NATIONAL BIODIVERSITY FUTURE CENTER

PhD STM
Course in Marine Science and Technologies
Curriculum: Marine Ecosystem Science

Health status of aquacultured bivalves and fish: immune responses of *Mytilus galloprovincialis* to bacterial isolates and monitoring growth of *Sparus aurata* and *Dicentrarchus labrax*

PhD student: Martina Leonessi

Supervisor: Prof. Laura Canesi
Co-supervisor: Manon Auguste, PhD

Università di Genova
DISTAV DIPARTIMENTO DI SCIENZE DELLA TERRA, DELL'AMBIENTE E DELLA VITA

Finanziato dall'Unione europea NextGenerationEU
Ministero dell'Università e della Ricerca
Italiadomani PIANO NAZIONALE DI RIPRESA E RESILIENZA
NATIONAL BIODIVERSITY FUTURE CENTER

Università di Genova | DISTAV DIPARTIMENTO DI SCIENZE DELLA TERRA, DELL'AMBIENTE E DELLA VITA

PhD STM

Course in Marine Science and Technologies (CODE: 9530) Curriculum: Marine Ecosystem Science

Thesis:

Health status of aquacultured bivalves and fish: immune responses of *Mytilus galloprovincialis* to bacterial isolates and monitoring growth of *Sparus aurata* and *Dicentrarchus labrax*

PhD student: Martina Leonessi

Supervisor:

Prof. Laura Canesi

Co-supervisor:

Manon Auguste, PhD

XXXVIII Cycle

Acknowledgement – Ringraziamenti

My first acknowledgements go to my supervisor Professor Laura Canesi, who gave me the opportunity to pursue and successfully complete my PhD journey, and to all the members of the Physiology group on the 5th floor. I would like to thank also the microbiology team, in particular Professor Luigi Vezzulli for his precious collaboration and Caterina for her patience in teaching me how to properly work in a microbiology lab.

Thanks to Professor Dolors Furones for kindly welcoming me at IRTA during my abroad period and for giving me the opportunity to learn new experimental approaches and develop new skills.

Mentre scrivo i ringraziamenti mi rendo conto di essere fortunata: così tante persone mi sono state vicine che non so né da chi iniziare né cosa dire perché ognuno si meriterebbe una pagina intera. Continuerò con la mia co-supervisor Manon Auguste. Il titolo di co-supervisor è solo l'ultimo che si aggiunto alla lista di tutte le figure che hai rappresentato per me in questi miei 5 anni a Genova: amica, confidente, punchball nei miei giorni peggiori. Grazie per avermi supportato e sopportato quotidianamente, per i tuoi consigli e per tutte le risate. E poi ovviamente grazie per tutta la sfera lavorativa: per avermi insegnato tutto in laboratorio e per tutte le ore spese insieme a fare esperimenti, per le discussioni scientifiche arricchenti. Grazie perché mi spingi a migliorarmi ogni giorno.

Il più grande dei ringraziamenti va alla mia famiglia, i miei genitori e mia sorella. Grazie babbo e grazie mamma per non avermi dato limiti e avermi permesso di perseguire il mio desiderio di provare a fare della ricerca il mio lavoro. Grazie per avermi spronata ad andare avanti e non mollare, per avermi sempre sostenuto. Grazie perché siete casa. Non c'è casa però senza la Carlo. Grazie perché ci sei sempre, incondizionatamente. Grazie perché sei sempre la prima a credere in me, molto prima che sia io a farlo. Questo mi spinge e sprona a dare il meglio di me per non deludere le tue aspettative.

Grazie alle mie amiche di una vita: Alice e Sofia. Grazie perché nonostante la distanza siete rimaste, perché ogni volta che torno a casa vi ritagliate del tempo per vedermi. Grazie Ali per il tuo entusiasmo smisurato e buonumore contagioso. Grazie Sofi per i piccoli gesti, tutt'altro che scontanti. Grazie ad entrambe per avermi ascoltata, consigliata, rimproverata quando necessario, ma soprattutto avermi spronata a credere in me stessa. Vi voglio bene.

Poi ci sono tutte quelle persone che ho incontrato durante i miei 5 anni passati a Genova che la vita mi ha regalato. Grazie Fra per la tua gentilezza e per avermi accolto a braccia aperte 5 anni fa, e per continuare ad essere un'amica fantastica anche dalla Francia! Grazie Vale: innumerevoli sono le volte che mi hai accolto a casa, pronta ad ascoltare ore delle mie lamentele. Grazie per avermi strappato un sorriso con il tuo sarcasmo, quando farlo non era per niente facile. Grazie anche a te Mari, per il tuo inguaribile ottimismo e per aver condiviso con me questa esperienza pazza che è il dottorato. Grazie alle mie coinquiline Ire, Mariv e Nuha. Grazie per le serate interminabili passate in cucina a discutere di qualsiasi argomento, grazie per avermi ascoltato tutte le volte che ne avevo bisogno.

Thank you also to all the amazing people I met during my abroad period in Spain. In particular I am very grateful to Alberto and Paula. Alberto, thank you for all the late nights spent at IRTA and the even later dinners we shared, it was always so much fun! Paula, thank you for your kindness and for being such a wonderful long-distance friend.

Grazie a tutta la mia famiglia, nonno, zii, cugini, Sandra, Davide, Richi per supportarmi ogni giorno.

Grazie mille a tutti, vi voglio bene!

Summary

This PhD project was carried out within the framework of the Italian National Biodiversity Future Center (NBFC), National Recovery and Resilience Plan (NRRP). The NRRP is the national program through which Italy used the European NextGenerationEU funds to promote economic recovery, innovation, sustainability, and social resilience after the COVID-19 crisis. The plan was organized into six missions, including digitalization, ecological transition, infrastructure, education and research, inclusion, and health. This project was enrolled within Mission 4 – Education and Research. This mission gave birth also to the National Biodiversity Future Center (NBFC), a national research centre funded to study, monitor, restore, and valorize biodiversity in Italy and the Mediterranean area. It involved dozens of universities, research centers, and private partners working together to develop scientific knowledge and technological solutions to address biodiversity loss and promote sustainable development. NBFC research topics were divided into 8 different spokes regarding: Sea (Spoke 1-2), Land (Spoke 3-4), Urban (Spoke 5-6) and Impact (Spoke 7-8). Within Spoke 2 (Marine biodiversity and sustainable management of marine resources), Activity 3 included research tasks aimed at improving sustainability, resilience, and animal welfare in aquaculture systems. This PhD thesis was enrolled in two relevant tasks belonging to Activity 3, Task 3.3 and Task 3.4, which focused on fish welfare and disease resilience respectively. Tasks 3.3 and 3.4 addressed sustainable aquaculture from complementary points of view: together they contribute to healthier aquaculture systems with lower disease incidence and reduced dependence on antimicrobials, supporting long-term sustainability.

- **Task 3.4** - *Selective breeding for disease resistance and resilience to environmental challenges for sustainable fish and shellfish aquaculture:* **Responses of aquacultured bivalves to environmental stressors and potential pathogens**
- **Task 3.3** - *Better health and welfare of fish without antimicrobials:* **Assessment of fish welfare in different farming systems**

Therefore, within the planned activities, **the first part of the research (Section I) is related to Task 3.4,** and it is focused on the marine mussel *Mytilus galloprovincialis*, and on the role of immune system in the response to challenge with bacterial isolates from bivalve mortality events (**Chapters 1-4**).

Chapter 1, 2 and 3 report data on a new potential bivalve pathogen isolated from a mortality event affecting adult *M. galloprovincialis* in 2022 in the Ebro Delta (Spain).

Chapter 1: this bacterium was firstly identified as *Vibrio ostreicida* and a PCR protocol was developed for its detection in mussel tissues and water samples. These data represented the first evidence for the association of *V. ostreicida* with a mortality episode in mussels.

Chapter 2: the immune interactions between a strain of *V. ostreicida* and bivalve hosts, the mussel

M. galloprovincialis and the oyster *Magallana gigas* were evaluated. The results revealed distinct immune profiles, indicating species-specific differences in susceptibility to *V. ostreicida*.

Chapter 3: the infection dynamics and immune responses of adult *M. galloprovincialis* challenged with *V. ostreicida* were investigated using different *in vivo* experimental approaches: injection/cohabitation experiments and bath infections. The results showed that *M. galloprovincialis* is able to cope with challenge with *V. ostreicida*, indicating that this *Vibrio* species is moderately pathogenic to mussels under the established experimental conditions.

Chapter 4 reports data on the immune responses of *M. galloprovincialis* to polymicrobial infection with two bacteria previously isolated from an oyster mortality event occurred in the Ebro Delta: *Vibrio aestuarianus* strain 106 and *Malaciobacter marinus* strain R1. Both *in vivo*/*in vitro* and *in vivo*/*in vivo* cross-infections challenges were performed to determine whether prior exposure to either isolate could influence immune responses to subsequent challenge with the other. The results demonstratethat first infection with *V. aestuarianus* weakened mussel immune defences, thus favoring the subsequent opportunistic behaviour of *M. marinus*.

Chapter 5 the results are reported of a seasonal study on variations in immunocompetence and in the specificity of immune responses of mussels towards three different bacteria: *Escherichia coli* MG 1655 (not pathogenic to bivalves, used as reference strain), *Vibrio aestuarianus* 01/32 (pathogenic to oysters but not to mussels), *Vibrio tasmaniensis* LGP32 (pathogenic to both oysters and mussels). The results support the specificity of mussel immune responses to different bacteria and indicate periods of higher susceptibility to *Vibrio* infection in winter months, in the spawning season.

In **the second part (Section II) the research activities related to Task 3.3** on farmed fish are presented **(Chapter 6 and 7).**

A multibiomarker approach was applied to monitor the growth and health status of gilthead seabream *Sparus aurata* (**Chapter 6**) and European seabass *Dicentrarchus labrax* (**Chapter 7**) reared in an offshore farm in the Ligurian Sea (Lavagna, Genoa, Italy) fed commercial standard diets (Skretting). Monitoring of *S. aurata* was conducted from the fry to marketable size (15

months), whereas that of *D. labrax* from a juvenile stage until market size (9 months). Standard morphometric and physiological measurements at the whole organism level indicate good growth performance and health conditions for the examined period for both species. Consistently, biomarker data at the tissue level indicate the absence of oxidative stress conditions or induction of biotransformation processes. In both species, the microbiota composition of anterior intestine samples along growth was evaluated.

SECTION I: Health of farmed bivalves in a global change scenario: immune responses of *Mytilus galloprovincialis* to potential bacterial pathogens

Introduction:

1. Health of farmed bivalves in a changing ocean: emerging issues and concerns
2. The model: *Mytilus galloprovincialis*
3. Mussel immune system
4. Functional immune biomarkers as tools for evaluating immunocompetence
5. Bivalve Microbiota
6. Mussel immune system - Bacteria interactions
    6.1 *In vitro* experiments
    6.2 *In vivo* experiments
7. Seasonal fluctuations in immunocompetence

Aim and Objectives

Results:

Chapter 1: First description of *Vibrio ostreicida* as putative causal agent of disease in Mediterranean mussel (*Mytilus galloprovincialis*) and development of a PCR protocol for its rapid diagnosis.

Chapter 2: Interactions between the oyster larvae pathogen *Vibrio ostreicida* and the bivalve hosts *Mytilus galloprovincialis* and *Magallana gigas*.

Chapter 3: Dynamics of *Vibrio ostreicida* in *Mytilus galloprovincialis* through *in vivo* infections. **Chapter 4:** Deciphering Host-Pathogen dynamics in *Mytilus galloprovincialis*: immune responses to multiple infections with bacterial isolates from bivalve mortality outbreaks.

Chapter 5: Seasonal variations in immunocompetence of *Mytilus galloprovincialis* and its specificity towards different bacteria

Conclusions and perspectives

SECTION II: Monitoring health and growth of farmed fish by a multibiomarker approach

Introduction:

1. Off-shore aquaculture
2. The models:
    2.1 Gilthead seabream *Spaura aurata*
    2.2 European seabass *Dicentrarchus labrax*

Aims and objectives

Materials and Methods

Results:

Chapter 6: Seabream

Chapter 7: Seabass

Discussion

Conclusions and perspectives

SECTION I

Health of farmed bivalves in a global change scenario: immune responses of *Mytilus galloprovincialis* to potential bacterial pathogens

Introduction

1. Bivalve Health in a Changing ocean: Emerging Issues and Concerns

Marine bivalves, as key foundation species in the marine environment, are the biotic basis for coastal ecosystems, providing structural habitat, food, and protection for myriad of plants and animals, as well as many ecosystem services (Wernberg et al., 2024). Moreover, bivalve aquaculture (in particular mussels, oysters and clams) is economically relevant, representing the 49 % of the total aquaculture production in EU in 2021(European Climate, Infrastructure and Environment Executive Agency, 2023) (EUMOFA 2024).

However, wild and farmed shellfish are facing new threats related to global climate changes. United Nations Framework Convention on Climate Change (UNFCCC), in its Article 1, defines climate change as: *a change of climate which is attributed directly or indirectly to human activity that alters the composition of the global atmosphere, and which is in addition to natural climate variability observed over comparable time periods* (Intergovernmental Panel On Climate Change (Ipcc), 2023). Climate change has started to affect ocean environmental parameters and more is to come: effects are recorded on temperature increase in the ocean, sea level rise, ocean acidification, changes in rainfall and therefore salinity, and concentration and quality of nutrients (Doney et al., 2020). The IPCC report (Intergovernmental Panel On Climate Change (Ipcc), 2023) has predicted for coastal waters about 3 °C warming and decrease in 0.4 pH units for the 21st century, with an estimated annual economic loss of 1 billion US$ by 2100 of European shellfish production caused by acidification only (Doney et al., 2020).

The ability of water of absorbing heat has increased proportionally the heat content of the oceans (Baker-Austin et al., 2024). Year 2023 was recorded as the warmest since modern records began in 1850 and global climate data, from January to December 2023, showed that oceans were 0.91 °C higher than the average (Rowley et al., 2024). The gradual increase in global temperatures varies geographically: warming of coastal areas is considered the most pervasive, with observations showing substantial and rapid warming in most of the world's coastlines (Baker-Austin et al., 2024). Heatwaves, defined as a period of at least three to five days during which mean or maximum temperature anomalies were at least 3–5 °C above normal (Hobday et al., 2016), and gradual temperature increases in surface sea water are one of the driving impacts of climate change in aquatic ecosystems. In 2024, severe to extreme marine heatwaves occurred in waters home to 17 % of shellfish farms along European coasts (Von Schuckmann et al., 2025), leading to financial distress in aquaculture farms (*FAO's work on climate change - Fisheries and aquaculture 2020*, 2021; Lattos et al., 2022). These events have

been studied intensively in recent decades and the results correlated them with down-regulation of both physiological and immunological functions in marine bivalves(Lattos et al., 2022), leading to aquatic diseases due to bacteria proliferation (Rowley et al., 2024; Scanes et al., 2021).

In a changing world, where the climate crisis is a global threat to species, biodiversity, and ecosystems, affecting individual organisms and their interactions (Bracchetti et al., 2024a; Wernberg et al., 2024), bivalve mortality events have become a big concern, with increasing records of mortalities and diseases affecting both farmed and natural stocks worldwide (Bracchetti et al., 2024a; Charles et al., 2020a; Lattos et al., 2022; Lupo et al., 2021; Mandic et al., 2024). The exact causes are not always clear, and mortality outbreaks are generally considered both multifactorial (Lupo et al., 2021) and polymicrobial. Indeed, fluctuations of biotic (e.g. different types of potentially harmful microorganisms including viruses, bacteria or protozoans) and abiotic parameters (e.g. seawater salinity, temperature, pH), as well as prolonged emersion at high temperatures during heatwaves, may induce multiple stress conditions in different bivalve species, affecting physiological homeostasis, from respiration and metabolism to immune defences. These effects may facilitate the proliferation of pathogenic and opportunistic microorganisms, bacteria in particular, and promote further cascade impacts on bivalve communities (leading not only to mortality but also altered development and reproductive success) (Cohen et al., 2018).

A great diversity of bacteria can be found in different marine sources, including both biotic and abiotic substrates (Stincone and Brandelli, 2020). Marine bacteria play important roles in the marine environment such as nutrient cycling, food sources for other species, and influencing host health (Beaz-Hidalgo et al., 2010; De Schryver and Vadstein, 2014; Travers et al., 2015a; Zilber-Rosenberg and Rosenberg, 2008a).

The association between bivalves and bacteria has a long evolutionary history, and there are several type of interactions that bacteria can establish with their hosts. As filter-feeding animals, bivalves have the ability to concentrate bacteria in their tissues and body fluids, including the hemolymph, that thus can represent habitats for bacteria, in particular those of the Vibrionaceae family (*vibrios*). *Vibrios*, gram-negative and rod-shape gamma-proteobacteria representing one of the most abundant culturable fraction of the marine microbial community (Baker-Austin et al., 2024; Ceccarelli et al., 2019), show a wide range of niche specialization, from free-living forms to those attached to biotic (e.g. copepods, crustacean, fish, algae and bivalves) and abiotic surfaces, from symbionts to pathogens, contributing to their growth and persistence in the natural environment (Ceccarelli et al., 2019). The temperature of seawater is

key role for *Vibrio* proliferation, which tends to be more present in warmer waters, especially above 17 °C; moreover, different vibrio species and strains can tolerate a large range of salinities (5 to 25 ppt) (Vezzulli et al., 2018a).

Several members of the genus *Vibrio* have been isolated and identified from different bivalve species (Barbosa Solomieu et al., 2015; Charles et al., 2020a; Travers et al., 2015a), where they can be present at concentrations 100-fold higher than those present in the surrounding water (Ceccarelli et al., 2019; Vezzulli et al., 2018a). As a matter of fact, *Vibrios* appeared to be important members of the oyster *Magallana gigas* and the mussel *Mytilus galloprovincialis* microbiota (Auguste et al., 2024a; Vezzulli et al., 2018a). The microbiota-host interactions and the path that separates *Vibrios* from being solely members of the natural microbial communities associated with the host to become pathogen (see below) are still blurred (Mesnil et al., 2023; Vezzulli et al., 2018a). Most of our knowledge on *Vibrios* isolated from bivalves comes from studies on pathological contexts; indeed, the presence of many *Vibrio*s has been associated with disease and mortality events of cultivated bivalves, leading to the conclusion that they represent the main infectious agents (Barbosa Solomieu et al., 2015; Charles et al., 2020a; Travers et al., 2015a).

Vibrio species can be primary pathogens, e.g. capable of causing pathological changes associated with disease in a healthy bivalve, or opportunistic pathogens, which cause disease when bivalves are compromised by a break in protective barriers or immunosuppression (Destoumieux-Garzón et al., 2020). In the literature, oysters have been shown to be historically more affected, with several *Vibrio* species identified as main pathogens. These include members of the *Splendidus* clade (*V. splendidus*, *V. tasmaniensis*, and *V. crassostreae* and *V. aestuarianus)*, consistently associated with disease outbreaks of oyster larvae, juveniles and adults (Azéma et al., 2017; Carrasco et al., 2017). Vibrioses have been also described in other bivalve species, such as those caused by *V. tubiashii* in the scallop *Argopecten irradians*, or by *V. tapetis*, the causative agent of the well known Brown Ring Disease in the clam *Ruditapes philippinarum* (Beaz-Hidalgo et al., 2010; Travers et al., 2015a).

Other *Vibrios* have been also implicated in larval mortalities across different host species, such as *V. tubiashii* in the oysters *M. gigas* and *Ostrea edulis* and in the scallop *A. irradians* (Travers et al., 2015a). Also *M. galloprovincialis* early larval stages have been shown to be susceptible to challenge with different *Vibrios*, such as *V. bathipelagicus*, which induced larval death (Lasa et al., 2021), or *V. coralliilyticus* and *V. tasmaniensis* LGP32 (Balbi et al., 2019b; Lasa et al., 2021) that induced developmental arrest.

Although adult mussels (*Mytilus* spp.) generally show a remarkable resistance to invading *Vibrios* with respect to other bivalve species, essentially due to the efficiency of their immune system (Destoumieux-Garzón et al., 2020; Eggermont et al., 2014), this advantageous trait seems to be not sufficient to face the more recent threats hitting European coastal waters.

Increasing reports of mortality events, often associated with microbial infections, in *M. edulis* and *M. galloprovincialis* have been recorded across Europe since 2014 (see the number of studies on musselmortality events reported in Figure 1); however, little is known on infection dynamics and kinetics of potentially pathogenic *Vibrio* species in mussels (Azizan et al., 2024, 2022; Beaz-Hidalgo et al., 2010; Benabdelmouna et al., 2018; Capelle et al., 2021; Charles et al., 2020b; Lupo et al., 2021).

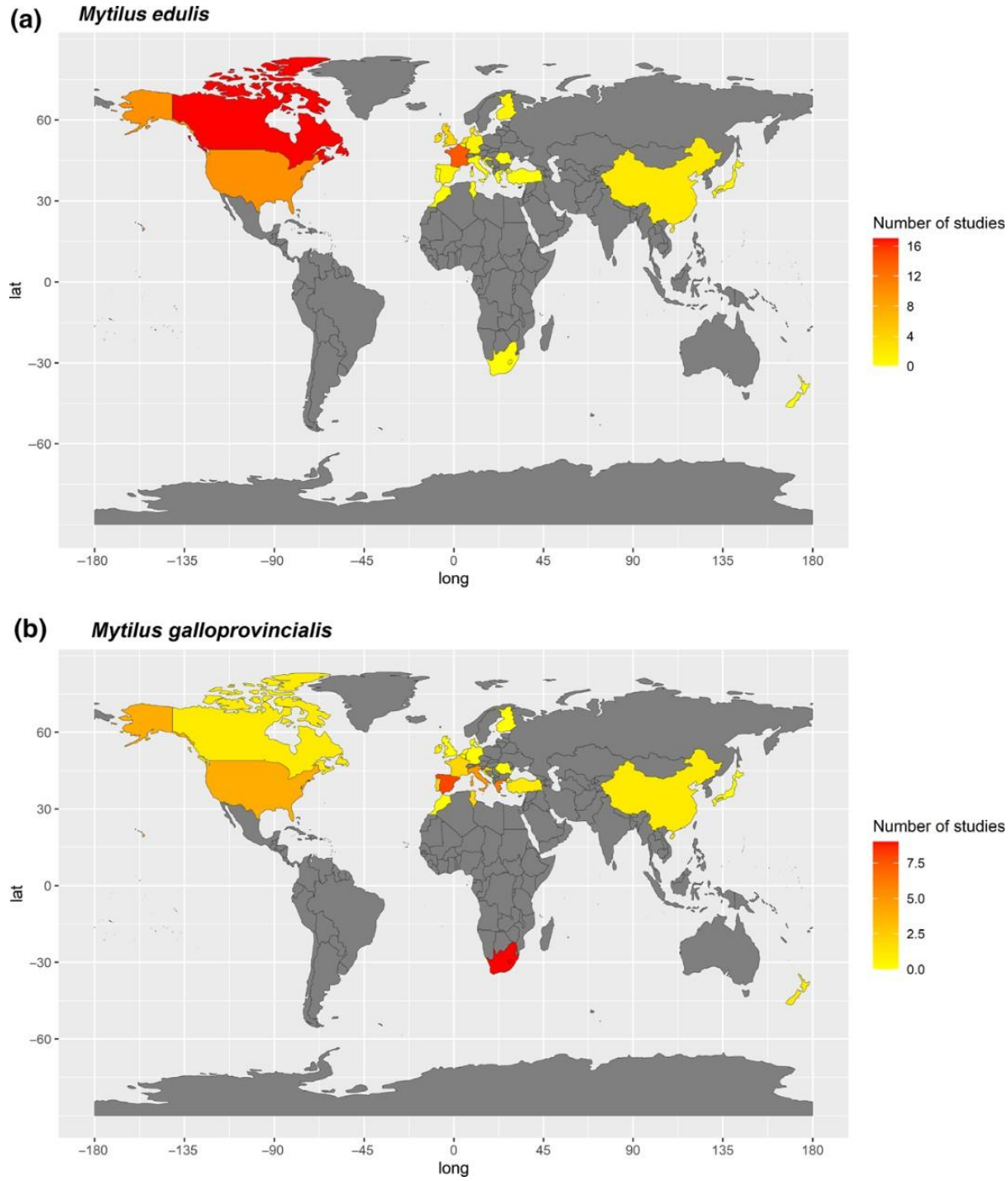

Figure 1: Geographical distribution of studies about (a) *Mytilus edulis* (N = 66) and (b) *Mytilus galloprovincialis* (N = 48). Grey shading indicates countries without included research about mussel mortality risk factors. The other colors represent the number of studies for each country. Figure from Lupo et al., 2021.

2. The model: *Mytilus galloprovincialis*

Among marine bivalves, the Mediterranean mussel *M. galloprovincialis* is one of the most aquacultured species, and apart from its economic importance and value, it has long been utilized in biomonitoring of marine pollution by a multi-biomarker approach (Curpan et al., 2022). It is considered an indigenous species of the Mediterranean Sea and Black Sea (Bownes and McQuaid, 2006). Nowadays, because of the growing mussel mariculture industry and the global increase in long-range maritime transport, it has been introduced to areas far outside their native range, and became an invasive species widely distributed all around the globe (Beyer et al., 2017). The optimal temperature conditions for growth are comprised between 8 °C and 25 °C and the salinity around 27- 30 ‰.

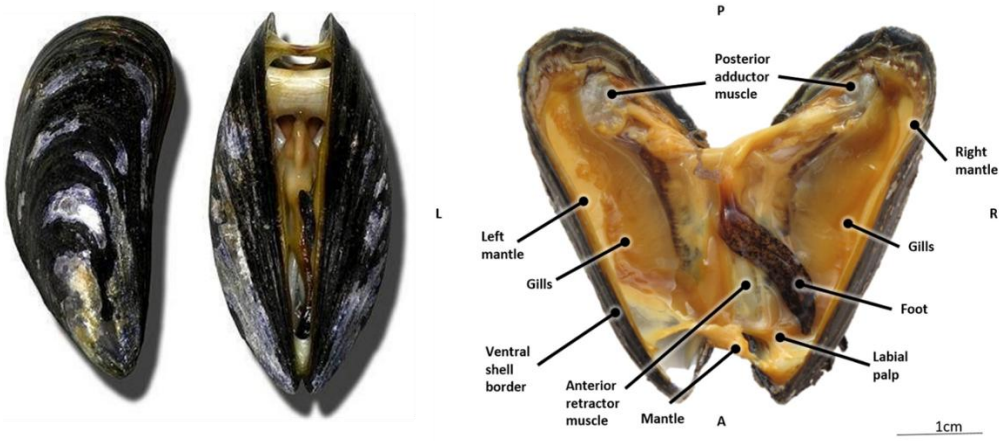

Figure 2: *Mytilus galloprovincialis* (Lamark, 1819), image from Eggermont et al., 2020

Mussels are sessile organisms and anchor themselves mainly to hard substrates or other mussels by the byssus, a keratinous and filamentous substance secreted by the foot. As a bivalve, the animal body is protected within two valves whose opening is modulated by the relaxation and contraction of the adductor muscles. Anterior and posterior retractor muscles are also attached to the shell, and these control the movement of the foot (Gosling, 2015).

The internal part of the body is composed principally by the mantle, which consists of two lobes of connective tissue which completely enclose the animal within the shell (Figure 2). The connective tissue presents hemolymph vessels, nerves and muscles. Cilia on the inner surface of the mantle play an important role in directing particles onto gills and in deflecting heavier material along rejection tracts towards the inhalant opening, the entry point on the mantle for incoming water.

The gills are inserted at the dorsal margin of the mantle, and have a dual role in respiration and feeding. Each gill is composed by numerous W shaped filaments, divided into “V” called demi- branch and each arm is called lamella (inner descending and outer ascending). The filaments are covered by cilia that allowed conveying the filtered particles toward the mouth (or to exhalant siphon for the particles that do not represent a feeding interest, that will be ejected directly as pseudofaeces). The filaments are made of a single layer of epithelial cells surrounding an hemolymph capillary, allowing the oxygen transport from the thin filament wall to the organs. The gills, due to their direct contact with surrounding water, can be the first tissue targeted by contaminants, several sorts of particles, or molecules can directly interact with gill cells (Gosling, 2015). Particles can be also trapped in pallial mucus and, through mucociliary transport, directed to digestive gland (Allam and Pales Espinosa, 2016).

The digestive gland, which is brown or black and consists of blind-ending tubules that connect to the stomach by several ciliated ducts, is the major site of intracellular digestion. The tubules are composed of two cell types: the digestive cells and the basophil (secretory) cells. Digestive cells take up material by pinocytosis and digest it within vacuoles. The released waste, enclosed in excretory spheres, is swept towards the stomach and ultimately to the intestine. The secretory cells carry out extensive protein synthesis, but their exact role is not yet known.

Mussels possess a simple nervous system, composed of 3 pairs of ganglia and several pairs of nerves: the cerebral ganglia (innervating the palp, anterior adductor muscle and part of the mantle), the pedal ganglia (foot) and the visceral ganglia (gills, heart, kidney, gonads, posterior adductor muscle and part of the mantle). The ganglia have a neurosecretory role, since they can produce neurotransmitters and neuropeptides released into the circulatory system (Gosling, 2015).

The circulatory system is open, and relies on the circulation of hemolymph fluid, whose osmotic concentration is equal or very similar to that of the surrounding seawater. The roles of the hemolymph are very diversified: gas exchange, osmoregulation, nutrient distribution, waste elimination and internal defense. It represents 40 to 60% of the fresh tissue weight and gives rigidity to organs as a fluid skeleton (Gosling, 2015).

Mussels are dioecious, the sexes are separate, and the gonad develops within the mantle tissue. During the reproduction period, gametes differentiate within the connective tissue of the mantle: orange for the female eggs and creamy-white sperms for males (Gosling, 2015). Gametogenesis is influenced by different environmental factors, and it is likely subject to a year to year variability, mainly dependent on temperature and food availability. In particular, warmer temperatures reduce rates of gametogenesis in *M. galloprovincialis* (Fearman and

Moltschaniwskyj, 2010). It is well accepted also that gametogenesis influences the health status of the animals (OSPAR Commission, 2013).

3. Mussel immune system

The defense system of mussels can be divided in 2 different types of barriers: physical and biological. Physical barriers include the shell, that supports and protects the soft tissues from biological and physico-chemical insults, the skin, and the mucosal layer that covers it and that captures microbes simplifying their elimination via ciliary activity (Allam and Raftos, 2015). The mucosal layer is not only a physical barrier but, with the external epithelium, is also among the first actors in immune defense (Figueras, 2019). There are several lines in biological immune defense in mussels. Although mussels, as all invertebrates, lack an adaptative immune system, they can mount efficient responses to pathogens, trauma or environmental stress (Canesi et al., 2002a) (Figure 3). Indeed, innate immunity displays a wide variety of sensitive receptors, selective effectors, and synergistic genetic regulatory networks that help mussels coping with exposure to several abiotic and biotic stresses (Canesi et al., 2002a). In mussels, immunity involves both cell-mediated and humoral systems that operate in a coordinated way to provide protection from invading microorganisms. The primary effectors, the backbone of mussel immunity system, are the hemocytes, the circulating cells of the hemolymph which may act directly or in concert with humoral factors, present in the hemolymph, to defend the animal against infections (Allam and Raftos, 2015; Bouallegui, 2019; Burgos-Aceves and Faggio, 2017; Canesi et al., 2002a).

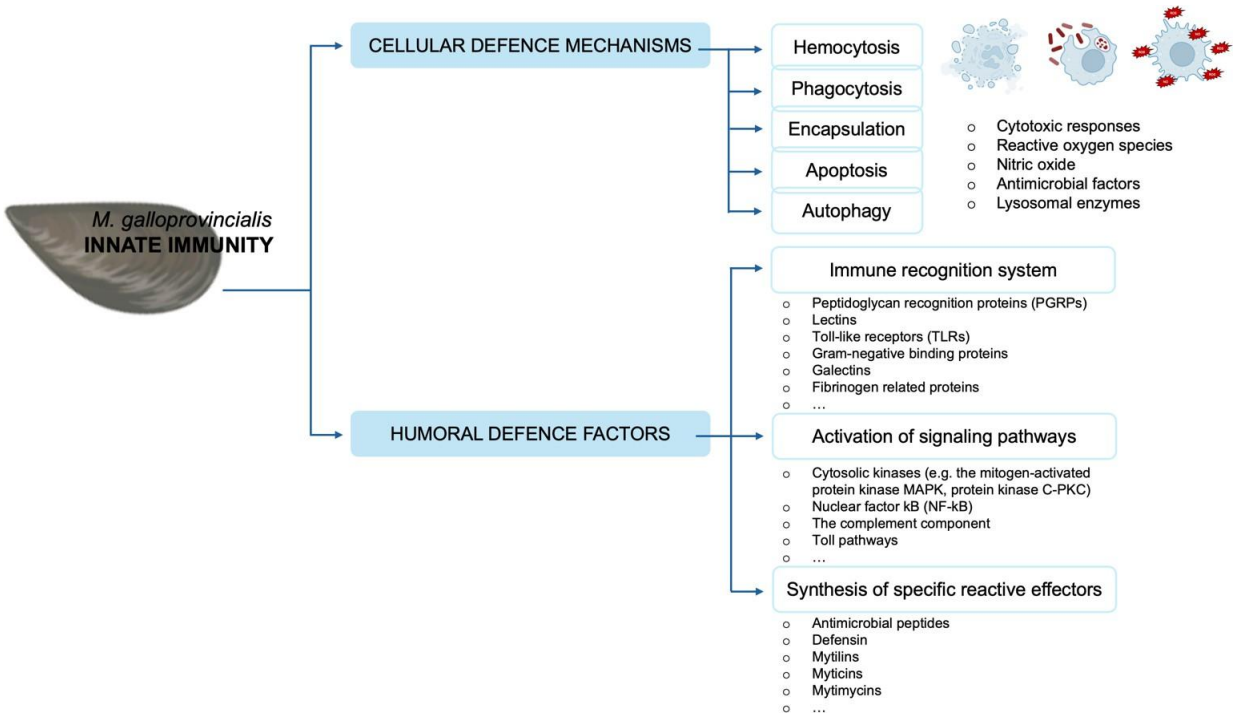

Figure 3: Summary of innate immunity of mussel *M. galloprovincialis*. Mechanisms of cellular defence and humoral defence factors are shown.

Mussel hemocytes, in both structure and function, resemble the vertebrate monocyte/macrophage lineage. Hemocytes move through the open circulatory system and migrate to other locations, such as the connective tissue and epithelia. Hemocytes have been classified into 4 main groups: large granular (R1), large semigranular (R2), small semigranular (R3) cells, hyaline (R4) cells (García- García et al., 2008). Generally, the most common differentiation is between granulocytes (cells with granules in the cytoplasm and typically a low nucleus/cytoplasm ratio, comprehensive of R1, R2 and R3) and hyalinocytes (cells containing few or no granules within the cytoplasm and higher nucleus/cytoplasm ratio, R4) (De La Ballina et al., 2022; García-García et al., 2008). Even if the relative abundance of each cell type in the hemolymph is variable, being affected by seasonal changes, temperature, size, sex, maturity, food availability and interindividual variability, granulocytes are generally considered the most abundant cell type in *M. galloprovincialis* (De La Ballina et al., 2022). Granulocytes are believed to be more efficient in killing microorganisms by producing extracellular toxic metabolites such as reactive oxygen intermediates (ROS), nitric oxide (NO) and by activating lysosomal enzymes, actors which can serve as killing agents. Unbalanced levels of these elements can lead to oxidative stress (Canesi and Pruzzo, 2016; Song et al., 2010a). What is more, granulocytes can phagocyte non-self particles, such as pathogens, mediated by either serum ligands (opsonins) or membrane receptors (Gerdol et al., 2018). Hyalinocytes, in contrast, are primarily associated with clotting and wound-healing processes, but they also play an active role in innate immunity through the production of ROS and NO (De La Ballina et al., 2022).

The fluid portion of mussel hemolymph, referred to as hemolymph serum, as in all invertebrates, lacks immunoglobulins, and must rely on other molecules for self- nonself-recognition necessary for internal defense. Indeed, mussel serum has been demonstrated to contain diverse proteins, including lysosomal enzymes, various antimicrobial peptides (AMPs) and soluble lectins that, together with the hemocytes, contribute to recognition and elimination of potential pathogens. Lysosomal enzymes play a role in defense by breaking down the bacteria cell wall due to their muramidase activity: indeed, they catalyze the hydrolysis of β-1,4-glycosidic linkage between N-acetylmuramic acid and N-acetylglucosamine of peptidoglycans (PGN). AMPs are small size (12-100 amino acids), widespread group of

heterogenous gene-encoded peptides with heat stability, cationic hydrophobic nature and antibiotic functions (Gerdol and Pallavicini, 2025). *M. galloprovincialis* is one of the species with the highest amount of different families of AMPs in the animal kingdom. Moreover, the complexity of the immune repertoire is further enhanced by the presence in mussel genome of extensive hemizygous regions, which exhibit extensive presence/absence variation (PAV) among individuals, and affects all known AMP families to varying degrees. *M. galloprovincialis* AMPs have been divided into 7 principal classes: myticins, mytilins, defensins, big defensins, mytimycins, mytimacins and myticalins (Gerdol and Pallavicini, 2025). Lectins, that are present both in a free in serum and bound to hemocyte membranes, are involved in cell recognition and have an opsonic and agglutinating role of non self-material in hemocyte phagocytosis. They firstly take part to immune recognition as pattern recognition receptors (PRRs), recognizing pathogen-associated molecular patterns (PAMPs). PRRs selectively recognize a large family of conserved foreign PAMPs commonly present in microorganisms but rare or absent in host animals such as lipopolysaccharides (LPS) or peptidoglycans (PGN) (both present in bacterial cell walls) (Song et al., 2010b). Upon successful recognition, activated PRRs trigger different intracellular signaling pathways that may lead to the rapid activation of phagocytosis, ROS production, release of preexisting enzymes or antimicrobial molecules, as well as to changes in the transcription of immune, or stress response genes at the nuclear level (Allam and Raftos, 2015; Canesi and Pruzzo, 2016; Gerdol et al., 2018).
The phagocytosis is the main actor in killing of many bacteria. The phagocytic process can be summarized in 4 steps: chemotaxis, attraction and migration (not always required or involved in phagocytosis), recognition and attachment mediated by lectins, internalization and intracellular degradation. These processes result in the formation of a primary phagosome, where the intracellular destruction and killing of microorganisms take place. Lysosomes migrate toward the phagosome where they fuse with it and discharge their contents (hydrolytic enzymes), contributing to the enzymatic degradation of engulfed microorganisms. After the engulfment, the target is destroyed within the phagosomes by lysosomal enzymes, ROS, nitric oxides NO as well as antimicrobial factors (AMPs) (Canesi and Pruzzo, 2016; Gerdol et al., 2018; Song et al., 2010b).

The immune response is dependent on gene expression. Genomic and transcriptomic studies have revealed a wide variety of immune-related genes in mussels, whose expression is modulated in response to bacterial challenge, particularly those involved in bacteria recognition, signaling, and effector functions (Gerdol and Venier, 2015; Moreira et al., 2020).

Hemocytes exhibit high basal and inducible expression of different immune-related genes, (Romero et al., 2011). Among the most studied genes, there are those encoding pattern recognition receptors (PRRs), such as *Toll-like receptors* (TLRs), *C-type lectins*, *galectins*, and *peptidoglycan recognition proteins* (PGRPs), which mediate the detection of bacterial molecular patterns (Romero et al., 2011; Song et al., 2010b). Recognition of bacteria and bacterial products promotes the expression of key signaling genes, including Myeloid differentiation factor88 (MyD88), Tumor Necrosis factor (TNF) Receptor- Associated Factors6 (TRAFs), and *NF-κB–like transcription factors*, which regulate immune gene networks (Gerdol and Venier, 2015). MyD88 transduces signals from TLRs and interleukin-1 receptors (IL-1Rs) after they detect pathogen-associated molecular patterns (PAMPs). Activation of MyD88-dependent pathways leads to the transcription of immune effector genes, including cytokines, antimicrobial peptides (AMPs), and other inflammatory mediators (Gerdol et al., 2018; Song et al., 2010b). TRAFs transduce signals from TLRs, TNF receptors (TNFRs), and activation of IL-1Rs results in transcription of immune-related genes, including AMPs, cytokines, and genes involved in oxidative stress responses (Song et al., 2010b). Upon stimulation by receptors such as TLRs or TNFRs, *NF-κB–like transcription factors* activate target genes including AMPs, cytokines, lysozymes, oxidative stress enzymes, and other immune regulators (Gerdol and Venier, 2015; Song et al., 2010b).

However, the strongest transcriptional responses to bacterial infections are often observed in effector genes encoding AMPs such as *mytilins, myticins,* and *defensins*, which are widely used as molecular markers of immune activation in mussels (Costa et al., 2009; Gerdol and Pallavicini, 2025). AMP genes are predominantly expressed in hemocytes, although expression in epithelial and barrier tissues suggests additional roles in local defense. Both constitutive expression and inducible regulation have been described, enabling a balance between continuous immune surveillance and enhanced responses upon microbial challenge or tissue damage (Gerdol and Pallavicini, 2025).

Among the different AMP families, myticins are known for their functional versatility. Indeed, firstly characterized for their antibacterial properties, they have been demonstrated to play a more prominent role in antiviral defense. This discover was strongly supported by a study demonstrating the direct antiviral activity of myticin C against ostreid herpesvirus 1 (OsHV-1), a common oyster pathogen (Barbosa Solomieu et al., 2015). The study showed that mussel hemolymph, containing myticin C, conferred protection from infection to oyster hemocytes, naturally lacking myticin C, when incubated together (Novoa et al., 2016). Mussels and oysters do not share the same AMPs: mussels express myticins, including myticin C, which are absent

in oysters. However, oysters possess their own distinct antimicrobial peptides (De San Nicolas et al., 2022). These findings help explaining the resistance of mussels to OsHV-1 infection, as mussels do not experience significant mortality in contrast to oysters, which exhibit near-complete lethality under similar experimental conditions (Gerdol and Pallavicini, 2025). Among myticins, Myticin C (MytC), the most expressed AMP in adult mussels, has the highest RNA polymorphism relative to other mussel AMPs (Canesi et al., 2022). MytC has been shown to inhibit the replication of bacteria, fish viruses, and to have chemotactic and wound healing properties (Balseiro et al., 2011). *In vivo* studies suggested that overexpression of MytC in hemocytes could alter the transcription of other immune-related genes (other AMPs, complement proteins, lysozyme). These data suggested that MytC may also play a role as an immune system modulator with chemokine-like activities (Balseiro et al., 2011). In *M. galloprovincialis*, the extensive repertoire of AMPs, endowed with a broad spectrum of immune functions, might have significantly contributed to the evolutionary advantage of mussels in adapting to extremely changing environments (Figueras, 2019; Gerdol et al., 2020). Myticalins demonstrated notable antimicrobial activity at relatively low concentrations against a broad spectrum of Gram-positive and Gram-negative bacteria, which was exerted through membrane permeabilization (Gerdol and Pallavicini, 2025). Myticalins are, however, not the only mussel AMPs to lack hemocyte-specificity, since also mytimacins and big defensins are expressed in a broad range of tissues, which would confirm the importance of antimicrobial defense at mucosal interfaces. Big defensins (BD), the ancestors of b- Defensins, essential components of innate immunity in vertebrates and invertebrates, are a large family of AMPs characterized by a highly hydrophobic globular N- terminal domain, which is present in different phylogenetically distant species, including both marine and freshwater bivalves (Gerdol et al., 2020). BDs are characterized by antimicrobial activities over a wide range of osmolarity. Studies in bivalves showed that the presence of the conserved hydrophobic domain confers bactericidal activity even at high salt concentrations (Loth et al., 2019).

Another effector of humoral defence is represented by the complement system. The complement system is an ancient pro-inflammatory and microbial destruction system based on serum and cell surface proteins, that lead to pathogen neutralization and pro-inflammatory responses (Bouallegui, 2019; Sun et al., 2023). The complement system pathway relies on several interacting proteins to recognize and then eliminate foreign microorganisms, with a pivotal role in the initiation of defense mechanisms, including agglutination, adhesion, opsonization, and cell lysis. Once activated, the complement system promotes target

proteolytic reactions that operate following classical, lectin, or alternative pathways. C1q, a subcomponent of the complement C1 complex, is considered to be a versatile PRP, binding directly to a broad range of PAMPs of bacteria, viruses, and parasites as well as enhancing pathogen phagocytosis (Canesi and Pruzzo, 2016; Nayak et al., 2012; Sun et al., 2023). In *M. galloprovincialis*, proteins from the complement system, such as MgC1q, with specific ligand recognition properties have been described and characterized (Gestal et al., 2010).

Additional immune genes frequently analyzed include *lysozyme*, *phenoloxidase*, and genes associated with oxidative stress and cytotoxic responses, such as *superoxide dismutase* and *catalase* (Romero et al., 2011) which together mediate bacterial killing and immune defense (Costa et al., 2009; Gerdol et al., 2012).

In addition to hemolymph, immune gene expression has been documented in barrier and metabolically active tissues, including the gills, mantle, digestive gland, and foot, which are directly exposed to the external environment or involved in filtration and digestion (Pallavicini et al., 2008). These tissues express a broad set of immune genes, often at lower basal levels than hemocytes, but can show significant transcriptional modulation during bacterial exposure, particularly for genes associated with antimicrobial activity, oxidative stress responses, and immune regulation, such as *superoxide dismutase* and *catalase* (Romero et al., 2011).

In addition to the classical innate immune mechanisms described above, increasing attention has been directed toward the possibility that invertebrate immune systems can retain information from previous pathogen encounters, a phenomenon referred to as innate immune memory. Innate immune memory, or priming, can be defined as the ability of the immune system to store or simply use the information on a previously encountered antigen or parasite upon a secondary exposure (Milutinovic´ and Kurtz, 2016). From an evolutionary perspective, it is difficult to accept the hypothesis that immune memory evolved exclusively in vertebrates, which represent a small percentage of living animals. Few studies have emerged in the immune priming in different human cell lines, including macrophages (Boraschi and Italiani 2018) but in the past two decades, some evidence has been provided also for a memory of innate immunity in invertebrates (Gourbal et al., 2018; Lanz-Mendoza and Contreras-Garduno 2022; Kurtz et al., 2025). Three main mechanisms have been identified: the first is called recall or trained response, expressed as potentiation (with immune parameters showing enhanced response/activity upon the second exposure); the second is represented by a sustained, unique response which corresponds to the maintenance of a high response between successive

exposures; and the last is characterized by an immune shift, a change in the type of response observed between several exposures (Gourbal et al., 2018; Melillo et al., 2018). Evidence for epigenetic reprogramming of immune cells (i.e., histone acetylation/deacetylation and DNA methylation) leading to changes in gene expression, which represent the characteristic hallmark of immune training or memory, has not been provided yet in most invertebrate groups, including bivalve mollusks (Gourbal et al., 2018; Pradeu et al., 2018; Montagnani et al., 2023). On the other hand, evidence for immune stimulation induced by repeated challenge with natural pathogens is available in scallops and oysters (Wang et al., 2013; Zhang et al., 2014; Liu et al., 2016; Green et al., 2018; Arfatahery et al 2024). In the mussel *M. galloprovincialis*, increased bactericidal activity was observed after *in vivo* and subsequent *in vitro* challenge with *V. anguillarum* (Ciacci et al., 2009). Recent transcriptomics data obtained in *M. galloprovincialis* hemocytes after repeated challenge with *V. splendidus* demonstrated a shift from a pro-inflammatory response to an anti-inflammatory and probably regenerative phenotype, indicating the existence of a secondary immune response in mussels oriented to tolerate infection (Rey-Campos et al., 2019). A similar response has been described following repeated *in vivo* exposures to nanoplastics in *Mytilus*, where the immune parameters were modulated differently after the second exposure and this shift in immune parameters could act as compensatory mechanisms to maintain immune homeostasis after a second encounter with NPs. (Auguste et al., 2020).

4. Functional Immune biomarkers as tools for evaluating immunocompetence

A biomarker is defined as a measurable biological response, at different levels, in a marine organism that reflects exposure to, or effects of, chemical contaminants or other environmental stressors in the environment (OSPAR Commission, 2013). In a context of host-bacteria interactions, immune-related biomarkers allow the identification of molecular, biochemical, physiological, genetic, and cellular changes in the host (Qureshi and Niazi, 2020). These changes occur due to the interaction of three factors: the host, the microbes, and the environment, known as *the epidemiological triangle* (Lane et al., 2022). In mussels, immunocompetence relies entirely on innate immune defenses, including hemocyte-mediated cellular responses, humoral factors such as AMPs and enzymes, and oxidative and detoxification pathways. Biomarkers that quantify these responses therefore provide valuable proxies for assessing immunocompetence and responses to pathogen infection.

Immunological parameters have been developed for both tissues (mainly digestive gland and

gills) and hemolymph. However, since hemocytes are the key of the innate immune system, acting as defensive cells in several different ways and compartments, many biomarkers have been therefore developed to assess hemolymph immune functions, in particular in response to bacterial challenge (Azizan et al., 2024). Hereafter some of the most utilized biomarkers are described.

The first important cellular parameter that can be used to investigate bacteria-immune system interactions is hemocyte viability. It can be studied by measuring metabolic activity through reduction of cell-permeable fluorescent probes such as CTB (CellTiter-Blue) or the colorimetric MTT (thiazolyl blue tetrazolium bromide) assay. Alternative methods are represented by the use of a counter stain dye such as trypan blue or the use of DNA-binding fluorescent dyes are alternative methods (Azizan et al., 2024). Apoptosis and preapoptosis evaluation methods can be used as early markers for cell viability through the use of specific fluorescent dyes (e.g., annexin V staining/ 4′,6-diamidino-2- phenylindole-DAPI).

In addition to measuring the overall immune cell viability, quantifying changes in hemocyte number and the ratios of different hemocyte subpopulations (e.g., total hemocyte counts-THC, granulocytes- hyalinocytes ratio) by flow cytometry can give a more detailed view of the impact of bacteria (Ciacci et al., 2010; Parisi et al., 2019). Moreover, subcellular effects of bacteria can be identified via assessment of the integrity of organelles, membranes, and other cellular compartments. Lysosomal functional integrity is an evolutionarily conserved marker of stress, and it is commonly evaluated by measuring neural red retention time (NRRT) (OSPAR Commission, 2013). Microscopy techniques can reveal the change in cell morphologies and subcellular structures (e.g., vacuoles, phagosomes, endosomes) and give hints regarding the general activation or damages that the cell has undergone (Auguste et al., 2020; Balbi et al., 2017, 2019b).

Phagocytic capacity of hemocytes is considered as a proxy of immunocompetence of the whole organism, since it represents the main parameter of cell-mediated immunity in invertebrates. Phagocytosis can be evaluated by colorimetric and fluorescent methods by microscopy and flow cytometry (Canesi et al., 2002a). Upon contact with bacteria, hemocytes can be activated and produce cytotoxic factors inside the cells; among them, the oxidative burst, which involves the production of several radicals from oxygen (ROS) and nitrogen (RNS) derivatives. To quantify ROS, several methods can be utilized, including the use of fluorescent probes (e.g., Dichlorofluorescein-DCF or calcein), UV-vis spectroscopy (e.g., cytochrome C reduction) or histochemical staining (Auguste et al., 2022a; Ciacci et al., 2010; Panebianco et al., 2023). As

for the quantification of RNS nitric oxide (NO) can be measured spectrophotometrically in hemolymph samples using the Griess reagent (Auguste et al., 2024a; Balbi et al., 2018, 2019b).

Upon activation of the immune cells, lysozyme and radicals can also be released by hemocytes in the extracellular medium, to directly destroy bacteria in close proximity to the cell. Lysosomal enzymes play a role in defense by breaking down the bacteria cell wall due to their muramidase activity. The release of lysozyme into the extracellular medium can easily be determined spectrophotometrically by measuring the lytic activity towards *Micrococcus lysodeikticus*. Fluorescent probes can be also used to monitor the evolution of the lysosomal compartment and acidification in the cell (Auguste et al., 2022a; Balbi et al., 2013, 2019a). An important immunological parameter often analyzed in mussels is the measurement of phenoloxidase (PO) activity. This enzyme, produced via the pro-PO cascade, is involved in melanin synthesis. Upon pathogen recognition, hemocytes rapidly encapsulate the foreign body, and melanin is deposited around the encapsulated pathogen, contributing to its elimination. PO activity can be assessed by monitoring spectrophotometrically the formation of a reddish-brown pigment in the hemolymph (Luna-Acosta et al., 2017).

In addition immune responses can be measured through transcriptomic approaches, whose the main advantages are their high-throughput potential a specificity, allowing for the assessment of entire immunological pathways instead of focusing on specific functional endpoints (Moreira et al., 2020).

Moreover, gene expression offers alternative possibilities to study several proteins involved in the immune response, such as the effects of bacteria on AMP modulation (Tanguy et al., 2018). However, major limitations of these methods are that they require species-specific primers and the availability of transcriptomes. Moreover, gene expression is highly regulated and time-dependent, so careful consideration must be given in terms of stimulation/exposure time, and cell collection technique. Thus, in order to understand the environmental relevance of any change in immune homeostasis, a combination of both functional assays and cutting-edge technology (transcriptomics, proteomics, and metabolomics) is required (Balbi et al., 2021).

Overall, current knowledge on mussel immune biomarkers highlights both strengths and limitations. Immunological biomarkers offer several advantages, including the ability to quantify responses to bacterial exposure, integrate the effects of polymicrobial mixtures, support mechanistic interpretations, and serve as surrogate indicators of physiological health

status. They are also valuable for assessing recovery following environmental stress (Azizan et al., 2024).

However, limitations remain. Immune biomarkers (both functional and molecular) lack specificity and their basal levels can be affected by both abiotic and biotic factors, such as temperature, salinity, reproductive stage and nutritional status (Azizan et al., 2024). Finally, a single biomarker is obviously not sufficient to fully evaluate immune competence in mussels. Therefore, a multiple-biomarker approach is strongly recommended for optimal use in biological monitoring programs and in laboratory experiments to evaluate immune responses to challenge with different bacterial species and strains. Finally, immune parameters in mussels may also be influenced by the composition of the microbiota in the hemolymph and various tissues. Indeed, the microbiota composition can alter the outcome of bacterial infections.

5. Bivalve Microbiota

The 'hologenome' concept, introduced by Zilber-Rosenberg and Rosenberg, 2008, considers the host and its associated microorganisms (microbiota) as a single evolutionary and ecological unit: the holobiont. This concept is based on (1) existing symbiotic relationships between host and several microorganisms; (2) the transmission of the symbiotes; (3) the benefits of the symbiotic association between the host and the microorganisms; and (4) the genetic plasticity enhancement of the holobiont, through change in the microbiotic composition under environmental pressure (Desriac et al., 2014). Mussels can be described as holobionts, due to their life-long association with host-selected symbiont microbial communities known as microbiota (Glasl et al., 2016; Pita et al., 2018). These symbionts can endow the host with a set of probiotic functions (i.e. defense against pathogens, immunological regulation and improved nutritional efficiency), supporting homeostasis and health. Thus, mussel microbiota should be considered as an integral component of the host physiology and immunity (Ben Cheikh et al., 2024; Musella et al., 2020). Microbiota can be divided in core and transient. The core microbiome is represented by groups of microbes constantly present among individuals, and thus considered as a stable community established within the host (Auguste et al., 2023). As filter feeders able to concentrate microorganisms, mussels have highly plastic transient microbiome, that is especially influenced by the surrounding seawater and environmental conditions. These bacteria can be rapidly eliminated upon depuration in clean seawater, a common method employed for removing waterborne microbial contaminants from bivalves (Destoumieux-Garzón et al., 2024; Gignoux- Wolfsohn et al., 2024).

In healthy mussels, bacteria abundance in the hemolymph can reach 10^3 CFU/mL (Li et al., 2019; Vezzulli et al., 2018b); they are essential for maintaining homeostasis and resisting disease. Disturbances of these microbial communities can negatively impact host fitness, inhibiting growth or even leading to death (Li et al., 2019). Shifts from symbiotic bacteria to pathogen-dominated communities, due to environmental factors and stress, highlight the importance of crosstalk between environment and host-associated microbial communities (Li et al., 2019). The impairment of microbial community can lead to dysbiosis, causing a disruption in the mutual harmony bacteria-host. Healthy balanced microbiota can turn into a disease-inducing pathobiota (Ben Cheikh et al., 2024; Paillard et al., 2022). In mussels, stressful conditions such as pollutant exposure (Auguste et al., 2020, 2019), bacterial challenge (Ben Cheikh and Travers, 2022) or changes in water chemico-physical parameters (Li et al., 2019) can affect the physiological status which could lead to shifts in microbiota composition.

Analyses on hemolymph microbiome of *M. galloprovincialis* cultivated in north-western Italy (La Spezia) sampled from February to November showed seasonal changes. Although hemolymph microbiota was characterized by the constant presence of 8 bacterial genera (*Vibrio*, *Pseudoalteromonas, Tenacibaculum*, *Colwellia*, *Shewanella*, *Amphritea*, and 2 from the *Arcobacteracea* family: *Halarcobacter* and *Arcobacter*-like), distinct patterns in term of abundance in winter (February–November) and summer (July, September) were observed. Water temperature contributed to shaping the microbiota composition, in particular with regards to the abundance of *Vibrios*, *Psychrilobacter* and *Photobacterium*, *Halarcobacter* and *Arcobacter*-like, that was favored by higher temperatures. Some of these bacteria were reported as primary or opportunistic pathogens for bivalves and found in association with diseased bivalves and mortality outbreaks (Auguste et al., 2022b; Lasa et al., 2019).

6. Mussel immune system - Bacteria interactions

The presence of complex host-associated microbial communities is a characteristic shared by most animal species, and the type of interactions that they can establish with their host can range from mutualistic to pathogenic (Destoumieux-Garzón et al., 2020; Fraune and Bosch, 2010). Bacterial pathogens can impact the health status of marine bivalves, and a number of bacterial diseases have emerged or re-emerged in the last two decades. Among these bacteria, some are implicated in human seafood-borne infections, by consumption of raw or undercooked seafood, representing a threat for human health (Odeyemi, 2016). Many studies on marine mussels, both economical important and appreciated seafood, supported the

knowledge that the persistence of bacteria in bivalve tissues largely depends on their sensitivity to hemolymph bactericidal activity (Auguste et al., 2022b; Balbi et al., 2013; Pruzzo et al., 2005).

Therefore, studying host-bacteria interactions is fundamental for understanding mussel physiology, immune responses and susceptibility to disease. The family *Vibrionaceae* is among the most prevalent bacterial groups in marine environments, and its members exhibit a high colonization potential, partially due to their metabolic versatility and genetic variability (Le Roux et al., 2016). Most studies on host–bacteria interactions have focused on *Vibrio* species often isolated during mortality events affecting various bivalve species. Actually, some *Vibrio* species have been described as primary pathogens for certain bivalve species (see paragraph "Bivalve Health in a Changing ocean: Emerging Issues and Concerns"); however, so far, no particular bacterium has been identified as an etiological agent of disease in *Mytilus* spp.

Several *in vitro* and *in vivo* studies have investigated the diverse interactions between *Vibrio* spp. and *Mytilus* (Destoumieux-Garzón et al., 2020; Travers et al., 2015b), and different experimental approaches have been utilized to study how mussel immune system responds to potential opportunistic or pathogenic bacteria.

6.1 *In vitro* experiments

In vitro assays are essential tools for immunological studies. First, they allow for the investigation of the molecular and cellular interactions between bacteria and innate immunity of bivalves. In addition, the highly controlled experimental conditions enable reproducible experiments while reducing biological variability. Circulating hemocytes, together with soluble factors present in hemolymph serum, are a system that responds very quickly upon the encounter with foreign particles and bodies, making it a suitable *in vitro* model to evaluate the effects of a number of effectors, from contaminants to bacteria, on immune responses. The utilization of primary cells or cell lines is already established for vertebrates, but these existing protocols need to be adapted and/or improved for bivalve *in vitro* assays (Canesi et al., 2017). Hemocytes freshly isolated from adult mussels can be maintained in different media (artificial seawater, salt-enriched culture medium or hemolymph serum) for some hours, without impacting cell survival and biochemical/ functional features (Auguste et al., 2022b). In particular, in isolated mussel hemocytes, the utilization of a battery of immune-related biomarkers has proven useful in the evaluation of the effects of different bacterial strains (Destoumieux-Garzón et al., 2020). These studies underlined how mussel hemocytes represent a

sensitive target for different bacteria and their potential application as a starting point to more accurately design further studies that are relevant at the whole animal level.

Freshly isolated hemocytes are therefore commonly utilized as a model for *in vitro* experiments on mussel immunity studies. Hemolymph is extracted from the posterior adductor muscle of adult mussels under sterile conditions and kept at 18°C. Hemolymph and hemocytes, alone or in combination, are then exposed for a short time to bacterial suspensions (from 15 min to 2 h). Functional parameters such as lysosomal membrane stability (LMS) and phagocytic activity can be assessed directly on hemocyte monolayers by adding the bacterial suspension on the cells. Other parameters, including lysozyme activity, extracellular ROS and NO production are evaluated in serum. For these analyses, aliquots of whole hemolymph are incubated with bacterial suspensions for different periods of time (ranging from 0 to 90/120 min, according to the endpoint). At the end of the incubation, samples are centrifuged at 100 x g for 10 min and the supernatant collected for subsequent analyses.

Interactions between *M. galloprovincialis* and heat-killed and live suspensions of *V. tasmaniensis* LGP32, isolated from moribund *M. gigas* oysters (Gay et al., 2004a) (previously: *V. splendidus* LGP32) at 10^7 CFU/mL have been investigated *in vitro* (Balbi et al., 2013; Ciacci et al., 2010). Short- term exposure showed that both bacterial suspensions induced strong lysosomal destabilization, assessed by lysosomal membrane stability (LMS), a core cellular stress biomarker (OSPAR Commission, 2013). Notably, live bacterial suspension caused a stronger effect, with up to an 80% of reduction in LMS. Both suspensions induced persistent lysozyme release, and heat-killed bacteria stimulated also extracellular ROS and NO production. These responses were associated with persistent activation of the stress-related kinases p38 MAPK and protein kinase C (PKC), two highly conservated signaling molecules. Although analyses by transmission electron microscopy (TEM) further revealed rapid internalization of live *V. tasmaniensis* by hemocytes, *V. tasmaniensis* was able to survive within the hemocytes. These data demonstrated the existence of specific interactions between mussel hemocytes and *V. tasmaniensis* LGP32 and suggest that this strain is able to evade host bactericidal activity by disregulating immune signaling pathways (Balbi et al., 2013; Ciacci et al., 2010).

Stronger effects on lysosomal membrane stability were observed following *in vitro* exposure to live suspensions of *V. coralliilyticus* at the same bacterial concentration (10^7 CFU/mL) (Balbi et al., 2017).

V. corallyliticus has been described as an emerging pathogen for corals throughout the Indo-

Pacific reef, and responsible for oyster larval mortalities worldwide (Genard et al., 2013; Kesarcodi-Watson et al., 2012; Richards et al., 2015; Sussman et al., 2008; Y. and E., 2002). *In vitro* experiments showed a dose-dependent decrease in LMS. and no bacterial killing by hemocytes was observed. At lower concentrations (10^6 CFU/mL), no activation of immune parameters was observed in response to the challenge, except for an extremely rapid extracellular lysozyme release. At high concentrations (10^8 CFU/mL), *V. coralliilyticus* was cytotoxic (Balbi et al., 2017).

Environmental strains isolated from Adriatic Sea coastal areas - *V. parahaemolyticus* Conero, *V. alginolyticus* 1513, and *V. vulnificus* 509 - were tested, alongside *V. parahaemolyticus* ATCC 43996 as a reference strain, in short-term *in vitro* exposures at 10^7 CFU/mL (Balbi et al., 2017). The results revealed species- and strain-specific effects on hemocyte function : all strains stimulated extracellular lysozyme release, total ROS, O_2^- and NO production by hemocytes, but solely *V. parahaemolyticus* strains induced significant LMS decrease (- 40 % respect to the controls) and only *V. vulnificus* 509 induced dysregulation of the phosphorylation state of p38 MAP Kinase and of apoptotic processes. Overall, the results indicate that mussel hemocytes can mount an efficient immune response towards

V. parahaemolyticus and *V. alginolyticus* strains, whereas *V. vulnificus* 509 may affect the hemocyte function (Canesi et al., 2017). The results support the specificity of hemocyte immune responses to different vibrio species and strains.

Among *Vibrio* species associated with mollusk diseases, *V. tapetis* deserves particular attention. Approximately 40 strains of *V. tapetis* have been identified worldwide in mollusks and fish, with strain CECT4600 recognized as the causative agent of brown ring disease (BRD) in the Manila clam *Ruditapes philippinarum* (Paillard et al., 2008). *V. tapetis* strain LP2 was tested *in vitro* at 10^7 CFU/mL on mussel hemocytes (Balbi et al., 2017). The latter were unable to mount an efficient immune response towards this strain. Moreover, *V. tapetis* even reduced the basal ROS production, indicating impairment of the oxidative burst response, and was not killed by hemocytes even at low bacterial concentrations. However, *V. tapetis* induced a moderate lysosomal membrane destabilization (< 50%), corresponding to activation of the lysosomal machinery in response to mild stress conditions in the absence of cytotoxicity. Moreover, TEM observations showed that *V. tapetis* resulted in rapid formation of autophagosomes and autolysosomes (Balbi et al., 2017).

In addition to these coastal pathogens, the interaction between mussel hemocytes and bacteria from remote environments has also been investigated. A deep-sea bacterium, *V. bathopelagicus*, isolated from a remote Mediterranean bathypelagic site, was tested *in vitro* on mussel hemocytes at 10^7 CFU/mL (Lasa et al., 2021). Exposure resulted in a large decrease in LMS, even stronger than that of the bivalve pathogen *V. tasmaniensis* LGP32 (Balbi et al., 2013) and comparable to that of *V. coralliilyticus* (Balbi et al., 2019a). However, despite this pronounced cellular stress, data on bactericidal activity showed that mussel cells retained a significant and sustained ability to kill *V. bathopelagicus* over time (up to 60% of cells were killed after 60 min), indicating substantial recovery. Since evidence suggests that the external (non-host) environments might play a greater role in the evolution of certain pathogens and their virulence traits than previously thought (Hasan et al., 2015; Vezzulli et al., 2008), these findings emphasize the importance of investigating bacteria beyond those directly associated with disease outbreaks. Two deep-sea *Vibrio* strains collected hydrothermal vents in the Pacific Ocean, EPR225 and EPR117 (belonging to *V. alginolyticus* and *V. diabolicus* clades, respectively) were tested in *in vitro* assay on mussel hemocytes at 10^7 CFU/mL. The results showed how *in vitro* challenge of EPRs elicits a strong cellular stress, the LMS reduction induced by the EPR strains was comparable, if not greater, to *V. tasmaniensis* (Balbi et al., 2013; Lasa et al., 2021). Data on bactericidal activity indicated that hemocytes were not able to recognize and kill EPR strains efficiently (Bosi et al., 2024).

The interactions of mussel immune system with other bacteria not belonging to *Vibrio* species have been also investigated. *Arcobacter-like species*, emerging foodborne zoonotic pathogens in humans and animals, are frequently detected in diseased oysters and stressed bivalve species, and poor data are available so far on its potential pathogenicity or interactions with the immune system of the bivalve host. (Auguste et al., 2022b) evaluated the responses of *M. galloprovincialis* to two *Malaciobacter marinus* strains (IRTA-19-131 and IRTA-19-132; final concentration 10^7 CFU/mL), isolated from *M. gigas* during a mortality event occurred in 2019 in Spain. Both strains decreased hemocyte LMS and stimulated extracellular ROS production and lysozyme activity. *In vitro* assays with strain R1 showed reduced LMS, lysosomal enlargement, increased extracellular ROS and lysozyme release, and evidence of phagocytosis supported by changes in mTOR and LC3 activation. Hemolymph exhibited significant bactericidal activity, largely mediated by serum components.

Actually, mussel hemolymph serum factors have been shown to play a crucial role in

determining the outcome of immune response towards certain bacteria. Studies involving *Vibrio cholerae* O1 El Tor, the etiological agent of the seventh cholera pandemic, and *Escherichia coli* Mg1655, used as a model for enteric bacteria, showed that *M. galloprovincialis* hemolymph serum promotes D-mannose- sensitive (MS) adhesion and killing by mussel hemocytes of these bacteria. This effect depends on the presence on the bacterial surface of MS adhesins, i.e., the MS hemagglutinin (MSHA) pilus that is present in *V. cholerae* O1 El Tor strains, and type 1 fimbriae expressed by *E. coli* strains and other enteric bacteria including pathogenic strains (e.g*., Salmonella spp*.) (Canesi et al., 2016).

The importance of these opsonin-mediated interactions was highlighted by studies on *V. aestuarianus* 01/032, a strain isolated from oyster mortality outbreaks (Balbi et al., 2013). *In vitro* challenge (10^7 CFU/mL) did not induce strong lysosomal stress in hemocytes or significant lysozyme release. TEM analyses showed rapid internalization of 01/032, consistent with the observed high bacterial killing capacity of hemocytes. These findings were supported by the presence of extrapallial protein (EP) in serum of *M. galloprovincialis* (MgEP), which promotes hemocyte adhesion to and killing of *V. aestuarianus* 01/032 through D-mannose sensitive (MS) interactions of the strain with the hemocytes. MgEP is absent in oyster hemolymph, suggesting that the differential sensitivity of strains, such as 01/032, to the antibacterial activity of oyster and mussel hemolymph, may partly depend on the lack of MgEP-like opsonins in *M. gigas* serum (Balbi et al., 2013). The role of MgEP in adhesion and killing of other bacteria carrying MS sensitive ligands was investigated. Purified MgEP enhanced adhesion to and killing by hemocytes of *V. cholerae* ElTor N16961, as well as of *E. coli* MG1655. These results further support that the multifunctional MgEP also acts as an opsonin involved in mussel defense towards bacteria carrying MSHA ligands (Canesi et al., 2016).

6.2 *In vivo* experiments

In vivo experiments are essential for studying mussel immunity because they can capture the full biological complexity that cannot be reproduced in isolated systems, and represent a more realistic host-pathogen interaction scenario. The most utilized infection method is by injecting directly the bacterial suspensions into hemolymph sinus of the posterior abductor muscle. Since a large number of studies are available using this approach (a search for 'Mytilus bacteria injection' gave over 40 hits on PUBMED), few representative examples are reported here of functional immune responses of *M. galloprovincialis* to bacterial challenge.

Injection with *V. tasmaniensis* LGP32 and *V. aestuarianus* 01/032 (10^7 CFU/mL final

concentration) induced transient decreases in hemocyte LMS, with total destabilization for *V. tasmaniensis* and approximately 80% for *V. aestuarianus* 01/032 at 24 h post injection (p.i.), followed by complete recovery after 96 h p.i. for both strains. Progressive increases in serum lysozyme activity were observed, with *V. tasmaniensis* > *V. aestuarianus*. Moreover, whereas *V. aestuarianus* was efficiently cleared from hemolymph, *V. tasmaniensis* showed significant growth, that was maximal at 24 h p.i. when lowest LMS values were recorded in the hemocytes (Balbi et al., 2013).

Injection of *V. coralliilyticus* at a lower concentration (10^6 CFU/mL) caused a weaker LMS reduction (about 23 %) 24 h p.i. and no activation of other immune parameters. Similar to *V. tasmaniensis*, bacterial loads in hemolymph increased markedly after 24 h p.i., indicating that *V. coralliilyticus* can proliferate within the hemolymph (Balbi et al., 2019a)(Balbi et al., 2019).

In contrast, responses to challenge with *M. marinus* (10^6 CFU/mL in hemolymph) at 24 h p.i. showed that this strain induced strong lysosomal stress in hemocytes (evaluated as a decrease in LMS, around 60 %), but also a large stimulation of extracellular defenses (ROS production and lysozyme activity) was observed, indicating that hemolymph components of adult mussels are able to mount an efficient defense response against *M. marinus* infection (Auguste et al., 2022b).

In vivo injection experiments are also widely utilised in transcriptomic studies. For example, the effects of *V. tasmaniensis* LGP32 on hemocyte gene expression were also investigated (Rey-Campos et al., 2019). Mussels were injected with a non-lethal concentration of *V. splendidus* LGP32 (100 µL of 1×10^7 CFU/mL). Total clearance of the injected bacteria was observed 7 days p.i.. A total of 1,216 differentially expressed genes (DEGs) were detected at 24 hpi, most of them were related to the immune system, such as those regulating pathogen recognition, cell migration and pro-inflammatory response. After the first exposure, several genes showed high expression values and were significantly decreased after 7 days. This was the case for perlucin-like protein, which is directly involved in pathogen recognition, the spore cortex-lytic enzyme, which can destroy the bacterial cell wall, and the henna protein, which is important for melanization; all of these genes could play crucial roles in the killing and sequestration of invading pathogens (Rey-Campos et al., 2019).

A different *in vivo* approach involves injection–cohabitation models to study horizontal transmission of bacteria from infected (donors) to non-infected (recipients) individuals. Ben Cheikh et al., 2017 tested *V. splendidus* 10/068 1T1, a strain of the *Splendidus* clade, isolated

from mortality events affecting *M. edulis*. To better investigate infection dynamics and potential horizontal transfer, they injected donors with *V. splendidus* 10/068 1T1 GFP-tagged (10^6 CFU/mL). The injection- cohabitation experiment revealed successful transmission of *V. splendidus* from donors to recipients through seawater. Moreover, colonization of hemocytes and multiple tissue necrosis, particularly in gills, were observed in donors.

Another *in vivo* approach is represented by the bath (waterborne) infection model, which consists in spiking the bacterial suspensions directly into the tank water to mimic a more environmentally realistic exposure scenario. Romero et al., 2014 utilized this approach to investigate the pathogenicity of different isolates of *V. splendidus* and *V. aestuarianus* in mussels under different environmental conditions. Temperature changes and hypoxic stress were included to simulate environmental changes potentially en implicated in bivalve deaths. The results showed that mortality only occurred when animals were infected with a high concentration of bacteria (10^{11} CFU/mL) in adverse environmental conditions (hypoxia and 25 °C). This result reflects the extreme resistance of mussels to the bacterial pathogens tested.

Using a bath experiment set up, Saco et al., 2020 investigated the role of gills in response to bacterial infection. After the bath infection with *V. splendidus* LGP32 at 10^8 CFU/mL final concentration r, mussels were able to remove the bacteria from their bodies and from the water tank. Accordingly, antibacterial activity was detected in gill extracts, demonstrating that this tissue plays a central role in removing and clearing potential pathogens. A transcriptomic study, performed after the bath infection, identified a total of 1,156 differentially expressed genes. The expression levels of genes contributing to a number of biological processes, such as immune response activation pathways and their regulation with cytokines, cell recognition, adhesion and apoptosis, were significantly modulated after infection, suggesting that the gills play important roles in pathogen recognition, as well as being activators and regulators of the mussel innate immune response. When the transcriptomic response of gills after bath infection was compared with that previously observed in hemocytes after injection with the same strain (Rey-Campos et al., 2019), the results indicate that recognition processes of waterborne first occur in the gills, thereby activating the effector agents of the immune response (Saco et al., 2020).

Overall, an understanding of the complexity of signals and responses between bacteria and mussel immune system obviously requires more detailed analyses of the multiple interactions occurring between these bacteria and not only hemocytes, but other mussel cells and tissues.

Moreover, a complete description of the environment in which these interactions occur and a study of its influence on bivalve health status are also necessary for elucidating how these processes develop and persist in natural conditions.

Finally, it is widely demonstrated that health status of mussels shows seasonal fluctuations driven by the complex interactions between natural environmental factors (temperature, salinity, food availability, etc.) and endogenous factors (sex, age, gametogenic stage) (Balbi et al., 2017; Jarque et al., 2014; Wathsala et al., 2021). Gametogenesis is influenced by different environmental factors, and it is likely subject to a year to year variability, mainly depending on temperature and food availability. In particular, warmer temperatures reduce rates of gametogenesis in *M. galloprovincialis* (Fearman and Moltschaniwskyj, 2010). The reproductive effort, which usually occurs during winter months, has a strong effect on mussel physiology (Balbi et al., 2017).

Overall, both *in vitro* and *in vivo* studies revealed how the immune response of mussel to bacterial challenge can be both species- and strain specific. These studies contribute to understand not only the interactions between mussel immune system and bacteria, but also to predict the potential pathogenicity of certain bacteria, or their opportunistic behaviour, depending on both environmental factors and physiological conditions.
In the context of global change, the environmental impact on sustainability of mussel aquaculture production is raising particular concerns. Understanding how mussel can respond to the challenge with different types of bacteria in a seasonal framework is therefore essential for future prediction of further potential impacts in changing environmental conditions.

References

Allam, B., Pales Espinosa, E., 2016. Bivalve immunity and response to infections: Are we looking at the right place? Fish & Shellfish Immunology 53, 4–12. https://doi.org/10.1016/j.fsi.2016.03.037

Allam, B., Raftos, D., 2015. Immune responses to infectious diseases in bivalves. Journal of Invertebrate Pathology 131, 121–136. https://doi.org/10.1016/j.jip.2015.05.005

Arfatahery N, Rafaluk C, Rolff J, Wegner KM. Evidence for immune priming specificity and cross-protection against sympatric and allopatric Vibrio splendidus strains in the oyster Magalana (Crassostrea) gigas. Dev Comp Immunol. 2024 Oct;159:105221. doi: 10.1016/j.dci.2024.105221. Epub 2024 Jun 24. PMID: 38925430.

Auguste, M., Lasa, A., Balbi, T., Pallavicini, A., Vezzulli, L., Canesi, L., 2020. Impact of nanoplastics on hemolymph immune parameters and microbiota composition in Mytilus galloprovincialis. Marine Environmental Research 159, 105017. https://doi.org/10.1016/j.marenvres.2020.105017

Auguste M, Balbi T, Ciacci C, Canonico B, Papa S, Borello A, Vezzulli L and Canesi L (2020) Shift in Immune Parameters After Repeated Exposure to Nanoplastics in the Marine Bivalve Mytilus. Front. Immunol. 11:426. doi: 10.3389/fimmu.2020.00426

Auguste, M., Lasa, A., Pallavicini, A., Gualdi, S., Vezzulli, L., Canesi, L., 2019. Exposure to TiO2 nanoparticles induces shifts in the microbiota composition of Mytilus galloprovincialis hemolymph. Science of The Total Environment 670, 129–137. https://doi.org/10.1016/j.scitotenv.2019.03.133

Auguste, M., Leonessi, M., Balbi, T., Doni, L., Oliveri, C., Vezzulli, L., Canesi, L., 2024a. Seasonal fluctuations of hemolymph microbiota and immune parameters in Mytilus galloprovincialis farmed at La Spezia, Italy. Aquaculture 578, 740028. https://doi.org/10.1016/j.aquaculture.2023.740028

Auguste, M., Leonessi, M., Balbi, T., Doni, L., Oliveri, C., Vezzulli, L., Canesi, L., 2024b. Seasonal fluctuations of hemolymph microbiota and immune parameters in Mytilus galloprovincialis farmed at La Spezia, Italy. Aquaculture 578, 740028. https://doi.org/10.1016/j.aquaculture.2023.740028

Auguste, M., Leonessi, M., Bozzo, M., Risso, B., Cutroneo, L., Prandi, S., Kokalj, A.J., Drobne, D., Canesi, L., 2023. Multiple responses of Mytilus galloprovincialis to plastic microfibers. Science of The Total Environment 890, 164318. https://doi.org/10.1016/j.scitotenv.2023.164318

Auguste, M., Melillo, D., Corteggio, A., Marino, R., Canesi, L., Pinsino, A., Italiani, P., Boraschi, D., 2022a. Methodological Approaches To Assess Innate Immunity and Innate Memory in Marine Invertebrates and Humans. Front. Toxicol. 4, 842469. https://doi.org/10.3389/ftox.2022.842469

Auguste, M., Rahman, F.U., Balbi, T., Leonessi, M., Oliveri, C., Bellese, G., Vezzulli, L., Furones, D., Canesi, L., 2022b. Responses of Mytilus galloprovincialis to challenge with environmental isolates of the potential emerging pathogen Malaciobacter marinus. Fish & Shellfish Immunology 131, 1–9. https://doi.org/10.1016/j.fsi.2022.09.048

Azéma, P., Lamy, J.-B., Boudry, P., Renault, T., Travers, M.-A., Dégremont, L., 2017. Genetic parameters of resistance to Vibrio aestuarianus, and OsHV-1 infections in the Pacific oyster, Crassostrea gigas, at three different life stages. Genet Sel Evol 49, 23. https://doi.org/10.1186/s12711-017-0297-2

Azizan, A., Alfaro, A.C., Jaramillo, D., Venter, L., Young, T., Frost, E., Lee, K., Van Nguyen, T., Kitundu, E., Archer, S.D.J., Ericson, J.A., Foxwell, J., Quinn, O., Ragg, N.L.C., 2022.

Pathogenicity and virulence of bacterial strains associated with summer mortality in marine mussels (*Perna canaliculus*). FEMS Microbiology Ecology 98, fiac140. https://doi.org/10.1093/femsec/fiac140

Azizan, A., Venter, L., Alfaro, A.C., 2024. Biomarkers of mussel exposure to Vibrionaceae: A review. Aquacult Int 32, 7595–7627. https://doi.org/10.1007/s10499-024-01531-2

Baker-Austin, C., Lake, I., Archer, E., Hartnell, R., Trinanes, J., Martinez-Urtaza, J., 2024. Stemming the rising tide of Vibrio disease. The Lancet Planetary Health 8, e515–e520. https://doi.org/10.1016/S2542-5196(24)00124-4

Balbi, T., Auguste, M., Ciacci, C., Canesi, L., 2021. Immunological Responses of Marine Bivalves to Contaminant Exposure: Contribution of the -Omics Approach. Front. Immunol. 12, 618726. https://doi.org/10.3389/fimmu.2021.618726

Balbi, T., Auguste, M., Cortese, K., Montagna, M., Borello, A., Pruzzo, C., Vezzulli, L., Canesi, L., 2019a. Responses of Mytilus galloprovincialis to challenge with the emerging marine pathogen Vibrio coralliilyticus. Fish & Shellfish Immunology 84, 352–360. https://doi.org/10.1016/j.fsi.2018.10.011

Balbi, T., Ciacci, C., Canesi, L., 2019b. Estrogenic compounds as exogenous modulators of physiological functions in molluscs: Signaling pathways and biological responses. Comparative Biochemistry and Physiology Part C: Toxicology & Pharmacology 222, 135–
144. https://doi.org/10.1016/j.cbpc.2019.05.004

Balbi, T., Cortese, K., Ciacci, C., Bellese, G., Vezzulli, L., Pruzzo, C., Canesi, L., 2018. Autophagic processes in Mytilus galloprovincialis hemocytes: Effects of Vibrio tapetis. Fish & Shellfish Immunology 73, 66–74. https://doi.org/10.1016/j.fsi.2017.12.003

Balbi, T., Fabbri, R., Cortese, K., Smerilli, A., Ciacci, C., Grande, C., Vezzulli, L., Pruzzo, C., Canesi, L., 2013. Interactions between Mytilus galloprovincialis hemocytes and the bivalve pathogens Vibrio aestuarianus 01/032 and Vibrio splendidus LGP32. Fish & Shellfish Immunology 35, 1906–1915. https://doi.org/10.1016/j.fsi.2013.09.027

Balbi, T., Fabbri, R., Montagna, M., Camisassi, G., Canesi, L., 2017. Seasonal variability of different biomarkers in mussels (Mytilus galloprovincialis) farmed at different sites of the Gulf of La Spezia, Ligurian sea, Italy. Marine Pollution Bulletin 116, 348–356. https://doi.org/10.1016/j.marpolbul.2017.01.035

Balseiro, P., Falcó, A., Romero, A., Dios, S., Martínez-López, A., Figueras, A., Estepa, A., Novoa, B., 2011. Mytilus galloprovincialis Myticin C: A Chemotactic Molecule with Antiviral Activity and Immunoregulatory Properties. PLoS ONE 6, e23140. https://doi.org/10.1371/journal.pone.0023140

Barbosa Solomieu, V., Renault, T., Travers, M.-A., 2015. Mass mortality in bivalves and the intricate case of the Pacific oyster, Crassostrea gigas. Journal of Invertebrate Pathology 131, 2–10. https://doi.org/10.1016/j.jip.2015.07.011

Beaz-Hidalgo, R., Balboa, S., Romalde, J.L., Figueras, M.J., 2010. Diversity and pathogenecity of *Vibrio* species in cultured bivalve molluscs. Environ Microbiol Rep 2, 34–43. https://doi.org/10.1111/j.1758-2229.2010.00135.x

Ben Cheikh, Y., Massol, F., Giusti-Petrucciani, N., Travers, M.-A., 2024. Impact of epizootics on mussel farms: Insights into microbiota composition of Mytilus species. Microbiological Research 280, 127593. https://doi.org/10.1016/j.micres.2023.127593

Ben Cheikh, Y., Travers, M.A., 2022. Vibrio splendidus infection induces dysbiosis in the blue mussel and favors pathobiontic bacteria. Microbiological Research 261, 127078. https://doi.org/10.1016/j.micres.2022.127078

Ben Cheikh, Y., Travers, M.-A., Le Foll, F., 2017. Infection dynamics of a V. splendidus strain pathogenic to Mytilus edulis: In vivo and in vitro interactions with hemocytes. Fish & Shellfish Immunology 70, 515–523. https://doi.org/10.1016/j.fsi.2017.09.047

Benabdelmouna, A., Garcia, C., Ledu, C., Lamy, P., Maurouard, E., Dégremont, L., 2018. Mortality investigation of Mytilus edulis and Mytilus galloprovincialis in France: An experimental survey under laboratory conditions. Aquaculture 495, 831–841. https://doi.org/10.1016/j.aquaculture.2018.06.075

Beyer, J., Green, N.W., Brooks, S., Allan, I.J., Ruus, A., Gomes, T., Bråte, I.L.N., Schøyen, M., 2017. Blue mussels (Mytilus edulis spp.) as sentinel organisms in coastal pollution monitoring: A review. Marine Environmental Research 130, 338–365. https://doi.org/10.1016/j.marenvres.2017.07.024

Bosi, E., Taviani, E., Avesani, A., Doni, L., Auguste, M., Oliveri, C., Leonessi, M., Martinez-Urtaza, J., Vetriani, C., Vezzulli, L., 2024. Pan-Genome Provides Insights into *Vibrio* Evolution and Adaptation to Deep-Sea Hydrothermal Vents. Genome Biology and Evolution 16, evae131. https://doi.org/10.1093/gbe/evae131

Bouallegui, Y., 2019. Immunity in mussels: An overview of molecular components and mechanisms with a focus on the functional defenses. Fish & Shellfish Immunology 89, 158–169. https://doi.org/10.1016/j.fsi.2019.03.057

Bownes, S.J., McQuaid, C.D., 2006. Will the invasive mussel Mytilus galloprovincialis Lamarck replace the indigenous Perna perna L. on the south coast of South Africa? Journal of Experimental Marine Biology and Ecology 338, 140–151. https://doi.org/10.1016/j.jembe.2006.07.006

Bracchetti, L., Capriotti, M., Fazzini, M., Cocci, P., Palermo, F.A., 2024a. Mass Mortality Event of Mediterranean Mussels (Mytilus galloprovincialis) in the Middle Adriatic: Potential Implications of the Climate Crisis for Marine Ecosystems. Diversity 16, 130. https://doi.org/10.3390/d16030130

Bracchetti, L., Capriotti, M., Fazzini, M., Cocci, P., Palermo, F.A., 2024b. Mass Mortality Event of Mediterranean Mussels (Mytilus galloprovincialis) in the Middle Adriatic: Potential Implications of the Climate Crisis for Marine Ecosystems. Diversity 16, 130. https://doi.org/10.3390/d16030130

Burgos-Aceves, M.A., Faggio, C., 2017. An approach to the study of the immunity functions of bivalve haemocytes: Physiology and molecular aspects. Fish & Shellfish Immunology 67, 513–517. https://doi.org/10.1016/j.fsi.2017.06.042

Canesi, L., Auguste, M., Balbi, T., Prochazkova, P., 2022. Soluble mediators of innate immunity in annelids and bivalve mollusks: A mini-review. Front. Immunol. 13, 1051155. https://doi.org/10.3389/fimmu.2022.1051155

Canesi, L., Ciacci, C., Balbi, T., 2017. Invertebrate Models for Investigating the Impact of Nanomaterials on Innate Immunity: The Example of the Marine Mussel Mytilus spp. CBNT 2, 77–83. https://doi.org/10.2174/2213529402666160601102529

Canesi, L., Gallo, G., Gavioli, M., Pruzzo, C., 2002a. Bacteria–hemocyte interactions and phagocytosis in marine bivalves. Microscopy Res & Technique 57, 469–476. https://doi.org/10.1002/jemt.10100

Canesi, L., Gallo, G., Gavioli, M., Pruzzo, C., 2002b. Bacteria–hemocyte interactions and phagocytosis in marine bivalves. Microscopy Res & Technique 57, 469–476. https://doi.org/10.1002/jemt.10100

Canesi, L., Grande, C., Pezzati, E., Balbi, T., Vezzulli, L., Pruzzo, C., 2016. Killing of Vibrio cholerae and Escherichia coli Strains Carrying D-mannose-sensitive Ligands by Mytilus Hemocytes is Promoted by a Multifunctional Hemolymph Serum Protein. Microb Ecol 72, 759–762. https://doi.org/10.1007/s00248-016-0757-1

Canesi, L., Pruzzo, C., 2016. Chapter 6 - Specificity of Innate Immunity in Bivalves: A Lesson From Bacteria, in: Ballarin, L., Cammarata, M. (Eds.), Lessons in Immunity. Academic Press, pp. 79–91. https://doi.org/10.1016/B978-0-12-803252-7.00006-0

Capelle, J.J., Garcia, A.B., Kamermans, P., Engelsma, M.Y., Jansen, H.M., 2021. Observations on recent mass mortality events of marine mussels in the Oosterschelde, the Netherlands. Aquacult Int 29, 1737–1751. https://doi.org/10.1007/s10499-021-00713-6

Carrasco, N., Gairin, I., Pérez, J., Andree, K.B., Roque, A., Fernández-Tejedor, M., Rodgers, C.J., Aguilera, C., Furones, M.D., 2017. A Production Calendar Based on Water Temperature, Spat Size, and Husbandry Practices Reduce OsHV-1 µvar Impact on Cultured Pacific Oyster Crassostrea gigas in the Ebro Delta (Catalonia), Mediterranean Coast of Spain. Front. Physiol. 8. https://doi.org/10.3389/fphys.2017.00125

Ceccarelli, D., Amaro, C., Romalde, J.L., Suffredini, E., Vezzulli, L., 2019. *Vibrio Species*, in: Doyle, M.P., Diez-Gonzalez, F., Hill, C. (Eds.), Food Microbiology. ASM Press, Washington, DC, USA, pp. 347–388. https://doi.org/10.1128/9781555819972.ch13

Charles, M., Bernard, I., Villalba, A., Oden, E., Burioli, E.A.V., Allain, G., Trancart, S., Bouchart, V., Houssin, M., 2020a. High mortality of mussels in northern Brittany – Evaluation of the involvement of pathogens, pathological conditions and pollutants. Journal of Invertebrate Pathology 170, 107308. https://doi.org/10.1016/j.jip.2019.107308

Charles, M., Trancart, S., Oden, E., Houssin, M., 2020b. Experimental infection of *Mytilus edulis* by two *Vibrio splendidus* -related strains: Determination of pathogenicity level of strains and influence of the origin and annual cycle of mussels on their sensitivity. Journal of Fish Diseases 43, 9–21. https://doi.org/10.1111/jfd.13094

Ciacci, C., Betti, M., Canonico, B., Citterio, B., Roch, P., Canesi, L., 2010. Specificity of anti-Vibrio immune response through p38 MAPK and PKC activation in the hemocytes of the mussel Mytilus galloprovincialis. Journal of Invertebrate Pathology 105, 49–55. https://doi.org/10.1016/j.jip.2010.05.010

Ciacci, C., Manti, A., Canonico, B., Campana, R., Camisassi, G., Baffone, W., Canesi, L., 2017. Responses of Mytilus galloprovincialis hemocytes to environmental strains of Vibrio parahaemolyticus, Vibrio alginolyticus, Vibrio vulnificus. Fish & Shellfish Immunology 65, 80–87. https://doi.org/10.1016/j.fsi.2017.04.002

Cohen, R., James, C., Lee, A., Martinelli, M., Muraoka, W., Ortega, M., Sadowski, R., Starkey, L., Szesciorka, A., Timko, S., Weiss, E., Franks, P., 2018. Marine Host-Pathogen Dynamics: Influences of Global Climate Change. Oceanog 31. https://doi.org/10.5670/oceanog.2018.201

Costa, M.M., Prado-Alvarez, M., Gestal, C., Li, H., Roch, P., Novoa, B., Figueras, A., 2009. Functional and molecular immune response of Mediterranean mussel (Mytilus galloprovincialis) haemocytes against pathogen-associated molecular patterns and bacteria. Fish & Shellfish Immunology 26, 515–523. https://doi.org/10.1016/j.fsi.2009.02.001

Curpan, A.-S., Impellitteri, F., Plavan, G., Ciobica, A., Faggio, C., 2022. Review: Mytilus galloprovincialis: An essential, low-cost model organism for the impact of xenobiotics on oxidative stress and public health. Comparative Biochemistry and Physiology Part C: Toxicology & Pharmacology 256, 109302. https://doi.org/10.1016/j.cbpc.2022.109302

Dagnino, A., Allen, J.I., Moore, M.N., Broeg, K., Canesi, L., Viarengo, A., 2007. Development of an expert system for the integration of biomarker responses in mussels into an animal health index. Biomarkers 12, 155–172. https://doi.org/10.1080/13547500601037171

De La Ballina, N.R., Maresca, F., Cao, A., Villalba, A., 2022. Bivalve Haemocyte Subpopulations: A Review. Front. Immunol. 13, 826255.

https://doi.org/10.3389/fimmu.2022.826255
De San Nicolas, N., Asokan, A., Rosa, R., Voisin, S., Travers, M.-A., Rocha, G., Dantan, L., Dorant, Y., Mitta, G., Petton, B., Charrière, G., Escoubas, J.-M., Boulo, V., Pouzadoux, J., Meudal, H., Loth, K., Aucagne, V., Delmas, A., Bulet, P., Montagnani, C., Destoumieux-Garzón, D., 2022. Functional Diversification of Oyster Big Defensins Generates Antimicrobial Specificity and Synergy against Members of the Microbiota. Marine Drugs 20, 745. https://doi.org/10.3390/md20120745
De Schryver, P., Vadstein, O., 2014. Ecological theory as a foundation to control pathogenic invasion in aquaculture. The ISME Journal 8, 2360–2368. https://doi.org/10.1038/ismej.2014.84
Desriac, F., Le Chevalier, P., Brillet, B., Leguerinel, I., Thuillier, B., Paillard, C., Fleury, Y., 2014. Exploring the hologenome concept in marine bivalvia: haemolymph microbiota as a pertinent source of probiotics for aquaculture. FEMS Microbiol Lett 350, 107–116. https://doi.org/10.1111/1574-6968.12308
Destoumieux-Garzón, D., Canesi, L., Oyanedel, D., Travers, M., Charrière, G.M., Pruzzo, C., Vezzulli, L., 2020. *Vibrio* –bivalve interactions in health and disease. Environmental Microbiology 22, 4323–4341. https://doi.org/10.1111/1462-2920.15055
Destoumieux-Garzón, D., Montagnani, C., Dantan, L., Nicolas, N.D.S., Travers, M.-A., Duperret, L., Charrière, G.M., Toulza, E., Mitta, G., Cosseau, C., Escoubas, J.-M., 2024. Cross-talk
and mutual shaping between the immune system and the microbiota during an oyster's life. Phil. Trans. R. Soc. B 379, 20230065. https://doi.org/10.1098/rstb.2023.0065
Doney, S.C., Busch, D.S., Cooley, S.R., Kroeker, K.J., 2020. The Impacts of Ocean Acidification on Marine Ecosystems and Reliant Human Communities. Annu. Rev. Environ. Resour. 45, 83–112. https://doi.org/10.1146/annurev-environ-012320-083019
Eggermont, M., Tamanji, A., Nevejan, N., Bossier, P., Sorgeloos, P., Defoirdt, T., 2014. Stimulation of heterotrophic bacteria associated with wild-caught blue mussel (Mytilus edulis) adults results in mass mortality. Aquaculture 431, 136–138. https://doi.org/10.1016/j.aquaculture.2014.01.014
European Climate, Infrastructure and Environment Executive Agency (Ed.), 2023. EU aquaculture sector: socioeconomic development (2008-2020). Publications Office, Luxembourg. https://doi.org/10.2926/34713
FAO (Ed.), 2018. Meeting the sustainable development goals, The state of world fisheries and aquaculture. Rome.
FAO's work on climate change - Fisheries and aquaculture 2020, 2021. . FAO. https://doi.org/10.4060/cb3414en
Fearman, J., Moltschaniwskyj, N.A., 2010. Warmer temperatures reduce rates of gametogenesis in temperate mussels, Mytilus galloprovincialis. Aquaculture 305, 20–25. https://doi.org/10.1016/j.aquaculture.2010.04.003
Figueras, A., 2019. Genomics and immunity of the Mediterranean mussel Mytilus galloprovincialis in a changing environment.
Fraune, S., Bosch, T.C.G., 2010. Why bacteria matter in animal development and evolution. BioEssays 32, 571–580. https://doi.org/10.1002/bies.200900192
García-García, E., Prado-Álvarez, M., Novoa, B., Figueras, A., Rosales, C., 2008. Immune responses of mussel hemocyte subpopulations are differentially regulated by enzymes of the PI 3-K, PKC, and ERK kinase families. Developmental & Comparative Immunology 32, 637–653. https://doi.org/10.1016/j.dci.2007.10.004
Garnier, M., Labreuche, Y., Garcia, C., Robert, M., Nicolas, J.-L., 2007. Evidence for the Involvement of Pathogenic Bacteria in Summer Mortalities of the Pacific Oyster Crassostrea gigas. Microb Ecol 53, 187–196. https://doi.org/10.1007/s00248-006-9061-

9
Garnier, M., Labreuche, Y., Nicolas, J.-L., 2008. Molecular and phenotypic characterization of Vibrio aestuarianus subsp. francensis subsp. nov., a pathogen of the oyster Crassostrea gigas. Systematic and Applied Microbiology 31, 358–365. https://doi.org/10.1016/j.syapm.2008.06.003
Gay, M., Berthe, F., Le Roux, F., 2004a. Screening of Vibrio isolates to develop an experimental infection model in the Pacific oyster Crassostrea gigas. Dis. Aquat. Org. 59, 49–56. https://doi.org/10.3354/dao059049
Gay, M., Berthe, F., Le Roux, F., 2004b. Screening of Vibrio isolates to develop an experimental infection model in the Pacific oyster Crassostrea gigas. Dis. Aquat. Org. 59, 49–56. https://doi.org/10.3354/dao059049
Genard, B., Miner, P., Nicolas, J.-L., Moraga, D., Boudry, P., Pernet, F., Tremblay, R., 2013. Integrative Study of Physiological Changes Associated with Bacterial Infection in Pacific Oyster Larvae. PLoS ONE 8, e64534. https://doi.org/10.1371/journal.pone.0064534
Gerdol, M., De Moro, G., Manfrin, C., Venier, P., Pallavicini, A., 2012. Big defensins and mytimacins, new AMP families of the Mediterranean mussel Mytilus galloprovincialis. Developmental & Comparative Immunology 36, 390–399. https://doi.org/10.1016/j.dci.2011.08.003
Gerdol, M., Gomez-Chiarri, M., Castillo, M.G., Figueras, A., Fiorito, G., Moreira, R., Novoa, B., Pallavicini, A., Ponte, G., Roumbedakis, K., Venier, P., Vasta, G.R., 2018. Immunity in Molluscs: Recognition and Effector Mechanisms, with a Focus on Bivalvia, in: Cooper, E.L. (Ed.), Advances in Comparative Immunology. Springer International Publishing, Cham, pp. 225–341. https://doi.org/10.1007/978-3-319-76768-0_11
Gerdol, M., Moreira, R., Cruz, F., Gómez-Garrido, J., Vlasova, A., Rosani, U., Venier, P., Naranjo- Ortiz, M.A., Murgarella, M., Greco, S., Balseiro, P., Corvelo, A., Frias, L., Gut, M., Gabaldón, T., Pallavicini, A., Canchaya, C., Novoa, B., Alioto, T.S., Posada, D., Figueras, A., 2020. Massive gene presence-absence variation shapes an open pan-genome in the Mediterranean mussel. Genome Biol 21, 275. https://doi.org/10.1186/s13059-020-02180-3
Gerdol, M., Pallavicini, A., 2025. Exploring the immune resilience of Mediterranean mussels: Recent advances and future directions. Fish & Shellfish Immunology 158, 110147. https://doi.org/10.1016/j.fsi.2025.110147
Gerdol, M., Venier, P., 2015. An updated molecular basis for mussel immunity. Fish & Shellfish Immunology 46, 17–38. https://doi.org/10.1016/j.fsi.2015.02.013
Gestal, C., Pallavicini, A., Venier, P., Novoa, B., Figueras, A., 2010. MgC1q, a novel C1q-domain-containing protein involved in the immune response of Mytilus galloprovincialis. Developmental & Comparative Immunology 34, 926–934. https://doi.org/10.1016/j.dci.2010.02.012
Gignoux-Wolfsohn, S., Garcia Ruiz, M., Portugal Barron, D., Ruiz, G., Lohan, K., 2024. Bivalve microbiomes are shaped by host species, size, parasite infection, and environment. PeerJ 12, e18082. https://doi.org/10.7717/peerj.18082
Glasl, B., Herndl, G.J., Frade, P.R., 2016. The microbiome of coral surface mucus has a key role in mediating holobiont health and survival upon disturbance. The ISME Journal 10, 2280– 2292. https://doi.org/10.1038/ismej.2016.9
Gosling, E., 2015. Marine Bivalve Molluscs, 1st ed. Wiley. https://doi.org/10.1002/9781119045212
Gourbal B, Pinaud S, Beckers GJM, Van Der Meer JWM, Conrath U, Netea MG. Innate immune memory: An evolutionary perspective. Immunol Rev. 2018 May;283(1):21-40. doi: 10.1111/imr.12647. PMID: 29664574.
Green TJ, Speck P. Antiviral Defense and Innate Immune Memory in the Oyster. Viruses. 2018

Mar 16;10(3):133. doi: 10.3390/v10030133. PMID: 29547519; PMCID: PMC5869526.
Hasan, I., Sugawara, S., Fujii, Y., Koide, Y., Terada, D., Iimura, N., Fujiwara, T., Takahashi, K., Kojima, N., Rajia, S., Kawsar, S., Kanaly, R., Uchiyama, H., Hosono, M., Ogawa, Y., Fujita, H., Hamako, J., Matsui, T., Ozeki, Y., 2015. MytiLec, a Mussel R-Type Lectin, Interacts with Surface Glycan Gb3 on Burkitt's Lymphoma Cells to Trigger Apoptosis through Multiple Pathways. Marine Drugs 13, 7377–7389. https://doi.org/10.3390/md13127071
Hemraj, D.A., Russell, B.D., 2025. Consistency in marine heatwave experiments for ecological relevance and application: Key problems and solutions. Limnol Oceanogr Letters 10, 1–4. https://doi.org/10.1002/lol2.10418
Hobday, A.J., Alexander, L.V., Perkins, S.E., Smale, D.A., Straub, S.C., Oliver, E.C.J., Benthuysen, J.A., Burrows, M.T., Donat, M.G., Feng, M., Holbrook, N.J., Moore, P.J., Scannell, H.A., Sen Gupta, A., Wernberg, T., 2016. A hierarchical approach to defining marine heatwaves. Progress in Oceanography 141, 227–238. https://doi.org/10.1016/j.pocean.2015.12.014
Intergovernmental Panel On Climate Change (Ipcc), 2023. Climate Change 2021 – The Physical Science Basis: Working Group I Contribution to the Sixth Assessment Report of the Intergovernmental Panel on Climate Change, 1st ed. Cambridge University Press. https://doi.org/10.1017/9781009157896
Jarque, S., Prats, E., Olivares, A., Casado, M., Ramón, M., Piña, B., 2014. Seasonal variations of gene expression biomarkers in Mytilus galloprovincialis cultured populations: Temperature, oxidative stress and reproductive cycle as major modulators. Science of The Total Environment 499, 363–372. https://doi.org/10.1016/j.scitotenv.2014.08.064
Kesarcodi-Watson, A., Miner, P., Nicolas, J.-L., Robert, R., 2012. Protective effect of four potential probiotics against pathogen-challenge of the larvae of three bivalves: Pacific oyster (Crassostrea gigas), flat oyster (Ostrea edulis) and scallop (Pecten maximus). Aquaculture 344–349, 29–34. https://doi.org/10.1016/j.aquaculture.2012.02.029
Kurtz et al 2025 Trained immunity and immune priming in plants and invertebrates DOI: https://doi.org/10.7554/eLife.106597
Labreuche, Y., Le Roux, F., Henry, J., Zatylny, C., Huvet, A., Lambert, C., Soudant, P., Mazel, D., Nicolas, J.-L., 2010. Vibrio aestuarianus zinc metalloprotease causes lethality in the Pacific oyster Crassostrea gigas and impairs the host cellular immune defenses. Fish & Shellfish Immunology 29, 753–758. https://doi.org/10.1016/j.fsi.2010.07.007
Labreuche, Y., Soudant, P., Goncalves, M., Lambert, C., Nicolas, J., 2006. Effects of extracellular products from the pathogenic Vibrio aestuarianus strain 01/32 on lethality and cellular immune responses of the oyster Crassostrea gigas. Developmental & Comparative Immunology 30, 367–379. https://doi.org/10.1016/j.dci.2005.05.003
Lane, H.S., Brosnahan, C.L., Poulin, R., 2022. Aquatic disease in New Zealand: synthesis and future directions. New Zealand Journal of Marine and Freshwater Research 56, 1–42. https://doi.org/10.1080/00288330.2020.1848887
Lanz-Mendoza and Contreras-Garduno 2022 Innate immune memory in invertebrates: Concept and potential mechanisms https://doi.org/10.1016/j.dci.2021.104285
Lasa, A., Auguste, M., Lema, A., Oliveri, C., Borello, A., Taviani, E., Bonello, G., Doni, L., Millard, A.D., Bruto, M., Romalde, J.L., Yakimov, M., Balbi, T., Pruzzo, C., Canesi, L., Vezzulli, L., 2021. A deep-sea bacterium related to coastal marine pathogens. Environmental Microbiology 23, 5349–5363. https://doi.org/10.1111/1462-2920.15629
Lasa, A., Di Cesare, A., Tassistro, G., Borello, A., Gualdi, S., Furones, D., Carrasco, N., Cheslett, D., Brechon, A., Paillard, C., Bidault, A., Pernet, F., Canesi, L., Edomi, P., Pallavicini, A., Pruzzo, C., Vezzulli, L., 2019. Dynamics of the Pacific oyster pathobiota during mortality episodes in Europe assessed by 16S rRNA gene profiling

and a new target enrichment next- generation sequencing strategy. Environmental Microbiology 21, 4548–4562. https://doi.org/10.1111/1462-2920.14750

Lattos, A., Papadopoulos, D.K., Feidantsis, K., Karagiannis, D., Giantsis, I.A., Michaelidis, B., 2022. Are Marine Heatwaves Responsible for Mortalities of Farmed Mytilus galloprovincialis? A Pathophysiological Analysis of Marteilia Infected Mussels from Thermaikos Gulf, Greece. Animals 12, 2805. https://doi.org/10.3390/ani12202805

Le Roux, F., Wegner, K.M., Polz, M.F., 2016. Oysters and Vibrios as a Model for Disease Dynamics in Wild Animals. Trends in Microbiology 24, 568–580. https://doi.org/10.1016/j.tim.2016.03.006

Li, H., Venier, P., Prado-Alvárez, M., Gestal, C., Toubiana, M., Quartesan, R., Borghesan, F., Novoa, B., Figueras, A., Roch, P., 2010. Expression of Mytilus immune genes in response to experimental challenges varied according to the site of collection. Fish & Shellfish Immunology 28, 640–648. https://doi.org/10.1016/j.fsi.2009.12.022

Li, Y.-F., Chen, Y.-W., Xu, J.-K., Ding, W.-Y., Shao, A.-Q., Zhu, Y.-T., Wang, C., Liang, X., Yang, J.-L., 2019. Temperature elevation and Vibrio cyclitrophicus infection reduce the diversity of haemolymph microbiome of the mussel Mytilus coruscus. Sci Rep 9, 16391. https://doi.org/10.1038/s41598-019-52752-y

Liu B, Liu Q, Yang L, Palaniappan SK, Bahar I, Thiagarajan PS, Ding JL. Innate immune memory and homeostasis may be conferred through crosstalk between the TLR3 and TLR7 pathways. Sci Signal. 2016 Jul 12;9(436):ra70. doi: 10.1126/scisignal.aac9340. PMID: 27405980; PMCID: PMC5087126.

Loth, K., Vergnes, A., Barreto, C., Voisin, S.N., Meudal, H., Da Silva, J., Bressan, A., Belmadi, N., Bachère, E., Aucagne, V., Cazevielle, C., Marchandin, H., Rosa, R.D., Bulet, P., Touqui, L., Delmas, A.F., Destoumieux-Garzón, D., 2019. The Ancestral N-Terminal Domain of Big Defensins Drives Bacterially Triggered Assembly into Antimicrobial Nanonets. mBio 10, e01821-19. https://doi.org/10.1128/mBio.01821-19

Luna-Acosta, A., Breitwieser, M., Renault, T., Thomas-Guyon, H., 2017. Recent findings on phenoloxidases in bivalves. Marine Pollution Bulletin 122, 5–16. https://doi.org/10.1016/j.marpolbul.2017.06.031

Lupo, C., Bougeard, S., Le Bihan, V., Blin, J.L., Allain, G., Azéma, P., Benoit, F., Béchemin, C., Bernard, I., Blachier, P., Brieau, L., Danion, M., Garcia, A., Gervasoni, E., Glize, P., Lainé, A., Lapègue, S., Mablouké, C., Poirier, L., Raymond, J.C., Treilles, M., Chauvin, C., Le Bouquin, S., 2021. Mortality of marine mussels *Mytilus edulis* and *M. galloprovincialis* : systematic literature review of risk factors and recommendations for future research.
Reviews in Aquaculture 13, 504–536. https://doi.org/10.1111/raq.12484

Mandic, M., Gvozdenović Nikolić, S., Kokić, I., Jokanović, S., 2024. Mass mortality of farmed mussels – a phenomenon without explanation? https://doi.org/10.5281/ZENODO.12749090

Melillo D, Marino R, Italiani P, Boraschi D. Innate Immune Memory in Invertebrate Metazoans: A Critical Appraisal. Front Immunol. 2018 Aug 22;9:1915. doi: 10.3389/fimmu.2018.01915. PMID: 30186286; PMCID: PMC6113390.

Mesnil, A., Jacquot, M., Garcia, C., Tourbiez, D., Canier, L., Bidois, A., Dégremont, L., Cheslett, D., Geary, M., Vetri, A., Roque, A., Furones, D., Garden, A., Orozova, P., Arzul, I., Sicard, M., Charrière, G.M., Destoumieux-Garzón, D., Travers, M., 2023. Emergence and clonal

expansion of *Vibrio aestuarianus* lineages pathogenic for oysters in Europe. Molecular Ecology 32, 2869–2883. https://doi.org/10.1111/mec.16910

Milutinović B, Kurtz J. Immune memory in invertebrates. Semin Immunol. 2016 Aug;28(4):328-42. doi: 10.1016/j.smim.2016.05.004. Epub 2016 Jul 9. PMID:

27402055.
Montagnani et al., 2023 Trained immunity: Perspectives for disease control strategy in marine mollusc aquaculture DOI: 10.1111/raq.12906
Moreira, R., Romero, A., Rey-Campos, M., Pereiro, P., Rosani, U., Novoa, B., Figueras, A., 2020. Stimulation of Mytilus galloprovincialis Hemocytes With Different Immune Challenges Induces Differential Transcriptomic, miRNomic, and Functional Responses. Front. Immunol. 11, 606102. https://doi.org/10.3389/fimmu.2020.606102
Musella, M., Wathsala, R., Tavella, T., Rampelli, S., Barone, M., Palladino, G., Biagi, E., Brigidi, P., Turroni, S., Franzellitti, S., Candela, M., 2020. Tissue-scale microbiota of the Mediterranean mussel (Mytilus galloprovincialis) and its relationship with the environment. Science of The Total Environment 717, 137209. https://doi.org/10.1016/j.scitotenv.2020.137209
Nayak, A., Pednekar, L., Reid, K.B., Kishore, U., 2012. Complement and non-complement activating functions of C1q: A prototypical innate immune molecule. Innate Immun 18, 350–363. https://doi.org/10.1177/1753425910396252
Novoa, B., Romero, A., Álvarez, Á.L., Moreira, R., Pereiro, P., Costa, M.M., Dios, S., Estepa, A., Parra, F., Figueras, A., 2016. Antiviral Activity of Myticin C Peptide from Mussel: an Ancient Defense against Herpesviruses. J Virol 90, 7692–7702. https://doi.org/10.1128/JVI.00591-16
Odeyemi, O.A., 2016. Incidence and prevalence of Vibrio parahaemolyticus in seafood: a systematic review and meta-analysis. SpringerPlus 5, 464. https://doi.org/10.1186/s40064- 016-2115-7
OSPAR Commission, 2013. Background documents and technical annexes for biological effects monitoring. p. 239.
Paillard, C., Gueguen, Y., Wegner, K.M., Bass, D., Pallavicini, A., Vezzulli, L., Arzul, I., 2022. Recent advances in bivalve-microbiota interactions for disease prevention in aquaculture. Current Opinion in Biotechnology 73, 225–232. https://doi.org/10.1016/j.copbio.2021.07.026
Paillard, C., Korsnes, K., Le Chevalier, P., Le Boulay, C., Harkestad, L., Eriksen, A., Willassen, E., Bergh, Ø., Bovo, C., Skår, C., Mortensen, S., 2008. Vibrio tapetis-like strain isolated from introduced Manila clams Ruditapes philippinarum showing symptoms of brown ring disease in Norway. Dis. Aquat. Org. 81, 153–161. https://doi.org/10.3354/dao01950
Panebianco, A., Rey-Campos, M., Romero, A., Diz, A.P., Novoa, B., Figueras, A., 2023. Mytilus galloprovincialis releases immunologically functional haemocytes to the intervalvar space in response to tissue injury and infection. Fish & Shellfish Immunology 138, 108806. https://doi.org/10.1016/j.fsi.2023.108806
Parisi, M.G., Maisano, M., Cappello, T., Oliva, S., Mauceri, A., Toubiana, M., Cammarata, M., 2019. Responses of marine mussel Mytilus galloprovincialis (Bivalvia: Mytilidae) after infection with the pathogen Vibrio splendidus. Comparative Biochemistry and Physiology Part C: Toxicology & Pharmacology 221, 1–9. https://doi.org/10.1016/j.cbpc.2019.03.005
Pezzati, E., Canesi, L., Damonte, G., Salis, A., Marsano, F., Grande, C., Vezzulli, L., Pruzzo, C., 2015. Susceptibility of *V ibrio aestuarianu* s 01/032 to the antibacterial activity of *M ytilus* haemolymph: identification of a serum opsonin involved in mannose-sensitive interactions. Environmental Microbiology 17, 4271–4279. https://doi.org/10.1111/1462-2920.12750
Pita, L., Rix, L., Slaby, B.M., Franke, A., Hentschel, U., 2018. The sponge holobiont in a

changing ocean: from microbes to ecosystems. Microbiome 6, 46. https://doi.org/10.1186/s40168- 018-0428-1
Pradeu T, Du Pasquier L. Immunological memory: What's in a name?. Immunol Rev. 2018;283:7–20. https://doi.org/10.1111/imr.12652
Pruzzo, C., Gallo, G., Canesi, L., 2005. Persistence of vibrios in marine bivalves: the role of interactions with haemolymph components. Environmental Microbiology 7, 761–772. https://doi.org/10.1111/j.1462-2920.2005.00792.x
Qureshi, A., Niazi, J.H., 2020. Biosensors for detecting viral and bacterial infections using host biomarkers: a review. Analyst 145, 7825–7848. https://doi.org/10.1039/D0AN00896F
Rey-Campos, M., Moreira, R., Gerdol, M., Pallavicini, A., Novoa, B., Figueras, A., 2019. Immune Tolerance in Mytilus galloprovincialis Hemocytes After Repeated Contact With Vibrio splendidus. Front. Immunol. 10, 1894. https://doi.org/10.3389/fimmu.2019.01894
Richards, G.P., Watson, M.A., Needleman, D.S., Church, K.M., Häse, C.C., 2015. Mortalities of Eastern and Pacific Oyster Larvae Caused by the Pathogens Vibrio coralliilyticus and Vibrio tubiashii. Appl Environ Microbiol 81, 292–297. https://doi.org/10.1128/AEM.02930-14
Romero, A., Costa, M., Forn-Cuni, G., Balseiro, P., Chamorro, R., Dios, S., Figueras, A., Novoa, B., 2014. Occurrence, seasonality and infectivity of Vibrio strains in natural populations of mussels Mytilus galloprovincialis. Dis. Aquat. Org. 108, 149–163. https://doi.org/10.3354/dao02701
Romero, A., Dios, S., Poisa-Beiro, L., Costa, M.M., Posada, D., Figueras, A., Novoa, B., 2011. Individual sequence variability and functional activities of fibrinogen-related proteins (FREPs) in the Mediterranean mussel (Mytilus galloprovincialis) suggest ancient and complex immune recognition models in invertebrates. Developmental & Comparative Immunology 35, 334–344. https://doi.org/10.1016/j.dci.2010.10.007
Rowley, A.F., Baker-Austin, C., Boerlage, A.S., Caillon, C., Davies, C.E., Duperret, L., Martin, S.A.M., Mitta, G., Pernet, F., Pratoomyot, J., Shields, J.D., Shinn, A.P., Songsungthong, W., Srijuntongsiri, G., Sritunyalucksana, K., Vidal-Dupiol, J., Uren Webster, T.M., Taengchaiyaphum, S., Wongwaradechkul, R., Coates, C.J., 2024. Diseases of marine fish and shellfish in an age of rapid climate change. iScience 27, 110838. https://doi.org/10.1016/j.isci.2024.110838
Rubio, T., Oyanedel, D., Labreuche, Y., Toulza, E., Luo, X., Bruto, M., Chaparro, C., Torres, M., De Lorgeril, J., Haffner, P., Vidal-Dupiol, J., Lagorce, A., Petton, B., Mitta, G., Jacq, A., Le Roux, F., Charrière, G.M., Destoumieux-Garzón, D., 2019. Species-specific mechanisms of cytotoxicity toward immune cells determine the successful outcome of *Vibrio* infections.
Proc. Natl. Acad. Sci. U.S.A. 116, 14238–14247.
https://doi.org/10.1073/pnas.1905747116 Saco, A., Rey-Campos, M., Novoa, B., Figueras, A.,
2020. Transcriptomic Response of Mussel
Gills After a Vibrio splendidus Infection Demonstrates Their Role in the Immune Response. Front. Immunol. 11, 615580. https://doi.org/10.3389/fimmu.2020.615580
Scanes, E., Parker, L.M., Seymour, J.R., Siboni, N., King, W.L., Wegner, K.M., Dove, M.C., O'Connor, W.A., Ross, P.M., 2021. Microbiome response differs among selected lines of Sydney rock oysters to ocean warming and acidification. FEMS Microbiology Ecology 97, fiab099. https://doi.org/10.1093/femsec/fiab099
Smaal, A.C., Ferreira, J.G., Grant, J., Petersen, J.K., Strand, Ø. (Eds.), 2019. Goods and Services of Marine Bivalves. Springer International Publishing, Cham. https://doi.org/10.1007/978-3- 319-96776-9
Sokolova, I., 2021. Bioenergetics in environmental adaptation and stress tolerance of aquatic ectotherms: linking physiology and ecology in a multi-stressor landscape. Journal of

Experimental Biology 224, jeb236802. https://doi.org/10.1242/jeb.236802
Song, L., Wang, L., Qiu, L., Zhang, H., 2010a. Bivalve Immunity, in: Söderhäll, K. (Ed.), Invertebrate Immunity, Advances in Experimental Medicine and Biology. Springer US, Boston, MA, pp. 44–65. https://doi.org/10.1007/978-1-4419-8059-5_3
Song, L., Wang, L., Qiu, L., Zhang, H., 2010b. Bivalve Immunity, in: Söderhäll, K. (Ed.), Invertebrate Immunity, Advances in Experimental Medicine and Biology. Springer US, Boston, MA, pp. 44–65. https://doi.org/10.1007/978-1-4419-8059-5_3
Stincone, P., Brandelli, A., 2020. Marine bacteria as source of antimicrobial compounds. Critical Reviews in Biotechnology 40, 306–319. https://doi.org/10.1080/07388551.2019.1710457
Sun, J., Wang, L., Song, L., 2023. The primitive complement system in molluscs. Developmental & Comparative Immunology 139, 104565. https://doi.org/10.1016/j.dci.2022.104565
Sussman, M., Willis, B.L., Victor, S., Bourne, D.G., 2008. Coral Pathogens Identified for White Syndrome (WS) Epizootics in the Indo-Pacific. PLoS ONE 3, e2393. https://doi.org/10.1371/journal.pone.0002393
Tanguy, M., Gauthier-Clerc, S., Pellerin, J., Danger, J.-M., Siah, A., 2018. The immune response of Mytilus edulis hemocytes exposed to Vibrio splendidus LGP32 strain: A transcriptomic attempt at identifying molecular actors. Fish & Shellfish Immunology 74, 268–280. https://doi.org/10.1016/j.fsi.2017.12.038
Travers, M.-A., Boettcher Miller, K., Roque, A., Friedman, C.S., 2015a. Bacterial diseases in marine bivalves. Journal of Invertebrate Pathology 131, 11–31. https://doi.org/10.1016/j.jip.2015.07.010
Travers, M.-A., Boettcher Miller, K., Roque, A., Friedman, C.S., 2015b. Bacterial diseases in marine bivalves. Journal of Invertebrate Pathology 131, 11–31. https://doi.org/10.1016/j.jip.2015.07.010
Vezzulli, L., Repetto, B., Pezzati, E., Stauder, M., Giusto, G., Pruzzo, C., 2008. Adhesins acquired in the aquatic environment and *Vibrio cholerae* colonization of intestinal cells. Microbial Ecology in Health and Disease 20, 193–196. https://doi.org/10.1080/08910600802333517
Vezzulli, L., Stagnaro, L., Grande, C., Tassistro, G., Canesi, L., Pruzzo, C., 2018a. Comparative 16SrDNA Gene-Based Microbiota Profiles of the Pacific Oyster (Crassostrea gigas) and the Mediterranean Mussel (Mytilus galloprovincialis) from a Shellfish Farm (Ligurian Sea, Italy). Microb Ecol 75, 495–504. https://doi.org/10.1007/s00248-017-1051-6
Vezzulli, L., Stagnaro, L., Grande, C., Tassistro, G., Canesi, L., Pruzzo, C., 2018b. Comparative 16SrDNA Gene-Based Microbiota Profiles of the Pacific Oyster (Crassostrea gigas) and the Mediterranean Mussel (Mytilus galloprovincialis) from a Shellfish Farm (Ligurian Sea, Italy). Microb Ecol 75, 495–504. https://doi.org/10.1007/s00248-017-1051-6
Viarengo, A., Lowe, D., Bolognesi, C., Fabbri, E., Koehler, A., 2007. The use of biomarkers in biomonitoring: A 2-tier approach assessing the level of pollutant-induced stress syndrome in sentinel organisms. Comparative Biochemistry and Physiology Part C: Toxicology & Pharmacology 146, 281–300. https://doi.org/10.1016/j.cbpc.2007.04.011
Von Schuckmann, K., Moreira, L., De Pascual Collar, Á., Grégoire, M., Brasseur, P., Garric, G., Karstensen, J., Lionello, P., Marcos, M., Poulain, P.-M., Staneva, J., 2025. 9th edition of the Copernicus Ocean State Report (OSR9). Copernicus GmbH. https://doi.org/10.5194/sp-6- osr9
Wang, J., Wang, L., Yang, C., Jiang, Q., Zhang, H., Yue, F., Huang, M., Sun, Z., Song, L., 2013. The response of mRNA expression upon secondary challenge with Vibrio anguillarum suggests the involvement of C-lectins in the immune priming of scallop Chlamys farreri. Dev. Comp. Immunol. 40, 142–147.

Wathsala, R.H.G.R., Musella, M., Valbonesi, P., Candela, M., Franzellitti, S., 2021. Variability of metabolic, protective, antioxidant, and lysosomal gene transcriptional profiles and microbiota composition of Mytilus galloprovincialis farmed in the North Adriatic Sea (Italy). Marine Pollution Bulletin 172, 112847. https://doi.org/10.1016/j.marpolbul.2021.112847

Wernberg, T., Thomsen, M.S., Baum, J.K., Bishop, M.J., Bruno, J.F., Coleman, M.A., Filbee-Dexter, K., Gagnon, K., He, Q., Murdiyarso, D., Rogers, K., Silliman, B.R., Smale, D.A., Starko, S., Vanderklift, M.A., 2024. Impacts of Climate Change on Marine Foundation Species. Annu. Rev. Mar. Sci. 16, 247–282. https://doi.org/10.1146/annurev-marine-042023- 093037

Y., B.-H., E., R., 2002. A novel Vibrio sp. pathogen of the coral Pocillopora damicornis. Marine Biology 141, 47–55. https://doi.org/10.1007/s00227-002-0797-6

Yang, J., He, J., Liu, L., He, M., Zhang, X., Buttino, I., Guo, B., Yan, X., Liao, Z., 2022. Expression profiles of antimicrobial peptides in Mytilus coruscus. Aquaculture 548, 737709. https://doi.org/10.1016/j.aquaculture.2021.737709

Zhang T, Qiu L, Sun Z, Wang L, Zhou Z, Liu R, Yue F, Sun R, Song L. The specifically enhanced cellular immune responses in Pacific oyster (Crassostrea gigas) against secondary challenge with Vibrio splendidus. Dev Comp Immunol. 2014 Jul;45(1):141-50. doi: 10.1016/j.dci.2014.02.015. Epub 2014 Mar 6. PMID: 24607288.

Zilber-Rosenberg, I., Rosenberg, E., 2008a. Role of microorganisms in the evolution of animals and plants: the hologenome theory of evolution. FEMS Microbiol Rev 32, 723–735. https://doi.org/10.1111/j.1574-6976.2008.00123.x

Zilber-Rosenberg, I., Rosenberg, E., 2008b. Role of microorganisms in the evolution of animals and plants: the hologenome theory of evolution. FEMS Microbiol Rev 32, 723–735. https://doi.org/10.1111/j.1574-6976.2008.00123.x

Aim and objectives

In a context of increasing mortality outbreaks in bivalve populations, driven by polymicrobial and multifactorial causes, understanding the interactions between bacterial strains and the immune system of their bivalve hosts is essential for predicting and potentially preventing bacterial infections, supporting the development of effective disease management strategies for aquacultured species, and ultimately protecting marine biodiversity.

The research activity carried out in the first section of this thesis was developed within the framework of the Italian National Recovery and Resilience Plan (PNRR), Activity 3, Task 3.4, focusing on selective breeding for disease, resistance and resilience to environmental challenges for shellfish aquaculture.

In the present work, the interactions between the immune system of *M. galloprovincialis* and bacterial strains isolated from bivalve mortality outbreaks were investigated. This activity was carried out in collaboration with the Aquaculture research group of the Institute of Agrifood Research and Technology (IRTA, La Rapita, Spain), who provided bacterial isolates from recent bivalve mortality episodes occurring at different aquaculture sites in the Ebro Delta.

The research activity was developed into 4 sections:

1 Isolation of potentially pathogenic bacteria from a mortality event occurred in aquacultured mussel populations in 2022 in the Ebro Delta (Spain). After its characterization as *Vibrio ostreicida*, the effects of a selected strain (r172) were first evaluated on *M. galloprovincialis* early larval development. *In vitro* interactions with the immune system of adult mussels were subsequently investigated and compared with those obtained in the oyster *M. gigas.*

2 Evaluation of *in vivo* experimental infection dynamics and immune responses of adult *M. galloprovincialis* challenged with *V. ostreicida* r172.

3 Evaluation of immune responses of *M. galloprovincialis* to multiple infections with two different bacterial strains isolated from an oyster mortality event in the Ebro Delta (Spain, 2019): *V. aestuarianus* (strain IRTA-19-106) and *M. marinus* (IRTA-19-131). Both *in vivo/in vitro* and *in vivo/in vivo* experimental multi-infection approaches were employed,

and several immune parameters were evaluated.

4 Evaluation of seasonal changes in immunocompetence of *M. galloprovincialis* cultivated in the Ligurian Sea (La Spezia, Italy). Basal immune parameters were evaluated in musselssampled across 1 year; moreover, seasonal changes in the specificity of immune responses were investigated in *in vitro* experiments of hemolymph samples challenged with different bacterial species and strains.

Results

Chapter 1:

First description of *Vibrio ostreicida* as putative causal agent of disease in Mediterranean mussel (*Mytilus galloprovincialis*) and development of a PCR protocol for its rapid diagnosis.

The results of this work have been published in Journal of Invertebrate Pathology 212 (2025) 108399. https://doi.org/10.1016/j.jip.2025.108399

Data are presented on the isolation and characterization of a bacterium isolated in April 2022, from a mortality outbreak of adult *M. galloprovincialis* occurred in Alfacs Bay (Spain). The episode involved 25 % of individuals, and was observed at a water temperature of 18 °C. Mussel samples from mortality site (3M) were investigated for the presence of potentially pathogenic bacteria. A parallel group of animals that did not experience the morality outbreak was analysed as negative control (3N). Bacterial isolates from both 3M and 3N samples were analysed by the ERIC-PCR, and the obtained band patterns showed a distinct profile in the 3M samples, covering 13% of the isolates. Three representative isolates from this distinct profile (r167, r172, r190) were chosen for the genotypic and phenotypic characterization, resulting in their identification as *V. ostreicida*. In addition, the complete genome of isolate r172 was sequenced to identify functional features of interest. Moreover, histological examination in 3M samples revealed bacterial colonies and tissue damage compatible with bacterial toxicity. A preliminary virulence test was performed by injecting r172 isolate (9×10^6 CFU/mussel) into mussels. A mean mortality of 50 % was observed in infected animals at 5 days. Finally, a specific PCR protocol was designed for *V. ostreicida* using the *gyrB* gene as a target, able to detect the pathogen from both pure cultures and from tissues. This is the first evidence of the association of *V. ostreicida* with a mortality episode in cultured *M. galloprovincialis*, highlighting its potential as an emerging pathogen of concern in marine ecosystems.

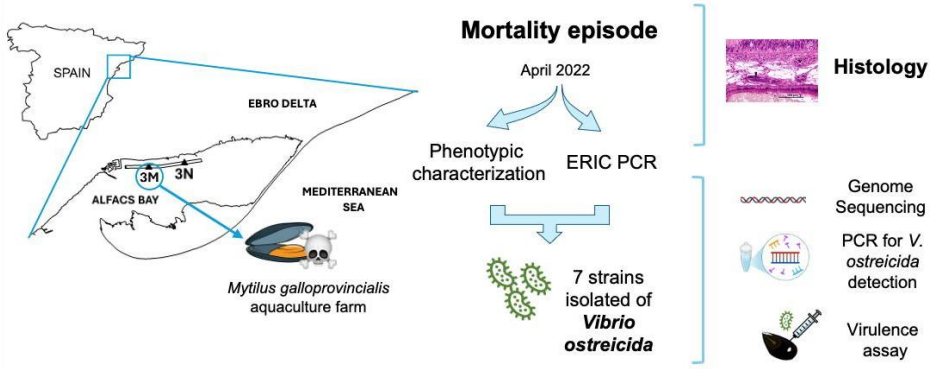

Journal of Invertebrate Pathology 212 (2025) 108399

Contents lists available at ScienceDirect

Journal of Invertebrate Pathology

journal homepage: www.elsevier.com/locate/jip

First description of *Vibrio ostreicida* as putative causal agent of disease in Mediterranean mussel (*Mytilus galloprovincialis*) and development of a PCR protocol for its rapid diagnosis

Jose R. Lopez [a,b,*], Martina Leonessi [c,d], Margarita Fernandez-Tejedor [a], Manon Auguste [c,d], Lapo Doni [c,d], Yanis Cruz-Quintana [a,e], Emanuele Bosi [c,d], Luigi Vezzulli [c,d], Karl Andree [a], Laura Canesi [c,d], Dolors Furones [a]

[a] Institut de Recerca i Tecnologia Agroalimentaries (IRTA), La Ràpita, Spain
[b] Universidade de Santiago de Compostela, Santiago de Compostela, Spain
[c] Department of Earth, Environmental and Life Sciences (DISTAV), University of Genoa, Genoa 16132, Italy
[d] National Biodiversity Future Center, Palermo, Italy
[e] Grupo de Investigación en Sanidad Acuícola, Inocuidad y Salud Ambiental (SAISA), Departamento de Acuicultura, Pesca y Recursos Naturales Renovables, Facultad de Acuicultura y Ciencias del Mar, Universidad Técnica de Manabí, Bahía de Caráquez 130104, Ecuador

ARTICLE INFO

Keywords:
Vibrio ostreicida
Mussel
Mytilus galloprovincialis
Disease
Mortality
Diagnosis

ABSTRACT

In April 2022, mussels (*Mytilus galloprovincialis*) cultivated in the Ebro River delta (Spain) were affected by a mortality episode, involving 25 % of individuals, observed at a water temperature of 18 °C. Mussel samples from this site (3 M) were analysed for the presence of potentially pathogenic bacteria, in parallel with those obtained from an area where no mortality was reported (3 N). From all samples, a total of 113 bacterial isolates were obtained. When subjected to ERIC-PCR, the obtained band patterns showed a distinct profile in the 3 M samples, covering 13 % of the isolates. The genotypic and phenotypic characterization of three representative isolates of this profile (r167, r172, r190) allowed their identification as *Vibrio ostreicida*. In addition, the complete genome of isolate r172 was sequenced to identify functional features of interest. Histological examination revealed bacterial colonies and tissue damage compatible with bacterial toxicity in 3 M samples. From a preliminary assessment of the virulence of the r172 isolate by mussel challenge via injection (9×10^6 cfu/mussel), a mean mortality of 50 % was observed in infected animals at 5 days. Moreover, a specific PCR protocol was designed for *V. ostreicida* using the *gyrB* gene as a target, able to detect the pathogen from both pure cultures and from tissues. To our knowledge, this is the first evidence of the association of *V. ostreicida* with a mortality episode in cultured *M. galloprovincialis*. The PCR protocol developed will be useful for screening and diagnosis of this vibrio species in different matrices and to clarify its importance as shellfish possible pathogen.

1. Introduction

Infectious diseases caused by bacteria from the genus *Vibrio* are among the most important threats that affect bivalve mollusk cultures worldwide. Species such as *Vibrio tapetis*, *Vibrio splendidus*, *Vibrio neptunius*, *Vibrio aestuarianus*, *Vibrio pectenicida* and *Vibrio alginolyticus*, have been described associated with mortality outbreaks in a variety of bivalve species (*Crassostrea gigas*, *Ostrea edulis*, *Ruditappes decussatus*, *Ruditapes philippinarum*, *Pecten maximus*), their pathogenicity having been demonstrated in virulence assays (Beaz-Hidalgo et al., 2010). In 2014, Prado *et al.* described a new *Vibrio* species, *Vibrio ostreicida*, associated with mortalities in oyster (*Ostrea edulis*) larvae in northwest Spain. The type strain, PP-203, proved its capacity to cause mortality in oyster larvae. Apart from the draft genome of this type strain reported by Kumar et al. (2020), no further mentions of *V. ostreicida* have appeared in the literature.

Emergent bacterial pathogens like some *Vibrio* species pose an increasing threat to aquaculture, fuelled by global climate change and stock's movements, which can create favourable conditions for the proliferation and increased virulence of these organisms. Rising sea

* Corresponding author at: IRTA La Rapita. Carretera de Poble Nou, km 5.5. La Rapita, 43540 Tarragona, Spain.
E-mail address: lasacias@yahoo.es (J.R. Lopez).

https://doi.org/10.1016/j.jip.2025.108399
Received 13 March 2025; Received in revised form 17 June 2025; Accepted 9 July 2025
Available online 11 July 2025
0022-2011/© 2025 Elsevier Inc. All rights are reserved, including those for text and data mining, AI training, and similar technologies.

surface temperatures, shifts in salinity and other environmental changes have been linked to increased incidence and severity of some *Vibrio*-related outbreaks (Charles et al., 2020a; Romero et al., 2014a).

Oysters and mussels are the most important species in the European aquaculture sector, accounting for over 45 % of the production volume in 2021 (EUMOFA, 2024). However, while oyster cultures have suffered extensive recurrent mortality episodes across their different life stages, reports of mass mortality caused by infectious diseases in mussels remain relatively rare (Ben Cheikh et al., 2016; Destoumieux-Garzón et al., 2020; Eggermont et al., 2017). Pathogenic bacteria associated with mortality in different mussel species include strains related to *V. splendidus* in blue mussel (*Mytilus edulis*) in France (Ben Cheikh et al., 2016, Ben Cheikh et al., 2017), strains of *V. splendidus* and *Vibrio coralliilyticus/V. neptunius*-like in Greenshell mussel (*Perna canalicula*) larvae (Kesarcodi-Watson et al., 2009), and strains of *Francisella halioticida* in *M. edulis* in France (Bouras et al., 2023; Charles et al., 2020b). Virulence assays confirmed these strains capable (to varying degrees) to cause mortality in their respective host species. However, to our knowledge no mass mortalities associated with infectious diseases have been described in the Mediterranean mussel (*M. galloprovincialis*) (Lupo et al., 2021).

Given the challenges posed by traditional phenotypic and biochemical methods, which are labor-intensive, require cultivation and limited sensitivity, molecular detection technologies have become essential for rapid and accurate identification of bacteria. Polymerase chain reaction (PCR) technology has facilitated the detection of pathogens in aquaculture, offering notable advantages such as versatility, cost-effectiveness, rapid diagnosis and high sensitivity. Historically, PCR-based techniques relied on 16S ribosomal genes. However, although Vibrio can be identified to the level of genus by their 16 s ribosomal DNA signatures, there are many species whose 16S sequences are nearly identical (Thompson et al., 2005) and therefore coding sequences, which often have synonymous mutations in the third position of the codon, can provide sufficient phylogenetic information for species identification and also targeted PCR diagnostics. Consequently, recent approaches increasingly focus on protein-coding genes, such as *gyrB* (Bunpa et al., 2018; Wang et al., 2024).

Here, we present the first report of *Vibrio ostreicida* associated with a mortality outbreak in *M. galloprovincialis*. Furthermore, we propose a PCR-based protocol for the detection of this pathogen, offering a valuable tool to enhance diagnostic capabilities in aquaculture.

2. Materials and methods

2.1. Study site and mussel sampling

The two bays of the Ebro delta, Alfacs and Fangar, hold aquaculture farms were mussels and oysters grow attached to ropes in structures (bateas) fixed to the sea bottom, with different production among the bays, with Alfacs dedicated customarily to mussels, whereas Fangar accommodates most of the oyster culture. The production in both bays during the year of this study (2022) was 2,905 t of mussels and 397 t of oysters. Lowest temperatures occur in January with means of 10 °C and extremes of 6 °C; while the highest hit in August, with means of 28 °C and extremes of 30 °C (Llebot et al., 2011). Drainage channels from the Ebro delta's agriculture fields provide vital freshwater inputs to the bays, favouring water circulation and preventing high salinity peaks. Thus, the surface water salinity ranges between 34 and 35.5 ppt. In April 2022, an adult mussel mortality episode was reported in Alfacs Bay by local mussel farmers, with a 25 % estimated mortality. The surface seawater temperature recorded during the outbreak was 18 °C, in line with average values for the period. To investigate the potential causes of mortality, mussels from two farms (2.5 km far from each other) differentially affected by the event according to the producers' estimations, were sampled. The samples from the farm where mortality was detected were coded as 3 M and the samples from the farm where mortality was not registered, were coded as 3 N (Fig. 1). Noteworthy, the mussel ropes in 3 N were not covered by sediment; on the contrary, the mussels in the bottom of the 3 M mussel ropes (where mortality was higher), were covered by sediments, although not buried.

Mussels (approx. 6 kg) were collected from ropes at each farm, representing their whole length. Mortality was assessed on arrival at the laboratory by counting dead animals in a group of 200 individuals, resulting in 20 % in 3 M and 9 % in 3 N. Biometry (length and weight) was taken from 50 individuals of 3 M and 3 N, 63 ± 7 and 68 ± 5 mm respectively (average ± sd). A total of 60 live adult mussels (about 9 g weight) were sampled for histopathological analyses, 30 from 3 M, and 30 from 3 N.

2.2. Bacterial isolation and typing

Soft mussel tissues (gills, mantle, hepatopancreas) were dissected, and for each group (3 M and 3 N) 6 pools of 5 individuals each were made. Pools were homogenized by Ultraturrax in PBS pH 7.4 (ratio 1:1). For bacterial isolation, aliquots of 100 µl of homogenate were seeded onto Marine Agar (MA) and Thiosulfate-Citrate-Bile Salts-Sucrose (TCBS) plates and incubated at 23 °C, 24–48 h. The obtained isolates were frozen in sterile seawater supplemented with 20 % (v/v) glycerol and stored at −80 °C.

DNA extraction from pure cultures was carried out using the boiling method (briefly: 95 °C 5 min in distilled water, spin for 2 min at 13200 rpm). The concentration and purity of the DNA were calculated using NanoDrop 2000. Molecular typing of the isolates was performed using the ERIC-PCR technique according to Zhang et al. (2019), using 100 ng of DNA for each isolate. PCR products were electrophoresed on a 1.2 % agarose Tris-acetate-EDTA buffer (TAE) gel stained with ethidium bromide. The Invitrogen 1 Kb Plus Ladder was used as a molecular weight marker.

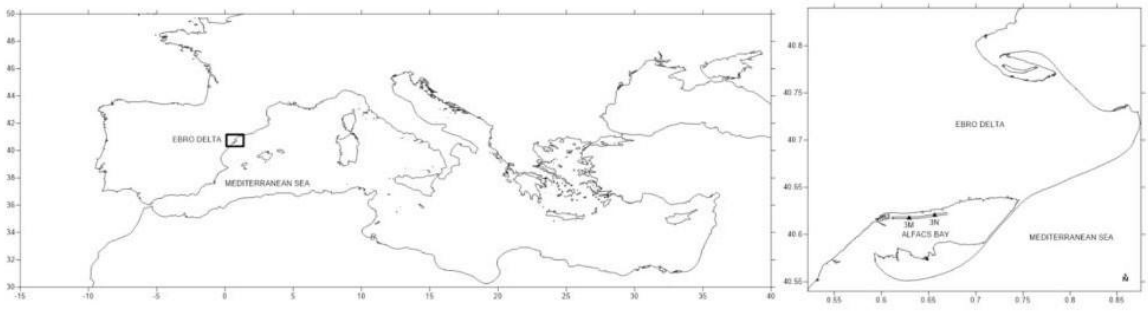

Fig. 1. Map of the Ebro delta showing the location of the farms from Alfacs Bay where the samples were obtained; 3 M is where mortality was detected and 3 N is where did not occur. The polygons inside the bays show the area where the mussel and oyster farms are located.

2.3. Phenotypic characterization

A basic phenotypic characterization of representative isolates was carried out according to López et al. (2017), including the following tests: gram staining, glucose fermentation/oxidation test (OF), cytochrome oxidase and catalase activity, growth at different temperatures on MA plates (4, 8. 15, 25, 30, 35, 40 and 45 °C), tolerance of salinity (growth on basal medium −neopeptone 4 g/l, yeast extract 1 g/l, agar 15 g/l- supplemented with 0, 3, 6, 8, 10 and 12 % NaCl), and growth on TCBS agar. Commercial miniaturized API 20E galleries (bioMerieux), were also utilized according to the manufacturer's instructions, but saline solution (0.85 % NaCl) was used as diluent. With the exception of the temperature tests, all other tests were carried out at 23 °C. Drug sensitivity to antimicrobial compounds was determined on Mueller-Hinton (+2 % NaCl) by the disc diffusion method, for the vibriostatic agent O/129 (10 and 150 μg/disc), novobiocin (30 μg), erythromycin (15 μg), cefoxitin (30 μg), trimethoprim (5 μg), ampicillin (10 μg), nitrofurantoin (100 and 300 μg), ciprofloxacin (5 μg), kanamycin (30 μg) and amoxicillin (25 μg). Antibiogram readings were performed after 48 h incubation at 23 °C. The type strain of *V. ostreicida* (CECT7398^T = PP-203^T) was characterized together with the isolates under study with the same methodology.

2.4. Phylogenetic analysis

Partial sequences were obtained from representative isolates according to Weisburg et al. (1991) for 16S rRNA gene, Thompson et al. (2005) for *rpoA* gene, and Sawabe et al. (2007) for *gyrB*, *ftsZ* and *pyrH* genes. PCRs were carried out basically as indicated in the literature, in a total reaction volume of 25 μl, using the Invitrogen Taq DNA Polymerase. PCR products were purified with the QIAquick PCR Purification kit (Quiagen) and sequencing of purified PCR products was performed by Sistemas Genomicos (Valencia, Spain). The sequences were analyzed with Chromas LITE and BioEdit programs and subjected to BLAST and EzTaxon searches to retrieve close related sequences. Concatenated gene sequences were also used; they were constructed by joining the in-frame sequences in the following order: 16S-*ftsZ*-*gyrB*-*pyrH*-*rpoA* (1321, 572, 572, 417 and 831 nt, respectively). DNA sequences alignments were performed using Clustal Omega software and phylogenetic trees were constructed according to the neighbor-joining method (Saitou & Nei, 1987) by using the program MEGA (bootstrap of 1000 replicates).

2.5. Complete genome sequence of V. ostreicida r172

Genomic DNA was extracted from colonies of *Vibrio ostreicida* strain r172 grown on MA plate (Sharlab) at 23 °C for 24 h, using an DNeasy Blood and tissue kit (Qiagen). The libraries (151 bp paired-end) were prepared using Nextera XT DNA Library Preparation Kit (Ref. Guide 15,031,942 v03) and run on an Illumina NovaSeq 6000 system.

2.5.1. Genome assembly and annotation

The sequencing reads were assembled with the SPAdes genome assembler (v3.13.1) using the following command-line options: −k 21,33,55,77 −-careful. The performed analysis included read error correction with BayesHammer. The obtained contigs were filtered discarding sequences shorter than 1000 bp. Genome annotation was performed with Prokka (v1.14.6). Protein-encoding sequences were further annotated using the emapper.py script (v2.1.10) from EggNOG (v5.0.2) to define their corresponding orthologous group with a two-step annotation process. Seed orthologs were identified with the following command: emapper.py −m diamond –sensmode more-sensitive –no_annot. Then, the hit tables have been annotated with the following command emapper.py −m no_search –annotate_hits_table –dbmem –report_orthologs –target_orthologs one2one.

The presence of genes related to virulence was assessed using Abricate (v. 1.0.1) (Seemann) to map annotated genes on the Virulence Factors Database (VFDB) (Chen et al., 2016) with options –db vfdb GBK, using the GenBank file generated by Prokka (GBK) as input. Putative ARGs were named with AMRFinderPlus (v. 3.11.2).

2.5.2. Phylogenetic analysis

The phylogenetic relationships between *V. ostreicida* and other *Vibrio* species were assessed using a pan-genome we previously defined for this genus (Bosi et al., 2024). Briefly, comparing ortholog groups shared between the different species we identified a group of 380 single-copy genes present in all species. The corresponding aminoacid sequences were aligned separately with Muscle (Edgar, 2004), using the "clwstrict" and "diags" parameters. Multiple sequence alignments were concatenated and used to compute phylogeny with iqtree2 (Minh et al., 2020) with the parameters –alrt 1000 −B 1000, resulting in a maximum likelihood phylogeny with 1000 bootstrap. As implemented in iqtree2, model selection was performed with ModelFinder (Kalyaanamoorthy et al., 2017) by selecting the best-fit model according to Bayesian Information Criteria minimisation. Phylogenetic tree visualisation was performed with ITOL (Letunic & Bork, 2021).

The phylogenetic relationships within the *V. ostreicida* species were determined by downloading all genomes available for this taxon, then aligning the sequences to the reference genome (GCA_001957165.1) to identify conserved polymorphic sites. This was achieved by applying Snippy (https://github.com/tseemann/snippy), and the snippy-core utility to extract universally shared single-nucleotide variants. The resulting alignment was used to derive a phylogeny with iqtree2 as above.

2.6. Mussel histopathological analysis

For histopathological evaluation, a transverse section (0.3 cm) including digestive tissue, gill, foot, and gonad was obtained from each *M. galloprovincialis* individual, sampled from both mortality and no-mortality sites (n = 30). Tissue samples were fixed in Davidson's solution for 48–72 h (Howard et al., 2004). After fixation, samples were dehydrated through a graded ethanol series, cleared with xylene (MYR STP 120, Especialidades Médicas Myr, Spain), and embedded in paraffin (MYR EC-350, Especialidades Médicas Myr). Serial sections (5 μm thick) were cut using a microtome (Leica RM2155, Leica Microsystems, Germany) and stained with hematoxylin and eosin (H&E) using automated staining equipment (MYR MYREVA SS-30, Especialidades Médicas Myr). The slides were examined under a light microscope (Leica DM LB, Leica Microsystems) and images were captured using an Olympus DP70 digital camera (Olympus Europa, Germany) and processed with Analysis software (Olympus Soft Imaging Solutions, Germany).

2.7. Development of a PCR-based diagnostic protocol for V. ostreicida

DNA sequences from *rpoA*, *gyrB*, *ftsZ* and *pyrH* genes from *V. ostreicida* and related species, obtained from GenBank database and this study, were aligned using the program Bioedit v.7.1.11 (Hall, 1999) and examined for areas of similarity and variability between different species and strains. On the basis of the alignments, variable regions were chosen and specific primers were designed using the PRIMER3 program (Rozen & Skaletsky, 2000). Primers were synthesized by Sigma Aldrich. All DNA extractions mentioned in this section (from pure bacterial cultures, and tissues) were performed with the DNeasy Blood & Tissue kit (Quiagen) according to the manufacturer's instructions.

The PCR amplifications were carried out in a mixture (total reaction volume of 25 μl) composed of 1U Taq Polymerase (Invitrogen), 2.5 μl of 10x buffer, 1 mM $MgCl_2$, 0.05 mM of each dNTP, 0.5 μM of each primer, and autoclaved deionized water. PCR reaction was performed with the following conditions: an initial denaturation at 94 °C for 5 min followed by 50 amplification cycles of denaturation at 94 °C for 30 s, annealing at 63 °C for 30 s, and extension at 72 °C for 30 s; and a final elongation at 72 °C for 5 min. DNA from type strain *V. ostreicida* CECT7398^T was used

as a positive control and deionized water was employed as a negative control. PCR products were electrophoresed on a 1.2 % agarose TAE gel stained with ethidium bromide. The Invitrogen 1 Kb Plus Ladder was used as a molecular weight marker.

In order to test the specificity of the proposed PCR protocol, four *V. ostreicida* strains (the type strain, *V. ostreicida* CECT7398^T, and 3 isolates from this study) and 31 strains of other 25 species were employed (Table1). For PCR amplification, the same amount of DNA template (100 ng) was used for each strain. The detection limit of the protocol was evaluated using 4 different approaches: 1) using 10-fold serially diluted DNA (in ultrapure water) from *V. ostreicida* CECT 7398^T, over the range from 100 ng to 1 fg; 2) in order to determine the sensibility in the presence of mollusk DNA, the same DNA dilutions mentioned above were used mixed with 1 μg of DNA from healthy mussels and oysters (separately); 3) using 10-fold serially diluted cell suspensions (CECT 7398^T) over the range from 5x10^5 cfu to 0.5 cfu by PCR tube; and 4) in order to test the sensitivity in the presence of tissue debris, samples of 30 mg of mussel tissue (mantle) were seeded with a range of 3x10^5 to 0.3 cfu of CECT 7398^T; after DNA extraction, 400 ng were used for each PCR reaction. Bacterial concentration was estimated by absorbance of bacterial suspensions at 580 nm wavelength and real doses were confirmed with total viable counts in MA plates.

Finally, the ability of the PCR protocol to detect *V. ostreicida* from naturally infected mussel tissues was evaluated using the 6 pools (tissue homogenate of 5 individuals each) obtained in this study from the area where mortality had been observed. With these 6 samples, 400 ng DNA template was used for each PCR reaction. All the assays mentioned in this section were performed at least in duplicate.

Table 1
Bacterial species and strains/isolates used to test the specificity of the proposed PCR protocol.

Species	Strains/ isolates	Source/Origin
Aeromonas salmonicida	CECT 5234	Water from La Platjola Lagoon, Spain
Malaciobacter marinus	CECT 7727	Sea water, Korea
Photobacterium damselae damselae	CECT 626	Skin ulcer in damsel fish Chromis punctipinnis, USA
Photobacterium damselae piscicida	CECT 5895	Dicentrarchus labrax
Streptococcus iniae	CECT 7363 T	Fresh water dolphin Inia geoffrensis, USA
Tenacibaculum maritimum	CECT 4276	Kidney of diseased black seabream Acanthopagrus schlegeli, Japan
Vibrio aestuarianus	CECT 625 T	Oyster from Yaquina Bay, USA
	01/032	Oyster mortality outbreak
	02/041	*Crassostrea gigas*
Vibrio alginolyticus	CECT 521 T	Horse mackerel Trachurus trachurus, Japan
Vibrio anguillarum	CECT 522 T	Ulcerous lesion in cod Gadus morhua, Norway
Vibrio campbellii	CECT 523 T	Sea water
Vibrio celticus	Bivalife Unige 8	*Ruditapes philippinarum* and *Venerupis pullastra*
Vibrio coralliilyticus	LMG 20984 T	Diseased coral *Pocillopora damicornis*, Indian ocean
	TAV24	Diseased *Paramuricea clavata* colonies
Vibrio harveyi	CECT 525 T	Amphipod Talorchestia sp., USA
Vibrio ichthyoenteri	CECT 5675 T	Diseased Japanese flounder larvae, Paralichthys olivaceus, Japan
Vibrio natriegens	ATCC 14048 T	Salt marsh mud
Vibrio orientalis	CECT 629 T	Sea water, Yellow Sea, China
Vibrio ostreicida	CECT 7398 T (= PP203T)	Inner surface of containers in a mollusc hatchery in Galicia, Spain
	r167	This study
	r172	This study
	r190	This study
Vibrio owensii	LMG 25443 T	Spiny lobster *Panulirus ornatus*, Australia
Vibrio parahaemolyticus	ATCC 43,996	Cockles causing fatal food poisoning
Vibrio pectenicida	LMG 19642 T	Scallop *Pecten maximus* larvae, France
Vibrio rotiferianus	LMG 21460 T	Rotifer *Branchionus plicatilis* flow-through culture system, Belgium
Vibrio scophthalmi	CECT 4638 T	Gastrointestinal tract of turbot Scophthalmus maximus, Spain
Vibrio splendidus	CECT 528 T	Marine fish
	LGP32	Oyster mortality outbreak
Vibrio tasmaniensis	LGP32	Oyster farm
Vibrio tapetis	CECT 4600 T	*Tapes philippinarum*, clam
	LP2	*Symphodus melops*, fish
Vibrio vulnificus	ATCC 27562 T	Blood
	CECT 897	Diseased pond-cultured eels, Anguilla japonica and Anguilla anguilla

2.8. Virulence assay

In order to evaluate the pathogenic potential of mussel isolates, an *in vivo* virulence test was carried out with isolate r172, using a dose of 9x10^6 cfu/mussel. Bacteria were grown on MA plates at 23 °C for 24 h and resuspended in PBS (pH 7.4). The concentration was estimated by absorbance at 580 nm wavelength, and the actual doses were determined by total viable counts on MA plates after 24 h at 23 °C.

Bacterial challenge was performed by intravalvar injection (100 μl doses, in PBS pH 7.4), using 2 groups of 10 mussels each, with an average weight of 9 g. A parallel negative control was run in duplicate, with two groups of 10 mussels injected with PBS. After the injection, the mussels were kept in 20 l tanks at 24 °C for 5 days, with both water renewal and feeding starting 48 h after the beginning of the assay. The death toll was reviewed daily. Dead mussels were removed and tissue sample homogenates of each individual were plated on MA at 23 °C for 24 h. Detection of *V. ostreicida* among the bacteria grown on the plates was carried out using the PCR protocol described above, using 400 ng of DNA in each PCR reaction.

3. Results

3.1. Bacterial isolation and typing

A total of 113 bacterial isolates were obtained, 54 from the mortality site (3 M) and 59 from the no mortality one (3 N). DNA samples from the 113 isolates were analysed by ERIC-PCR. Among these, a group of 7 isolates (r167, r169, r172, r173, r174, r175 and r190) shared a similar band profile (Fig. 2A, lanes 1–7). The 7 isolates showed a DNA profile similar to *V. ostreicida* type strain, as reported in Fig. 2B. These isolates were distributed in 3 out of 6 pools of the 3 M samples, representing 13 % of total recovered isolates. No isolate with a similar profile appeared in the 3 N samples (not shown).

Three isolates (r167, r172 and r190), representative from the 3 positive pools, were selected for phylogenetic analysis and phenotypic characterization. The results obtained were identical for these 3 isolates. So, one strain (r172) was selected to perform the virulence test and the whole genome sequencing. Once the PCR protocol for detecting *V. ostreicida* was designed, the 7 isolates sharing the ERIC profile were tested positive for *V. ostreicida*.

3.2. Phenotypic characterization

Phenotypic characterization was performed on 3 representative isolates (r167, r172 and r190), each of them recovered from a different 3 M pool. These isolates were recovered from MA plates, where the colonies had a colour that varied between translucent grey and opaque white. In all cases the colonies showed swarming (although this characteristic was not always present in successive cultures) and did not show adhesion to the agar, nor diffusible pigments. All isolates consist of gram-negative, fermentative, oxidase- and catalase-positive bacilli, capable of growing with 3–6 % NaCl and between 15–30 °C (growth at 8 and 35 °C showed variable results). Except for isolate r190, all others were able to grow on TCBS plates, displaying green colonies. In the API

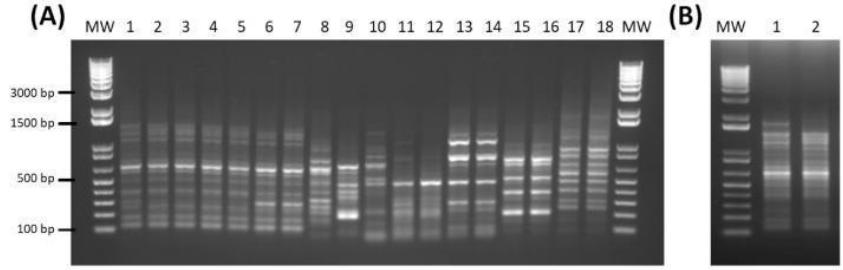

Fig. 2. (A) ERIC-PCR band profiles obtained with some of the isolates recovered from 3 M samples. MW: Invitrogen 1 Kb Plus Ladder; lanes 1–7: *V. ostreicida* isolates r172, r173, r174, r175, r167, r169 and r190, respectively; lanes 8–18, unidentified isolates from 3 M samples. (B) comparison between ERIC-PCR band profiles from *V. ostreicida* type strain (lane 1) and *V. ostreicida* mussel isolate r172 (lane 2). The type strain of *V. ostreicida* shows a band profile practically identical to that of the mussel isolates. Numbers on the left indicate the position of molecular size marker in bp.

20E miniaturized system, all tests gave negative results except gelatinase, which was positive for all isolates. Antibiogram readings showed that all isolates were sensitive to all antimicrobial compounds tested except ampicillin and amoxicillin (no isolate was sensitive to these two antibiotics). The type strain of *V. ostreicida*, characterized together with the mussel isolates, showed results similar to these, except in the API 20E strip, where it showed some discrepancies (acid production from glucose and mannitol was positive).

3.3. Genomic and phylogenetic analysis

Partial sequences were obtained from the 3 isolates (r167, r172 and r190) used for phenotypic characterization, for 16S rRNA, *ftsZ*, *gyrB*, *pyrH* and *rpoA* genes (GenBnk/EMBL/DDBJ accession numbers PP702166-PP702168, PP724677-PP724688). For the 16S gene, the similarity percentages between the three isolates were 99.63–99.92 %. According to the EzTaxon database, the percentage of similarity with the type strain of *V. ostreicida* was 99.35–99.64 %, while with the type strains of other Vibrio species it was always below 98 %. The results obtained for the *ftsZ*, *gyrB*, *pyrH* and *rpoA* genes confirmed the identification of the isolates as *V. ostreicida*. In all cases, the percentages of similarity between the 3 isolates obtained in this work, and with the *V. ostreicida* type strain, ranged between 99.26–100 %, while with other species the values were always below 88 %, 84 %, 87 % and 95 % for the mentioned genes, respectively. The concatenated sequences of the 5 genes (16S rRNA, *ftsZ*, *gyrB*, *pyrH* and *rpoA*; 3713 nt) showed similarity values of 99.73–99.89 % between the isolates and the type strain of *V. ostreicida*. However, the results with other type strains were always below 91 %, being *V. pectenicida*, *Vibrio coralliilyticus* and *V. neptunius* the closest species. The phylogenetic tree obtained from the concatenated sequences (Fig. 3A) showed consistent results with those observed for each gene individually, clearly grouping the mussel isolates with the *V. ostreicida* clade.

To better clarify the taxonomic relationships of the *V. ostreicida* strain

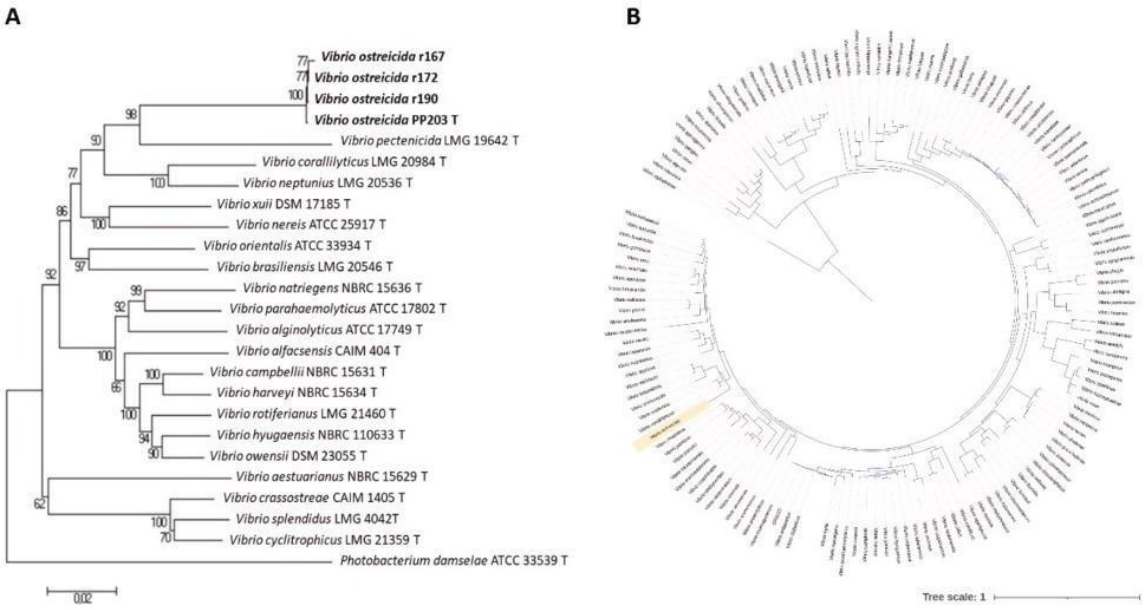

Fig. 3. (A) Phylogenetic tree based on concatenated sequences of five housekeeping genes (16S rDNA, 1321 nt; *ftsZ*, 572 nt; *gyrB*, 572 nt; *pyrH*, 417 nt; *and rpoA*, *831* nt) by the neighbour-joining method, showing the relationships between the 3 isolates recovered from mussels (r167, r172 and r190), and related species of the genus *Vibrio*. The numbers at the nodes indicate the levels of bootstrap based on 1000 replicates. (B) Phylogenetic reconstruction of the Vibrio genus obtained aligning a set of single-copy shared genes. Bootstrap values lower than 80 % are reported. The highlighted clade corresponds to *V. ostreicida* strain r172.

r172, the genome sequence was compared with all the other *Vibrio* species using a phylogenomic approach (Fig. 3B), and with the 3 other genomes of *V. ostreicida* strains available in GenBank (Supplementary Fig. S1) aligning the core SNP sites. Considering the phylogeny of the genus, *V. ostreicida* forms a sister clade to the group comprising *V. coralliilyticus*, *V. neptunius*, *V. pectenicida*, *V. tetraodonis* and *V. aquimaris* (these last two species has been effectively published but not validly published under the rules of the International Code of Nomenclature of Prokaryotes). Compared with the other representatives of the *V. ostreicida* species, *V. ostreicida* r172 is placed between the reference strain UCD-KL16 and the type strain (CECT 7398 and PP-203 T) (isolated from young oyster spat in a bivalve hatchery in Galicia (NW Spain) (Kumar et al., 2020; Prado et al., 2014).

3.4. Mussel histopathological analysis

Mussel tissue sections from both 3 M and 3 N samples were investigated for possible histopathological alterations and representative images are reported in Fig. 4. The 3 N samples did not show any particular tissue damage (see representative image of the hepatopancreas in Fig. 4A).

In contrast, 50 % of 3 M mussels showed atrophy of the hepatopancreas; moreover, 43.3 % exhibited necrosis and hemocytic infiltration in different tissues (hepatopancreas, gills, and mantle) to varying degrees. In cases of minor tissue alterations, there was a loss of absorptive cells in the hepatopancreatic epithelium, focal necrosis, and peeling, but the organ retained its overall normal appearance (Fig. 4B). More severe alterations included extensive necrosis of the tubular epithelium, along with hemocytic infiltration and abundant bacterial colonies, which distorted the tissue architecture, making the tubules indistinguishable (Fig. 4C). Bacilliform bacterial colonies were also found in the connective tissue (Fig. 4D). In worst cases, necrosis and peeling of the mantle epithelium, along with hemocytic infiltrates, were present (Fig. 4E), as well as necrosis of the epithelial cells of the branchial filaments, resulting in loss of cilia and cell shedding (Fig. 4F).

3.5. Development of a PCR-based diagnostic protocol for V. ostreicida

After the analysis of the alignments obtained with different genes, *gyrB* gene was selected as target, and a pair of primers that amplify a 491 bp DNA fragment were designed (c172-F1: 5′-GACAACGGGAACAAAAATCC-3′; c172-R1: 5′-ACACGACCGCGGTTAGGC-3′). The

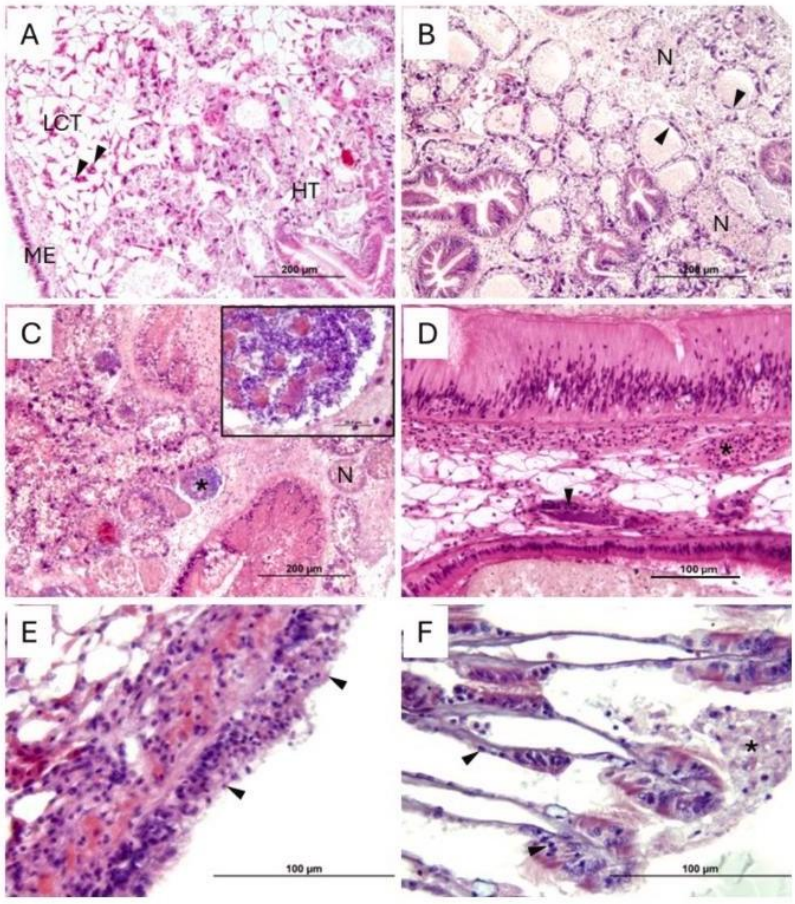

Fig. 4. Histological sections of *Mytilus galloprovincialis* from mortality (3 M) and no mortality (3 N) samples. (A) Section of healthy *M. galloprovincialis* (3 N samples) showing the hepatopancreatic tissue (HT), mantle epithelium (ME) and adipogranular cells (arrowheads) in the loose connective tissue (LCT). (B) Mussel with minor tissue alterations: atrophy (arrowhead) and necrosis (N) in mussels hepatopancreas. (C) Severe necrosis (N) in hepatopancreas of mussel with bacterial colonies (*). Note the appearance of bacteria bacilli (in insert) (D) Hemocytic infiltrate (*) and bacterial colony (arrowhead) in the loose connective tissue around the intestine. (E) Necrosis of the mantle epithelium (arrowheads) and underlying hemocytic infiltrate. (F) Necrosis of the branchial filaments (arrowheads). Note the presence of cell peeling and detritus (*). H&E stain.

specificity of the protocol was tested using DNA from target and non-target strains shown in Table 1. The *V. ostreicida* isolates recovered from mussels and the type strain of this species showed the expected amplification product of 491 bp, whereas no amplicon was detected from strains belonging to other species (Fig. 5).

The detection limit of the protocol, using DNA dilutions, was 100 fg (up to 10 fg in some cases) when pure DNA from *V. ostreicida* CECT 7398^T was used, and also 100 fg when 1 μg of oyster DNA (extracted from whole tissue) was added to the same dilutions. On the contrary, when 1 μg of mussel DNA was added to the same dilutions, the results varied between individuals. With two of the mussels used, the detection limit ranged between 1 and 100 fg; however, when DNA from two other different mussels was used, a total blockage of the PCR was observed. The tissues of one of these mussels were used to determine if the possible inhibitor was located in the mantle and/or in the hepatopancreas. When the assay was repeated using 1 μg of mantle DNA, the detection limit was 1 fg, but when 1 μg of hepatopancreas DNA from the same individual was used, a complete blockage of the PCR was again observed. When cell dilutions were used, the detection limit was of 0.5 cfu/PCR tube, whereas when dilutions of cells were used mixed with mussel tissue (mantle), the protocol was able to detect $3x10^2$ cfu/30 mg of tissue. On the other hand, no bands of the expected size (nor non-specific bands) were observed when only mollusk DNA (from mussel, or from oyster) was used as a template.

Finally, the protocol was used with DNA samples from the 6 pools obtained from the area where mortality had been observed (3 M samples). Five of the 6 pools tested were positive by PCR, including the 3 pools from which the isolates r167, r172 and r190 were recovered, and from another 2 pools where *V. ostreicida* had not been detected by cultural methods (Fig. 6).

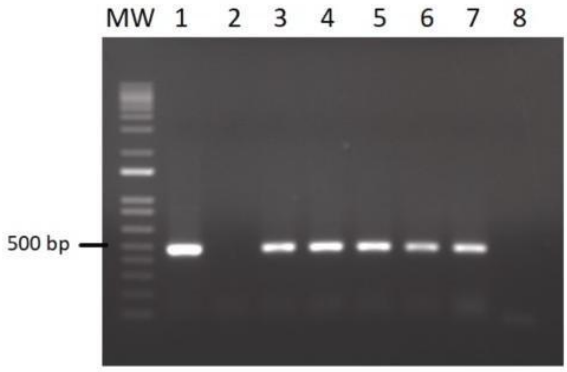

Fig. 6. PCR profiles using the set of primers based on *gyrB* gene with DNA templates from 3 M sampling pools (tissue homogenates). MW: Invitrogen 1 Kb Plus Ladder; lane 1: positive control (*V. ostreicida* CECT 7398^T); lanes 2–7: DNA samples from pools 1 to 6, respectively; lane 8: negative control. Numbers on the left indicate the position of molecular size marker in bp. Except for pool 1, in all cases the 491 bp band was detected. Previously, *V. ostreicida* had been detected by culture in pools 2, 3 and 6.

3.6. Virulence assay

The 2 groups of mussels inoculated with isolate *V. ostreicida* r172 presented an average mortality of 50 ± 10 % at 5 days. PCRs carried out from the cultures obtained from the samples of these dead mussels were all positive for *V. ostreicida*, confirming the recovery of the viable pathogen from them (data not shown). Mortality in the 2 control groups was 10 %.

4. Discussion

This article describes for the first time the appearance of *V. ostreicida* strains associated with mortality in the Mediterranean mussel *M. galloprovincialis*, an economically important species in the context of aquaculture in Europe. Although mortality in this species is usually high in the studied area (Ebro delta, northeast Spain) in summer, due to the high water temperatures reached in the growing areas (Ramón et al., 2007), in this case, the mortality episode was relevant given that, contrary to usual, it took place in spring, with a water temperature of 18 °C. Temperature plays a determining role in the development of other diseases caused by vibrios; this is the case, for example, of brown ring disease caused by *V. tapetis*, which usually appears at temperatures between 12–17 °C, while temperatures above 21 °C usually prevent the appearance of the disease (López et al., 2023; Paillard, 2004). High temperatures can also be implicated in oyster's summer mortalities linked with *V. aestuarianus* (Cowan et al., 2024). On the other hand, interestingly, the lowest part of the mussel ropes at the farm where mortality was observed (3 M) had high contents of mud; this could have been a stressful factor (Collinson & Rees, 1978) since mortality was mainly observed at the bottom of the ropes and not at the surface. A sediment resuspension event in this area could also have favoured the proliferation of different vibrios, including *V. ostreicida* (Turner et al., 2009).

In the case of *V. ostreicida*, little is known about its epidemiology, host range and the factors that determine its virulence. The species was detected in April 1999 by Prado et al. (2005, 2014) associated with mortalities in oyster *O. edulis* larvae in Galicia (northwest Spain). The type strain, isolated from the surface of the affected tanks, was capable of causing a mortality of 98.5 % in virulence tests carried out with oyster larvae at a temperature of 22 °C. In this work, the preliminary evaluation of the virulence of one of the *V. ostreicida* isolates (r172), carried out

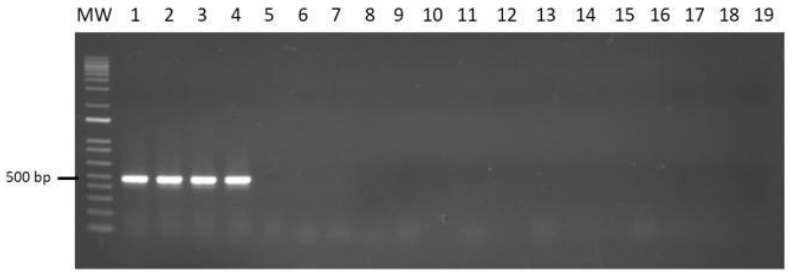

Fig. 5. PCR profiles using the set of primers based on *gyrB* gene with DNA templates from *V. ostreicida* strains and some non-target related species. MW: Invitrogen 1 Kb Plus Ladder; lanes 1–4: *V. ostreicida* strains CECT 7398^T, r167, r172 and r190, respectively; lanes 5–18: type strains of *V. aestuarianus*, *V. alginolyticus*, *V. anguillarum*, *V. campbellii*, *V. coralliilyticus*, *V. harveyi*, *V. ichthyoenteri*, *V. orientalis*, *V. owensii*, *V. pectenicida*, *V. rotiferianus*, *V. scophtahlmi* and *V. splendidus*, respectively; lane 19: negative control. Numbers on the left indicate the position of molecular size marker in bp. Only the *V. ostreicida* strains showed the expected 491 bp band.

by injection of a dose of $9x10^6$ cfu/mussel, caused an average mortality of 50 % in 5 days, a result that seems to corroborate the pathogenicity of this strain for *M. galloprovincialis*. This species of mussel is generally considered to be very resistant to infectious diseases, due to the apparent absence of mass mortalities in its populations, but also due to the results obtained by different authors when carrying out virulence tests with it. Thus, Ben Cheikh et al. (2024) found that *M. galloprovincialis* was more resistant to *V. splendidus*-like strains than other *Mytilus* species, and Romero et al. (2014b) found that *V. splendidus* and *V. aestuarianus* strains recovered from oyster mortalities, were capable of causing mortality only when extremely high bacterial doses (10^{10} cfu/mussel) were used under stressful conditions. In the present work, although we did not seek to create stressful conditions during the virulence assay, for technical reasons, the trial had to be carried out at 24 °C instead of the 18 °C observed in the outbreak; therefore the thermal stress was probably greater than that during the mortality episode. In the near future, tests will be carried out using a wider range of temperatures, in order to clarify the influence of this factor on the development of the disease. It is, however, worth mentioning that the recurrent mass mortality episodes in the Delta shellfish growing area have been consistently associated with heatwaves, when temperatures rise above 28 °C and holds for weeks (Soriano-González et al., 2019); this was clearly not the case in the mortality episode described here. Further studies should also investigate the virulence of this species on mussel larvae, as well as their mechanisms to evade the host immune systems.

Histopathological analysis of mussels naturally infected by *V. ostreicida* (3 M) showed necrosis and hemocytic infiltration in the gills and mantle, similar to what has been reported in mass mortality events of Pacific oysters (*Magallana gigas*) infected with *V. aestuarianus* (Cowan et al., 2024). However, the hepatopancreas was the most affected organ, suggesting that it could be the primary target organ of *V. ostreicida*. Similar damage to the hepatopancreas has been reported in larvae of the mussel *Perna canaliculus* experimentally infected with *V. splendidus* and strains of the *V. coralliilyticus/neptunius*-like complex (Kesarcodi-Watson et al., 2009). Extensive necrosis of the hepatopancreas tubules, accompanied by low hemocytic infiltration observed primarily in the early stages of infection, could be related to the release of extracellular products by *V. ostreicida*. However, this remains unknown. Future studies should focus on elucidating the pathogenesis of the disease and investigating the relationship between the observed damage and the production of extracellular products.

The identification of the *V. ostreicida* isolates was based on both phenotypic and genotypic data. The phenotypic profiles of the bacterial mussel isolates shared the same characteristics of the strains associated with the oyster larvae mortality in Galicia (including the CECT 7398^T type strain), except for their negativity to acid production from glucose and mannitol. The ERIC-PCR band profiles of *V. ostreicida* isolates were similar to the type strain, despite of being strains isolated with a difference of 23 years, coming from different geographical locations (Atlantic Ocean and Mediterranean Sea) and different hosts (oyster and mussel), which could indicate that this species is quite homogeneous in this respect. We need to consider, however, that shellfish movements happen frequently, associated with different human activities such aquaculture, ballast water from ships, etc., which could be in the origin of this finding.

The analysis of the sequences of 5 housekeeping genes (16S, *ftsZ*, *gyrB*, *pyrH*, *rpoA*) allowed the identification of the isolates as *V. ostreicida*. The 16S gene sequences of mussel isolates showed similarity values clearly above the intraspecific variability limit of 98.7 % proposed by Stackebrandt & Ebers (2006), between them and with the *V. ostreicida* type strain, while these values were below 98 % with the type strains of other Vibrio species. The rest of the genes analyzed showed even more discriminating results, and the phylogenetic analysis carried out with the concatenated sequences of the 5 genes clearly grouped the mussel isolates with the *V. ostreicida* cluster. Moreover, the MLSA phylogenetic analysis coincides with that obtained in the sequencing of the complete genome of r172.

Finally, the lack of rapid diagnostic methods for *V. ostreicida* not only makes it difficult to work with this species, but also to determine its real importance as a mollusk pathogen. All detection methods so far available require cultivation and are therefore time-consuming; moreover, the great bacterial diversity present in samples of filter-feeding organisms makes the detection of potential pathogens even more challenging. These limitations could have played a role in the fact that *V. ostreicida* has not been described in association with other mortality outbreaks in mollusks. This led us to develop a diagnostic method based on PCR that would allow rapid detection of the pathogen from pure cultures, as well as from tissues. The specificity of the protocol was validated with strains of 25 species, ecologically or taxonomically related, with no false positives nor non-specific amplifications observed in any case. The detection limit with pure samples was as low as 100 fg of DNA or 0.5 cells per tube. The addition of 1 μg of oyster DNA kept the detection range unchanged, with the target DNA being detected at a target:background ratio of $1:10^7$. However, when mussel DNA was added, the results were variable depending on the individuals, and while in some cases detection limits similar to those observed with oyster DNA were obtained, in other cases the PCR was completely blocked. It is known that high amounts of non-target DNA and tissue debris can act as PCR inhibitors (Becker et al., 2000; Wilson, 1997). In this case, the problem does not seem to be due to an excess amount of DNA, but to the presence of inhibitors in mussel tissues, probably in the hepatopancreas, since with mantle samples a blockage of the PCR was not observed (similar results to those observed with oysters were obtained). The detection of *V. ostreicida* in mussel samples naturally infected by this species (3 M), however, did not appear to be affected in this regard. The samples used consisted of whole mussel homogenates that included a mixture of tissues (gills, mantle, hepatopancreas…); even so, 5 of the 6 pools used gave positive results in the PCR, demonstrating a greater sensitivity than by culture (where only 3 of the pools were positive). Despite this good result, it would be of interest for the future to determine the nature of the inhibitors present in the mussel tissues, also clarifying whether they are typical of some mussel tissue or are due to some type of contamination. Another possible explanation could be the high content of lysosomal hydrolases (including DNAses) in mussel hepatopancreas.

In conclusion, the results of this work allow us to expand the number of susceptible hosts of *V. ostreicida*, while constituting the first documented case of mass mortality associated to infectious disease in one of the most relevant species in European aquaculture, *M. galloprovincialis*. The discovery of *V. ostreicida* in Mediterranean mussels highlights its potential as an emerging pathogen of concern in marine ecosystems; its ability to evade the immune systems of a host as resilient as *M. galloprovincialis* (Figueras et al., 2019) suggests a significant risk not only to mussel populations but also to other bivalves. The impact of this potential pathogen in a transforming environment underscores the need for further research on its pathogenicity, infection mechanisms, and potential mitigation strategies. In this context, the PCR protocol developed here will contribute to easier diagnosis and to clarify the relevance of this pathogen in the future. Further studies will investigate also the influence of temperature on virulence, as well as the effect of *V. ostreicida* isolates on mussel larvae, and on host immune responses.

CRediT authorship contribution statement

Jose R. Lopez: Writing – review & editing, Writing – original draft, Methodology, Investigation, Data curation, Conceptualization. **Martina Leonessi:** Writing – review & editing, Writing – original draft, Data curation. **Margarita Fernandez-Tejedor:** Writing – review & editing, Writing – original draft, Validation, Supervision, Project administration, Methodology, Funding acquisition, Data curation, Conceptualization. **Manon Auguste:** Writing – review & editing, Writing – original draft, Data curation. **Lapo Doni:** Software, Formal analysis. **Yanis Cruz-Quintana:** Writing – review & editing, Writing – original draft,

Investigation, Data curation. **Emanuele Bosi:** Software, Formal analysis. **Luigi Vezzulli:** Writing – review & editing, Writing – original draft, Supervision. **Karl Andree:** Writing – review & editing. **Laura Canesi:** Writing – review & editing, Writing – original draft, Supervision. **Dolors Furones:** Writing – review & editing, Writing – original draft, Supervision, Project administration, Methodology, Investigation, Funding acquisition, Data curation, Conceptualization.

Funding

This work was supported by the project "Emergent risks related to shellfish mortalities in the Ebro delta-REMBE". ARP140/20/000011, funded by the European Maritime and Fisheries Fund (EMFF)-European Commission and Generalitat de Catalunya.

Declaration of competing interest

The authors declare that they have no known competing financial interests or personal relationships that could have appeared to influence the work reported in this paper.

Appendix A. Supplementary material

Supplementary data to this article can be found online at https://doi.org/10.1016/j.jip.2025.108399.

References

Beaz-Hidalgo, R., Balboa, S., Romalde, J.L., Figueras, M.J., 2010. Diversity and pathogenecity of Vibrio species in cultured bivalve molluscs. Environ. Microbiol. Rep. 2 (1), 34–43. https://doi.org/10.1111/j.1758-2229.2010.00135.x.

Becker, S., Böger, P., Oehlmann, R., Ernst, A., 2000. PCR bias in ecological analysis: a case study for quantitative Taq nuclease assays in analyses of microbial communities. Appl. Environ. Microbiol. 66 (11), 4945–4953. https://doi.org/10.1128/AEM.66.11.4945-4953.2000.

Ben Cheikh, Y., Massol, F., Giusti-Petrucciani, N., Travers, M.-A., 2024. Impact of epizootics on mussel farms: Insights into microbiota composition of Mytilus species. Microbiol. Res. 280, 127593. https://doi.org/10.1016/j.micres.2023.127593.

Ben Cheikh, Y., Travers, M.-A., Le Foll, F., 2017. Infection dynamics of a *V. splendidus* strain pathogenic to *Mytilus edulis*: *In vivo* and *in vitro* interactions with hemocytes. Fish Shellfish Immunol. 70, 515–523. https://doi.org/10.1016/j.fsi.2017.09.047.

Ben Cheikh, Y., Travers, M.-A., Morga, B., Godfrin, Y., Rioult, D., Le Foll, F., 2016. First evidence for a Vibrio strain pathogenic to Mytilus edulis altering hemocyte immune capacities. Dev. Comp. Immunol. 57, 107–119. https://doi.org/10.1016/j.dci.2015.12.014.

Bosi, E., Taviani, E., Avesani, A., Doni, L., Auguste, M., Oliveri, C., Leonessi, M., Martinez-Urtaza, J., Vetriani, C., Vezzulli, L., 2024. Pan-genome provides insights into vibrio evolution and adaptation to deep-sea hydrothermal vents. Genome Biol. Evol. 16 (7), evae131. https://doi.org/10.1093/gbe/evae131.

Bouras, H., Quesnelle, Y., Barozet, A., Goux, D., Blin, J.-L., Savary, M., Zatylny-Gaudin, C., Houssin, M., 2023. First isolation of Francisella halioticida strains from blue mussel (Mytilus edulis) in Normandy. France. J. Invert. Pathol. 200, 107950. https://doi.org/10.1016/j.jip.2023.107950.

Bunpa, S., Nishibuchi, M., Thawonsuwan, J., Sermwittayawong, N., 2018. Genetic heterogeneity among Vibrio alginolyticus strains, and design of a PCR-based identification method using gyrB gene sequence. Can. J. Microbiol. 64 (1), 1–10. https://doi.org/10.1139/cjm-2017-0269.

Charles, M., Bernard, I., Villalba, A., Oden, E., Burioli, E.A.V., Allain, G., Trancart, S., Bouchart, V., Houssin, M., 2020a. High mortality of mussels in northern Brittany—evaluation of the involvement of pathogens, pathological conditions and pollutants. J. Invertebr. Pathol. 170, 107308. https://doi.org/10.1016/j.jip.2019.107308.

Charles, M., Villalba, A., Meyer, G., Trancart, S., Lagy, C., Bernard, I., Houssin, M., 2020b. First detection of Francisella halioticida in mussels Mytilus spp. experiencing mortalities in France. Dis. Aquat. Organ. 140, 203–208. https://doi.org/10.3354/dao03505.

Chen, L., Zheng, D., Liu, B., Yang, J., Jin, Q., 2016. VFDB 2016: Hierarchical and refined dataset for big data analysis—10 years on. Nucleic Acids Res. 44 (D1), D694–D697. https://doi.org/10.1093/nar/gkv1239.

Collinson, R.I., Rees, C.P., 1978. Mussel mortality in the Gulf of La Spezia. Italy. Marine Pollut. Bull. 9 (4), 99–101.

Cowan, M.W., Pearce, C.M., Green, T.J., Finston, T., Meyer, G.R., McAmmond, B., Van Hamme, J.D., Bottos, E.M., Marshall, R., Evans, W., Sutherland, T.F., de la Bastide, P. Y., 2024. Abundance of Vibrio aestuarianus, water temperature, and stocking density are associated with summer mortality of Pacific oysters in suspended culture. Aquac. Int. 32 (4), 5045–5066. https://doi.org/10.1007/s10499-024-01415-5.

Destoumieux-Garzón, D., Canesi, L., Oyanedel, D., Travers, M.-A., Charrière, G.M., Pruzzo, C., Vezzulli, L., 2020. Vibrio–bivalve interactions in health and disease. Environ. Microbiol. 22 (10), 4323–4341. https://doi.org/10.1111/1462-2920.15055.

Edgar, R.C., 2004. MUSCLE: Multiple sequence alignment with high accuracy and high throughput. Nucleic Acids Res. 32 (5), 1792–1797. https://doi.org/10.1093/nar/gkh340.

Eggermont, M., Bossier, P., Pande, G.S.J., Delahaut, V., Rayhan, A.M., Gupta, N., Islam, S.S., Yumo, E., Nevejan, N., Sorgeloos, P., Gomez-Gil, B., Defoirdt, T., 2017. Isolation of Vibrionaceae from wild blue mussel (Mytilus edulis) adults and their impact on blue mussel larviculture. FEMS Microbiol. Ecol. 93 (4). https://doi.org/10.1093/femsec/fix039.

EUMOFA. & European Commission. Directorate General for Maritime Affairs and Fisheries. (2024). *Study on the challenges of aquaculture products in food outlets.* Publications Office. https://data.europa.eu/doi/10.2771/967261.

Figueras, A., Moreira, R., Sendra, M., Novoa, B., 2019. Genomics and immunity of the Mediterranean mussel Mytilus galloprovincialis in a changing environment. Fish Shellfish Immunol. 90, 440–445. https://doi.org/10.1016/j.fsi.2019.04.064.

Hall, T., 1999. BioEdit: a user-friendly biological sequence alignment editor and analysis program for Windows 95/98/ NT. Nucleic Acids Symp. Ser. 41, 95–98.

Howard, Dorothy W., Sarbanes Cooperative Oxford Laboratory, & National Centers for Coastal Ocean Science (U.S.). (2004). *Histological techniques for marine bivalve mollusks and crustaceans.* https://repository.library.noaa.gov/view/noaa/1790.

Kalyaanamoorthy, S., Minh, B.Q., Wong, T.K.F., Von Haeseler, A., Jermiin, L.S., 2017. ModelFinder: fast model selection for accurate phylogenetic estimates. Nat. Methods 14 (6), 587–589. https://doi.org/10.1038/nmeth.4285.

Kesarcodi-Watson, A., Kaspar, H., Lategan, M.J., Gibson, L., 2009. Two pathogens of Greenshell mussel larvae, Perna canaliculus: vibrio splendidus and a V. coralliilyticus/neptunius-like isolate. J. Fish Dis. 32 (6), 499–507. https://doi.org/10.1111/j.1365-2761.2009.01006.x.

Kumar, R.S., Galvis, F., Wasson, B.J., Saw, J.H., Oline, D.K., Barja, J.L., Ushijima, B., Koyack, M.J., Prado, S., Videau, P., 2020. Draft genome sequence of vibrio ostreicida strain PP-203, the type strain of a pathogen that infects bivalve larvae. Microbiol. Resour. Announce. 9 (35), e00913–e00920. https://doi.org/10.1128/MRA.00913-20.

Letunic, I., Bork, P., 2021. Interactive tree of Life (iTOL) v5: an online tool for phylogenetic tree display and annotation. Nucleic Acids Res. 49 (W1), W293–W296. https://doi.org/10.1093/nar/gkab301.

Llebot, C., Solé, J., Delgado, M., Fernández-Tejedor, M., Camp, J., Estrada, M., 2011. Hydrographical forcing and phytoplankton variability in two semi-enclosed estuarine bays. J. Mar. Syst. 86 (3), 69–86. https://doi.org/10.1016/j.jmarsys.2011.01.004.

López, J.R., Lorenzo, L., Alcantara, R., Navas, J.I., 2017. Characterization of Aliivibrio fischeri strains associated with disease outbreak in brill Scophthalmus rhombus. Dis. Aquat. Organ. 124 (3), 3. https://doi.org/10.3354/dao03123.

López, J.R., Romalde, J.L., López-Sanmartín, M., Navas, J.I., 2023. First evidence of vibrio tapetis as causal agent of disease outbreak in meagre (argyrosomus regius). Fishes 8 (1), 1. https://doi.org/10.3390/fishes8010022.

Lupo, C., Bougeard, S., Le Bihan, V., Blin, J.L., Allain, G., Azéma, P., Benoit, F., Béchemin, C., Bernard, I., Blachier, P., Brieau, L., Danion, M., Garcia, A., Gervasoni, E., Glize, P., Lainé, A., Lapègue, S., Mablouké, C., Poirier, L., Le Bouquin, S., 2021. Mortality of marine mussels Mytilus edulis and M. galloprovincialis: systematic literature review of risk factors and recommendations for future research. Rev. Aquac. 13 (1), 1. https://doi.org/10.1111/raq.12484.

Minh, B.Q., Schmidt, H.A., Chernomor, O., Schrempf, D., Woodhams, M.D., Von Haeseler, A., Lanfear, R., 2020. IQ-TREE 2: new models and efficient methods for phylogenetic inference in the genomic era. Mol. Biol. Evol. 37 (5), 1530–1534. https://doi.org/10.1093/molbev/msaa015.

Paillard, C., 2004. A short-review of brown ring disease, a vibriosis affecting clams, Ruditapes philippinarum and Ruditapes decussatus. Aquat. Living Resour. 17 (4), 4. https://doi.org/10.1051/alr:2004053.

Prado, S., Dubert, J., Romalde, J.L., Toranzo, A.E., Barja, J.L., 2014. Vibrio ostreicida sp. Nov., a new pathogen of bivalve larvae. Int. J. Syst. Evol. Microbiol. 64 (Pt 5), 1641–1646. https://doi.org/10.1099/ijs.0.051417-0.

Prado, S., Romalde, J.L., Montes, J., Barja, J.L., 2005. Pathogenic bacteria isolated from disease outbreaks in shellfish hatcheries. First description of Vibrio neptunius as an oyster pathogen. Dis. Aquat. Organ. 67 (3), 209–215. https://doi.org/10.3354/dao067209.

Ramón, M., Fernández, M., Galimany, E., 2007. Development of mussel (*Mytilus galloprovincialis*) seed from two different origins in a semi-enclosed Mediterranean Bay (N.E. Spain). Aquaculture 264 (1), 148–159. https://doi.org/10.1016/j.aquaculture.2006.11.014.

Romero, A., Chamorro, R., Dios, S., Figueras, A., & Novoa, B. (2014). *Occurrence, seasonality and infectivity of Vibrio strains in natural populations of mussels Mytilus galloprovincialis.*

Romero, A., del Costa, M., Forn-Cuni, G., Balseiro, P., Chamorro, R., Dios, S., Figueras, A., Novoa, B., 2014b. Occurrence, seasonality and infectivity of Vibrio strains in natural populations of mussels Mytilus galloprovincialis. Dis. Aquat. Organ. 108 (2), 149–163. https://doi.org/10.3354/dao02701.

Rozen, S., Skaletsky, H., 2000. Primer3 on the WWW for general users and for biologist programmers. *Methods in Molecular Biology (Clifton, N.J.)* 132, 365–386. https://doi.org/10.1385/1-59259-192-2:365.

Saitou, N., Nei, M., 1987. The neighbour-joining method: a new method for reconstructing phylogenetic trees. Mol. Biol. Evol. https://doi.org/10.1093/oxfordjournals.molbev.a040454.

Sawabe, T., Kita-Tsukamoto, K., Thompson, F.L., 2007. Inferring the evolutionary history of vibrios by means of multilocus sequence analysis. J. Bacteriol. 189 (21), 7932–7936. https://doi.org/10.1128/JB.00693-07.

Soriano-González, J., Angelats, E., Fernández-Tejedor, M., Diogene, J., Alcaraz, C., 2019. First results of phytoplankton spatial dynamics in two NW-Mediterranean bays from chlorophyll-a estimates using sentinel 2: potential implications for aquaculture. Remote Sens. (Basel) 11 (15), 15. https://doi.org/10.3390/rs11151756.

Stackebrandt, E., Ebers, J., 2006. Taxonomic parameters revisited: tarnished gold standards. Microbiol. Today 8, 6–9.

Thompson, F.L., Gevers, D., Thompson, C.C., Dawyndt, P., Naser, S., Hoste, B., Munn, C. B., Swings, J., 2005. Phylogeny and molecular identification of vibrios on the basis of multilocus sequence analysis. Appl. Environ. Microbiol. 71 (9), 5107–5115. https://doi.org/10.1128/AEM.71.9.5107-5115.2005.

Turner, J.W., Good, B., Cole, D., Lipp, E.K., 2009. Plankton composition and environmental factors contribute to Vibrio seasonality. ISME J. 3 (9), 1082–1092. https://doi.org/10.1038/ismej.2009.50.

Wang, D., Ma, L., Xiong, B.B., Zhu, J., Lu, J.Z., Meng, L.-L., Liu, Y.-G., 2024. Rapid identification of related species of *vibrio* by *gyr*B gene degenerative primers. LWT 191, 115594. https://doi.org/10.1016/j.lwt.2023.115594.

Weisburg, W.G., Barns, S.M., Pelletier, D.A., Lane, D.J., 1991. 16S ribosomal DNA amplification for phylogenetic study. J. Bacteriol. 173 (2), 697–703. https://doi.org/10.1128/JB.173.2.697-703.1991.

Wilson, I.G., 1997. Inhibition and facilitation of nucleic acid amplification. Appl. Environ. Microbiol. 63 (10), 3741–3751.

Zhang, X., Alter, T., Gölz, G., 2019. Characterization of Arcobacter spp. Isolated from retail seafood in Germany. Food Microbiol. 82, 254–258. https://doi.org/10.1016/j.fm.2019.02.010.

Supplementary material to:

First description of *Vibrio ostreicida* as putative causal agent of disease in Mediterranean mussel (*Mytilus galloprovincialis*) and development of a PCR protocol for its rapid diagnosis

Results

Phylogenetic analysis

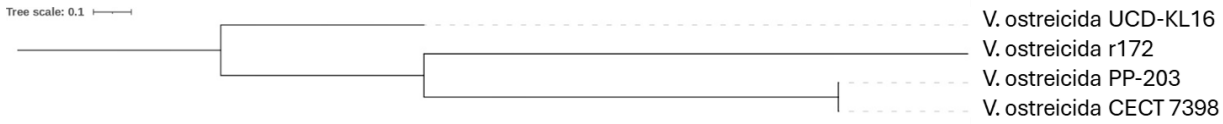

Fig. S1. Core-SNP phylogeny of the *V. ostreicida* species. The tree reports the phylogenetic relationships between *V. ostreicida* strains with a sequenced genome.

Phylogenetic and functional characterisation of the *V. ostreicida* strain r172

The genome assembly features of the *V. ostreicida* strain *r172* are reported in Supplementary Table S2. Briefly, we obtained a complete genome with 81 contigs with a total size of 4657173 base pairs, for which 4303 genes have been predicted, 4249 of which are protein-coding. A taxonomic classification has been performed with ANI, identifying the reference strain of the *V. ostreicida* species (UCD-KL16) (isolated on seagrass *Zostera marina*) collected from Bodega Bay, California, (Lujan et al., 2017) as the most similar (ANI=99.42%). By comparison, the reference strain genome embeds 60 contigs for a total size of 4496068 base pairs. The genome sequence was scanned to identify functional elements. In particular, we focused on two classes of genes, i.e. those associated with virulence and antibiotic resistance. Regarding the putative virulence factors, we identified a total of 4 genes: *flgB*, *flgC*, *cheW* and *cheY* (Table S3). The phyletic distribution of these genes revealed a substantial conservation within the clade comprising *V. corallilyticus* and *V. neptunius*. Moreover, they can be found also in other pathogenic species such as *V. vulnificus*. For what concern antibiotic resistance genes, there were a total of 5 resistance genes, which are the tetracycline-resistance gene *tet(34)*, three chloramphenicol acetyltransferase (*catC*, *catB* and *catB9*) and the beta-lactamase *bla* (Table S3).

Table S1: Genome assembly information

	Contigs	Size (bp)	GC%	Genes	CDSs	tRNA	tmRNA
V.ostreicida r172	81	4,657,173	45.25	4303	4249	53	1

Table S2: Virulence factors and antibiotic resistance genes identified in *V. ostreicida r172*. The table reports the antibiotic resistance genes identified in *V. ostreicida r172*.

Putative virulence factors	*flgB*
	flgC
	cheW
	cheY

Antibiotic resistance genes	tetracycline-resistance	*tet(34)*
	chloramphenicol	*catC*
chloramphenicol acetyltransferase gene		*catC* *catB* *catB9*
beta-lactamase		*bla*

Chapter 2:

Interactions between the oyster larval pathogen *Vibrio ostreicida* and the bivalve hosts *Mytilus galloprovincialis* and *Magallana gigas*.

The results of this work have been published in Frontiers in Immunology 16:1711477. doi: 10.3389/fimmu.2025.1711477

In this chapter the results of *in vitro* short-term exposure experiments of *V. ostreicida* r172 towards

M. galloprovincialis and *M. gigas* are reported. Using *in vitro* short-term exposure experiments, the effects of *V. ostreicida* on mussel early larval development and hemolymph immune responses were evaluated. Immune responses were compared with those of the oyster *M. gigas* (see graphical abstract). Both live and heat-killed *V. ostreicida* significantly impaired normal mussel larval development with a dose-concentration effect (EC50 $\approx 10^3$ - 10^4 CFU/mL), with live bacteria inducing shell malformations and heat-killed *Vibrio* causing developmental arrest. In adult mussel hemocytes, exposure to heat-killed *V. ostreicida* led to dose-dependent lysosomal destabilization, reduced phagocytic activity, and increased intracellular ROS production evaluated by Confocal Fluorescence Microscopy. Similar lysosomal destabilization was observed with live *V. ostreicida*, which also stimulated extracellular ROS and nitric oxide release, but only in the presence of hemolymph serum (HS). Mussel HS displayed a strong bactericidal activity towards *V. ostreicida*, highlighting a key role for soluble immune effectors. In oyster hemocytes, *V. ostreicida* induced similar lysosomal stress; however, neither hemocytes nor serum showed any bactericidal activity towards this strain. This data represents the first results on the interactions of an environmental strain of *V. ostreicida* with marine bivalve immune system. The species-specific differences observed in immune responses highlight the complexity of host-pathogen interactions in these organisms and emphasize the need for further investigation into immune responses of different aquacultured species.

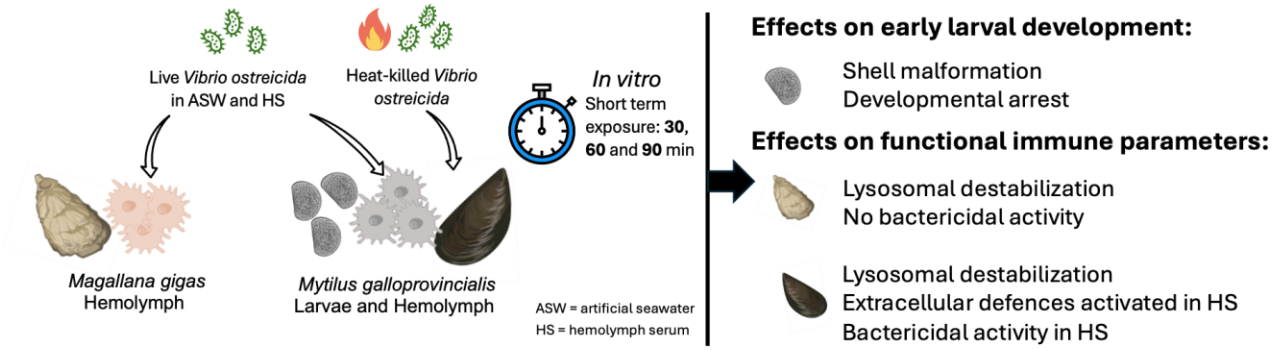

frontiers | Frontiers in Immunology

TYPE Original Research
PUBLISHED 26 November 2025
DOI 10.3389/fimmu.2025.1711477

Check for updates

OPEN ACCESS

EDITED BY
Antonio Figueras,
Spanish National Research Council (CSIC), Spain

REVIEWED BY
Marco Gerdol,
University of Trieste, Italy
Patricia Diaz-Rosales,
Spanish National Research Council (CSIC), Spain

*CORRESPONDENCE
Martina Leonessi
martina.leonessi@edu.unige.it

RECEIVED 23 September 2025
REVISED 03 November 2025
ACCEPTED 12 November 2025
PUBLISHED 26 November 2025

CITATION
Leonessi M, Auguste M, Lopez JR, Balbi T, Ciacci C, Oliveri C, Vezzulli L, Furones D and Canesi L (2025) Interactions between the oyster larvae pathogen *Vibrio ostreicida* and the bivalve hosts *Mytilus galloprovincialis* and *Magallana gigas*.
Front. Immunol. 16:1711477.
doi: 10.3389/fimmu.2025.1711477

COPYRIGHT
© 2025 Leonessi, Auguste, Lopez, Balbi, Ciacci, Oliveri, Vezzulli, Furones and Canesi. This is an open-access article distributed under the terms of the Creative Commons Attribution License (CC BY). The use, distribution or reproduction in other forums is permitted, provided the original author(s) and the copyright owner(s) are credited and that the original publication in this journal is cited, in accordance with accepted academic practice. No use, distribution or reproduction is permitted which does not comply with these terms.

Interactions between the oyster larvae pathogen *Vibrio ostreicida* and the bivalve hosts *Mytilus galloprovincialis* and *Magallana gigas*

Martina Leonessi [1,2]*, Manon Auguste [1,2], Jose R. Lopez [3,4], Teresa Balbi [1,2], Caterina Ciacci [5], Caterina Oliveri [1], Luigi Vezzulli [1,2], Dolors Furones [3] and Laura Canesi [1,2]

[1]Department of Earth, Environmental and Life Sciences (DISTAV), University of Genoa, Genoa, Italy, [2]National Biodiversity Future Center, Palermo, Italy, [3]Aquaculture Program, Institute of Agrifood Research and Technology (IRTA), La Ràpita, Spain, [4]Universidade de Santiago de Compostela, Santiago de Compostela, Spain, [5]Department of Biomolecular Sciences (DIBS), University 'Carlo Bo' of Urbino, Urbino, Italy

Introduction: Marine bivalves are continuously exposed to a variety of environmental stressors, including different Vibrio species potentially involved in disease outbreaks that have severely impacted farmed populations over the past two decades. *Vibrio ostreicida* was firstly identified as a lethal pathogen for oyster larvae (*Ostrea edulis*), but its interactions with the immune system of the bivalve host are largely unexplored.
Methods: In this study, we investigated the pathogenic potential of a *V. ostreicida* strain r172, isolated from a 2022 mortality event in adult *Mytilus galloprovincialis* in the Ebro Delta (Spain), focusing on mussel early larval development and hemolymph immune responses in *in vitro* short-term exposure experiments. Immune responses were compared with those of the oyster *Magallana gigas*.
Results: Both live and heat-killed *V. ostreicida* significantly impaired normal larval development with a dose-concentration effect ($EC_{50} \approx 10^3$ - 10_4 CFU/mL), with live bacteria inducing shell malformations and heat-killed Vibrio causing developmental arrest. In the hemocytes of adult mussels, exposure to heat-killed *V. ostreicida* led to dose-dependent lysosomal destabilization, reduced phagocytic activity, and increased intracellular ROS production. Similar lysosomal destabilization was observed with live *V. ostreicida*, which also stimulated extracellular ROS and nitric oxide release, but only in the presence of hemolymph serum (HS). Mussel HS displayed a strong bactericidal activity towards *V. ostreicida*, highlighting a key role for soluble immune effectors. In oyster hemocytes, *V. ostreicida* induced similar lysosomal stress; however, neither hemocytes nor serum showed any bactericidal activity towards this strain.
Discussion: This data represents the first attempt to elucidate the mechanisms underlying the interactions of an environmental strain of *V. ostreicida* with marine

bivalves. The species-specific differences observed in immune responses highlight the complexity of host-pathogen interactions in these organisms and emphasize the need for further investigation into immune responses of different aquacultured species.

KEYWORDS

bivalves, *Vibrio ostreicida*, larvae, hemocytes, immune response, mussel, oyster

1 Introduction

In the last decade, recurrent disease and mass mortality events of both farmed and natural stocks of marine bivalves have been observed throughout Europe. Even though the exact causes are not always clear, and these events are generally considered both multifactorial and polymicrobial, bacteria, in particular members of the genus *Vibrio*, have been identified as the main infectious agents in different bivalve species (1–6).

Among bivalves, oysters have been shown to be historically more affected, with several Vibrio species identified as main pathogens. In particular, members of the Splendidus clade (*V. splendidus*, *V. tasmaniensis*, and *V. crassostreae*) and *V. aestuarianus*, have been associated with disease outbreaks across France, Ireland (7) and Spain, notably in the Ebro Delta in 2016–2019 (8). Several vibrio isolates were confirmed as virulent in experimental infections (9–13). Vibrioses have been also described in other bivalve species, such as those caused by *V. tubiashii* in the scallop *Argopecten irradians*, or by *V. tapetis*, the causative agent of the well-known Brown Ring Disease in *Ruditapes philippinarum* (1, 2).

Some vibrios have been also implicated in larval mortalities across different host species, such as *V. tubiashii* in the oysters *Magallana gigas* and *Ostrea edulis*, and in the scallop *Argopecten irradians* (2). Also *Mytilus galloprovincialis* early larval stages have been shown to be susceptible to challenge with different vibrios, such as V. *bathipelagicus*, which induced larval death (14), or. *V. coralliilyticus* and *V. tasmaniensis* LGP32 (14, 15) that induced developmental arrest.

On the other hand, adult mussels (*Mytilus* spp.) generally show a remarkable resistance to invading vibrios with respect to other bivalve species, essentially due to the efficiency of their immune system. Differences in immune effectors between oysters and mussels may underlie the generally greater resilience of mussels to bacterial infections (16, 17). However, this advantageous trait seems to be not sufficient to face the more recent threats hitting European coastal waters. Indeed, increasing reports of mortality events in *M. edulis* and *M. galloprovincialis* have been recorded across Europe since 2014 (18–21). The fast changes of environmental variables seemed to be a triggering factor (17, 22); in addition, some bacteria belonging to the *Vibrio* genus, *V. splendidus* in particular, were also isolated from mussel mortality episodes (6, 22, 23). However, so far, no particular bacterium has been identified as an etiological agent of disease in *Mytilus* spp.

Previous episodes of disease and severe mortalities were observed in young oyster spat (*O. edulis*) in a bivalve hatchery in Galicia (NW Spain) from 1999 (24). Among the bacterial strains isolated from samples of oysters, water tanks, and surface of the affected tanks, one *Vibrio* species induced > 98.5% mortality in virulence tests carried out with oyster larvae (10–12 days old) at 22°C (Prado et al., 2005). The type strain, PP-203T (5CECT 7398T5DSM 21433T), isolated from the inner surface of containers, was subsequently identified as *V. ostreicida* (25), and its draft genome subsequently released in 2020 (26). However, since no further mentions of *V. ostreicida* interactions with oysters or other bivalves have appeared in the literature since then, little is known about its epidemiology, host range or virulence.

We have recently reported the isolation of strains of *V. ostreicida* from a mortality episode occurred in spring 2022 in adult *M. galloprovincialis* farmed in the Ebro River Delta in NW Spain, involving 25% of individuals, but observed at a water temperature of 18 °C, lower than in the other usual summer outbreaks (27). Histological examination revealed bacterial foci and tissue damage compatible with bacterial toxicity. Bacterial isolates from mussel sampled at the affected site showed a distinct profile; the phenotypic characterization of three representative isolates of this profile (r167, r172, r190) allowed their identification as *Vibrio ostreicida* (27). The complete genome of the r172 isolate was sequenced and preliminary virulence experiments in adult mussels showed mortality of 50% at 5 days post infection (27). This data suggested that this *V. ostreicida* strain may also represent a pathogen for mussels. However, to our knowledge, no data is available on the virulence of *V. ostreicida* in adult oysters or other bivalve species.

In this work, responses to the *V. ostreicida* r172 were investigated in *M. galloprovincialis*. *In vivo* experiments were performed in mussel larvae (48 h post-fertilization, hpf), in order to evaluate pathogenicity with early developmental stages. *In vitro*, short term responses of mussel hemolymph components to both heat-killed and live *V. ostreicida* were evaluated in terms of hemocyte lysosomal membrane stability (LMS), phagocytosis and bactericidal activity. Extracellular lysozyme release, Reactive Oxygen Species (ROS) and Nitric oxide (NO) production were also evaluated. The main results (LMS and bactericidal activity)

were compared with those obtained with hemolymph components of the oyster *Magallana gigas*.

2 Materials and methods

2.1 Bacterial cultures and inoculum preparation

The *V. ostreicida* strain *r172* was isolated from an adult mussel mortality episode that occurred in April 2022 in an aquaculture farm in Alfacs Bay, Ebro River Delta (Tarragona, Spain) (27), close to the research center of IRTA- La Ràpita. *V. ostreicida r172* was cultured in Zobell Marine Broth at 23°C under static conditions. After 5–6 h growth, cells in exponential phase were harvested by centrifugation (4,500 x g for 10 min), washed once with filter-sterilized artificial sea water (ASW, 35 ‰ for mussel experiments and 31 ‰ for oysters), and resuspended in ASW or mussel hemolymph serum (HS) to obtain a concentration of about 10^8 CFU/mL (determined spectrophotometrically as an Abs 600 = 0.38 of a suspension diluted 1:10). Marine agar (MA) was used throughout the experiments. For assays with heat-killed bacteria, samples were boiled for 10 min in a water bath, stored at 4°C and the whole unwashed suspensions suitably diluted in ASW to obtain the desire concentrations. This type of preparation was previously utilized in first *in vitro* studies on mussel hemocytes challenged with the known bivalve pathogen *V. splendidus* LGP32. as previously described (28).

2.2 Animals

Mytilus galloprovincialis, 4–6 cm long, were purchased from a mussel farm in the Ligurian Sea (La Spezia, Italy) in November 2022 (for larval assays) and in spring-summer 2023 (for immune assays). Animals were transferred to the laboratory and acclimatized in static tanks containing aerated ASW (1 L/animal), pH 7.9-8.1, 35 ‰ at 18°C for 24 h. Mussels were not fed during experiments. Specimens of *Magallana gigas*, 8–10 cm long, were purchased from an aquaculture farm (Bretagne, France) and acclimatized for 24 h in the same conditions, except for lower ASW salinity (31 ‰).

2.3 Effects of *V. ostreicida* on mussel early larval development

The mussel 48-h embryotoxicity assay (29) was carried out in 96-microwell plates as previously described (15, 30, 31). At 30 min post-fertilization, aliquots of 20 µL of live and heat-killed *V. ostreicida* suspensions, suitably diluted, were added to fertilized eggs in each microwell to reach the nominal final concentrations (from 10^2 to 10^8 CFU/mL) in a 200 µL volume. Control samples in ASW were run in parallel. Microplates were then incubated for 48 h at 18°C ± 1°C, with a 16:8 h light: dark photoperiod. All the procedures were carried out following (29). At the end of incubation, samples were fixed with buffered formalin (4%). A larva was considered normal when the shell was D-shaped (straight hinge) and the mantle did not protrude out of the shell, and malformed if had not reached the stage typical for 48 h (trocophora or earlier stages) or when some developmental defects were observed (concave, malformed or damaged shell, protruding mantle). The recorded endpoint was the percentage of normal D-larvae in each well with respect to the total, including malformed larvae and pre-D stages. The acceptability of test results was based on controls for a percentage of normal D-shell stage larvae >75% (29). Experiments were performed using fertilized eggs obtained by different parental pairs (N = 3), each in 6 replicate wells per condition (see Methods in Supplementary Information for details). All larvae in each well were examined by optical microscopy using an inverted Olympus IX53 microscope (Olympus, Milano, Italy) at 400 x, equipped with a CCD UC30 camera and a digital image acquisition software (cellSens Entry).

2.4 *In vitro* challenge of *Mytilus galloprovincialis* hemocytes with *V. ostreicida*

2.4.1 Hemolymph sampling and sample preparation

All procedures were performed as previously described (30). Hemolymph was extracted from the posterior adductor muscle of 10–15 mussels using a sterile 1 mL syringe with an 18 G1/2" needle, filtered through sterile gauze and pooled in Falcon tubes at 18°C as previously described. Hemolymph serum (HS) was obtained by centrifugation of whole hemolymph at 100 *x g* for 10 min and the supernatant was sterilized through a 0.22 µm-pore filter. Hemocyte monolayers were prepared by depositing 20 µL drops of whole hemolymph on microscope slides and the cells were left to adhere at 18°C for 20 min before removing the excess hemolymph (30). Hemocyte monolayers or aliquots of 500 µL of whole hemolymph samples (according to the endpoint) were incubated with either live or heat-killed *V. ostreicida* suspensions suitably diluted in ASW or HS at different final concentrations (from 10^8 to 10^5 CFU/mL) from 30 to 90 minutes. Untreated samples in ASW or HS were run in parallel. All experiments were carried out at 35 ‰ salinity.

2.4.2 Hemocyte functional parameters

Lysosomal membrane stability (LMS) and phagocytic activity were evaluated in hemocyte monolayers as previously described (15, 30, 32). LMS was determined after 30 min incubation with either heat-killed (in ASW) or live bacteria (resuspended in ASW or HS) or at different concentrations (from 10^5 to 10^8 CFU/mL). In all functional assays the bacteria:hemocyte ratio was 3:1 for a bacterial concentration of 10^6 CFU/mL. This ratio changed accordingly at different vibrio concentrations.

The phagocytic activity was evaluated by the uptake of NR-stained zymosan incubated for 60 min with only heat-killed bacteria (from 10^6 to 10^8 CFU/mL).This experimental choice was made because some bacteria are known to evade the host immune defense

by interfering with phagocytic process of the host cells (33). Therefore, in the presence of live bacteria, with this method it cannot be identified whether a change in particle uptake may reflect a preference of hemocytes towards *V. ostreicida* with respect to zymosan (or vice versa) or interference with the phagocytic process by live vibrios.

Lysozyme activity, extracellular reactive oxygen species (ROS) and nitric oxide (NO) production were determined in whole hemolymph samples as previously described (15, 30, 32). See more details in Supplementary Information (Methods).

The effects of heat-killed *V. ostreicida* (10^6 and 10^7 CFU/mL, 30 min) were further investigated by confocal fluorescence microscopy in hemocytes loaded with LysoTracker Green (LTG) (250 nM, 30 min) (Thermo Fisher Scientific, Massachusetts, USA) and 2',7'-Dichlorofluorescein (DCF) (2 µM, 30 min) (Sigma, Milan, Italy) as previously described (34). LTG is a green, fluorescent dye that stains acidic compartments in live cells. DCF fluorescence is used as an indicator for production reactive oxygen species (ROS) in live cells. Fluorescence of Lysotracker Green (ex: 504 nm, em: 511 nm) and DCF (ex: 495 nm, em: 520 nm) were detected using a Leica TCS SP5 confocal setup mounted on a Leica DMI 6000 CS inverted microscope (Leica Microsystems, Heidelberg, Germany) using 63 ×1.4 oil objective (HCX PL APO ×63.0 1.40 OIL UV). Images were analyzed by the Leica Application Suite Advanced Fluorescence (LASAF) and ImageJ Software (Wayne Rasband, Bethesda, MA).

Bactericidal activity of hemocytes towards live *V. ostreicida* was evaluated as previously described (30). Briefly, hemocyte monolayers (obtained from 500 µL hemolymph) were incubated in 24 multi-well plates with live *V. ostreicida* (5×10^6 CFU/mL) at 18 °C in ASW or HS for different periods of time (0, 30 and 90 min). The bactericidal activity of HS alone (aliquots of 500 µL) was also evaluated. *V. ostreicida* in ASW was used as a control for bacterial growth over the experimental time. Immediately after the inoculum (time 0) and after 30 and 90 min of incubation, supernatants were collected and hemocytes were lysed by adding filter-sterilized ASW with 0.05% Triton x-100 and by 10 s agitation. Supernatants and lysates were pooled and tenfold serial diluted in ASW. Aliquots of 100 µL of the diluted samples were plated onto MA. Samples of *V. ostreicida* resuspended in ASW or HS at the same concentrations were directly diluted and plated. After 24 h incubation at 23°C, the number of CFU per hemocyte monolayer was determined. Percentages of killing were determined in comparison to values obtained at time zero. The number of CFU in control hemocytes never exceeded 0.1% of those counted in vibrio-exposed samples. In all experiments, ASW at 35 ‰ salinity was utilized.

2.5 *In vitro* challenge of *Magallana gigas* hemocytes with *V. ostreicida*

Hemolymph sampling and monolayer preparations were performed as described above with slight modifications (14). Effects of heat-killed and live suspensions of *V. ostreicida* were evaluated on lysosomal membrane stability (LMS) and bactericidal activity was evaluated as described above following (30). In all experiments, ASW at 31 ‰ salinity was utilized.

2.6 Data analysis

Embryotoxicity test data, representing the mean ± SD of 3 independent experiments, carried out in 6 replicate samples in 96-microwell plates, were analyzed by ANOVA plus Tukey's post-test. EC_{50} values for embryotoxicity and LMS data were calculated at 95% confidence intervals (C.I.). Data on hemocyte and hemolymph functional parameters are the mean ± SD of at least 4 experiments, with each assay performed in triplicate. Statistical analyses were performed by the non-parametric Kruskal-Wallis test followed by Dunn's test ($p \leq 0.05$). All statistical calculations were performed using the GraphPad Prism version 7.03 for Windows, GraphPad Software, San Diego, CA, USA.

3 Results

3.1 Effects on early larval development

We first tested the potential pathogenicity of *V. ostreicida*, an oyster larval pathogen (25), on early larval development of *M. galloprovincialis*. Fertilized eggs were exposed to different concentrations (from 10^2 to 10^7 CFU/mL) of live and heat-killed *V. ostreicida* and the percentage of normal D-larvae was evaluated after 48 h post fertilization (hpf) (15, 30) (Figure 1). In controls, the percentage of normal D-larvae at 48 hpf was 84 ± 3%. The results, reported in Figure 1A, show that live *V. ostreicida* induced a concentration dependent decrease in normal development, with an $EC_{50} = 9.64 \times 10^3$ CFU/mL (95% C.I.: 8.04 – 11.60) (corresponding to a ratio bacteria:larvae of about 4:1). A strong effect was observed from concentrations > 10^5 CFU/mL (-60% of normal D-larvae). Slightly lower EC_{50} values were obtained with heat-killed bacteria (3.09×10^3 CFU/mL, 95% C.I.: 2.03 – 4.69), corresponding to a ratio bacteria:larvae of 1.24:1.

When the effects of live and heat-killed bacteria on larval phenotypes were compared at 10^5 CFU/mL, the results indicate that live *V. ostreicida* mainly induced larval malformations (57% of total larvae), whereas challenge with heat-killed *V. ostreicida* resulted in 100% delayed or arrested larvae (Figure 1B).

3.2 *In vitro* effects of *V. ostreicida* on adult mussel hemocytes

3.2.1 Effects of heat-killed bacteria

In vitro responses of hemocytes to heat-killed *V. ostreicida* suspensions in ASW were first evaluated, and data obtained for LMS and phagocytosis are reported in Figure 2. As shown in Figure 2A, a large and concentration dependent decrease in LMS was observed (from -20% with respect to controls at 10^5 CFU/mL to

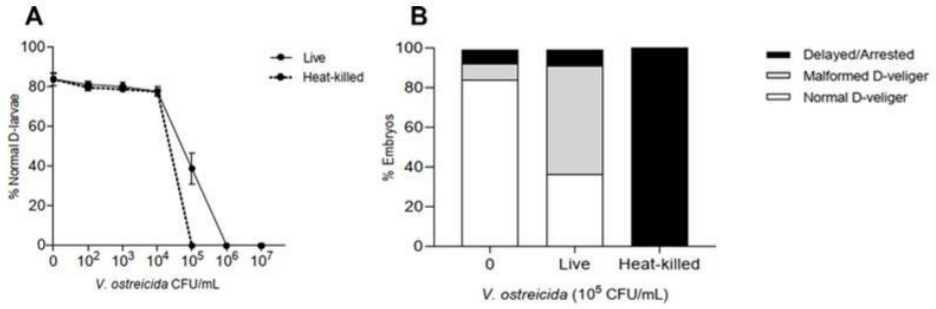

FIGURE 1
Effects of *V. ostreicida* on *M. galloprovincialis* embryo-larval development evaluated in the 48 h embryotoxicity assay. Fertilized eggs were exposed to different concentrations of live and heat-killed *V. ostreicida* suspension in ASW (from 10^2 to 10^7 CFU/mL). **(A)** Percentage of normal D-shaped larvae with respect to controls. **(B)** Percentage of larval phenotypes at 10^5 CFU/mL: normal D-veliger (white), malformed D-veliger (grey) and delayed/arrested larvae (black). Data represent the mean ± SD of 3 independent experiments carried out in 96-multiwell plates (6 replicates wells for each sample).

complete destabilization at 10^7 CFU/mL, Figure 3A), with an EC_{50} of about 10^6 CFU/ml (7.88 x 10^5 CFU/mL, 95% C.I.: 4.71 – 12.8). The hemocyte phagocytic activity was slightly reduced (about -20-25% respect with control) by exposure to the highest concentrations of bacteria, 10^7 and 10^8 CFU/mL (Figure 2B).

The effects of heat-killed bacteria on the lysosomal system were confirmed by CLSM (Confocal laser scanning microscopy) using LTG (Lysotracker green), a fluorescent dye that stains acidic compartments in live cells. As shown in Figure 3 (upper panel) an increase in LTG fluorescence was progressively observed at increasing concentrations of bacteria, indicating lysosome enlargement and fusion events. In the same conditions, increased intracellular ROS production, evaluated by DCF fluorescence, was also observed (Figure 3, lower panel).

In contrast, no significant effects were observed in activation of extracellular immune parameters (ROS, NO production and lysozyme activity) at any time and bacteria concentration (Supplementary Figure S1).

3.2.2 Effects of live bacteria

The *in vitro* effects of live *V. ostreicida* on mussel hemocytes were investigated in different media, ASW or HS, and the results are reported in Figure 4. As shown in Figure 4A, live *V. ostreicida* induced a similar dose-dependent decrease in LMS in both media, although with a slightly lower EC_{50} in ASW (2.23 x 10^5 CFU/mL, 95% C.I.: 1.11 – 5.39), than in HS (6.52 x 10^5 CFU/mL, 95% C.I.: 3.20 – 1.19). At the lowest concentration tested, the decrease in LMS induced by live *V. ostreicida* was larger (-40 and -30% with respect to controls in either ASW or HS) compared with that induced by heat-killed bacteria (see Figure 2A). However, complete lysosomal destabilization (>95%) was observed from 10^7 CFU/mL.

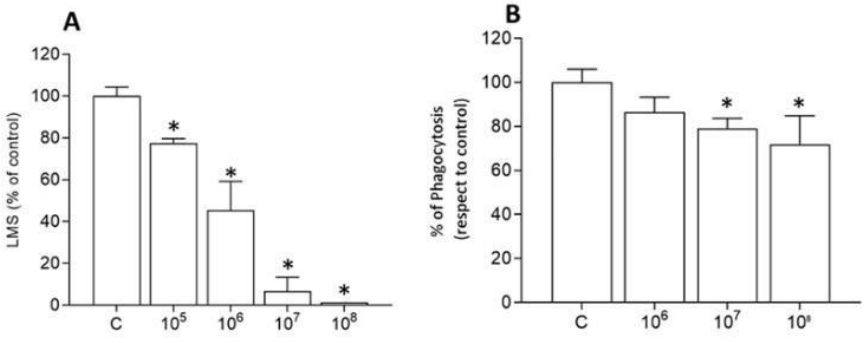

FIGURE 2
In vitro effects of heat-killed *V. ostreicida* on hemocyte lysosomal membrane stability (LMS) and phagocytic activity. **(A)** LMS: Hemocytes were exposed to different concentrations (from 10^5 to 10^8 CFU/mL) of heat-killed *V. ostreicida* suspensions in ASW for 30 min. **(B)** Phagocytosis: hemocytes were exposed to heat-killed *V. ostreicida* (from 10^6 to 10^8 CFU/mL) for 60 min. Data represent the mean ± SD of n=4 experiments. Statistical analyses were performed by non-parametric Kruskal-Wallis followed by Dunn's multiple comparisons test, *p < 0.05.

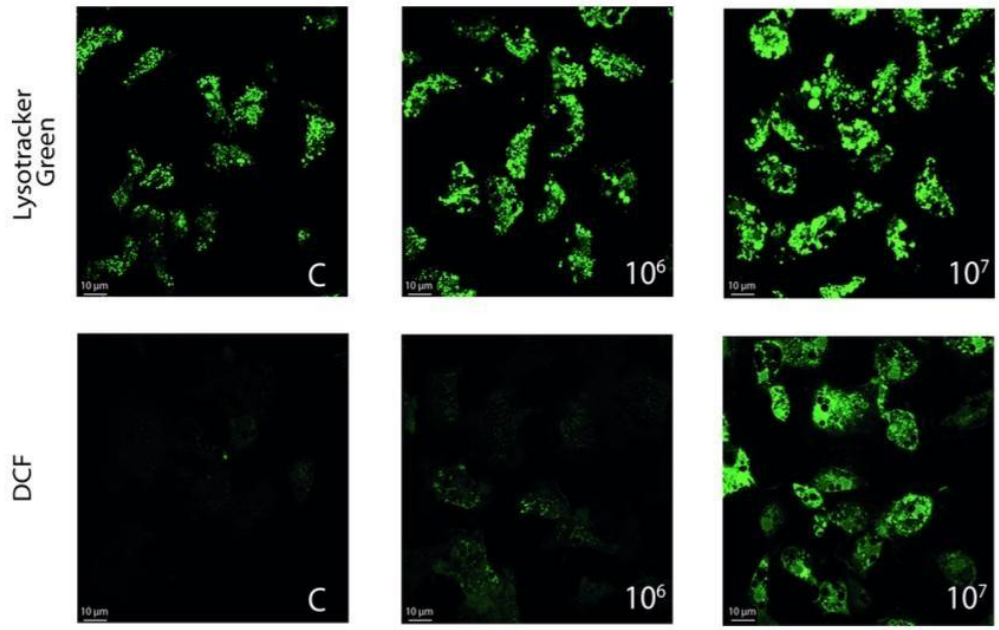

FIGURE 3
Confocal fluorescence microscopy: effects of *in vitro* exposure (30 min) of *Mytilus* hemocytes to heat-killed *V. ostreicida* suspensions at different concentrations (CFU/mL). Hemocytes from controls and challenged groups were loaded with LysoTracker Green (upper panel) and 2',7'-Dichlorofluorescein DCF (lower panel). Representative images are reported (LysoTracker Green: ex: 504 nm, em: 511 nm; DCF: ex: 495 nm, em: 520 nm).

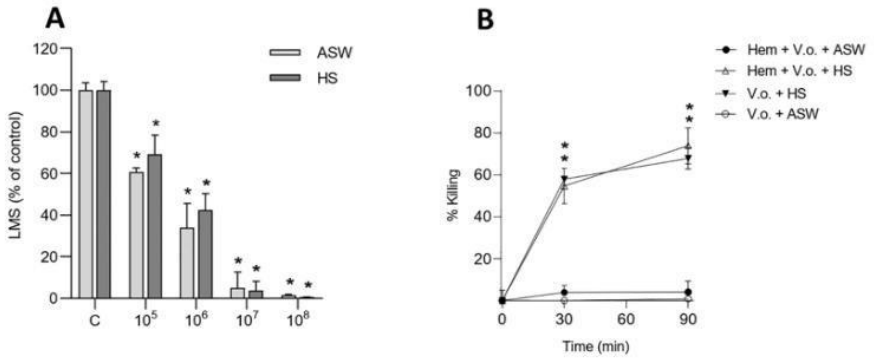

FIGURE 4
In *vitro* effects of live *V. ostreicida* in different media on hemocyte lysosomal membrane stability (LMS) and hemolymph bactericidal activity. **(A)** LMS: hemocyte monolayers were exposed to different concentrations (from 10^5 to 10^8 CFU/mL) of *V. ostreicida* resuspended in ASW or HS for 30 min. **(B)** actericidal activity: hemocyte monolayers were incubated for 30 and 90 min with *V. ostreicida* (5 x 10^6 CFU/mL) resuspended in ASW (Hem +V.o.+ASW) or in HS (Hem+V.o.+HS). In parallel, *V. ostreicida* were incubated in ASW (V.o.+ASW) or HS (V.o.+HS) alone. At each time point, the number of viable, cultivable bacteria (CFU) was evaluated, and the results are expressed as percent values respect to time zero. Data represent the mean ± SD of n=4 experiments. Statistical analyses were performed by non-parametric Kruskal-Wallis followed by Dunn's multiple comparisons test, *$p < 0.05$.

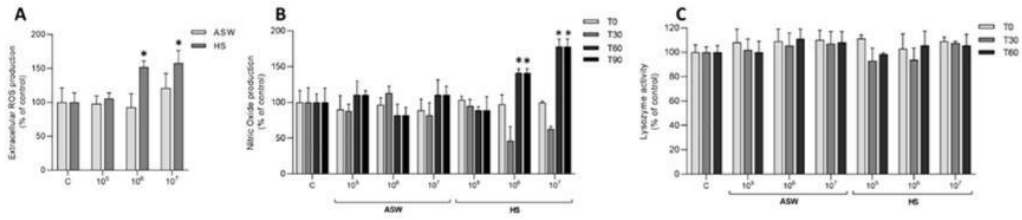

FIGURE 5
In *vitro* effects of live *V. ostreicida* on extracellular immune parameters of *M. galloprovincialis*. Extracellular ROS **(A)**, Nitric Oxide **(B)** production and lysozyme release **(C)**, were evaluated after incubation with *V. ostreicida* at 10^5, 10^6 and 10^7 CFU/mL in ASW or HS (hemolymph serum). Data represent the mean ± SD of n=4 experiments. Statistical analyses were performed by non-parametric Kruskal-Wallis followed by Dunn's multiple comparisons test, *p < 0.05.

The capacity of mussel hemocytes to kill *V. ostreicida* (5 x 10^6 CFU/mL) was investigated using a bactericidal assay that evaluates the number of live, culturable bacteria at different times of incubation (30 and 90 min) (30). The bactericidal activity was measured in hemocytes in the presence of ASW or HS, as well as in HS and ASW alone, and data are expressed as the percentage of killed bacteria with respect to time zero (Figure 4B). The results showed the absence of killing by hemocytes in ASW. In contrast, a high bactericidal activity was due to HS, irrespectively of the presence of hemocytes (60% and 70% respectively, at 30 and 90 min).

Live bacteria induced a significant stimulation of extracellular ROS (Figure 5A) and NO production (Figure 5B), although only in HS and at the highest concentrations tested. No stimulation of lysozyme activity was observed in any experimental condition (Figure 5C).

3.3 *In vitro* effects of heat-killed and live *V. ostreicida* on adult oyster *M. gigas*

Representative images of Giemsa staining of mussel and oyster hemocytes exposed to live *V. ostreicida* (30 min, 10^6 CFU/mL) are reported in Figure 6. Control hemocytes of both specimens were well spread on the support, showing different cytoplasmic extensions, with the nuclei colored in dark violet, the cytosol in

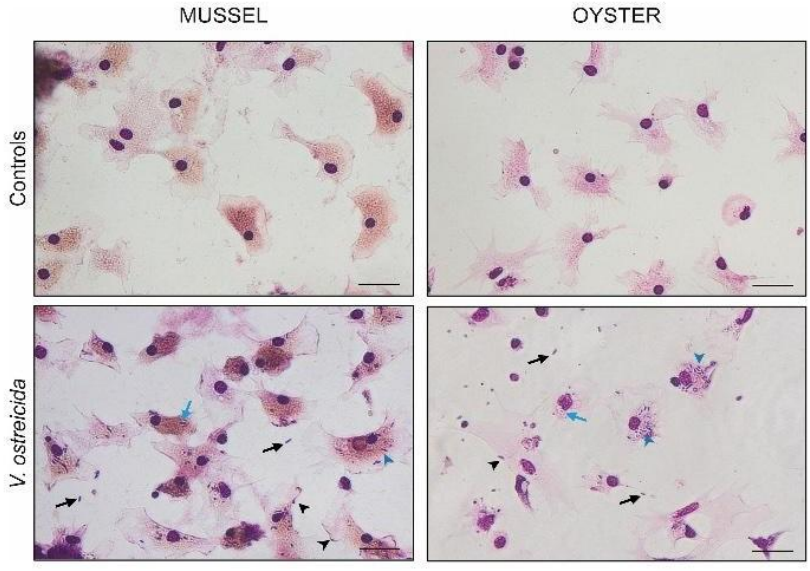

FIGURE 6
Giemsa staining of hemocytes of *M. galloprovincialis* and *M. gigas* (controls and incubated with live *V. ostreicida* suspensions in ASW (30 min, 10^6 CFU/mL). Black arrows: bacteria in extracellular medium; black arrowheads: bacteria adherent to cell membranes; blue arrowheads: bacteria in cytoplasm; blue arrows: bacteria in vacuolar structures. Scale bar: 20 µm.

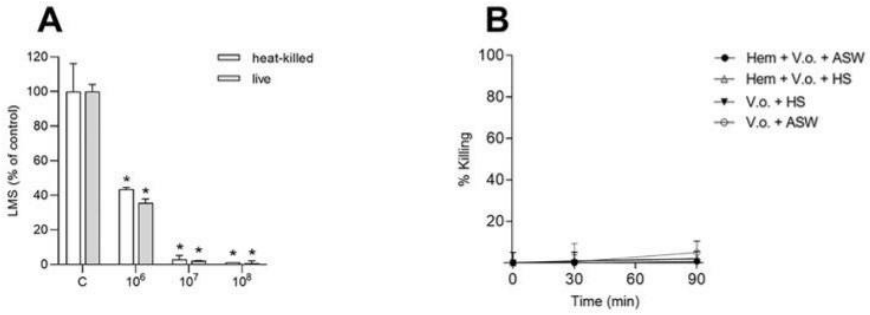

FIGURE 7
In vitro effects of *V. ostreicida* in *M. gigas* hemocytes. **(A)** LMS: hemocyte monolayers were exposed to different concentrations (from 10^6 to 10^8 CFU/mL) of heat-killed or live *V. ostreicida* suspensions for 30 min. **(B)** Bactericidal activity: hemocyte monolayers were incubated for 30 and 90 min with *V. ostreicida* (5 x 10^5 CFU/mL) resuspended in ASW (Hem+V.o.+ASW) or in HS (Hem+V.o.+HS). In parallel, *V. ostreicida* were incubated in ASW (V.o.+ASW) or HS (V.o.+HS) alone. At each time point, the number of viable, cultivable bacteria (CFU) was evaluated, and the results are expressed as percent values respect to time zero. Data represent the mean ± SD of n=4 experiments. Statistical analyses were performed by non-parametric Kruskal-Wallis followed by Dunn's multiple comparisons test, *p < 0.05.

pink, and intracellular vacuoles and lysosomes in pink-yellowish (much more evident in mussel hemocytes). In both mussel and oyster hemocytes challenged with *V. ostreicida*, bacteria were visible in the extracellular medium (black arrows), adherent to cell membranes (black arrow heads), as well within the cells, both in cytoplasm (blue arrowheads) and in vacuolar structures (blue arrows).

When oyster hemocytes were incubated with *V. ostreicida* suspensions in ASW, a similar dose-dependent decrease in LMS was observed with both heat-killed and live bacteria (Figure 7A). At the lowest concentration tested (10^6 CFU/mL), a decrease in LMS with respect to controls was observed (-60%), until almost complete destabilization (>95%) at 10^7 CFU/mL. LMS EC_{50} values were comparable with those obtained in mussel hemocytes, although slightly lower for oyster hemocytes challenged with live suspension (2.6 x 10^5 CFU/mL, 95% C.I.: 0.8 – 7.4), than with heat-killed bacteria (4.3 x 10^5 CFU/mL, 95% C.I.: 2.60 – 7.6).

The capacity of oyster hemocytes to kill *V. ostreicida* (5 x 10^6 CFU/mL) was evaluated in the bactericidal assay in the presence of ASW or HS, as well as in HS and ASW alone (Figure 7B). No bactericidal activity towards *V. ostreicida* was observed in any experimental condition (Figure 7B).

4 Discussion

The results of this work represent the first data on responses of *M. galloprovincialis* to *V. ostreicida*, a vibrio species previously identified as a larval oyster pathogen and associated with oyster mortalities in Spain (24, 25). Evidence is provided here of the effects of a *V. ostreicida* strain r172, isolated from a mortality episode of adult *M. galloprovincialis* in a shellfish production zone at the Ebro Delta River (27) on mussel larval development and hemolymph immune responses.

Since both mussel and oyster early developmental stages are likely to be more susceptible than adults to potential pathogens, not having fully developed the immune system (35, 36), we firstly tested the effects of *V. ostreicida* r172 in mussel early larvae. The results demonstrate that *V. ostreicida* affects normal *Mytilus* larval development, as shown by data from the 48 h embryo/larval assay. Heat-killed bacteria were also utilized in order to evaluate whether only live bacteria were able to interfere with larval development. Similar EC_{50} values, in the range of 10^3–10^4 CFU/mL, were obtained with both heat-killed and live bacteria. However, distinct effects on larval phenotypes were observed, with live bacteria mainly inducing shell malformations, and dead bacteria developmental arrest. The results indicate that normal development is affected by interactions of live *V. ostreicida* with mussel larvae, as previously observed with other bacterial isolated (15, 31). Moreover, the results obtained by heat-killed bacteria indicate that, products released by dead bacteria are involved in larval toxicity; these may include toxins, cell wall proteins, outer membrane proteins and lipopolysaccharides. Although the possible outcome of larval development at later stages cannot currently be predicted, the results indicate that *V. ostreicida* r172 is pathogenic to mussel early larvae. When compared with other live Vibrio tested so far in the same experimental conditions, the effect of *V. ostreicida* was comparable to those of other pathogenic bacterial species and strains: *V. bathipelagicus* induced larval death (14) and *V. coralliilyticus* and *V. tasmaniensis* LGP32 developmental arrest (14, 15).

V. ostreicida did not result in larval mortality; this is probably due to the low experimental ratio bacteria:larvae (about 4:1 at EC_{50} values for live bacteria). Although no data is available on concentrations of *V. ostreicida* in natural conditions in seawater, in this work, a wide range of concentrations were tested to fully cover also potentially natural environmental occurrence of *V. ostreicida*. In contrast, in oyster experimental trials focused on

larval pathogenicity, much higher bacteria:larvae ratios were utilized (10^4-10^5/larva), possibly simulating the worst scenarios occurring in contaminated hatcheries. In 10–15 day-old larvae of the flat oyster *O. edulis*, the *V. ostreicida* type strain PP-203T at 10_5-10_6 CFU/mL induced 98% mortality from 72 to 96 h after inoculation (24, 25).

In adult mussels, the outcome of infection depends on the capacity of hemolymph components (hemocytes and hemolymph serum) to recognize and mount an effective defense response towards invading pathogens (17, 37). The microbicidal activity of bivalve hemolymph results from the combined action of the phagocytic process, carried out by hemocytes, with humoral defense factors such as agglutinins (e.g. lectins), lysosomal enzymes (e.g. lysozyme), toxic oxygen intermediates and various antimicrobial peptides (37). Therefore, immune responses to challenge with *V. ostreicida* were tested in *in vitro* short-term experiments on hemolymph samples. The results indicate that both heat-killed and live *V. ostreicida* suspensions induced a dose dependent lysosomal stress in hemocytes.

In vitro incubation with *V. ostreicida* may cause some loss of cell adherence from hemocytes monolayers in particular at high concentrations, that induced strong lysosomal damage. However, previous data (28) showed that in the same experimental conditions with other pathogenic heat-killed vibrios (*V. splendidus* LGP32 and *V. anguillarum*), loss in adherence could be observed only at longer incubation times (3 h) than those utilized in the present study, and could be quantified only by flow cytometry analysis of different hemocyte subpopulations.

Heat-killed bacteria decreased hemocyte LMS and phagocytic activity, at the same time stimulating intracellular ROS production, but no activation of extracellular immune defenses. The results suggest that some components of *V. ostreicida* may interfere with hemocyte membranes and intracellular processes involved in immune responses.

When considering all data obtained with heat-killed *V. ostreicida*, experiments were performed as previously described using a whole (unwashed) bacterial suspension (28). Therefore, it must be underlined that the observed effects may be due to products that are not naturally released by bacteria, as well as to bacterial components released from bacteria killed by hemolymph components or by the larvae, or both. However, the results indicate that heat-killed *V. ostreicida* induced responses in mussel and oyster hemocytes similar to those elicited by the bivalve pathogen *V. splendidus* in the same experimental conditions (28).

Live bacteria induced a similar decrease in LMS, independent of the presence of soluble serum components; however, stimulation of extracellular ROS and NO production was observed, although only in the presence of HS, and at higher bacterial concentrations, indicating some role for soluble hemolymph components in recognition of bacteria by hemocytes and subsequent, although poor, immune activation. Accordingly, when hemocytes were incubated with live bacteria in ASW they were unable to kill *V. ostreicida*, suggesting that observed bactericidal activity was essentially due to hemolymph serum.

The results obtained with *M. gigas* indicate a similar effect of heat-killed and live bacteria on hemocyte LMS, confirming lysosomal stress. However, no activation of extracellular defenses (ROS, NO and lysozyme release) were observed in any condition (not shown). Moreover, in the oyster, neither hemocytes alone nor HS showed the capacity to kill *V. ostreicida*. The results indicate the presence in the hemolymph of *M. galloprovincialis*, but not in that of *M. gigas*, of specific soluble hemolymph components that are responsible for the direct bactericidal activity observed towards *V. ostreicida*. These may involve specific antimicrobial peptides or other factors specifically directed towards *V. ostreicida* whose identity needs further investigation.

This data further underlines the differences in the role of hemolymph components in the immune responses of mussels and oysters to potential invading pathogens (17). As recently reviewed in (38), advances in molecular immunobiology provided deeper insights into the cellular and molecular mechanisms underlying the robust defense system of *M. galloprovincialis*, which allows this species to efficiently cope with a broad range of infections. *M. galloprovincialis* is one of the species with the highest amount of different families of antimicrobial peptides (AMPs) in the animal kingdom. Moreover, the complexity of the immune repertoire is further enhanced by the presence in mussel genome of extensive hemizygous regions, which exhibit extensive presence/absence variation (PAV) among individuals, and affects all known AMP families to varying degrees (38). In this light, studies on the transcriptomic responses of different bivalve species can help unraveling the mechanisms underlying resilience to different pathogenic infections (39). In this work, the direct bactericidal activity towards *V. ostreicida* observed by the soluble hemolymph fraction of *M. galloprovincialis*, but not if *M. gigas*, suggests the presence in the Mediterranean mussel of constitutive plasma peptides/proteins specifically directed to this vibrio species. However, only proteomic/peptidomic studies can identify differences in the presence of hemolymph plasma of immune effectors between mussels and other bivalve species (40, 41).

Further experiments of *in vivo* challenge of mussels with *V. ostreicida* will provide information on its virulence, time course of infection and hemolymph immune responses. These data will help elucidating the capacity of *M. galloprovincialis* to cope with this bacterial infection. The results of these studies will contribute to increasing knowledge on the interactions between potentially pathogenic vibrios and the bivalve host, thus potentially predicting causes of mortalities which are increasingly affecting aquaculture farms worldwide causing significant ecological and economic losses.

Data availability statement

The raw data supporting the conclusions of this article will be made available by the authors, without undue reservation.

Ethics statement

Ethical approval was not required for the study involving animals in accordance with the local legislation and institutional

requirements because marine mussel and oyster invertebrates do not require ethical approvals.

Author contributions

ML: Conceptualization, Data curation, Formal Analysis, Investigation, Writing – original draft, Writing – review & editing. MA: Conceptualization, Investigation, Writing – review & editing. JL: Formal Analysis, Writing – review & editing. TB: Data curation, Formal Analysis, Software, Writing – review & editing. CC: Data curation, Formal Analysis, Writing – review & editing. CO: Data curation, Formal Analysis, Writing – review & editing. LV: Conceptualization, Resources, Supervision, Writing – review & editing. DF: Resources, Supervision, Writing – review & editing. LC: Conceptualization, Supervision, Writing – original draft, Writing – review & editing.

Funding

The author(s) declare financial support was received for the research and/or publication of this article. Project funded under the National Recovery and Resilience Plan (NRRP), Mission 4 Component 2 Investment 1.4 - Call for tender No. 3138 of 16 December 2021, rectified by Decree n.3175 of 18 December 2021 of Italian Ministry of University and Research funded by the European Union – NextGenerationEU; Award Number: Project code CN_00000033, Concession Decree No. 1034 of 17 June 2022 adopted by the Italian Ministry of University and Research, CUP D33C22000960007, Project title "National Biodiversity Future Center - NBFC".

Conflict of interest

The authors declare that the research was conducted in the absence of any commercial or financial relationships that could be construed as a potential conflict of interest.

Generative AI statement

The author(s) declare that no Generative AI was used in the creation of this manuscript.

Any alternative text (alt text) provided alongside figures in this article has been generated by Frontiers with the support of artificial intelligence and reasonable efforts have been made to ensure accuracy, including review by the authors wherever possible. If you identify any issues, please contact us.

Publisher's note

All claims expressed in this article are solely those of the authors and do not necessarily represent those of their affiliated organizations, or those of the publisher, the editors and the reviewers. Any product that may be evaluated in this article, or claim that may be made by its manufacturer, is not guaranteed or endorsed by the publisher.

Supplementary material

The Supplementary Material for this article can be found online at: https://www.frontiersin.org/articles/10.3389/fimmu.2025.1711477/full#supplementary-material

References

1. Beaz-Hidalgo R, Balboa S, Romalde JL, Figueras MJ. Diversity and pathogenecity of *Vibrio* species in cultured bivalve molluscs. *Environ Microbiol Rep.* (2010) 2:34–43. doi: 10.1111/j.1758-2229.2010.00135.x

2. Travers MA, Boettcher Miller K, Roque A, Friedman CS. Bacterial diseases in marine bivalves. *J Invertebr Pathol.* (2015) 131:11–31. doi: 10.1016/j.jip.2015.07.010

3. Barbosa Solomieu V, Renault T, Travers MA. Mass mortality in bivalves and the intricate case of the Pacific oyster, Crassostrea gigas. *J Invertebr Pathol.* (2015) 131:2–10. doi: 10.1016/j.jip.2015.07.011

4. Charles M, Bernard I, Villalba A, Oden E, Burioli EAV, Allain G, et al. High mortality of mussels in northern Brittany – Evaluation of the involvement of pathogens, pathological conditions and pollutants. *J Invertebr Pathol.* (2020) 170:107308. doi: 10.1016/j.jip.2019.107308

5. Azizan A, Alfaro AC, Jaramillo D, Venter L, Young T, Frost E, et al. Pathogenicity and virulence of bacterial strains associated with summer mortality in marine mussels (*Perna canaliculus*). *FEMS Microbiol Ecol.* (2022) 98:fiac140. doi: 10.1093/femsec/fiac140

6. Azizan A, Venter L, Alfaro AC. Biomarkers of mussel exposure to Vibrionaceae: A review. *Aquac Int.* (2024) 32:7595–627. doi: 10.1007/s10499-024-01531-2

7. Azéma P, Lamy JB, Boudry P, Renault T, Travers MA, Dégremont L. Genetic parameters of resistance to Vibrio aestuarianus, and OsHV-1 infections in the Pacific oyster, Crassostrea gigas, at three different life stages. *Genet Sel Evol.* (2017) 49:23. doi: 10.1186/s12711-017-0297-2

8. Carrasco N, Gairin I, Pérez J, Andree KB, Roque A, Fernández-Tejedor M, et al. A production calendar based on water temperature, spat size, and husbandry practices reduce osHV-1 µvar impact on cultured pacific oyster crassostrea gigas in the ebro delta (Catalonia), mediterranean coast of Spain. *Front Physiol.* (2017) 8:125/full. doi: 10.3389/fphys.2017.00125/full

9. Goudenège D, Travers MA, Lemire A, Petton B, Haffner P, Labreuche Y, et al. A single regulatory gene is sufficient to alter *V ibrio aestuarianus* pathogenicity in oysters. *Environ Microbiol.* (2015) 17:4189–99. doi: 10.1111/1462-2920.12699

10. Lemire A, Goudenège D, Versigny T, Petton B, Calteau A, Labreuche Y, et al. Populations, not clones, are the unit of vibrio pathogenesis in naturally infected oysters. *ISME J.* (2015) 9:1523–31. doi: 10.1038/ismej.2014.233

11. Bruto M, James A, Petton B, Labreuche Y, Chenivesse S, Alunno-Bruscia M, et al. *Vibrio crassostreae*, a benign oyster colonizer turned into a pathogen after plasmid acquisition. *ISME J.* (2017) 11:1043–52. doi: 10.1038/ismej.2016.162

12. Travers MA, Tourbiez D, Parizadeh L, Haffner P, Kozic-Djellouli A, Aboubaker M, et al. Several strains, one disease: experimental investigation of Vibrio aestuarianus infection parameters in the Pacific oyster, Crassostrea gigas. *Vet Res.* (2017) 48:32. doi: 10.1186/s13567-017-0438-1

13. Mesnil A, Jacquot M, Garcia C, Tourbiez D, Canier L, Bidois A, et al. Emergence and clonal expansion of *Vibrio aestuarianus* lineages pathogenic for oysters in Europe. *Mol Ecol.* (2023) 32:2869–83. doi: 10.1111/mec.16910

14. Lasa A, Auguste M, Lema A, Oliveri C, Borello A, Taviani E, et al. A deep-sea bacterium related to coastal marine pathogens. *Environ Microbiol.* (2021) 23:5349–63. doi: 10.1111/1462-2920.15629

15. Balbi T, Auguste M, Cortese K, Montagna M, Borello A, Pruzzo C, et al. Responses of Mytilus galloprovincialis to challenge with the emerging marine pathogen Vibrio coralliilyticus. *Fish Shellfish Immunol.* (2019) 84:352–60. doi: 10.1016/j.fsi.2018.10.011

16. Eggermont M, Tamanji A, Nevejan N, Bossier P, Sorgeloos P, Defoirdt T. Stimulation of heterotrophic bacteria associated with wild-caught blue mussel (Mytilus edulis) adults results in mass mortality. *Aquaculture*. (2014) 431:136–8. doi: 10.1016/j.aquaculture.2014.01.014

17. Destoumieux-Garzón D, Canesi L, Oyanedel D, Travers M, Charrière GM, Pruzzo C, et al. *Vibrio* –bivalve interactions in health and disease. *Environ Microbiol*. (2020) 22:4323–41. doi: 10.1111/1462-2920.15055

18. Lupo C, Bougeard S, Le Bihan V, Blin JL, Allain G, Azéma P, et al. Mortality of marine mussels *Mytilus edulis* and M. galloprovincialis: systematic literature review of risk factors and recommendations for future research. *Rev Aquac*. (2021) 13:504–36. doi: 10.1111/raq.12484

19. Lattos A, Papadopoulos DK, Feidantsis K, Karagiannis D, Giantsis IA, Michaelidis B. Are marine heatwaves responsible for mortalities of farmed mytilus galloprovincialis? A pathophysiological analysis of marteilia infected mussels from thermaikos gulf, Greece. *Animals*. (2022) 12:2805. doi: 10.3390/ani12202805

20. Bracchetti L, Capriotti M, Fazzini M, Cocci P, Palermo FA. Mass mortality event of mediterranean mussels (Mytilus galloprovincialis) in the middle adriatic: potential implications of the climate crisis for marine ecosystems. *Diversity*. (2024) 16:130. doi: 10.3390/d16030130

21. Mandic M, Gvozdenović Nikolić S, Kokić I, Jokanović S. Mass mortality of farmed mussels – a phenomenon without explanation? (2024). doi: 10.5281/zenodo.12749090

22. Charles M, Trancart S, Oden E, Houssin M. Experimental infection of *Mytilus edulis* by two *Vibrio splendidus* -related strains: Determination of pathogenicity level of strains and influence of the origin and annual cycle of mussels on their sensitivity. *J Fish Dis*. (2020) 43:9–21. doi: 10.1111/jfd.13094

23. Bechemin C, Soletchnik P, Polsenaere P, Moine OL, Pernet F, Protat M, et al. Episodes de mortalité massive de moules bleues observés en 2014 dans les Pertuis charentais. *Bulletin Epidémiologique* (2015) 67:6–9.

24. Prado S, Romalde J, Montes J, Barja J. Pathogenic bacteria isolated from disease outbreaks in shellfish hatcheries. First description of Vibrio neptunius as an oyster pathogen. *Dis Aquat Organ*. (2005) 67:209–15. doi: 10.3354/dao067209

25. Prado S, Dubert J, Romalde JL, Toranzo AE, Barja JL. Vibrio ostreicida sp. nov., a new pathogen of bivalve larvae. *Int J Syst Evol Microbiol*. (2014) 64:1641–6. doi: 10.1099/ijs.0.051417-0

26. Kumar RS, Galvis F, Wasson BJ, Saw JH, Oline DK, Barja JL, et al. Draft genome sequence of vibrio ostreicida strain PP-203, the type strain of a pathogen that infects bivalve larvae. *Microbiol Resour Announc*. (2020) 9:e00913–20. doi: 10.1128/MRA.00913-20

27. Lopez JR, Leonessi M, Fernandez-Tejedor M, Auguste M, Doni L, Cruz-Quintana Y, et al. First description of Vibrio ostreicida as putative causal agent of disease in Mediterranean mussel (Mytilus galloprovincialis) and development of a PCR protocol for its rapid diagnosis. *J Invertebr Pathol*. (2025) 212:108399. doi: 10.1016/j.jip.2025.108399

28. Ciacci C, Betti M, Canonico B, Citterio B, Roch P, Canesi L. Specificity of anti-Vibrio immune response through p38 MAPK and PKC activation in the hemocytes of the mussel Mytilus galloprovincialis. *J Invertebr Pathol*. (2010) 105:49–55. doi: 10.1016/j.jip.2010.05.010

29. ASTM. Int stand guide conduct static acute toxic tests start embryos four species salt water bivalve mollusks E724–798 reapproved 2012. (2004).

30. Auguste M, Rahman FU, Balbi T, Leonessi M, Oliveri C, Bellese G, et al. Responses of Mytilus galloprovincialis to challenge with environmental isolates of the potential emerging pathogen Malaciobacter marinus. *Fish Shellfish Immunol*. (2022) 131:1–9. doi: 10.1016/j.fsi.2022.09.048

31. Balbi T, Bozzo M, Auguste M, Montagna M, Miglioli A, Drouet K, et al. Impact of ocean warming on early development of the Mediterranean mussel Mytilus galloprovincialis: Effects on larval susceptibility to potential vibrio pathogens. *Fish Shellfish Immunol*. (2024) 154:109937. doi: 10.1016/j.fsi.2024.109937

32. Auguste M, Lasa A, Balbi T, Pallavicini A, Vezzulli L, Canesi L. Impact of nanoplastics on hemolymph immune parameters and microbiota composition in Mytilus galloprovincialis. *Mar Environ Res*. (2020) 159:105017. doi: 10.1016/j.marenvres.2020.105017

33. Celli J, Finlay BB. Bacterial avoidance of phagocytosis. *Trends Microbiol*. (2002) 10:232–7. doi: 10.1016/S0966-842X(02)02343-0

34. Balbi T, Ciacci C, Canesi L. Estrogenic compounds as exogenous modulators of physiological functions in molluscs: Signaling pathways and biological responses. *Comp Biochem Physiol Part C Toxicol Pharmacol*. (2019) 222:135–44. doi: 10.1016/j.cbpc.2019.05.004

35. Balseiro P, Moreira R, Chamorro R, Figueras A, Novoa B. Immune responses during the larval stages of Mytilus galloprovincialis: Metamorphosis alters immunocompetence, body shape and behavior. *Fish Shellfish Immunol*. (2013) 35:438–47. doi: 10.1016/j.fsi.2013.04.044

36. Song X, Wang H, Xin L, Xu J, Jia Z, Wang L, et al. The immunological capacity in the larvae of Pacific oyster Crassostrea gigas. *Fish Shellfish Immunol*. (2016) 49:461–9. doi: 10.1016/j.fsi.2016.01.009

37. Canesi L, Pruzzo C. Chapter 6 - Specificity of Innate Immunity in Bivalves: A Lesson From Bacteria. In: Ballarin L, Cammarata M, editors. *Lessons in Immunity [Internet]*. Academic Press. (2016) 79–91. Available online at: https://www.sciencedirect.com/science/article/pii/B9780128032527000060.

38. Gerdol M, Pallavicini A. Exploring the immune resilience of Mediterranean mussels: Recent advances and future directions. *Fish Shellfish Immunol*. (2025) 158:110147. doi: 10.1016/j.fsi.2025.110147

39. Saco A, Rey-Campos M, Panebianco A, Novoa B, Figueras A. Comparative transcriptomics reveals different grades of susceptibility to a bacterial infection in bivalves. *Fish Shellfish Immunol*. (2025) 165:110443. doi: 10.1016/j.fsi.2025.110443

40. Yang J, He J, Liu L, He M, Zhang X, Buttino I, et al. Expression profiles of antimicrobial peptides in Mytilus coruscus. *Aquaculture*. (2022) 548:737709. doi: 10.1016/j.aquaculture.2021.737709

41. Rey-Campos M, Novoa B, Pallavicini A, Gerdol M, Figueras A. Comparative genomics reveals a significant sequence variability of myticin genes in mytilus galloprovincialis. *Biomolecules*. (2020) 10:943. doi: 10.3390/biom10060943

Supplementary Material to

Interactions between the oyster larvae pathogen *Vibrio ostreicida* and the bivalve hosts *Mytilus galloprovincialis* and *Magallana gigas*.

Martina Leonessi[1,2*], Manon Auguste[1,2], Jose R. Lopez[3,4], Teresa Balbi[1,2], Caterina Ciacci[5], Caterina Oliveri[1], Luigi Vezzulli[1,2], Dolors Furones[3], Laura Canesi[1,2]

[1]Department of Earth, Environmental and Life Sciences (DISTAV), University of Genoa, Genoa 16132, Italy

[2]National Biodiversity Future Center, Palermo, Italy

[3]IRTA, Aquaculture Program. La Ràpita, Spain

[4]Universidade de Santiago de Compostela, Santiago de Compostela, Spain

[5]Department of Biomolecular Sciences (DIBS), University 'Carlo Bo' of Urbino, Urbino, Italy

1 Materials an Methods

Larval assays

All procedures were carried out following the protocol described in **(1)**. For each exposure condition experiments were carried out utilizing three different single pairings. Six replicates were made for each treatment, in 96 wells, each containing about 50 embryos. A total of 300 larvae were thus examined for each condition, according to the protocol ISO **(2)**. Observations were acquired manually by an operator blind to the experimental conditions.

Evaluation of functional hemocyte parameters

LMS was evaluated in hemocyte monolayers of *M. gigas* and *M. galloprovincialis* by the Neutral Red Retention Time (NRRT) assay (3) as previously described (4–6). Hemocyte monolayers were pre- incubated for 30 min with 20 µL of different *V. ostreicida* suspensions, either live (resuspended in ASW or HS) or heat-killed (in ASW), at different concentrations (from 10^8 to 10^5 CFU/mL). Samples were washed out and incubated with a neutral red (NR) (Sigma-Aldrich, Milan, Italy) solution: 20 µg/mL for 7 min and 40 µg/mL (in ASW) for 15 min for respectively oyster and mussel monolayers. At the end of incubation, excess dye removed, a drop of ASW was added and the slides were observed under an optical microscope from time zero every 15 min. The percentage of cells showing loss of dye from lysosomes in each field (10 fields each containing 8-10 cells) was evaluated until 50% of the cells showed sign of lysosomal leaking. All incubations were carried out at 18 °C.

Phagocytic activity was evaluated by the uptake of NR-stained zymosan by mussel hemocyte monolayers. Briefly, samples were incubated first with ASW (control) or heat-killed *V. ostreicida*

suspensions (from 10^5 to 10^8 CFU/mL) for 1 h and then with NR-stained zymosan in 0.05 M Tris-HCl buffer, pH 7.6 (TBS) for 1 h. Then monolayers were washed three times with ASW, fixed with Baker's calcium formol, and mounted in Kaiser's glycerol gelatine medium for microscopical examination with a fluorescent microscope. For each slide, the percentage of phagocytic hemocytes was calculated from minimum of 200 cells in triplicate samples (6,7).

Lysozyme activity, ROS and NO production were measured as previously described (6). Aliquots of whole hemolymph (500 µL) were incubated with either live and heat-killed suspension of *V. ostreicida* (final concentrations 10^5, 10^6 and 10^7 CFU/mL) at 18 °C for different times depending on the endpoint measured. Lysozyme activity was evaluated spectrophotometrically at 450 nm using a suspension of *Micrococcus lysodeikticus* (15 mg/100 mL in 66 mM phosphate buffer, pH 6.4) after incubation with bacteria for 0, 30 and 60 minutes. Nitric oxide (NO) production was evaluated by Griess reaction after incubation with bacteria for 0, 30, 60 and 90 minutes; samples were centrifuged (12000 x g for 30 min at 4 °C) and the supernatants were incubated for 10 min in the dark with 1% (w/v) sulphanilamide in 5% H_3PO_4 and 0.1% (w/v) N-(1-naphthyl)-ethylenediamine dihydrochloride. Samples were read at 540 nm and the molar concentration of NO_2^- in the samples were calculated from standard curves generated using known concentrations of sodium nitrite. Extracellular ROS generation was measured by the reduction of cytochrome c. Hemolymph samples were incubated for 30 min with a cytochrome c solution (75 µM ferricytochrome c in TBS). Samples were read at 550 nm. Cytochrome c in TBS was utilized as a blank. The results were expressed as changes in OD per mg protein. Protein content was determined using the Bradford method using bovine serum albumin (BSA) as standard. All data are reported per mg/protein sample and expressed a percentage of control values.

1 Results

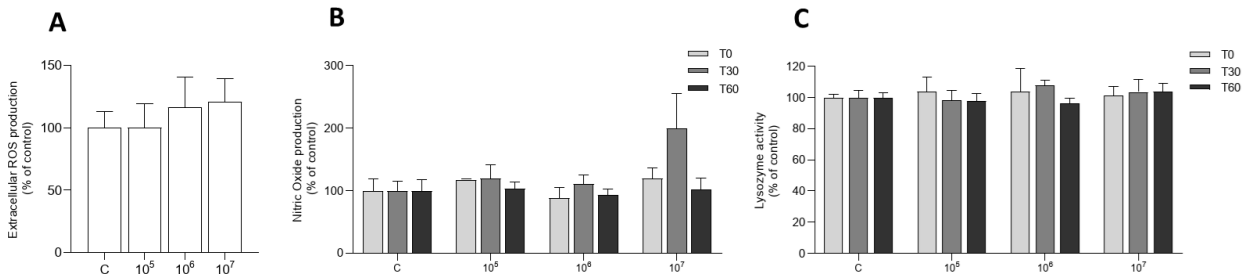

Supplementary Figure 1. *In vitro* effects of heat-killed *V. ostreicida* on extracellular immune parameters of *M. galloprovincialis*. Extracellular ROS (A), Nitric Oxide (B) production and lysozyme release (C), were evaluated after incubation with *V. ostreicida* at 10^5, 10^6 and 10^7 CFU/mL in ASW. Data represent the mean ±SD of n=4 experiments. Statistical analyses were performed by non- parametric Kruskal-Wallis followed by Dunn's multiple comparisons test. No significant differences were observed among different groups ($p > 0.05$).

2 References

1. Fabbri R, Montagna M, Balbi T, Raffo E, Palumbo F, Canesi L. Adaptation of the bivalve embryotoxicity assay for the high throughput screening of emerging contaminants in Mytilus galloprovincialis. Mar Environ Res. 2014 Aug;99:1–8.

1. Fabbri R, Montagna M, Balbi T, Raffo E, Palumbo F, Canesi L. Adaptation of the bivalve embryotoxicity assay for the high throughput screening of emerging contaminants in Mytilus galloprovincialis. Mar Environ Res. 2014 Aug;99:1–8.

2. International Standards Organization. Water quality — Determination of the toxicity of water samples on the embryo-larval development of Japanese oyster (Crassostrea gigas) and mussel (Mytilus edulis or Mytilus galloprovincialis). 2015; Available from: ISO:17244:2015

3. OSPAR Commission. Background documents and technical annexes for biological effects monitoring. In 2013. p. 239. Available from: www.ospar.org.

4. Lasa A, Auguste M, Lema A, Oliveri C, Borello A, Taviani E, et al. A deep-sea bacterium related to coastal marine pathogens. Environ Microbiol. 2021 Sep;23(9):5349–63.

5. Auguste M, Rahman FU, Balbi T, Leonessi M, Oliveri C, Bellese G, et al. Responses of Mytilus galloprovincialis to challenge with environmental isolates of the potential emerging pathogen Malaciobacter marinus. Fish Shellfish Immunol. 2022 Dec;131:1–9.

6. Auguste M, Leonessi M, Balbi T, Doni L, Oliveri C, Vezzulli L, et al. Seasonal fluctuations of hemolymph microbiota and immune parameters in Mytilus galloprovincialis farmed at La Spezia, Italy. Aquaculture. 2024 Jan;578:740028.

7. Balbi T, Cortese K, Ciacci C, Bellese G, Vezzulli L, Pruzzo C, et al. Autophagic processes in Mytilus galloprovincialis hemocytes: Effects of Vibrio tapetis. Fish Shellfish Immunol. 2018 Feb;73:66–74.

Chapter 3:

Dynamics of *Vibrio ostreicida* in *Mytilus galloprovincialis* through *in vivo* infections

The results of this work have been published in Frontiers in Immunology 16:1727164. doi: 10.3389/fimmu.2025.1727164

The results of infection dynamics and immune responses of adult *M. galloprovincialis* challenged *in vivo* with *V. ostreicida* strain r172 are presented. First, a temperature-dependent virulence assay was performed to assess the influence of environmental temperature on mortality. Injection of mussels with *V. ostreicida* (10^8 CFU/100 μL) produced moderate mortality (≈45–50%) at different temperatures (12–24°C), indicating that lethality was largely temperature-independent. Field screening to assess the background presence of *V. ostreicida* in local mussel populations (Fangar Bay, Alcanar, and Alfacs) revealed widespread natural infection, with Alcanar identified as the least contaminated site. An injection–cohabitation experiment was caried out and hemolymph immune responses, histopathology and potential horizontal transfer were evaluated. Mussels injected with *V. ostreicida* (10^8 CFU/mL) (Donors), partially transmitted *V. ostreicida* to uninfected animals (Recipients). Donors showed strong immune activation, and tissue lesions in gills and digestive gland. Recipients displayed milder and temporary alterations. Both groups cleared viable bacteria by day 4
p.i. and showed substantial tissue recovery by day 20. Bath infections at lower concentrations of bacteria (10^5 CFU/mL) caused only slight stress in hemocytes and no major histopathological changes at 3 days p.i.. Overall, adult *M. galloprovincialis* is able to cope with *V. ostreicida* under different types of experimental infection, supporting the view that *V. ostreicida* is only moderately pathogenic under natural conditions.

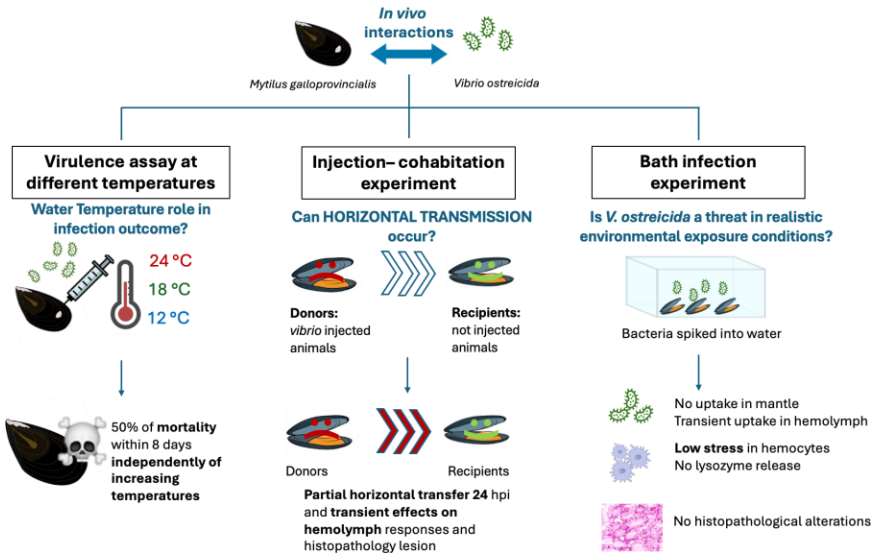
In vivo interactions
Mytilus galloprovincialis
Vibrio ostreicida
Virulence assay at different temperatures
Water Temperature role in infection outcome?
24 °C
18 °C
12 °C
50% of mortality within 8 days independently of increasing temperatures
Injection– cohabitation experiment
Can HORIZONTAL TRANSMISSION occur?
Donors: vibrio injected animals
Recipients: not injected animals
Donors
Recipients
Partial horizontal transfer 24 hpi and transient effects on hemolymph responses and histopathology lesion
Bath infection experiment
Is V. ostreicida a threat in realistic environmental exposure conditions?
Bacteria spiked into water
No uptake in mantle
Transient uptake in hemolymph
Low stress in hemocytes
No lysozyme release
No histopathological alterations

frontiers | Frontiers in Immunology

TYPE Original Research
PUBLISHED 26 November 2025
DOI 10.3389/fimmu.2025.1727164

Check for updates

OPEN ACCESS

EDITED BY
Antonio Figueras,
Spanish National Research Council (CSIC), Spain

REVIEWED BY
Magalí Rey-Campos,
Spanish National Research Council (CSIC), Spain
Patricia Diaz-Rosales,
Spanish National Research Council (CSIC), Spain

*CORRESPONDENCE
Martina Leonessi
martina.leonessi@edu.unige.it

RECEIVED 17 October 2025
REVISED 12 November 2025
ACCEPTED 14 November 2025
PUBLISHED 26 November 2025

CITATION
Leonessi M, Lopez JR, Cruz-Quintana Y, Auguste M, Andree KB, Fernandez-Tejedor M, Vezzulli L, Furones D and Canesi L (2025) Dynamics of *Vibrio ostreicida* in *Mytilus galloprovincialis* through *in vivo* infections. *Front. Immunol.* 16:1727164. doi: 10.3389/fimmu.2025.1727164

COPYRIGHT
© 2025 Leonessi, Lopez, Cruz-Quintana, Auguste, Andree, Fernandez-Tejedor, Vezzulli, Furones and Canesi. This is an open-access article distributed under the terms of the Creative Commons Attribution License (CC BY). The use, distribution or reproduction in other forums is permitted, provided the original author(s) and the copyright owner(s) are credited and that the original publication in this journal is cited, in accordance with accepted academic practice. No use, distribution or reproduction is permitted which does not comply with these terms.

Dynamics of *Vibrio ostreicida* in *Mytilus galloprovincialis* through *in vivo* infections

Martina Leonessi [1,2]*, Jose R. Lopez [3,4], Yanis Cruz-Quintana [3,5], Manon Auguste [1,2], Karl B. Andree [3], Margarita Fernandez-Tejedor [3], Luigi Vezzulli [1,2], Dolors Furones [3] and Laura Canesi [1,2]

[1]Department of Earth, Environmental and Life Sciences (DISTAV), University of Genoa, Genoa, Italy, [2]National Biodiversity Future Center, Palermo, Italy, [3]IRTA, Aquaculture Program, La Ràpita, Spain, [4]Universidade de Santiago de Compostela, Santiago de Compostela, Spain, [5]Facultad de Acuicultura y Ciencias del Mar, Universidad Técnica de Manabí, Bahía de Caráquez, Ecuador

Introduction: *Vibrio species* are widespread in coastal environments, where they are being increasingly associated with mortality episodes of farmed bivalves. This is the case for *Vibrio ostreicida* strain r172 isolated from a mortality event of adult mussels *Mytilus galloprovincialis* in Spain in 2022.

Methods and Results: In this study, the infection dynamics and immune responses of adult *M. galloprovincialis* challenged with *V. ostreicida* r172 were investigated using different *in vivo* experimental approaches. First, a virulence assay by injection (1 x 108 CFU/100 µL) was performed at different temperatures (12, 18 and 24 °C). The results showed that mussel mortality (about 50 % within 8 days) was independent of increasing temperatures. Subsequently, an injection/cohabitation experiment was carried out placing together in the same tank *V. ostreicida*-injected (Donors, 108 CFU/mL) with un-injected mussels (Recipients). The time course of infection was then followed by evaluating positivity to *V. ostreicida* by PCR, responses of haemolymph components (haemocyte lysosomal membrane stability and serum lysozyme activity) and tissue histopathology (gills and digestive gland). The results showed a partial horizontal transfer of *V. ostreicida* from infected to uninfected mussels, with transient effects on haemolymph responses and histopathological lesions in both groups. Finally, in order to mimic more realistic environmental conditions, a bath infection experiment was carried out, exposing mussels to *V. ostreicida* in seawater (105 CFU/mL). This condition resulted in lower stress in haemocytes; moreover, no lysozyme release or histopathological alterations were observed.

Discussion: Overall, the results show that *M. galloprovincialis* is able to cope with challenge with *V. ostreicida*, indicating that this Vibrio species is moderately pathogenic to adult mussels under the established experimental conditions.

KEYWORDS

***V. ostreicida* isolate, mussel mortality, cohabitation infection, bath infection, PCR, horizontal transmission, hemolymph responses, histopathology**

1 Introduction

The genus *Vibrio* represents one of the most diverse and important group of bacterial pathogens found in marine and coastal waters at the global scale. Some *Vibrio* species are responsible for a wide range of human infections *via* direct exposure to seawater or through the consumption of seafood, including farmed bivalves (1). In the last decade, *Vibrio* infections have been described as one of the main cause of diseases affecting all life stages of different species of bivalves (2–4). Recurrent mortality episodes may lead to the complete loss of production stocks, with serious economic consequences (5).

Different *Vibrio* species have been described as etiological agents of vibriosis that promote larval and spat mortalities of different bivalve species in hatcheries worldwide (6). Among them, *V. aestuarianus* has emerged as an important pathogenic species responsible of mass mortalities of spat and juveniles of the Pacific oyster (*Magallana gigas*) in France (7–10). Pathogenic infections of larvae of mussels, clams, scallops and oyster spat due to *V. splendidus*-related strains have been demonstrated as well (11–15). *V. coralliilyticus* was associated with disease outbreaks in multiple host larvae species including the oysters *M. gigas* and *Ostrea edulis*, the hard clam *Mercenaria*, and the Atlantic Bay scallop *Argopecten irradians* (6, 16, 17).

Adult bivalves can also be affected by mortality outbreaks. Mass mortality events of clams (*Venerupis philippinarum*) leading to serious economic losses in France and Spain have been associated with Brown Ring Disease (BRD) caused by *V. tapetis* (9). Among vibrios, *V. aestuarianus* has been identified as the main putative cause of oyster mortality in France since 2012 (3, 10), Spain (18), Ireland (19) and the United Kingdom (20).

Bivalves belonging to *Mytilus* spp., in particular *M. edulis* and *M. galloprovincialis*, have been so far considered to be very resistant to bacterial infections, in particular vibriosis, due to their particularly efficient innate immune system (4, 21). However, in the last decade, the frequency of mortality events of adult mussels, often associated with microbial infection, has dramatically increased in both natural and farmed populations (22). Indeed, during these events, different *Vibrio* strains, all from the *Splendidus* clade, have been isolated from moribund animals (3, 23–26).

However, little is known of infection kinetics of potentially pathogenic Vibrio species in mussels. Studying the interactions between vibrios and the immune system of the bivalve hosts may help preventing and predicting bacterial infections (27–30). In this context, understanding infection dynamics is an essential step in developing disease management strategies (14, 31).

V. ostreicida is an oyster larval pathogen first isolated from a nursery of flat oysters (*Ostrea edulis*) suffering from repeated disease outbreaks in Galicia (32, 33). A *V. ostreicida* strain r172 was recently isolated from a mortality episode of adult *M. galloprovincialis* that occurred in April 2022 in Alfacs Bay (Tarragona, Spain) (34). The phylogenetic analysis placed *V. ostreicida* r172 within a clade that included *Vibrio* species such as *V. coralliilyticus* and *V. neptunius*, both known for representing potential threats to mussel adults and larvae (12, 16). However, further studies are needed to evaluate the *in vivo* pathogenicity of this strain in adult mussels.

In the present work, the infection dynamics and immune responses of adult *M. galloprovincialis* challenged with the *V. ostreicida* strain r172 were investigated using different experimental protocols. We first carried out a virulence assay *via* injection at different water temperatures to evaluate the role of this key environmental variable in the outcome of infection. Subsequently, a model cohabitation experiment between infected and uninfected mussels was performed in order to investigate the possibility of horizontal transfer of bacteria among individuals. The time course of infection was followed in injected (Donors) and non-injected (Recipients) mussels by evaluating presence of *V. ostreicida* by PCR, responses of hemolymph components (in terms of hemocyte lysosomal stability and lysozyme activity), and histopathological conditions. Finally, a bath infection was performed to simulate a more natural environmental infection scenario, and the same parameters were evaluated.

2 Materials and methods

2.1 Bacterial cultures and inoculum preparation

The *V. ostreicida* strain *r172* utilized in this work was isolated from an adult mussel mortality episode that occurred in April 2022 in an aquaculture farm in Alfacs Bay, Ebro River Delta, (Tarragona, Spain) (34) close to the research center of IRTA- La Ràpita. *V. ostreicida r172* was grown on marine agar (MA) plates at 23°C for 24h and some colonies resuspended in PBS (phosphate buffered solution, pH 7.4) to obtain an Abs_{550} of about 0.8. Bacteria were then harvested by centrifugation (4,500 x *g* for 10min) and resuspended in 5 mL of PBS to obtain a final concentration of 10^9 CFU/mL. The final concentration was also determined by total viable counts on MA plates after 24h growth at 23°C. Marine agar (MA) was used for all culture preparations throughout the experiments.

2.2 Animals

Adult mussels (4–5 cm long) from local farms (IRTA), were collected in February 2023 (for virulence assay), and in May 2024 and July 2024 (for cohabitation and immersion experiments, respectively). Animals were transferred to the laboratory and acclimatized in static tanks containing aerated ASW (1 L/animal), pH 7.9–8.1, 35 ‰ for 24h at 18°C, unless otherwise indicated.

2.3 *In vivo* virulence assay at different temperatures (February 2023)

Experiments were carried out on adult mussels (5cm on average) purchased in February 2023 from Fangar Bay (Explotacions Marines, La Ràpita) at a seawater temperature of 12.8°C. Four groups of 10 mussels each (40 animals per condition) were acclimatized to three different temperatures: 12–14.5°C;

18–19.5°C; 23.5–24.5°C. After one week, two groups of mussels kept at each temperature were challenged with *V. ostreicida* by intravalvar injection (1 x 10^8 CFU/100 µL; 100 µL/mussel), and the other two were injected with PBS (control group). Therefore, data were obtained on two groups of 10 mussels each for each condition (20 mussels each). During the 14 days of the trial, each group was kept at the same acclimatization temperature. Mortality was checked daily. Dead mussels were removed and whole tissue homogenates of each individual were plated on MA at 23 °C for 24h. Detection of *V. ostreicida* among the bacterial colonies grown on the plates was carried out using the PCR protocol previously described (34), using 400 ng of DNA in each PCR reaction.

2.4 Detection of *V. ostreicida* in mussel samples from different aquaculture farms by real time PCR (April 2024)

A screening of mussel stocks from both Ebro bays (Alfacs and Fangar Bays) and from nearby open waters (Cases de Alcanar, Tarragona, Spain) (Supplementary Figure S1) was carried out in April 2024 to choose those with the lowest *V. ostreicida* background load for subsequent laboratory infection experiments. Adult mussels sampled from different sites were transferred to the laboratory, and 30 individuals were analyzed for detection of *V. ostreicida* by PCR, following the protocol described in (34), with slight modifications (see details in Supplementary Table S1 and Supplementary Table S2). PCR analysis was applied to either bacterial cultures from hemolymph pools or individual mantle as described below.

Hemolymph was extracted from the posterior adductor muscle using a sterile 1 mL syringe with an 18 G1/2" needle, filtered through sterile gauze and pooled in a Falcon tube at 18°C (35); 6 pools of derived from 5 animals each were made (n = 6). Aliquots of 100 µL of each hemolymph pool were plated on MA and incubated for 48h at 23°C to allow for bacterial growth. The same procedure was applied to single aliquots (100 µL) of seawater sampled from each tank at each time point. At the end of incubation, samples were collected into Eppendorf tubes. Using a 1 µL loop, a small quantity of samples from each tube was gathered and resuspended in 100 µL of Milli-Q water. DNA extraction was performed by incubating the resuspended samples for 5min at 95–99°C in a thermocycler; samples were then immediately put in ice, centrifuged for 5min at 8,000 x g at 4°C and the supernatants collected for PCR analyses. In both hemolymph and seawater bacterial cultures, PCR analyses allow for the determination of live, growing bacteria.

PCR analysis was also directly applied to mantle tissue to reveal the total bacterial load (live and dead bacteria). Individual mantle samples (n = 30) were dissected, frozen at -80°C, and were directly analyzed for the presence of *V. ostreicida*. DNA was extracted from 30 mg tissue using the DNeasy Blood & Tissue kit (Qiagen) according to the manufacturer's instructions. The DNA concentration was measured using a NanoDrop 2000.

The same sample preparation and PCR protocols were subsequently used for evaluating the presence of *V. ostreicida* in mussel samples from *in vivo* challenge experiments (before challenge, at day 0, and at different time points during each experiment). Data are reported as % of positive PCR samples with respect to the total number of samples analyzed.

2.5 Mussel infection by injection and water tank cohabitation model (May 2024)

Mussels obtained from Alcanar Bay in May 2024 (at a seawater T = 18.7°C) were injected into the posterior adductor muscle with 50 µL of bacterial suspension of *V. ostreicida* (10^8 CFU/mL final nominal concentration), as previously described in studies on determination of mussel immune responses to other vibrios (27, 36), as well as in previous cohabitation studies in oysters and mussels (31, 37–39). Injected mussels, hereafter indicated as Donors (D), were placed in the same tank filled with UV-treated and filtered seawater (0.5 L/animal), with un-injected animals, hereafter indicated as Recipients (R).A preliminary cohabitation experiment was performed testing different ratios between D and R in a total of 80 mussels for each tank (1D:1R, 1D:3R and 1D:10R, see Supplementary Figure S2). Different groups were separated in small netted containers in each tank. The experiment was run twice.

Since no significant mortality was observed in any experimental condition (see results Supplementary Figure S3), the intermediate ratio 1D:3R was chosen for final experiments (see Figure 1) as previously described (31, 39). In the cohabitation tank, a total of 160 mussels were thus utilized (40 D:120 R). Donors D were divided into 4 subgroups of 10 animals each. Recipients R were split into 4 subgroups of 30 animals each. Positive (*V. ostreicida*-injected) (C^+) controls and negative (PBS injected) controls (C^-) were run in parallel (4 subgroups of 10 animals each, for a total of 40 mussels).

Mussels were sampled from each tank at 1, 4 and 20 days post injection (p.i.). During the experiment, animals were maintained under static conditions at 18°C with aeration and without feeding. Mortality was monitored daily, and aliquots of 100 mL of SW were sampled from each tank before the daily water change.

At each time point, individual mantles were collected and frozen at -80°C (n = 10 for C^-, C^+ and D; n = 30 for R). Aliquots of water from tanks (100 µL) and of hemolymph pools (100 µL) were plated on MA for subsequent PCR analysis. Replicate samples were made of 3 pools of hemolymph from 3 mussels each (n = 3) for C^- and C^+ and D groups, and 6 hemolymph pools from 5 animals each (n = 6) for R, respectively. At each time point, individual histological sections were collected (n=10 for C^-, C^+ and D samples; n = 30 for R samples).

2.6 Mussel infection by immersion (July 2024)

In July 2024, another experiment was performed of mussel infection with *V. ostreicida* by water immersion, using mussels sampled from Alcanar (330 individuals). Seawater T at the day of sampling was 24.9°C). Before the experiment, the presence of *V. ostreicida* was evaluated in 30 animals by PCR as described above).

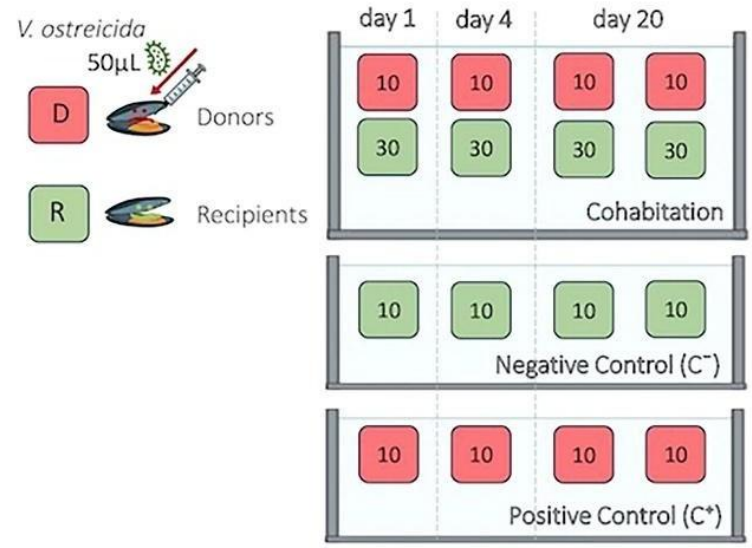

FIGURE 1
Cohabitation experimental set up.

After 24h acclimatization at 18°C, a suspension of *V. ostreicida* (final nominal concentration 10^5 CFU/mL) was spiked once into the water tank (150 animals) at day 0. A parallel group of control (unexposed) mussels was kept in clean seawater (150 animals). Mussels were divided into subgroups inside smaller netted containers within each tank (5 subgroups of 30 animals each). Seawater was changed daily with no addition of bacteria. Before daily water change, animals were fed with phytoplankton *Tetraselmis suecica* (200.000 cell/mL in the tank) in order to stimulate the filtration process. Mortality was checked daily in a group of 30 mussels for each condition. Mussels from all tanks (1 subgroup condition) were sampled at 1, 2, 3 and 4 days post infection. Hemolymph, mantle and water were collected. Individual mantles were dissected and frozen at -80 °C for PCR analysis (n = 30 for each experimental group). Hemolymph pools of 5 animals each were made (n = 6 for each experimental group). Individual mantles were dissected and frozen at –80°C for PCR analysis (n = 30 for each experimental group). Tissue samples for histopathological analysis were also collected and fixed as described below. All sampling procedures and assays were performed as described above for the cohabitation experiment.

2.7 Mussel hemolymph parameters

In both injection and immersion experiments, in all experimental conditions the remaining hemolymph from each pool was utilized for determination of functional parameters (16, 35, 40). Lysosomal membrane stability (LMS) was evaluated as an indicator of cellular stress in immune cells, the hemocytes, using the Neutral Red Retention Time assay (NRRT); lysozyme activity was determined spectrophotometrically as a marker of immune related enzymes in serum (see Methods in SI for experimental details). LMS and lysozyme activity were evaluated in 3 hemolymph pools for C^-, C^+ and D (n = 3) and 6 pools for R samples (n = 6) for the cohabitation experiment and in 6 pools for each condition (n = 6) for the bath infection.

2.8 Histopathological analysis

For histopathological evaluation, a transverse section (0.3 cm) including digestive gland, gill, foot, and gonad was obtained from each *M. galloprovincialis* individual from the injection and water tank cohabitation assay. In the cohabitation experiment, the number of individuals analyzed were 30 at T0, 10 from D, C^- and C^+ samples and 30 from R samples at 1 and 4 days, for a total number of n = 150). In the bath experiment 30 individuals from T0 and 30 animals from both control and challenged group were analyzed at 1, 2, 3 and 4 days, for a total number of n = 270). After fixation in Davidson's solution for 48–72 h (41), samples were dehydrated through a graded ethanol series, cleared with xylene (MYR STP 120, Especialidades Médicas Myr, Spain), and embedded in paraffin (MYR EC-350, Especialidades Médicas Myr). Serial sections (5 µm thick) were cut using a Leica RM2155 microtome (Leica Microsystems, Germany) and stained with hematoxylin and eosin (H&E) using automated staining equipment (MYR MYREVA SS-30, Especialidades Médicas Myr). For general evaluation and tissue description, the slides were examined under a light microscope (Leica DM LB, Leica Microsystems) and images were

captured using an Olympus DP70 digital camera (Olympus Europa, Germany) and processed with Image Analysis software (Olympus Soft Imaging Solutions, Germany). Quantification was performed for the adipogranular cells in the soft connective tissue among digestive tubules, the goblet cells in the gill filaments and the free intervalvar hemocytes between gill filaments (n = 10 field/mussel) at each sampling time (0, 1 and 4 days post injection). Cell counts were performed within a standardized rectangular area measuring 100 × 1000 µm (0.1 mm^2).

2.9 Data analysis

Data from experiments on hemocyte and hemolymph functional parameters are the mean ± SD of 3 hemolymph pools for C^-, C^+ and D (n = 3) and 6 hemolymph pools for R samples (n = 6) for the cohabitation experiment, and of 6 pools for each condition (n = 6) for the bath infection. Statistical analyses were performed by the non-parametric Kruskal-Walli's test followed by Dunn's test ($P \leq 0.05$). Statistical calculations were performed using the GraphPad Prism version 7.03 for Windows, GraphPad Software, San Diego, CA, USA.

Quantification of different cell types in digestive gland and gills samples from the cohabitation experiment, was performed analyzing 10 optical fields per animal (see 2.8 for the number of mussels analyzed per condition). The measured variables were compared across groups and sampling time using R (version 4.3.0 in RStudio). As data did not meet normality assumptions, non-parametric tests were applied. A Kruskal-Wallis test was used to detect overall differences among experimental groups, followed by pairwise Dunn's tests with Bonferroni correction. Superscript letters were assigned using the cld List function to indicate statistically significant differences ($P < 0.05$). Boxplots with group means and superscript letters were generated using the Minitab 18.1 software.

3 Results

3.1 Virulence of *V. ostreicida* at different temperatures

Infection with *V. ostreicida* r172 induced an average cumulative mortality of 45–50%, irrespectively of temperature, at 14 days p.i. (Figure 2A). Mortalities were recorded within 8 days p.i. in all groups, with no further increases up to 14 days (Figure 2B): however, the time course was affected by temperature, with maximal effects observed after 9, 7 and 6 days p.i., at 12, 18, and 24 °C, respectively (Figure 2B). In control mussels, mortality never exceeded 5%. PCR carried out on the cultures obtained from the whole tissue samples of dead mussels were all positive for *V. ostreicida*, confirming the recovery of the viable pathogen from them(not shown).

3.2 Detection of *V. ostreicida* in mussel samples from different aquaculture farms

The results of PCR analyses carried out in mussels sampled in April 2024 from different sites (Supplementary Figure S1) are reported in Table 1. The same data were obtained from both bacterial cultures of hemolymph pools (indicating the presence of viable bacteria) and individual mantles (where direct PCR analysis reveals the presence of both dead and live bacteria). All batch samples were positive for the presence of *V. ostreicida*; the highest value was detected in mussels from Fangar Bay, followed by those from Alfacs Bay. The lowest values were recorded in mussels from the open water farm in Alcanar; therefore, animals collected from this site were chosen for subsequent *in vivo* challenge experiments using two different experimental protocols of infection.

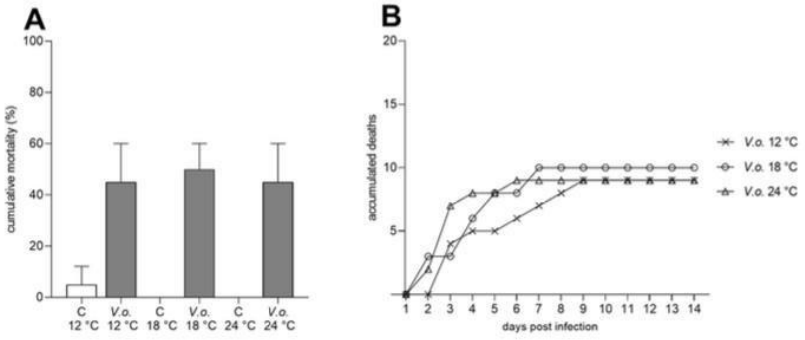

FIGURE 2
Effects of injection with *V. ostreicida* r172 (1 x 10^8 CFU/100 µL; 100 µL/animal) on mussel mortality at different temperatures (12, 18 and 24°C). **(A)** Percent cumulative mortality at 14 days p.i. **(B)** Accumulated deaths over the duration of the experiment in mussels injected with r172; each line represents the sum of deaths from two independent assays performed at each temperature.

10.3389/fimmu.2025.1727164

TABLE 1 Percentage (%) of *V. ostreicida* positive samples, evaluated by PCR, in mussels cultivated at different sites. Data represents the mean of both bacterial cultures of hemolymph pools and individual mantles.

Fangar Bay	Alfacs Bay	Alcanar
75%	40%	16%

3.3 Injection and cohabitation experiments

To investigate the effects of experimental infection of mussels with *V. ostreicida* and the possible horizontal transmission among individuals, a cohabitation experiment was first performed in May 2024 (see Methods for details). Mussels were injected with *V. ostreicida* (Donors-D, 10^8 CFU/mL final nominal concentration) and placed in the same tanks with un-injected mussels (Recipients-R), in a 1D:3R ratio. Samples were collected at different times post-infection (day 0, 1, 4 and 20). Both negative (C^-) and positive (C^+) control samples were kept in separate tanks for the duration of the experiments.

3.3.1 PCR detection of *V. ostreicida*

In bacterial cultures from hemolymph of mussels of the negative control group C^- (PBS-injected), *V. ostreicida* was detected in 33% of samples (Figure 3A). This value was higher than those recorded in the previous month (see Table 1). However, in these samples, a progressive clearance of live bacteria was observed over time. At day 1 p.i., both C^+ and D samples were 100% positive to *V. ostreicida*, confirming the successful injection; however, no positive samples were detected in the R group. Total clearance of live *V. ostreicida* was observed at day 4 p.i. in all samples. PCRs were also run on bacterial cultures of individual water samples from different tanks. Only those containing injected animals (C^+ and cohabitation tank) were positive to *V. ostreicida* at 1 day p.i.; at day 4 p.i., all water samples were negative (not shown).

PCR directly performed in individual mantle samples showed an initial detection of *V. ostreicida* in 10% of mussels at day 0. C^- samples showed a complete clearance from day 1 p.i. At day 1 p.i. *V. ostreicida* was detected in >50% of mantles from C^+ and D samples. Moreover, 40% positive samples were detected in R group. An overall decrease in positive samples was observed at day 4 in all groups, indicating bacterial clearance also from this tissue, that was higher for C^+ and R than in D samples (Figure 3B).

3.3.2 Hemolymph functional parameters

Hemocyte LMS and serum lysozyme activity were evaluated in hemolymph samples at different times p.i. and the results are reported in Figure 4. After 1 and 4 days a complete lysosomal destabilization (>95%) was observed in C^+ and D samples, indicating irreversible cellular stress (Figure 4A). In these conditions, significant increases in lysozyme activity were observed (Figure 4B). A smaller but significant lysosomal stress was observed in R samples at 1 and 4 days p.i. (about -50% LMS with respect to the negative control), with no changes in serum lysozyme activity (Figures 4A, B). However, after 20 days, a full recovery of LMS values was observed and lysozyme activities were comparable with those observed at 1 and 4 days in all groups (data not shown).

3.3.3 Histopathological analysis

Representative images of tissue sections from mussels at 1 and 4 days p.i. are shown in Figures 5 and 6, respectively. In negative controls (C^-) no tissue alterations such as atrophy, hemolytic infiltration, or necrosis were observed at any sampling time in digestive gland and gills (Figures 5 A, B, 6A, B). In the digestive gland, the tubules were closed together and displayed an irregular epithelium projecting into the lumen, with abundant vacuolation, indicating the presence of active, healthy digestive cells, and

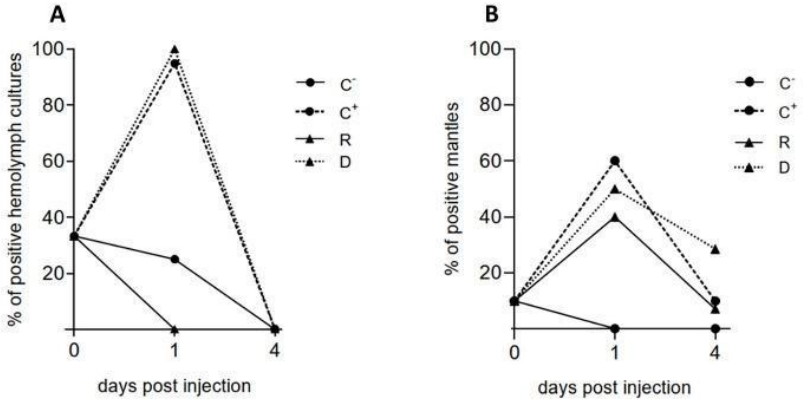

FIGURE 3
Detection of *V. ostreicida* by PCR in the cohabitation experiment in different experimental groups of mussels at different times post injection (day 0, 1 and 4). Negative (C-) and positive (C^+) controls, donors (D), recipients (R). **(A)** Bacterial cultures from hemolymph pools; **(B)** individual mantle samples. Data are expressed as % positive samples in hemolymph pools (n=3 for C^-, C^+ and D samples; n=6 for R samples) and individual mantles (n=10 for C^-, C^+ and D samples; n=30 for R samples) (see Methods 2.5).

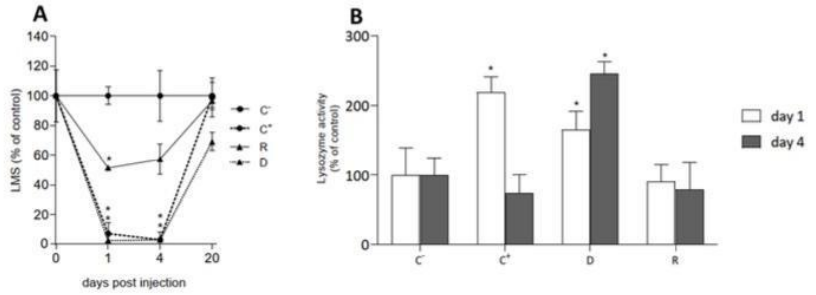

FIGURE 4
Hemolymph functional parameters in cohabitation experiment in different experimental groups of mussels at different times post injection (day 0, day 1 and day 4): negative (C-) and positive (C+) controls, donors (D), recipients (R). **(A)** Hemocyte lysosomal stability (LMS) and **(B)** serum lysozyme activity. Data are the mean ± SD evaluated in 3 pools for C^-, C^+ and D (n = 3) and 6 pools for R samples (n = 6). For more details see Methods 2.7. Statistical analyses were performed by non-parametric Kruskal-Wallis followed by Dunn's multiple comparisons test, * = $P < 0.05$.

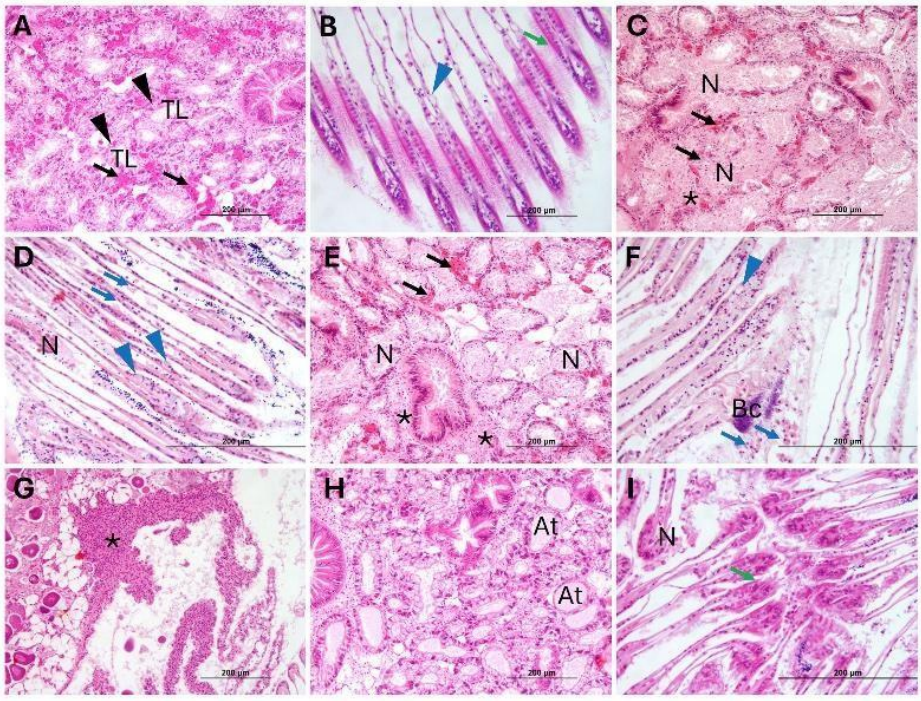

FIGURE 5
Representative H&E stain images of histological sections of *M. galloprovincialis* from the cohabitation experiment in negative controls, positive controls, donors and recipients at 1 day of exposure. **(A)** Digestive gland of negative control (C^-) showing the tubular epithelium (black arrowheads) and ADG (black arrows). **(B)** Gill of C^-. **(C)** Digestive gland of positive control (C^+). **(D)** Gill of C^+. **(E)** Digestive gland of Donor (D). **(F)** Gill of (D) **(G)** Hemolytic infiltrate (*) in soft connective tissue of (D) **(H)** Digestive gland of Recipient (R). **(I)** Gill of R. TL, Tubular lumen; N, Necrosis; At, Atrophied tubule; Bc, Bacterial colony; Blue arrowhead = goblet cell; Blue arrow = intervalvar hemocyte; Green arrow = Lamellar cilia. H&E Stain.

10.3389/fimmu.2025.1727164

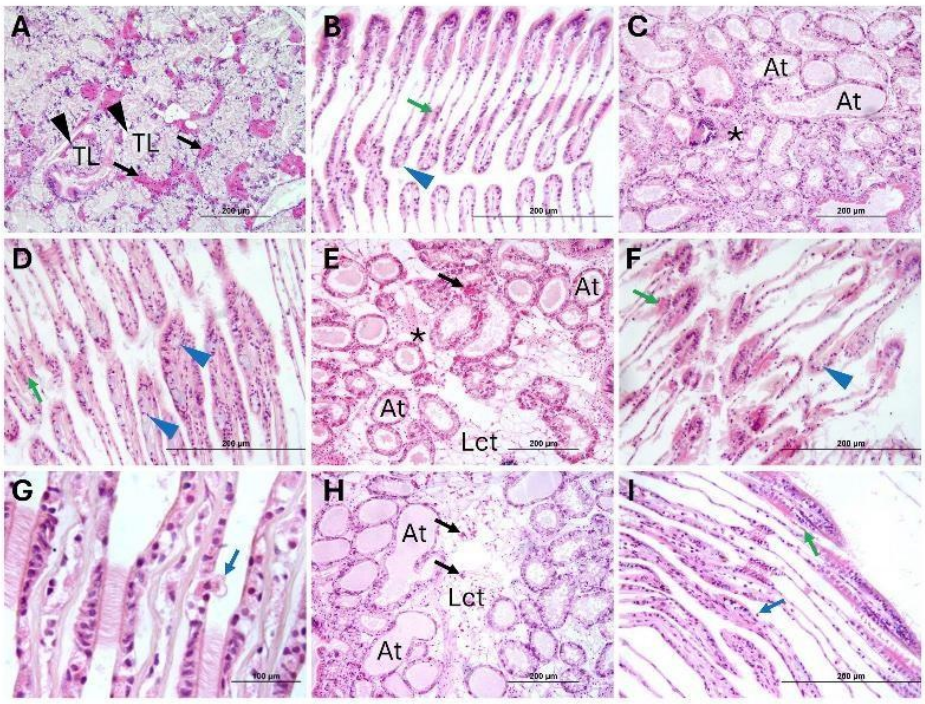

FIGURE 6
Representative H&E stain images of histological sections of *M. galloprovincialis* from the cohabitation experiment in negative controls, positive controls, donors and recipients at 4 days of exposure. **(A)** Digestive gland of negative control (C^-) showing the tubular epithelium (black arrowheads) and ADG (black arrows). **(B)** Gill of C^-. **(C)** Digestive gland of positive control (C^+). **(D)** Gill of C^+. **(E)** Digestive gland of Donor (D). **(F)** Gill of (D) **(G)** Hemocyte passing through the epithelium into the intervalvar space in (D) **(H)** Digestive gland of Recipient (R). **(I)** Gill of R. TL, Tubular lumen; At, Atrophied tubule. Lct, Loose connective tissue; * = hemocyte infiltrate; Blue arrowhead = goblet cell; Blue arrow = intervalvar hemocyte; Green arrow = Lamellar cilia. H&E Stain.

numerous adipogranular (ADG) cells in the intertubular spaces (Figures 5A, 6A). The connective tissue showed a regular appearance and contained abundant ADG cells in most individuals. Also, the gills exhibited a normal appearance, with few free intervalvar hemocytes and intact interlamellar cilia (Figures 5B, 6B).

At 1 day of exposure, C^+ (70%), D (80%), and R samples (30%) exhibited varying degrees of lesions in both the digestive gland and gills. Multifocal necrosis, degeneration with epithelial sloughing into the tubular lumen, hemolytic infiltration and atrophy were observed in the digestive gland of C^+ (Figure 5C), D (Figure 5E) and R (Figure 5H). Filament necrosis, epithelial sloughing, and interlamellar cilia damage were noted in the gills of C^+ (Figure 5D), D (Figure 5F) and R (Figure 5I). In some mussels from C^+ and D groups (Figure 5G), abundant hemolytic infiltration was observed in the loose connective tissue and mantle. In C^+, 20% showed mild lesions, 40% moderate, and 10% severe. Among D, 20% exhibited mild lesions, 50% moderate lesions, and 10% severe lesions. In the R group, 23.33% of mussels exhibited mild lesions, and 6.67% showed moderate lesions; no individuals in this group showed severe lesions.

At 4 days p.i., mussels from all groups showed fewer lesions compared to those observed at day 1 (Figure 6). However, individuals from C^+, D, and R groups exhibited some degree of digestive gland atrophy (50, 50 and 13.33%, respectively), with a reduction in the number of ADG cells and presence of hemocyte infiltration (Figures 6C, E, H), although no tissue necrosis was observed. In the gills, the presence of hemocytes into the intervalvar space (Figures 6G, I), an increase in the number of goblet cells (Figures 6B, D, F) and damaged interlamellar cilia were observed; however, the tissue generally showed signs of recovery. In C^+ and D 20% of the individuals exhibited mild lesions, while the remaining 30% showed moderate lesions. Among R, 10% of mussels exhibited mild lesions, and only 3.33% showed moderate lesions. No individuals showed severe lesions at 4 days of exposure.

Quantitative analysis showed that at 1 day of exposure, C^+, D and R samples exhibited a significant increase in the number of goblet cells in gills (Figure 7A) and free hemocytes in the intervalvar space (Figure 7B), compared to the C^- group, while the number of ADG cells in the digestive gland decreased significantly (Figure 7C). However, at 4 days of exposure, the number of goblet cells and free hemocytes in the inter-valvar space in individuals

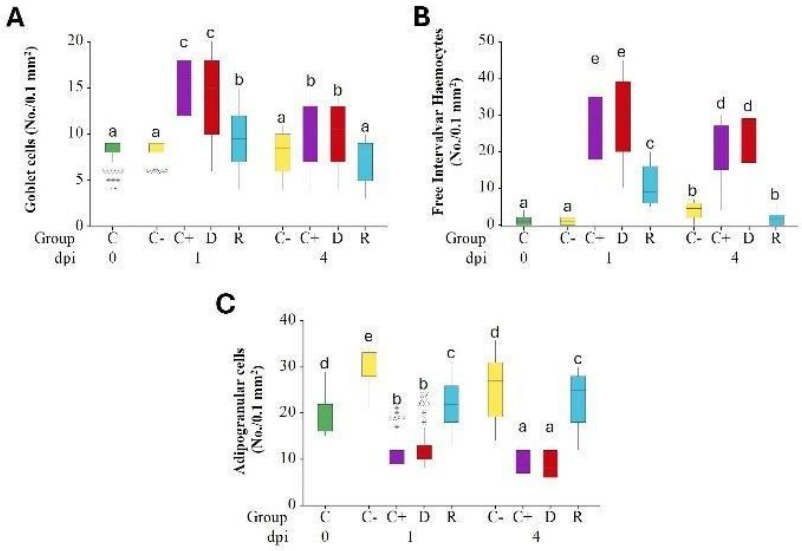

FIGURE 7
Boxplot graphs showing the number of goblet cells **(A)** and the free intervalvar hemocytes **(B)** in gill, and ADG(C) in digestive gland of *M. galloprovincialis* from the cohabitation experiment at 0, 1 and 4 days p.i. C_0 = control at time 0; negative (C^-) and positive (C^+) controls, donors **(D)**, recipients (R). For each group, the number of individuals analyzed were: 30 mussels at T0, 10 from D, C^- and C^+ samples and 30 from R samples at 1 and 4 days. Data were analyzed by the Kruskal-Wallis' test, followed by pairwise Dunn's tests with Bonferroni correction. Different superscript letters indicate statistically significant differences among groups. The line within each box represents the mean value; * = outlier points.

from C^+, D and R decreased significantly compared those observed at 1 day, approaching baseline values similar to those of the negative control C^- (Figure 7). In contrast, the number of ADG cells continued to decrease, at least in C^+ and D groups, which showed the greatest degree of tissue damage.

3.4 Bath infection experiments

The effects of bath infection with *V. ostreicida* were evaluated in mussels sampled from the Alcanar site in July 2024. Samplings were performed from 1 to 4 days and the same parameters were evaluated as in injection/cohabitation experiments. No mortality was observed in any experimental group.

As shown in Figure 8A, in July the presence of *V. ostreicida* in hemolymph cultures at day 0, before infection, was detected in 5 out of 6 sample pools (80%), a value much higher than those recorded in April and May (see Figure 3A). In contrast, no *V. ostreicida* was detected in any mantle samples at any sampling time (data not shown). In control samples a complete clearance of cultivable bacteria from hemolymph was observed after 1 day. Bath infected mussels (*V.o.*) showed a slower elimination of *V. ostreicida* (reaching 100% clearance at day 2). However, a subsequent progressive increase in positive samples was observed in the following days (up to 50% at day 4), indicating successful infection. Water samples were positive for *V. ostreicida* growth at 2 days in Control tanks, and from day 2 to day 4 in *V.o.* infected tanks (data not shown).

No changes in hemocyte LMS were recorded in control samples throughout the experiment. In contrast, a small but significant decrease (>30%), indicating mild stress conditions, was observed in infected mussels from day 1, followed by full recovery by day 4 (Figure 8B). No changes in lysozyme activity were recorded (Supplementary Figure S4).

No histological alterations were observed in mussels analyzed at the different time points. There were no differences in the overall tissue appearance between the control group and the mussels exposed to *V. ostreicida*: both showed abundant ADG cells between the digestive tubules and within the loose connective tissue, star-shaped digestive tubules with numerous vacuolated epithelial cells, and gills without lesions. No hemolytic infiltration or necrosis was detected in any specimens. Representative images are reported at day 0, 1, 2 and 3 (Supplementary Figures S2, S3). Similarly, no histopathological alterations were observed at day 1 and 4 (not shown).

4 Discussion

In this work, first data are reported on the effects of *in vivo* experimental infections of adult *M. galloprovincialis* with the potential bivalve pathogen *V. ostreicida*, utilizing a strain (r172)

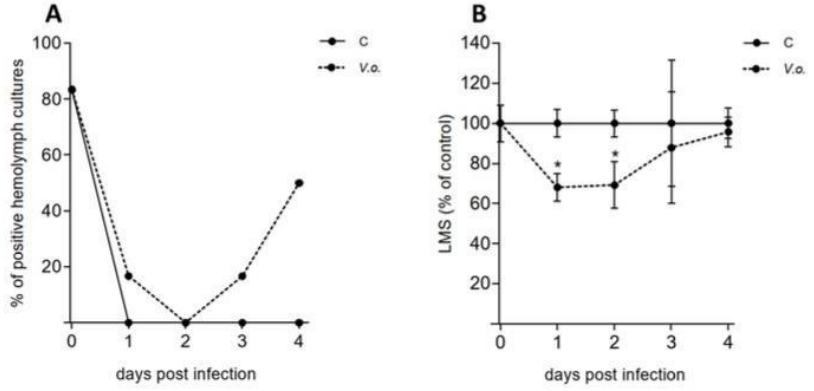

FIGURE 8
Bath infection experiment. Mussels were exposed to *V. ostreicida* spiked in water (10^5 CFU/mL) and samples of hemolymph were analyzed from day 0 to day 4 post infection. C: control mussels and *V.o.*: *V. ostreicida* challenged mussels. **(A)** Detection of viable, cultivable *V. ostreicida* in hemolymph pools. PCR data are expressed as % positive samples in hemolymph pools (n = 6). **(B)** Hemocyte lysosomal membrane stability (LMS): data are the mean ± SD evaluated in 6 pools for each condition (n = 6). For more details about number of animals per pool see method 2.6. Statistical analyses were performed by non-parametric Kruskal-Wallis followed by Dunn's multiple comparisons test, * = $P < 0.05$.

previously isolated from a mussel mortality episode that occurred at Alfacs Bay in the Ebro delta (Spain) in 2022 (34).

The results of a virulence assay carried out in animals from another mussel site at the Ebro delta (Fangar Bay) indicate an average 50% mortality within 5 days of infection by intravalvar injection. Moreover, the present data show that *V. ostreicida*-induced cumulative mortality in experimental infection was independent of increasing temperatures. Actually, the mortality episode from which this strain was isolated occurred in April 2022 at 18 °C, a temperature that is not generally associated with mussel mortality outbreaks. However, the slightly faster onset of mortality observed at increasing temperatures suggests that seawater warming may contribute to a faster growing rate of this strain.

Mussels collected from different sites in the Ebro delta were then screened for the presence of *V. ostreicida*, utilizing the PCR protocol recently developed (34) with slight modifications. In April 2024 the scaling of the percentage of individuals positive for *V. ostreicida* was Fangar Bay > Alfacs Bay > Alcanar. Therefore, mussels collected from Alcanar, a site nearby open waters (Cases de Alcanar, Tarragona, Spain) were utilized for subsequent *in vivo* experiments utilizing two different models of infection, injection and bath exposure, respectively.

A month later (May 2024), a first injection/cohabitation experiment was carried out in order to investigate the time course of infection, the possibility of horizontal transfer of bacteria among individuals and mussel hemolymph parameters (see experimental set up in Figure 1). The results indicate that at 1 day p.i. bacterial cultures from hemolymph of injected mussel groups (C^+ and D) were 100% positive for *V. ostreicida*, confirming successful infection. In contrast, no positive samples were detected in the R group, indicating the absence of transmission of live bacteria in hemolymph. By day 4 p.i. cultivable *V. ostreicida* was not detected in any sample group, indicating clearance of live bacteria from the circulation. Cultivable *V. ostreicida* was also detected in the water from both C^+ and cohabitation tanks at 1 day p.i. but not at 4 days p.i. These data may reflect the results of an *in vivo* bactericidal activity of mussels against *V. ostreicida* over time. In contrast, in mantle samples, where direct PCR analysis reveals the presence of both live and dead vibrios, *V. ostreicida* was detected at 1 day p.i. in both D and R mussel groups (with 50 and 40% positive samples, respectively), indicating that bacterial transfer occurs among individuals of different groups, probably due to the direct contact of this tissue with the surrounding water. At 4 days p.i., the percentage of mantle positive samples declined in all groups, indicating partial elimination also from this tissue.

Infection with *V. ostreicida* induced parallel transient responses in hemolymph components. A dramatic decrease in hemocyte LMS was observed at 1 and 4 days in injected mussels (C^+ and D) and a similar, although smaller effect, also in R samples. A parallel increase in serum lysozyme activity observed in C^+ and D at 1 and 4 days p.i. may indicate enzyme leakage from damaged hemocytes. At 20 days p.i., full recovery of both parameters was observed in all samples. Due to the large decrease in hemocyte LMS observed in injected mussels at shorter times of exposure, indicating irreversible cell damage and death (36), the subsequent recovery of LMS values can be ascribed either to the presence in hemolymph of healthy hemocytes derived from differentiation of new granular hemocytes in the circulation, or recruitment of pre-existing hemocytes from tissues during recovery from stress conditions, or both (42).

The effects of infection with *V. ostreicida* and subsequent recovery, as well as the partial horizontal transfer from infected to uninfected mussels, were confirmed by histopathology data obtained in digestive gland and gills, showing varying degrees of lesions in different experimental groups and times of exposure. At 1 day p.i. multifocal necrosis, degeneration with epithelial sloughing

into the tubular lumen, hemolytic infiltration and atrophy were observed in the digestive gland, along with filament necrosis, epithelial sloughing, and interlamellar cilia damage in the gills. These effects were recorded in the tissues of mussels from all experimental groups and were more severe in C^+ and D with respect to the R group. Severe lesions (10%) were observed only in injected mussels, but not in the R group. At 4 days p.i. both tissues showed signs of recovery, and no severe lesions were observed in any experimental group. In more detail, quantitative differences could be observed in the number of gill goblet cells and intervalvar (pallial) hemocytes, showing a transient increase at 1 day p.i. in both injected and R groups, followed by partial recovery at 4 days. Goblet cells are responsible for mucus secretion, that represents a first defense reaction in epithelia (43).

Bivalve hemocytes are able to move freely in a semi-open circulatory system, reaching the surface of the body and the extrapallial cavity: several studies underlined bidirectional exchanges between circulatory and pallial hemocytes (44–46). Since the pallial surfaces (epithelial tissues associated with the gills, mantle and palps) are directly exposed to the surrounding environment, and thus to the multitude of micro-organisms present in the water column, hemocytes associated with pallial organs represent the first host immune cells that can potentially interact with waterborne bacteria, and thus have major implications for the mechanisms of early host-pathogen interactions. In mussels, it has been shown that in response to temperature stress, hemocytes are released in seawater, where they can survive and remain functionally competent before entering other mussels; moreover, opportunistic bacteria can infect hemocytes in seawater and take advantage of the entry of hemocytes into other mussels to spread into healthy individuals (45). The transient increase observed in the number of intervalvar hemocytes in both injected and recipient mussels underlines a possible role for this hemocyte sub-population in response to mussel infection with *V. ostreicida*, and suggests a possible role in horizontal transfer of these vibrios among individuals (see Figure 9). Although mussel intervalvar hemocytes have been characterized for functional and molecular properties (46) further studies are needed on their role in spreading pathogen infection under different environmental stressors.

Finally, the results underline a persistent decrease in digestive gland ADG cells in injected mussel groups. ADG are storage cells present in different bivalve tissue containing lipid and glycogen reserves, that are essential for providing the energy and resources for maintaining bivalve health (47, 48). These data indicate the utilization of energy reserves to support defense responses during mussel infection with *V. ostreicida*.

Overall, the injection/cohabitation experiments indicate the possibility of horizontal transfer of *V. ostreicida* from infected to uninfected mussels. In this process, where intervalvar hemocytes may play a role (45, 46), the proximity of cultivated mussels at different sites may represents a significant risk of infection. Such a transfer has been previously described in cohabitation experiments of infected oysters and mussels, with stronger consequences on recipients mussels (31, 38). However, the results here obtained cannot be compared with those of previous studies, due to several differences in experimental set up and endpoints measured and, most of all, to the utilization of *V. splendidus* strains, that represent known bivalve pathogens (31, 38).

A bath infection experiment was then carried out in July 2024, exposing mussels to *V. ostreicida* at 10^5 CFU/mL in seawater. At this time of the year, the mantle tissues of mussels from Alcanar were negative for the presence of *V. ostreicida*; although in hemolymph cultures at the beginning of the experiment a high percentage of positive samples was recorded (80%), this value declined to 0% from 1 day of exposure in clean seawater in control (unexposed mussels) and from day 2 in exposed mussels, indicating a complete clearance of cultivable bacteria from hemolymph of control and infected mussels. However, a subsequent rise in bacterial growth was observed in the hemolymph of infected mussels, as a result of the filtration

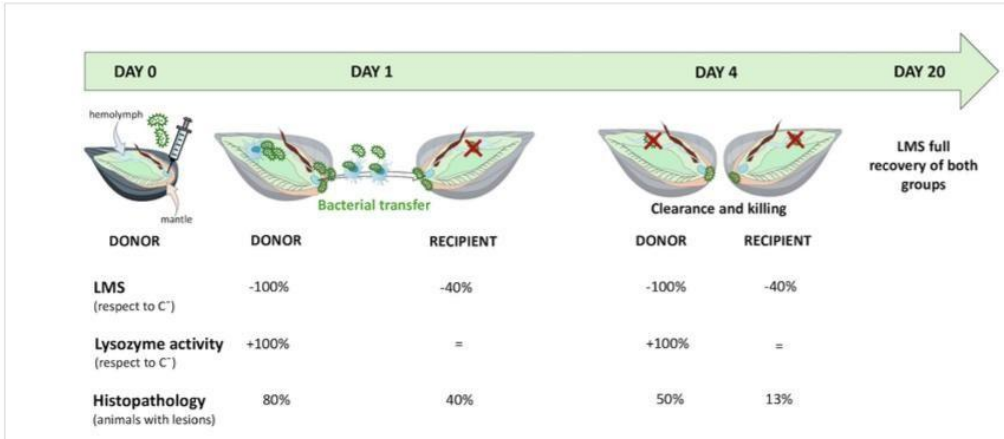

FIGURE 9
Summarized results from cohabitation experiment.

process of water by the gills and subsequent transfer of live bacteria to the circulation. Actually, water samples were positive for cultivable bacteria from day 2 to day 4 in the *V. ostreicida* infected tank, despite the daily water change, suggesting release of live bacteria from animals. LMS data indicate a fast and transient stress response in circulating hemocytes from 1 day of exposure to *V. ostreicida*. In mussel hemocytes, where LMS is an extremely sensitive parameter of cellular stress, such an effect could be induced by both cultivable and not cultivable or dead bacteria.

Finally, bath infection did not result in an increase of *V. ostreicida* positive samples in the mantle, or significant histopathological alterations in either gills or digestive gland. Although further data on the presence of live, cultivable *V. ostreicida* r172 in the sea water at the site of mussel collection will complement those on the positivity of mussel samples to this strain, the results indicate a fast depuration process from mussel tissues.

The results obtained from injection experiments demonstrate that *V. ostreicida* induces significant stress conditions in *M. galloprovincialis*, as shown by hemolymph parameters and tissue histopathology. However, all the observed responses were transient, and paralleled by a decrease in the presence of *V. ostreicida* within 4 days, indicating a capacity of the mussels to partially cope with infection. Such a capacity was confirmed in the more environmentally realistic exposure conditions of bath exposure experiments, that resulted in lower infection and stress conditions. The results of both *in vivo* experiments show that LMS represents a sensitive parameter to measure the response of mussel hemocytes to *V. ostreicida*, independent of the route of infection.

Overall, the results indicate a moderate pathogenicity of *V. ostreicida* r172 to mussels in *in vivo* infection models. These data provide further information on the interactions between the bivalve host and potential pathogenic vibrios. For *Mytilus* spp., these data may help understanding or predicting the onset and progression of disease in the context of increasing mortality outbreaks of farmed mussels in different environmental contexts.

From the present study, two additional points emerge that warrant further consideration.

The first concerns the background infection with cultivable *V. ostreicida* observed in hemolymph samples of control mussels used for laboratory experiments. Although mussels were initially collected from the site with the lowest *V. ostreicida* contamination (Alcanar), a progressive increase in the percentage of positive samples was recorded (from 16% in April to 33% in May and 80% in July) corresponding to seawater temperatures at the time of collection of 15.9, 18.7, and 24.9°C, respectively. While this variation could reflect natural differences among mussel groups, the data suggests that the presence of cultivable *V. ostreicida* in hemolymph increases with rising seawater temperature. In this context, the application of PCR to bacterial cultures from tissue samples may greatly enhance monitoring of *V. ostreicida* dynamics in mussel tissues under field conditions throughout the year.

With regards to the effects of *V. ostreicida* on mussel mortalities, significant effects were recorded in virulence assays carried out in mussels sampled from Fangar Bay in winter; however, no mortality was observed in subsequent injection and bath infections experiments carried out on mussels from Alcanar, a site from nearby open waters, sampled in late spring. The results indicate a distinct susceptibility of different populations of cultivated mussels, irrespectively of seawater temperatures recorded at sampling times. This may depend on other several factors, including salinity fluctuations, tissue loads of contaminants, mussel density and depth in the long line system (5), as well as to previous exposure history of mussels to other vibrios, leading to immune priming (42, 49). From the present data, temperature does not seem to represent a major conditioning factor in influencing the virulence of *V. ostreicida*; however, as underlined above, environmental temperatures may influence the presence of live bacteria in mussel hemolymph. Finally, since mussel stocks in the Ebro delta cultivation areas are imported from other growing sites, their genetic background would also play a role in resistance to infection (50).

Overall, the results underline the complexity of understanding the infection dynamics of environmental vibrio strains and their outcome in mussel populations.

Data availability statement

The raw data supporting the conclusions of this article will be made available by the authors, without undue reservation.

Ethics statement

The manuscript presents research on animals that do not require ethical approval for their study.

Author contributions

ML: Conceptualization, Data curation, Formal Analysis, Investigation, Writing – original draft, Writing – review & editing. JL: Investigation, Writing – review & editing. YC-Q: Data curation, Formal Analysis, Investigation, Writing – review & editing. MA: Conceptualization, Writing – review & editing. KA: Supervision, Writing – review & editing. MF-T: Resources, Writing – review & editing. LV: Conceptualization, Resources, Supervision, Writing – review & editing. DF: Resources, Supervision, Writing – review & editing. LC: Conceptualization, Supervision, Writing – original draft, Writing – review & editing.

Funding

The author(s) declare financial support was received for the research and/or publication of this article. This work was partially supported by the project "Emergent risks related to shellfish mortalities in the Ebro delta-REMBE". ARP140/20/000011, funded by the European Maritime and Fisheries Fund (EMFF)-European Commission and Generalitat de Catalunya. Project

funded under the National Recovery and Resilience Plan (NRRP), Mission 4 Component 2 Investment 1.4 -Call for tender No. 3138 of 16 December 2021, rectified by Decree n.3175 of 18 December 2021 of Italian Ministry of University and Research funded by the European Union -NextGenerationEU; Award Number: Project code CN_00000033, Concession Decree No. 1034 of 17 June 2022 adopted by the Italian Ministry of University and Research, CUP D33C22000960007, Project title "National Biodiversity Future Center -NBFC".

Conflict of interest

The authors declare that the research was conducted in the absence of any commercial or financial relationships that could be construed as a potential conflict of interest.

Generative AI statement

The author(s) declare that no Generative AI was used in the creation of this manuscript.

Any alternative text (alt text) provided alongside figures in this article has been generated by Frontiers with the support of artificial intelligence and reasonable efforts have been made to ensure accuracy, including review by the authors wherever possible. If you identify any issues, please contact us.

Publisher's note

All claims expressed in this article are solely those of the authors and do not necessarily represent those of their affiliated organizations, or those of the publisher, the editors and the reviewers. Any product that may be evaluated in this article, or claim that may be made by its manufacturer, is not guaranteed or endorsed by the publisher.

Supplementary material

The Supplementary Material for this article can be found online at: https://www.frontiersin.org/articles/10.3389/fimmu.2025.1727164/full#supplementary-material

References

1. Baker-Austin C, Lake I, Archer E, Hartnell R, Trinanes J, Martinez-Urtaza J. Stemming the rising tide of Vibrio disease. *Lancet Planet Health*. (2024) 8:e515–20. doi: 10.1016/S2542-5196(24)00124-4

2. Travers MA, Boettcher Miller K, Roque A, Friedman CS. Bacterial diseases in marine bivalves. *J Invertebr Pathol*. (2015) 131:11–31. doi: 10.1016/j.jip.2015.07.010

3. Charles M, Bernard I, Villalba A, Oden E, Burioli EAV, Allain G, et al. High mortality of mussels in northern Brittany – Evaluation of the involvement of pathogens, pathological conditions and pollutants. *J Invertebr Pathol*. (2020) 170:107308. doi: 10.1016/j.jip.2019.107308

4. Destoumieux-Garzón D, Canesi L, Oyanedel D, Travers M, Charrière GM, Pruzzo C, et al. *Vibrio* –bivalve interactions in health and disease. *Environ Microbiol*. (2020) 22:4323–41. doi: 10.1111/1462-2920.15055

5. Rowley AF, Baker-Austin C, Boerlage AS, Caillon C, Davies CE, Duperret L, et al. Diseases of marine fish and shellfish in an age of rapid climate change. *iScience*. (2024) 27:110838. doi: 10.1016/j.isci.2024.110838

6. Dubert J, Barja JL, Romalde JL. New insights into pathogenic vibrios affecting bivalves in hatcheries: present and future prospects. *Front Microbiol*. (2017) 8:762. doi: 10.3389/fmicb.2017.00762

7. Saulnier D, De Decker S, Haffner P, Cobret L, Robert M, Garcia C. A large-scale epidemiological study to identify bacteria pathogenic to pacific oyster crassostrea gigas and correlation between virulence and metalloprotease-like activity. *Microb Ecol*. (2010) 59:787–98. doi: 10.1007/s00248-009-9620-y

8. Madec S, Pichereau V, Jacq A, Paillard M, Boisset C, Guérard F, et al. Characterization of the secretomes of two vibrios pathogenic to mollusks. *PloS One*. (2014) 9:e113097. doi: 10.1371/journal.pone.0113097

9. Barbosa Solomieu V, Renault T, Travers MA. Mass mortality in bivalves and the intricate case of the Pacific oyster, Crassostrea gigas. *J Invertebr Pathol*. (2015) 131:2–10. doi: 10.1016/j.jip.2015.07.011

10. Azéma P, Lamy JB, Boudry P, Renault T, Travers MA, Dégremont L. Genetic parameters of resistance to Vibrio aestuarianus, and OsHV-1 infections in the Pacific oyster, Crassostrea gigas, at three different life stages. *Genet Sel Evol*. (2017) 49:23. doi: 10.1186/s12711-017-0297-2

11. Sandlund N, Torkildsen L, Magnesen T, Mortensen S, Bergh Ø. Immunohistochemistry of great scallop Pecten maximus larvae experimentally challenged with pathogenic bacteria. *Dis Aquat Organ*. (2006) 69:163–73. doi: 10.3354/dao069163

12. Kesarcodi-Watson A, Kaspar H, Lategan MJ, Gibson L. Two pathogens of Greenshell™ mussel larvae, *Perna canaliculus* : *Vibrio splendidus* and a V. coralliilyticus/neptunius -like isolate. *J Fish Dis*. (2009) 32:499–507. doi: 10.1016/j.aquaculture.2012.04.026

13. Rojas R, Miranda CD, Opazo R, Romero J. Characterization and pathogenicity of Vibrio splendidus strains associated with massive mortalities of commercial hatchery-reared larvae of scallop Argopecten purpuratus (Lamarck, 1819). *J Invertebr Pathol*. (2015) 124:61–9. doi: 10.1016/j.jip.2014.10.009

14. Ben Cheikh Y, Travers MA, Morga B, Godfrin Y, Rioult D, Le Foll F. First evidence for a Vibrio strain pathogenic to Mytilus edulis altering hemocyte immune capacities. *Dev Comp Immunol*. (2016) 57:107–19. doi: 10.1016/j.dci.2015.12.014

15. De Rijcke M, Van Acker E, Nevejan N, De Schamphelaere KAC, Janssen CR. Toxic dinoflagellates and Vibrio spp. act independently in bivalve larvae. *Fish Shellfish Immunol*. (2016) 57:236–42. doi: 10.1016/j.fsi.2016.08.027

16. Balbi T, Auguste M, Cortese K, Montagna M, Borello A, Pruzzo C, et al. Responses of Mytilus galloprovincialis to challenge with the emerging marine pathogen Vibrio coralliilyticus. *Fish Shellfish Immunol*. (2019) 84:352–60. doi: 10.1016/j.fsi.2018.10.011

17. Balbi T, Bozzo M, Auguste M, Montagna M, Miglioli A, Drouet K, et al. Impact of ocean warming on early development of the Mediterranean mussel Mytilus galloprovincialis: Effects on larval susceptibility to potential vibrio pathogens. *Fish Shellfish Immunol*. (2024) 154:109937. doi: 10.1016/j.fsi.2024.109937

18. Carrasco N, Gairin I, Pérez J, Andree KB, Roque A, Fernández-Tejedor M, et al. A production calendar based on water temperature, spat size, and husbandry practices reduce osHV-1 µvar impact on cultured pacific oyster crassostrea gigas in the ebro delta (Catalonia), mediterranean coast of Spain. *Front Physiol*. (2017) 8:125/full. doi: 10.3389/fphys.2017.00125/full

19. Coyle NM, O'Toole C, Thomas JCL, Ryder D, Feil EJ, Geary M, et al. Vibrio aestuarianus *Clade A and Clade B isolates are associated with Pacific oyster (*Crassostrea gigas*) disease outbreaks across Ireland*. (2023). doi: 10.1101/2023.04.06.535062.

20. Bean TP, Farley H, Nascimento-Schulze J, Regan T. Scottish oyster mortality event and association with Vibrio aestuarianus. *Aquac Rep*. (2024) 39:102480. doi: 10.1016/j.aqrep.2024.102480

21. Charles M, Trancart S, Oden E, Houssin M. Experimental infection of *Mytilus edulis* by two *Vibrio splendidus* -related strains: Determination of pathogenicity level of strains and influence of the origin and annual cycle of mussels on their sensitivity. *J Fish Dis*. (2020) 43:9–21. doi: 10.1111/jfd.13094

22. Lupo C, Bougeard S, Le Bihan V, Blin JL, Allain G, Azéma P, et al. Mortality of marine mussels *Mytilus edulis* and M. galloprovincialis : systematic literature review of risk factors and recommendations for future research. *Rev Aquac*. (2021) 13:504–36. doi: 10.1111/raq.12484

23. Bechemin C, Soletchnik P, Polsenaere P, Moine OL, Pernet F, Protat M, et al. Episodes de mortalité massive de moules bleues observés en 2014 dans les Pertuis charentais. *Bulletin Epidémiologique* (2015) 67:6–9. Available online at: https://hal.science/hal-02554385v1.

24. Oden E, Burioli EAV, Trancart S, Pitel PH, Houssin M. Multilocus sequence analysis of Vibrio splendidus related-strains isolated from blue mussel Mytilus sp. during mortality events. *Aquaculture*. (2016) 464:420–7. doi: 10.1016/j.aquaculture.2016.07.024

25. Polsenaere P, Soletchnik P, Le Moine O, Gohin F, Robert S, Pépin JF, et al. Potential environmental drivers of a regional blue mussel mass mortality event (winter of 2014, Breton Sound, France). *J Sea Res*. (2017) 123:39–50. doi: 10.1016/j.seares.2017.03.005

26. Capelle JJ, Garcia AB, Kamermans P, Engelsma MY, Jansen HM. Observations on recent mass mortality events of marine mussels in the Oosterschelde, the Netherlands. *Aquac Int*. (2021) 29:1737–51. doi: 10.1007/s10499-021-00713-6

27. Balbi T, Fabbri R, Cortese K, Smerilli A, Ciacci C, Grande C, et al. Interactions between Mytilus galloprovincialis hemocytes and the bivalve pathogens Vibrio aestuarianus 01/032 and Vibrio splendidus LGP32. *Fish Shellfish Immunol*. (2013) 35:1906–15. doi: 10.1016/j.fsi.2013.09.027

28. Restif O, Graham AL. Within-host dynamics of infection: from ecological insights to evolutionary predictions. *Philos Trans R Soc B Biol Sci*. (2015) 370:20140304. doi: 10.1098/rstb.2014.0304

29. Ciacci C, Manti A, Canonico B, Campana R, Camisassi G, Baffone W, et al. Responses of Mytilus galloprovincialis hemocytes to environmental strains of Vibrio parahaemolyticus, Vibrio alginolyticus, Vibrio vulnificus. *Fish Shellfish Immunol*. (2017) 65:80–7. doi: 10.1016/j.fsi.2017.04.002

30. Balbi T, Cortese K, Ciacci C, Bellese G, Vezzulli L, Pruzzo C, et al. Autophagic processes in Mytilus galloprovincialis hemocytes: Effects of Vibrio tapetis. *Fish Shellfish Immunol*. (2018) 73:66–74. doi: 10.1016/j.fsi.2017.12.003

31. Ben Cheikh Y, Travers MA, Le Foll F. Infection dynamics of a V. splendidus strain pathogenic to Mytilus edulis: *In vivo* and *in vitro* interactions with hemocytes. *Fish Shellfish Immunol*. (2017) 70:515–23. doi: 10.1016/j.fsi.2017.09.047

32. Prado S, Romalde J, Montes J, Barja J. Pathogenic bacteria isolated from disease outbreaks in shellfish hatcheries. First description of Vibrio neptunius as an oyster pathogen. *Dis Aquat Organ*. (2005) 67:209–15. doi: 10.3354/dao067209

33. Prado S, Dubert J, Romalde JL, Toranzo AE, Barja JL. Vibrio ostreicida sp. nov., a new pathogen of bivalve larvae. *Int J Syst Evol Microbiol*. (2014) 64:1641–6. doi: 10.1099/ijs.0.051417-0

34. Lopez JR, Leonessi M, Fernandez-Tejedor M, Auguste M, Doni L, Cruz-Quintana Y, et al. First description of Vibrio ostreicida as putative causal agent of disease in Mediterranean mussel (Mytilus galloprovincialis) and development of a PCR protocol for its rapid diagnosis. *J Invertebr Pathol*. (2025) :212:108399. doi: 10.1016/j.jip.2025.108399

35. Auguste M, Rahman FU, Balbi T, Leonessi M, Oliveri C, Bellese G, et al. Responses of Mytilus galloprovincialis to challenge with environmental isolates of the potential emerging pathogen Malaciobacter marinus. *Fish Shellfish Immunol*. (2022) 131:1–9. doi: 10.1016/j.fsi.2022.09.048

36. OSPAR Commission. *Background documents and technical annexes for biological effects monitoring* (2013). Available online at: www.ospar.org.

37. Gay M, Berthe F, Le Roux F. Screening of Vibrio isolates to develop an experimental infection model in the Pacific oyster Crassostrea gigas. *Dis Aquat Organ*. (2004) 59:49–56. doi: 10.3354/dao059049

38. De Decker S, Saulnier D. Vibriosis induced by experimental cohabitation in Crassostrea gigas: Evidence of early infection and down-expression of immune-related genes. *Fish Shellfish Immunol*. (2011) 30:691–9. doi: 10.1016/j.fsi.2010.12.017

39. Ben Cheikh Y, Travers MA. Vibrio splendidus infection induces dysbiosis in the blue mussel and favors pathobiontic bacteria. *Microbiol Res*. (2022) 261:127078. doi: 10.1016/j.micres.2022.127078

40. Leonessi M, Auguste M, Lopez JR, Balbi T, Ciacci C, Oliveri C, et al. Interactions between the oyster larvae pathogen Vibrio ostreicida and the bivalve hosts Mytilus galloprovincialis and Magallana gigas. In: *Interact Oyster Larvae Pathog Vibrio Ostreicida Bivalve Hosts Mytilus Galloprovincialis Magallana Gigas*. *Front Immunol*. (2025) 16:1711477. doi: 10.3389/fimmu.2025.1711477

41. Howard, Dorothy W, EJ L, BJ K, Smith CS. *NOAA Technical Memorandum NOS NCCOS 5*. (2004).

42. Auguste M, Balbi T, Ciacci C, Canonico B, Papa S, Borello A, et al. Shift in Immune parameters after repeated exposure to nanoplastics in the marine bivalve mytilus. *Front Immunol*. (2020) 11:426. doi: 10.3389/fimmu.2020.00426

43. Allam B, Pales Espinosa E. Bivalve immunity and response to infections: Are we looking at the right place? *Fish Shellfish Immunol*. (2016) 53:4–12. doi: 10.1016/j.fsi.2016.03.037

44. Lau YT, Gambino L, Santos B, Pales Espinosa E, Allam B. Regulation of oyster (Crassostrea virginica) hemocyte motility by the intracellular parasite Perkinsus marinus: A possible mechanism for host infection. *Fish Shellfish Immunol*. (2018) 78:18–25. doi: 10.1016/j.fsi.2018.04.019

45. Caza F, Bernet E, Veyrier FJ, Betoulle S, St-Pierre Y. Hemocytes released in seawater act as Trojan horses for spreading of bacterial infections in mussels. *Sci Rep*. (2020) 10:19696. doi: 10.1038/s41598-020-76677-z

46. Panebianco A, Rey-Campos M, Romero A, Diz AP, Novoa B, Figueras A. Mytilus galloprovincialis releases immunologically functional haemocytes to the intervalvar space in response to tissue injury and infection. *Fish Shellfish Immunol*. (2023) 138:108806. doi: 10.1016/j.fsi.2023.108806

47. Pipe RK. Ultrastructural and cytochemical study on interactions between nutrient storage cells and gametogenesis in the mussel Mytilus edulis. *Mar Biol*. (1987) 96:519–28. doi: 10.1007/BF00397969

48. Berthelin C, Kellner K, Mathieu M. Storage metabolism in the Pacific oyster (Crassostrea gigas) in relation to summer mortalities and reproductive cycle (West Coast of France). *Comp Biochem Physiol B Biochem Mol Biol*. (2000) 125:359–69. doi: 10.1016/S0305-0491(99)00187-X

49. Rey-Campos M, Moreira R, Gerdol M, Pallavicini A, Novoa B, Figueras A. Immune Tolerance in Mytilus galloprovincialis Hemocytes After Repeated Contact With Vibrio splendidus. *Front Immunol*. (2019) 10:1894. doi: 10.3389/fimmu.2019.01894

50. Gerdol M, Moreira R, Cruz F, Gómez-Garrido J, Vlasova A, Rosani U, et al. Massive gene presence-absence variation shapes an open pan-genome in the Mediterranean mussel. *Genome Biol*. (2020) 21:275. doi: 10.1186/s13059-020-02180-3

Supplementary Material to

Dynamics of *Vibrio ostreicida* in *Mytilus galloprovincialis* through *in vivo* infections

Martina Leonessi[1,2*], Jose R. Lopez[3,4], Yanis Cruz-Quintana[3,5], Manon Auguste[1,2], Karl B. Andree[3], Margarita Fernandez-Tejedor[3], Luigi Vezzulli[1,2], Dolors Furones[3], Laura Canesi[1,2]

[1]Department of Earth, Environmental and Life Sciences (DISTAV), University of Genoa, Genoa 16132, Italy

[2]National Biodiversity Future Center, Palermo, Italy

[3]IRTA, Aquaculture Program. La Ràpita, Spain

[4]Universidade de Santiago de Compostela, Santiago de Compostela, Spain

1 [5]Facultad de Acuicultura y Ciencias del Mar, Universidad Técnica de Manabí, Bahía de Caráquez 130104, EcuadorMaterial and methods

Evaluation of hemolymph functional parameters

All procedures were performed as previously described (1). Functional parameters were evaluated directly on hemolymph samples after challenge. Hemolymph was extracted from the posterior adductor muscle using a sterile 1 mL syringe with an 18 G1/2" needle, filtered through sterile gauze and pooled in Falcon tube at 18 °C as previously described. Hemocyte monolayers were prepared depositing 20 µL drops of whole hemolymph on microscope slides and the cells were let to adhere at 18 °C for 20 min before removing the excess hemolymph excess (1). LMS was evaluated in hemocyte monolayers by the Neutral Red Retention Time (NRRT) assay (2) as previously described (1,3). After the adhering time, samples were incubated with a neutral red (NR) (Sigma-Aldrich, Milan, Italy) solution (40 µg/mL in ASW). After 15 min, excess dye removed, a drop of ASW was added and the slides were observed under an optical microscope from time zero every 15 min. The percentage of cells showing loss of dye from lysosomes in each field (10 fields each containing 8-10 cells) was evaluated until 50% of the cells showed sign of lysosomal leaking. All incubations were carried out at 18 °C. For determination of lysozyme release aliquots of whole hemolymph were centrifuged for 10 min at 100 x g, 4 °C and the supernatants collected and frozen at -80 °C. Lysozyme activity was evaluated in the extracellular medium spectrophotometrically at 450 nm using a suspension of *Micrococcus lysodeikticus* (15 mg/100 mL in 66 mM phosphate buffer, pH 6.4). Protein content was determined using the Bradford method using bovine serum albumin (BSA) as a standard. Data are reported per mg/protein sample and expressed a percentage of control values.

PCR protocol

PCR amplifications were carried out in a mixture containing 0.5 U Q5 High-Fidelity DNA Polymerase (Biolabs), 1X Q5 Reaction Buffer (containing 2 mM Mg^{+2}), 200 µM of dNTPs, 0.5 µM of each primer,

1X of Q5 High GC Enhancer and Ultra Pure PCR water as previously described (4) using primers shown in **Table S1**. Optimal conditions for PCR reaction were chosen as follows (**Table S2**): an initial denaturation at 98 °C for 30 s followed by 35 amplification cycles of denaturation at 98 °C for 10 s, annealing at 55 °C for 30 s, extension at 72 °C for 30 s and a final elongation at 72 °C for 2 min. DNA from type strain *V. ostreicida* CECT7398T at 5 ng/µL was used as positive control, and Ultra Pure PCR water was employed as a negative control. Samples of PCR products were run on a 1.5 % agarose gel TAE (Tris-acetate-EDTA buffer) stained with ethidium bromide. The Invitrogen 1Kb Plus Ladder was used as a molecular weight marker.

1 Tables

Table S1. Primer sequences for amplification of *V. ostreicida* and the size of the obtained products.

Gene	Primers sequences from 5' to 3'	product size	Reference
gyr B	F: GACAACGGGAACAAAAATCC	491 bp	Lopez et al., 2025
	R: ACACGACCGCGGTTAGGC		

Table S2. PCR conditions

DNA concentration	mantles: 50 ng/µL bacterial cultures: 5 ng/µL
N° of cycles	35
Denaturation 1	98 °C x 30 s
Denaturation 2	98 °C x 10 s
Annealing	55 °C x 30 s
Extention	72 °C x 30 s
Final elongation	72 °C x 2 min

2 Figures

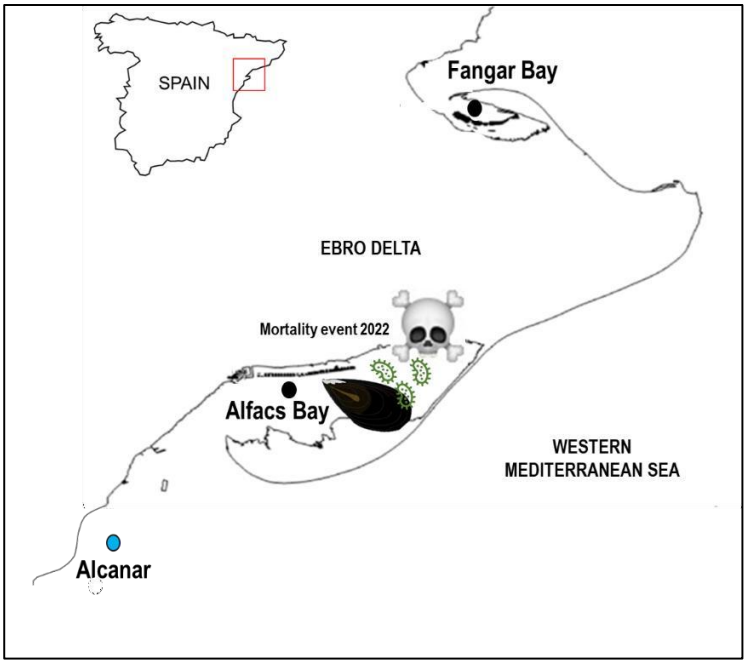

Figure S1. Locations of the 3 mussel farms in Ebro Delta (Spain): Fangar Bay, Alfacs Bay and Alcanar.

Figure S2. Experimental conditions in the preliminary cohabitation experiments. R: recipients, D: donors. 1D:1R (Tank 1), 1D:3R (Tank 2) and 1D:10R (Tank 3). Positive (*V. ostreicida* injected) (C^+) and negative (PBS injected) (C^-) controls were run in parallel. The number of D and R mussels in each tank is indicated, with a total of 80 mussels per each tank. The experiment was run twice. During the experiments, animals were maintained under static conditions in UV-treated and filtered seawater at 18 °C with aeration. The mortality in each tank was monitored daily, dead mussels were removed, and water was changed daily.

1 Results

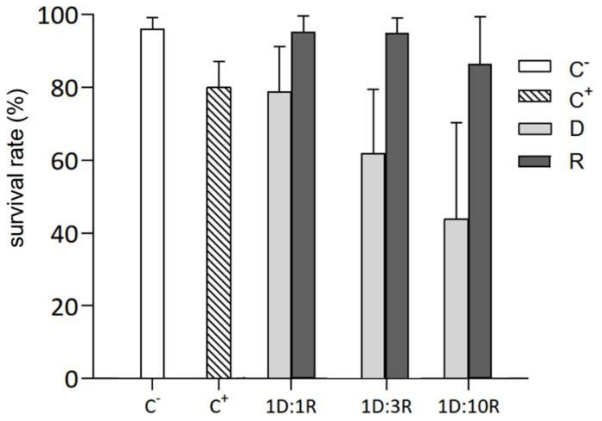

Figure S3. Survival rate (%) during the cohabitation experiments up to 20 days in Donors (D) and Recipients (R) in the different tanks: 1D:1R (Tank 1), 1D:3R (Tank 2) and 1D:10R (Tank 3). The experiment was run twice. C^-: negative control, C^+: positive control, R: recipients, D: donors.

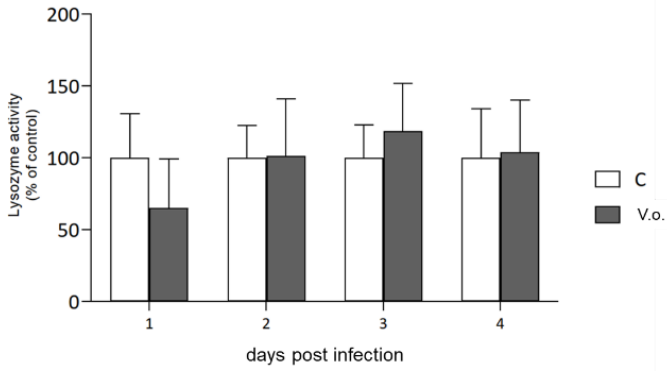

Figure S4. Effects of bath infection on lysozyme activity in hemolymph of *M. galloprovincialis*. Data, representing the mean ± SD of 6 pools of hemolymph samples for each condition (n=6), were analysed by non-parametric Kruskal-Wallis followed by Dunn's multiple comparisons test. No significant differences were observed among different groups ($p > 0.05$).

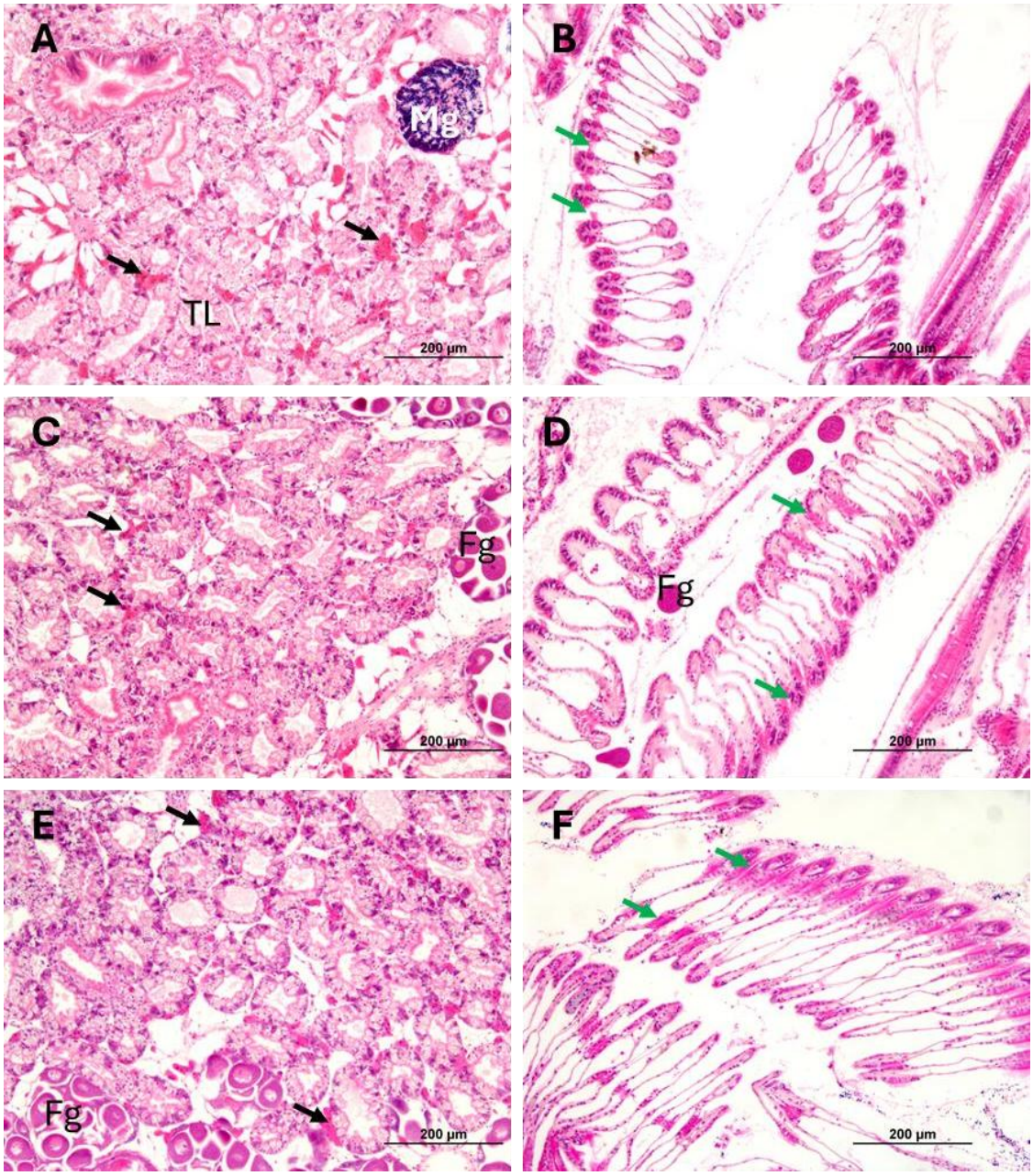

Figure S5. Representative histological sections of *M. galloprovincialis* from control and *V. ostreicida*- challenged groups in the bath infection experiment at 0 and 1 day of exposure. A) Digestive gland of
M. galloprovincialis at time 0 (prior to immersion) showing the adipogranular cells (black arrows) among tubular lumen (TL) and adjacent male gametes (Mg). B) Gill of the same specimen. C) Digestive gland of a mussel from the control group after 1 day of exposure. D) Gill of the same specimen. E) Digestive gland of a mussel from the *V. ostreicida*-challenged group after 1 day of exposure. F) Gill of the same specimen. TL = tubular lumen; Fg = female gametes; Mg = male gametes; Black arrow = adipogranular cells; Green arrow = lamellar cilia. H&E Stain.

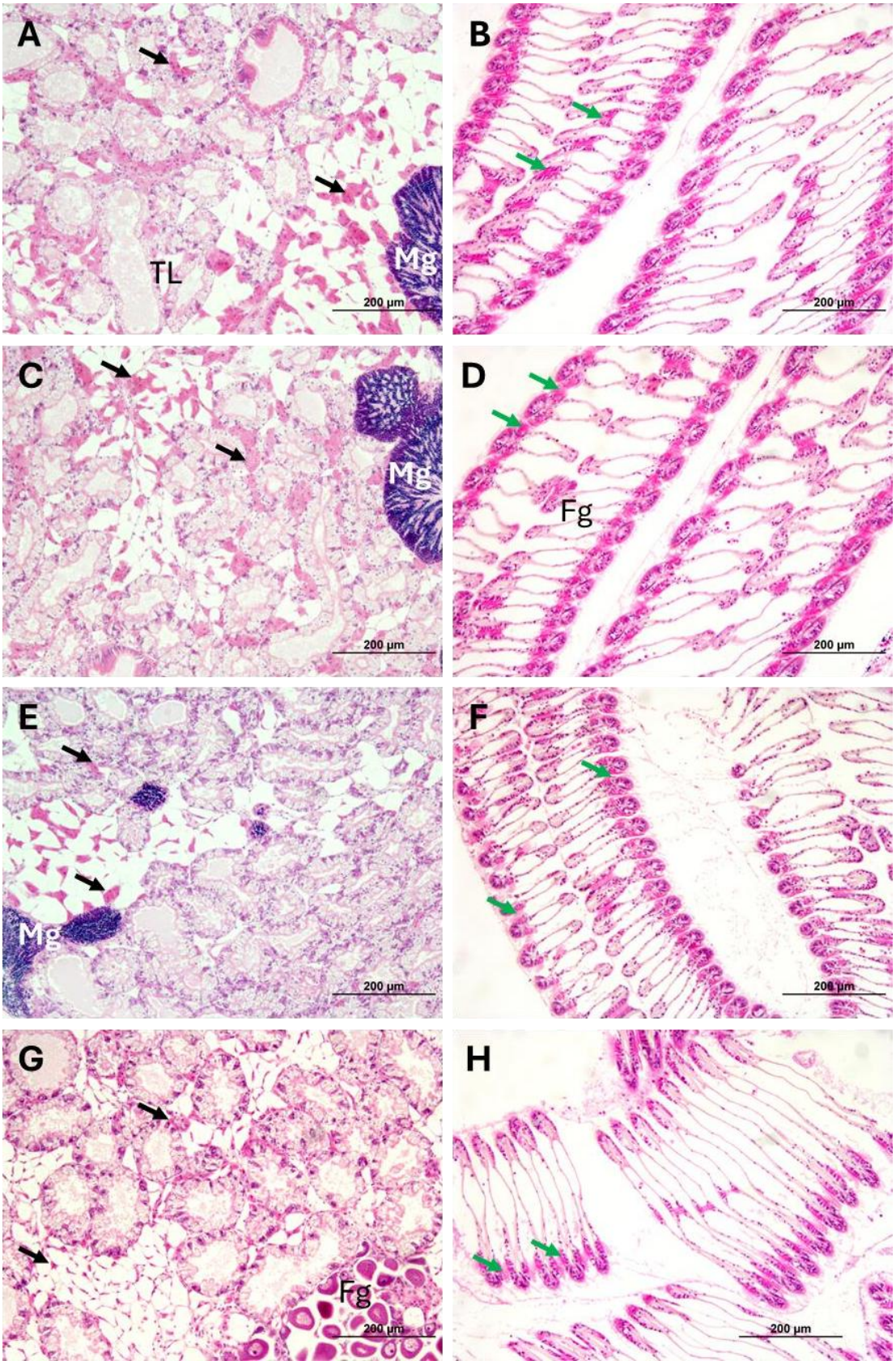
A
TL
Mg
200 µm
B
200 µm
C
Mg
200 µm
D
Fg
200 µm
E
Mg
200 µm
F
200 µm
G
Fg
200 µm
H
200 µm

Figure S6 - Representative histological sections of *M. galloprovincialis* from control and *V. ostreicida*- challenged groups in the bath infection experiment at 2 and 3 day exposure. A) Digestive gland of a mussel from the control group after 2 days of exposure. B) Gill of the same specimen. C) Digestive gland of a mussel from the *V. ostreicida*-challenged group after 2 days of exposure. D) Gill of the same specimen. E) Digestive gland of a mussel from the control group after 3 days of exposure. F) Gill of the same specimen. G) Digestive gland of a mussel from the *V. ostreicida*-challenged group after 3 days of exposure. H) Gill of the same specimen. TL = Tubular lumen; Fg = Female gametes; Mg = Male gametes; Black arrow = Adipogranular cells; Green arrow = Lamellar cilia. H&E Stain.

1 Bibliography

1. Auguste M, Rahman FU, Balbi T, Leonessi M, Oliveri C, Bellese G, et al. Responses of Mytilus galloprovincialis to challenge with environmental isolates of the potential emerging pathogen Malaciobacter marinus. Fish Shellfish Immunol. 2022 Dec;131:1–9.

2. OSPAR Commission. Background documents and technical annexes for biological effects monitoring. In 2013. p. 239. Available from: www.ospar.org.

3. Auguste M, Leonessi M, Bozzo M, Risso B, Cutroneo L, Prandi S, et al. Multiple responses of Mytilus galloprovincialis to plastic microfibers. Sci Total Environ. 2023 Sep;890:164318.

4. Lopez JR, Leonessi M, Fernandez-Tejedor M, Auguste M, Doni L, Cruz-Quintana Y, et al. First description of Vibrio ostreicida as putative causal agent of disease in Mediterranean mussel (Mytilus galloprovincialis) and development of a PCR protocol for its rapid diagnosis. J Invertebr Pathol. 2025 Sep;212:108399.

Chapter 4:

Deciphering Host-Pathogen dynamics in *Mytilus galloprovincialis*: immune responses to multiple infections with bacterial isolates from bivalve mortality outbreaks.

The results of this work have been published in Fish and Shellish Immunology 169 (2026) 111064. https://doi.org/10.1016/j.fsi.2025.111064

Immune response of *M. galloprovincialis* to infection with two bacterial strains isolated from an oyster mortality event in the Ebro Delta (Spain), *Vibrio aestuarianus* 106 (Va) and *Malaciobacter marinus* R1 (Mm) were evaluated. Previous studies showed that in mussels Mm R1 is moderately pathogenic to early larvae and elicits effective immune responses in adults, suggesting a limited pathogenic potential of this strain under laboratory conditions. In contrast, no data are available on the Va 106 strain. Therefore, firstly the effects of Va on early larval development and on *in vitro* immune responses of isolated hemocytes from adult mussels were evaluated. Subsequently, cross-infection experiments were performed to determine whether prior exposure to either pathogen could influence the mussel capacity to respond to subsequent challenge with the other. Both *in vivo*/*in vitro* and *in vivo*/*in vivo* experimental multi-infection approaches were employed, and several hemolymph parameters were analyzed, including hemocyte lysosomal membrane stability (LMS), extracellular reactive oxygen species (ROS) production, serum lysozyme activity, and bactericidal activity. Both *in vitro* and *in vivo* data indicate that Va 106 alone could represent a potential pathogenic strain for adult mussels, in contrast with other *V. aestuarianus* strains previously tested. Pre-challenge with Va reduced subsequent *in vitro* hemocyte responses to Mm, resulting in a lower bactericidal activity. In contrast, when hemocytes from Mm pre-injected mussels were incubated with Va, stimulation of extracellular defenses (ROS production and lysozyme release) prevailed, and the bactericidal activity towards Va was unaffected. The results were confirmed by *in vivo*/*in vivo* cross-exposure experiments: pre-injection with Va led to a significant reduction in the bactericidal activity towards subsequent infection with Mm. In contrast, pre-exposure to Mm increased the bactericidal activity towards subsequent challenge with Va. Overall, both *in vitro* and *in vivo* data demonstrate that, in *Mytilus*, first infection with certain potential pathogens (i.e. Va 106) can weaken immune defences of the host, thus favoring the subsequent opportunistic behaviour of other non-pathogenic bacteria (i.e. Mm R1).

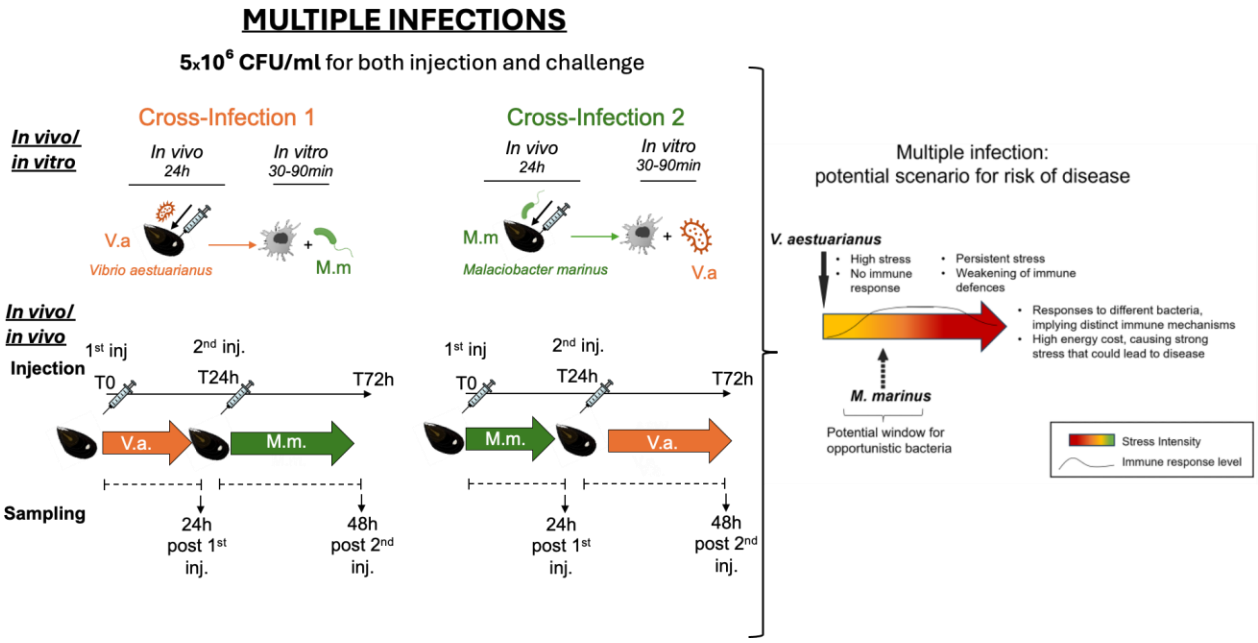
MULTIPLE INFECTIONS
5x10^6 CFU/ml for both injection and challenge
In vivo/ in vitro
Cross-Infection 1
In vivo 24h
In vitro 30-90min
V.a
Vibrio aestuarianus
M.m
Cross-Infection 2
In vivo 24h
In vitro 30-90min
M.m
Malaciobacter marinus
V.a
In vivo/ in vivo
Injection
1st inj
2nd inj.
T0
T24h
T72h
V.a.
M.m.
Sampling
24h post 1st inj.
48h post 2nd inj.
1st inj
2nd inj.
T0
T24h
T72h
M.m.
V.a.
24h post 1st inj.
48h post 2nd inj.
Multiple infection:
potential scenario for risk of disease
V. aestuarianus
High stress
No immune response
Persistent stress
Weakening of immune defences
Responses to different bacteria, implying distinct immune mechanisms
High energy cost, causing strong stress that could lead to disease
M. marinus
Potential window for opportunistic bacteria
Stress Intensity
Immune response level

Fish and Shellfish Immunology 169 (2026) 111064

Contents lists available at ScienceDirect

Fish and Shellfish Immunology

journal homepage: www.elsevier.com/locate/fsi

Full length article

Deciphering host–pathogen dynamics in *Mytilus galloprovincialis*: immune responses to multiple infections with bacterial isolates from bivalve mortality outbreaks

Manon Auguste [a,b,*,1], Martina Leonessi [a,b,1], Caterina Oliveri [b], Teresa Balbi [a,b], Faiz Ur Rahman [c,d], Luigi Vezzulli [a,b], Dolors Furones [c], Laura Canesi [a,b]

[a] DISTAV, Dept. of Environmental, Earth and Life Sciences, University of Genoa, Italy
[b] National Biodiversity Future Center, Palermo, Italy
[c] IRTA La Ràpita Centre, Aquaculture Program, Spain
[d] Unit of Microbiology, Department of Basic Health Sciences, Faculty of Medicine and Health Sciences, IISPV, Universitat Rovira i Virgili, Reus, Spain

ARTICLE INFO

Keywords:
Multiple infection
Marine bivalves
Bacterial isolates
Vibrio aestuarianus
Malaciobacter marinus
Immunity
Disease

ABSTRACT

Bivalve aquaculture is facing several challenges due to disease outbreaks, that are often multifactorial and polymicrobial. Increasing evidence shows that initial infection by primary pathogens, or exposure to environmental stressors, can disrupt the host-associated microbiota, creating a favorable environment for opportunistic pathogens. In adult bivalves, the outcome of bacterial infection depends on the capacity of the immune system to fight potential pathogens. Although immune responses to individual bacteria are well documented, data on polymicrobial infections remain scarce.

Mytilus spp. is generally considered resistant to bacterial challenge; however, increasing reports of mortality events have emerged across Europe more recently. In this study, we examined the immune response of *Mytilus galloprovincialis* to infection with two bacterial strains isolated from an oyster mortality event in the Ebro Delta (Spain): *Vibrio aestuarianus* 106 (Va) and *Malaciobacter marinus* R1 (Mm). The effects of Va alone on early larval development and on *in vitro* responses of hemocytes from adult mussels were first evaluated. Both *in vivo/in vitro* and *in vivo/in vivo* cross-infections were then performed to determine whether prior exposure to either isolate could influence immune responses to subsequent challenge with the other. The results demonstrate that first infection with Va weakened mussel immune defences, thus favoring the subsequent opportunistic behaviour of Mm.

These data indicate that the simple multiple infection approach used in *Mytilus* could be effectively applied to other, more susceptible bivalve species. These findings can help decipher the interaction dynamics between potential bacterial pathogens within bivalve hosts and predicting the risk of disease.

1. Introduction

Bivalve aquaculture, which includes shellfish such as oysters, mussels, and clams, is facing several challenges due to disease outbreaks that compromise the health of farmed species, reduce productivity, and result in substantial economic losses [1,2]. Among the most common etiological agents responsible for these mortality events are viruses, bacteria, fungi, and protozoans. These pathogens are increasingly recognized across various bivalve species, with particularly severe impacts observed during early life stages [3,4].

Bivalve diseases are often multifactorial and polymicrobial. Initial infections by primary pathogens or exposure to environmental stressors can disrupt the host-associated microbiota (a condition known as dysbiosis), creating a favorable environment for opportunistic pathogens [5]. A well-documented example is the Pacific oyster mortality syndrome (POMS) in juvenile oysters, caused by the interplay of *Ostreid herpesvirus type 1* (OsHV-1) and abiotic stressors [6]. Infection with OsHV-1-µVar induces immunosuppression in the host, leading to dysbiosis and subsequent bacteraemia by opportunistic bacteria, ultimately resulting in oyster death. Notably, opportunistic pathogens are

* Corresponding author. DISTAV, Dept. of Environmental, Earth and Life Sciences, University of Genoa, Italy.
E-mail address: manon.auguste@unige.it (M. Auguste).
[1] Equally contributed to the work.

https://doi.org/10.1016/j.fsi.2025.111064
Received 24 October 2025; Received in revised form 5 December 2025; Accepted 7 December 2025
Available online 8 December 2025
1050-4648/© 2025 Elsevier Ltd. All rights are reserved, including those for text and data mining, AI training, and similar technologies.

predominantly of the genus *Vibrio*, but also include *Arcobacter*-like species [4,7,8].

Although both groups are naturally present in the bivalve microbiota, increasing evidence indicates their *in vivo* proliferation in diseased or stressed bivalves, often in co-occurrence. For instance, *Arcobacter*-like spp. have been found at elevated levels in bivalves exhibiting disease symptoms, frequently alongside pathogenic *Vibrio* strains [9–12]. A study by Lasa et al. (2019) comparing the microbiota of healthy and diseased *Crassostrea gigas* across European aquaculture sites revealed that diseased oysters displayed disrupted microbiota, with reduced diversity and enrichment in potentially pathogenic *Vibrio* and *Arcobacter*-like species. These findings suggest that environmental disturbances and/or pathogen infections may drive *Arcobacter* to behave opportunistically, warranting further investigation into its role in polymicrobial infections [5].

Among *Vibrio* species isolated during disease outbreaks, several have been identified as primary pathogens for both adult and larval bivalves, including *V. alginolyticus*, *V. splendidus*, *V. aestuarianus*, *V. harveyi*, *V. anguillarum*, *V. tubiashii*, *V. tapetis*, and *V. neptunius* [7,13–15]. In particular, *V. aestuarianus* has emerged as a key pathogen responsible for mass mortalities in adult *C. gigas* populations [16–18]. Initially described in 2008 in association with oyster mortality in France [19,20], *V. aestuarianus* has been linked to mortality events in pre-commercial and commercial-sized oysters across France, Ireland [21], and Spain, notably in the Ebro Delta in 2016–2019 [17,22]. These recent events were associated with polymicrobial infections involving OsHV-1, various strains of *V. aestuarianus*, and *Arcobacter*-like species, particularly *Malaciobacter marinus* [17,23].

The susceptibility of bivalves to bacteria largely depends on the efficiency of their innate immune system, which varies across species [24]. In adult bivalves, where immune defenses are fully developed, the outcome of infection depends on the host's ability to recognize and respond to different bacterial components. For example, differences in immune effectors between oysters and mussels (*Mytilus* spp.) may underlie the generally greater resilience of mussels to bacterial infections [7]. Despite this, increasing reports of mortality events in *M. edulis* and *M. galloprovincialis* have emerged across Europe since 2014 [25].

While several studies have explored bivalve immune responses to specific pathogens, data on immune responses to mixed or sequential infections remain scarce. The best-documented case involves synergistic interactions between *V. harveyi* and *V. rotiferianus* during OsHV-1-associated infections in oysters [8]. However, to date, no such data exist for *Mytilus* species.

In this work, we investigated the immune responses of *M. galloprovincialis* to bacterial challenge with two strains isolated from an oyster mortality event in the Ebro Delta (Spain, 2019): *V. aestuarianus* (strain IRTA-19-106, hereafter Va) and *M. marinus* (IRTA-19-131, hereafter Mm) [17,23]. Previous studies have shown that in mussels Mm R1 is moderately pathogenic to early larvae and triggers effective immune responses in adults, suggesting limited pathogenicity of this strain under laboratory conditions [26].

We first evaluated the effects of Va on early larval development and on *in vitro* immune responses of isolated hemocytes from adult mussels. Cross-infection experiments were subsequently performed to determine whether prior exposure to either pathogen could influence the mussel capacity to respond to subsequent challenge with the other. Both *in vivo/in vitro* and *in vivo/in vivo* experimental multi-infection approaches were employed, and several hemolymph parameters were analyzed, including hemocyte lysosomal membrane stability (LMS), extracellular reactive oxygen species (ROS) production, serum lysozyme activity, and bactericidal activity.

2. Materials and methods

2.1. Animals

Mussels (*M. galloprovincialis* Lam.), 4–5 cm long, purchased from an aquaculture farm (La Spezia, Italy) in March or September–December 2023 (depending on the experiment), were transferred to the laboratory and acclimatized for 24 h in tanks containing aerated artificial sea water (ASW), pH 7.9–8.1, 35 ppt salinity (1 L per animal), at 18 ± 1 °C.

2.2. Bacterial cultures

Vibrio aestuarianus (Va) (strain IRTA-19-106) and *Malaciobacter marinus* (Mm) (strain IRTA-19-131 or R1) were isolated from adult diseased oysters (*C. gigas*) collected during a mortality event that occurred in Fangar bay (40° 46.506′ N; 0° 44.246′ E, Ebro Delta, Spain) in June 2019 [17,26]. Nine other strains of Va were also isolated and resulted clones from the stain IRTA-19-106 used in this study [17].

Va was cultured in Zobell medium at 23 °C under static conditions. After overnight growth, bacterial cells were collected by centrifugation (4500×*g*, 10 min), washed twice with ASW and the pellet resuspended in ASW to obtain a concentration of about 10^8 CFU/mL ($Abs_{600} = 0.25$).

Mm was cultured in *Arcobacter* broth (conventional broth media containing peptone 18 g/L, yeast extract 1 g/L, NaCl 5 g/L with the addition of 50 % ASW) at 30 °C in continuous agitation, as previously reported [26,27]. After 24 h growth, the inoculum was centrifuged (4500×*g*, 20 min), and the pellet resuspended in ASW to obtain a concentration of about 10^8 colony forming units (CFU)/mL (determined spectrophotometrically as an $Abs_{600} = 0.20$).

2.3. Effects of V. aestuarianus 106 on mussel early larval development

Gametes were obtained by spontaneous spawning of sexually mature mussels purchased in March 2023, further fertilization and larval development were carried out according to the 48 h embryotoxicity assay as previously described [26,28]). At 30 min post-fertilization, aliquots of Va, from a 10^8 CFU/mL stock suspension, were tenfold serially diluted in ASW and added to fertilized eggs to reach the nominal final concentration of 10^6 CFU/mL. Control samples in ASW were run in parallel. Samples were incubated for 48 h at 18 °C ± 1 °C, with a 16:8 h light: dark photoperiod. All procedures were carried out following ASTM (2021) [29]. At the end of incubation, larvae were fixed with buffered formalin (4 %) and examined using an inverted Olympus IX53 microscope (Olympus, Milano, Italy) at 40 × , equipped with a CCD UC30 camera and a digital image acquisition software (cellSens Entry). D-shaped (straight hinge) larvae with no protruding mantle were considered as normal; a larva was considered malformed if the typical stage at 48 hpf was not reached (trochophore or earlier stages) or when developmental impairments were observed (concave, malformed or damaged shell, protruding mantle). The acceptability of test results was based on controls for a percentage of normal D-shell larvae >75 %. Experiments were performed using fertilized eggs obtained from 4 parental pairs (n = 4) carried out in 6 replicate samples in 96-microwell plates.

2.4. Effects of in vitro challenge of mussel hemocytes with V. aestuarianus 106

For *in vitro* challenge, functional immune parameters were evaluated in hemolymph samples from adult mussels. Hemolymph was extracted from the posterior adductor muscle using a syringe (18 G1/2″ needle), filtered through sterile gauze and pooled (3 pools of 15 mussels each), as previously described [26,28]. Whole hemolymph samples were incubated with suspensions of Va at different concentrations (10^5, 10^6, 10^7 CFU/mL) from 30 to 90 min, depending on the endpoint measured.

For experiments of bactericidal activity, hemolymph serum (HS) was

obtained by centrifugation of whole hemolymph samples at 100×*g* for 10 min, and the supernatant was filtered through a 0.20 µm-pore filter.

2.5. Functional hemolymph parameters

Functional hemolymph parameters were evaluated in both *in vitro* and *in vivo* experiments as previously described [26,28]. Lysosomal membrane stability (LMS) was evaluated in hemocyte monolayers by the Neutral Red Retention time (NRRT) assay by optical microscopy. The endpoint of the assay was defined as the time at which 50 % of the cells showed sign of lysosomal leaking (the cytosol becoming red and the cells rounded). For morphological observations, hemocyte monolayers fixed in >50 % methanol were stained with a Giemsa kit (Diff-QuikTM, Medion Grifols Diagnostics AG, Switzerland), following the manufacturer instructions.

ROS production was evaluated by the reduction of cytochrome *c* (75 µM ferricytochrome c) at 550 nm, and data expressed as changes in OD/mg protein. Nitric Oxide (NO) production was evaluated by the Griess reaction, a spectrophotometric method for the quantification of nitrite content at 540 nm, and nitrite accumulation (nmol/mg prot/ml) was determined by a standard curve of known concentrations of sodium nitrite ($NaNO_2$). Soluble lysozyme activity was evaluated at 450 nm using *Micrococcus lysodeikticus* (15 mg/100 mL in 66 mM phosphate buffer, pH 6.4) and expressed as hen egg white (HEW) lysozyme equivalents (U/mg protein/mL).

Protein content was determined using the Bradford method with bovine serum albumin (BSA) as a standard.

Bactericidal activity was determined as previously reported [26,30]. In *in vitro* experiments, hemocyte monolayers were incubated with the bacterial suspensions (Va or Mm) in either ASW or HS (5×10^6 CFU/ml). The bactericidal activity of HS alone was also evaluated. To check bacterial growth or death over experimental time, control samples of Va or Mm alone incubated in ASW were run in parallel. Immediately after the addition of bacteria (T = 0) and after 30 and 90 min of incubation (at 18 °C), samples were collected and added with 0.05 % Triton X-100 in ASW and vortexed for 10s to lyse the hemocytes. The lysate was tenfold serially diluted in ASW and plated onto Marine Agar (MA) plates (Scharlab, Spain).

In *in vivo* experiments, aliquots (100 µl, in triplicate) of hemolymph samples collected at time 0 (30 min after injection) and at 24 or 48 h p.i., depending on the experiment, were serially diluted in ASW and plated onto MA plates. In both conditions, the number of CFUs was determined and the percentages of killing were compared with values obtained at zero time. All parameters were measured in triplicate. In all *in vivo* experiments, in ASW injected samples unspecific bactericidal activity never exceeded 10 % over time (7.6 ± 2.7 %).

2.6. Cross-infection experiments

The experimental set up for cross-infection experiments is depicted

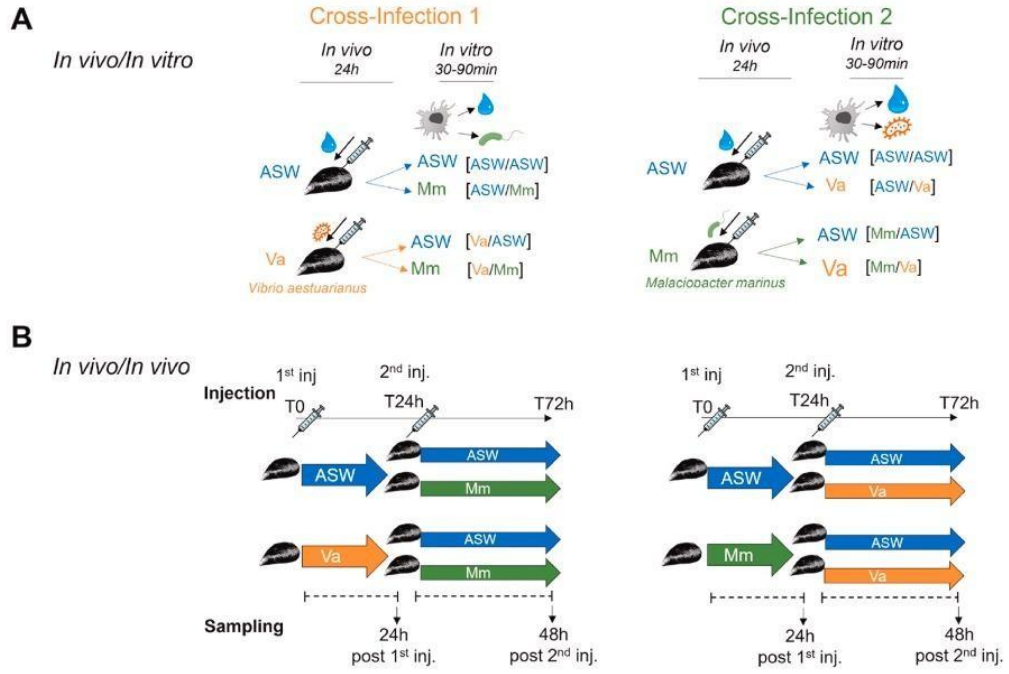

Fig. 1. Experimental plan of cross-infections.
A) *In vivo/in vitro* cross-infection
Left panel: mussels were injected with *V. aestuarianus* (Va) and at 24 h p.i. hemolymph samples were challenged *in vitro* with *M. marinus* (Mm). Right panel: mussels were injected with *M. marinus* (Mm) and at 24 h p.i. hemolymph samples were challenged *in vitro* with Va.
B) *In vivo/in vivo* cross-infection
Left panel: mussels were injected with *V. aestuarianus* (Va) or ASW. At 24 p.i., mussels were subjected to a second injection with *M. marinus* (Mm). Right panel: mussels were injected with *M. marinus* (Mm) or ASW. At 24 p.i., mussels were subjected to a second injection with *V. aestuarianus* (Va).
Hemolymph samples were collected at both 24 h p.i. and 48 h after the second injection for determination of functional parameters and bactericidal activity.
Final nominal concentrations of bacteria were $5x10^6$ CFU/ml for both *in vivo* injection and *in vitro* incubation. For each *in vivo* and *in vitro* condition, control samples with ASW (in blue) were run in parallel.

in Fig. 1. In both experiments (*in vivo/in vitro* and *in vivo/in vivo*), animals were injected into the posterior adductor muscle with 50 µL of a suspension of either Va or Mm (10^8 CFU/mL in ASW), in order to obtain a nominal concentration of 5×10^6 CFU/mL hemolymph. The bacterial doses used in the present study (5×10^6 CFU/mL) were selected on the basis of previous data obtained in mussels challenged with different bacterial species and strains ([26,31] and references therein). This sublethal dose has been shown to induce an immune response in mussels in the absence of mortality. In contrast, higher concentrations of the Va reference strain (01/032) (10^{11} CFU/ml) were shown to induce mortality in mussels [32]. Accordingly in oyster septicaemic individuals Va strains generally exceeded 10^8 CFU/ml hemolymph [19]. No data on bacterial loads (in terms of CFU/ml) encountered during natural mortality events are unfortunately not currently available for mussels. Control mussels were injected with ASW. Hemolymph (3 pools of 15 mussels for each condition) at 24h p.i. was sampled for both cross-infection experiments type.

2.6.1. In vivo/in vitro cross-infection

Mussels (45 per condition) were injected with either Va, Mm or ASW as described above. At 24 h p.i., hemolymph samples were collected (3 pools of 15 mussels for each condition); aliquots (1 mL) were used for measuring a) the effects of *in vivo* challenge on functional immune parameters and b) for short term *in vitro* cross-challenge (Fig. 1A). Samples from Va-injected mussels were incubated with Mm (5 x 10^6 CFU/mL) (Va/Mm) and those from Mm-injected mussels were incubated with Va (Mm/Va), in the same conditions described above for *in vitro* experiments (see 2.4). In parallel, hemolymph samples from ASW-injected mussels were challenged with either strain (ASW/Va and ASW/Mm) or kept in ASW (ASW/ASW). Corresponding controls for each *in vitro* condition were also performed (Va/ASW and Mm/ASW). Functional hemolymph parameters were evaluated as described above (see 2.5).

2.6.2. In vivo/in vivo cross-infection

Mussels were injected with Va, Mm or ASW as described above (150–160 animals per condition). Hemolymph was collected from 45 mussels at 24 h post first injection (p.i.); the remaining mussels challenged with Va (50 animals) were re-injected with Mm (Va/Mm), and those injected with Mm re-injected with Va (Mm/Va), respectively. Mussels injected with ASW were injected a second time with either strain (ASW/Va and ASW/Mm) or with ASW (ASW/ASW). Hemolymph samples were collected at 48 h post second injection (p.s.i), and at each sampling time (24 p.i. and 48 p.s.i.) hemolymph functional parameters were evaluated as described above (3 pools of 15 mussels for each condition). For evaluation of bactericidal activity at time 0, hemolymph was also sampled 30 min after the first or second injection. No mortality was observed during the experiments.

2.7. Data analysis

Embryotoxicity test data, representing the mean ± SD of 4 independent experiments, carried out in 6

replicate samples in 96-microwell plates, by non-parametric Mann-Whitney *U* test. All data from *in vitro* and *in vivo* experiments on hemocyte and hemolymph functional parameters are the mean ± SD of 3 independent experiments. Statistical analyses were performed by the ANOVA test followed by Tukey's post test ($p \leq 0.05$), control vs all conditions. All statistical calculations were performed using the GraphPad Prism version 7.03 for Windows (GraphPad Software, San Diego, CA, USA.)

3. Results

3.1. Effects of Vibrio aestuarianus 106 on early larval development

The possible pathogenicity of *V. aestuarianus* 106 (Va) towards mussel larvae was tested on early developmental stages of mussels using the 48 h embryotoxicity test as previously described [26,33]. Fertilized eggs were exposed to Va at 10^6 CFU/ml and the percentage of normal D-larvae at 48 hpf was evaluated. As shown in Fig. S1, Va induced a 30 % decrease in the percentage of normal D-larvae with respect to controls ($p < 0.05$), an effect comparable with that previously observed with *M. marinus* [26]. In both conditions, shell malformations represented the dominant altered larval phenotype (Fig. S1).

3.2. Effects of in vitro challenge with Vibrio aestuarianus 106 alone

The effects of Va were evaluated in short term *in vitro* experiments on hemolymph samples exposed to different concentrations of bacteria, and the results are reported in Fig. 2. Va induced a dose-dependent decrease in hemocyte LMS that was significant from the lowest concentration tested (−20 % at 10^5 CFU/ml $p < 0.05$), up to complete destabilization at 10^7 CFU/ml (−80 %) (Fig. 2A). Va did not trigger any extracellular immune responses in terms of ROS production and lysozyme release over time, irrespective of the concentration (Fig. S2 A and B); with regards to NO production, a concentration dependent inhibition was observed only immediately after the addition of bacteria, and no other effects were subsequently observed (Fig. S2 C).

In Fig. 2B data are reported on the hemolymph bactericidal activity towards Va (5 x 10^6 CFU/ml) expressed as the percentage of killed bacteria after 30 and 90 min incubation with respect time 0. No killing of Va was observed in ASW alone over time (Fig. 2B). Hemolymph components (hemocytes or HS) showed a time-dependent increase in bactericidal activity, with quantitative differences at each time point depending on the experimental conditions. The lowest bacterial killing was observed when hemocytes were challenged with Va in the presence of ASW (20 and 30 %, respectively, at 30 and 90 min). HS alone was responsible for a higher bactericidal activity (35 and 45 % at 30 and 90 min). The highest capacity to kill Va was observed by hemocytes in the presence of HS (60 and 70 % at 30 and 90 min, respectively). Moreover, as shown in Fig. S3, in presence of HS a higher, progressive internalization of Va by hemocytes was observed over time (Fig. S3A–B), whereas in ASW, a large number of bacteria were still visible in the extracellular medium (Fig. S3C–D).

3.3. Cross-infection experiments

3.3.1. Effects of in vivo challenge with either Va or Mm alone at 24 h.p.i

In Fig. 3, data are reported on hemolymph functional immune parameters evaluated in mussels challenged with either Va or Mm (final concentration 5×10^6 CFU/mL in hemolymph) at 24 h.p.i. The results are the mean obtained from both cross-infection experiments (Fig. 1A and B, left panels). Both strains induced a decrease in hemocyte LMS, with smaller effects of Va with respect to Mm (−23 % vs −43 %; $p < 0.05$) (Fig. 3A). Extracellular ROS production was inhibited by Va and stimulated by Mm (−40 % and +60 %, respectively; $p < 0.05$) (Fig. 3B). Va induced a smaller stimulation of lysozyme activity with respect to Mm (+40 % vs +115 %, $p < 0.05$) (Fig. 3C). Accordingly, these responses resulted in a much lower bactericidal activity of whole hemolymph samples towards Va than towards Mm (44 % vs 79 %, $p < 0.05$) (Fig. 3D).

3.3.2. In vivo/in vitro cross-infection

As shown in Fig. 1A, hemolymph samples from mussels injected with either Va, Mm or ASW (at 24 h p.i.) were tested for their capacity to respond to short term *in vitro* exposure to either Mm or Va (5×10^6 CFU/mL), respectively. Groups were thus identified as ASW/Mm, Va/Mm, and ASW/Va, Mm/Va and the results are reported in Fig. 4. Negative control values (ASW/ASW) are reported as 100 % values (dotted line).

Effect of pre-challenge with Va (Fig. 4: A-D): when hemolymph from Va-injected mussels was incubated with Mm (Va/Mm), a larger decrease in hemocyte LMS was observed compared to those of the corresponding

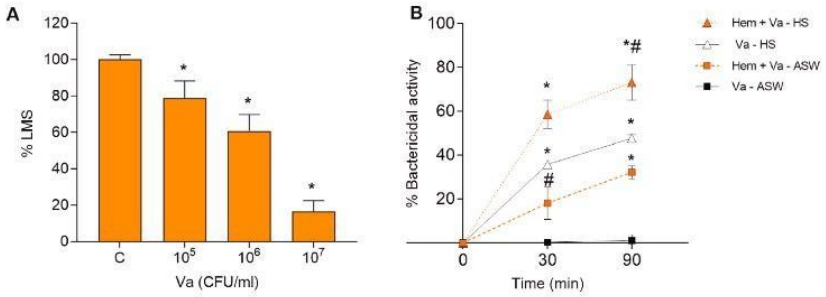

Fig. 2. *In vitro* effects of *V. aestuarianus* 106 (Va) on *M. galloprovincialis* **hemolymph.**
A) Lysosomal membrane stability (LMS). LMS was evaluated in hemocytes incubated for 30 min with different concentrations of bacteria suspended in hemolymph serum (HS). Data, expressed as percent values with respect to controls, represent the mean ± SD of 4 experiments in triplicate.
B) Bactericidal activity towards Va. Hemocytes were incubated for 30 and 90 min with suspensions of Va, at 5 x 10^6 CFU/ml in either ASW (Hem + Va + ASW) or HS (Hem + Va + HS). In parallel, Va were incubated in HS alone (Va- HS). Data, reported as the percentage of killed bacteria at different times of incubation with respect to time 0, are the mean ± SD of 3 experiments in triplicate.
Statistical analysis were performed by one way ANOVA followed by Tukey's multiple comparison test, at $p < 0.05$. In A: * = all concentrations vs control. In B: * = all conditions vs time 0 and # = differences between groups at each time point.

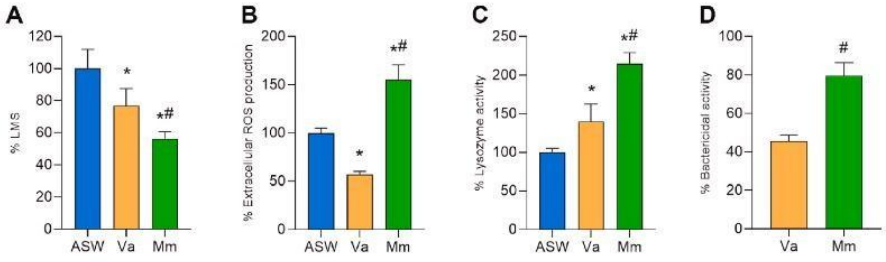

Fig. 3. Effects of *in vivo* exposure at 24h p.i. with either Va or Mm alone on functional hemolymph parameters of *M. galloprovincialis*.
A) hemocyte lysosomal membrane stability (LMS); B) extracellular ROS production; C) Lysozyme activity. Data are reported with respect to control values (ASW-injected). D) Bactericidal activity towards either Va or Mm, evaluated with respect to time 0. Data represent the mean ± SD of 6 experiments. Statistical analyses were performed by ANOVA followed by Tukey's multiple comparison test, $p < 0.05$: * = all treatments vs control (ASW); # = Mm vs Va.

control (ASW/Mm) (−57 % vs −35 %, $p < 0.05$) (Fig. 4A). *In vivo* pre-challenge with Va prevented the subsequent induction of ROS production induced by Mm *in vitro* (Fig. 4B), whereas no differences in lysozyme activity were observed (Fig. 4C). What is more, hemolymph from Va-injected mussels showed a significantly lower bactericidal activity towards Mm at all times of incubation with respect to that of ASW-injected mussels (37 % vs 74 %, respectively, at 90 min, $p < 0.05$) (Fig. 4D).

Effect of pre-challenge with Mm (Fig. 4: E-H): also in hemocytes from Mm-injected mussels, incubation with Va resulted in a larger decrease in LMS with respect to its corresponding control ASW/Va (−70 % vs −37 %, $p < 0.05$) (Fig. 4E). However, in Mm/Va samples, a larger ROS production was observed (+87 % vs +39 %) $p < 0.05$) (Fig. 4F), together with a significant increase in lysozyme activity (+29 %, $p < 0.05$) (Fig. 4G). Finally, hemolymph from Mm pre-exposed samples showed a bactericidal activity towards Va at 30 min that was about twice higher with respect to ASW/Va samples; however, similar values were reached by both samples at 90 min, the capacity to kill Va never exceeding 50 % in all conditions ($p < 0.05$) (Fig. 4H).

In Fig. S4 the results obtained for the same parameters in each respective *in vitro* control group (Va/ASW and Mm/ASW) are reported *vs* negative controls (ASW/ASW). Decreases in LMS were observed in both samples (−22 %, Va/ASW and −37 % Mm/ASW $p < 0.05$) (Fig. S4A). Only in Mm/ASW samples, stimulation of extracellular ROS production (+103 %, $p < 0.05$) (Fig. S4B), together with a slight increase in lysozyme activity (+16 %, $p < 0.05$) (Fig. S4C) were observed.

In Fig. 5 are reported representative images of hemocytes stained with NR and Giemsa after short *in vitro* incubation with either bacterium. In Va/Mm samples (Fig. 5A and B), NR live staining revealed a significant cellular damage, with lysosomal enlargement and fusion (arrows) as well as some rounded hemocytes (arrowhead) indicating cell damage/death (Fig. 5A); Giemsa staining also showed cell vacuolation corresponding to lysosome fusion (stars) (Fig. 5B). In Mm/Va samples, hemocytes showed less lysosomal enlargement and fusion (Fig. 5C, arrows) and were still well adherent to the substrate, with no apparent signs of cell damage (Fig. 5D).

3.3.3. *In vivo/In vivo cross infection*

Immune responses were evaluated after sequential *in vivo* challenge with different bacteria as shown in Fig. 1B. Mussels were injected with either Va or Mm; at 24 h p.i. they were subjected to a second injection with either Mm or Va respectively. At 48 h post second injection (p.s.i.) immune parameters were evaluated in whole hemolymph samples and the results are reported in Fig. 6. Groups were thus identified as Va/Mm and Mm/Va. For LMS, ROS and lysozyme, data are reported as percent values with respect to each corresponding control (Va/ASW and Mm/ASW). Negative control values (24 p.i. ASW/48 p.s.i. ASW) are reported as 100 % values (dotted line). For bactericidal activity, data are reported with respect to time zero.

Effect of pre-challenge with Va (A-D): as shown in Fig. 6A, in Va-injected mussels, subsequent challenge with Mm induced a larger decrease in hemocyte LMS with respect to ASW/Mm samples (−55 % vs

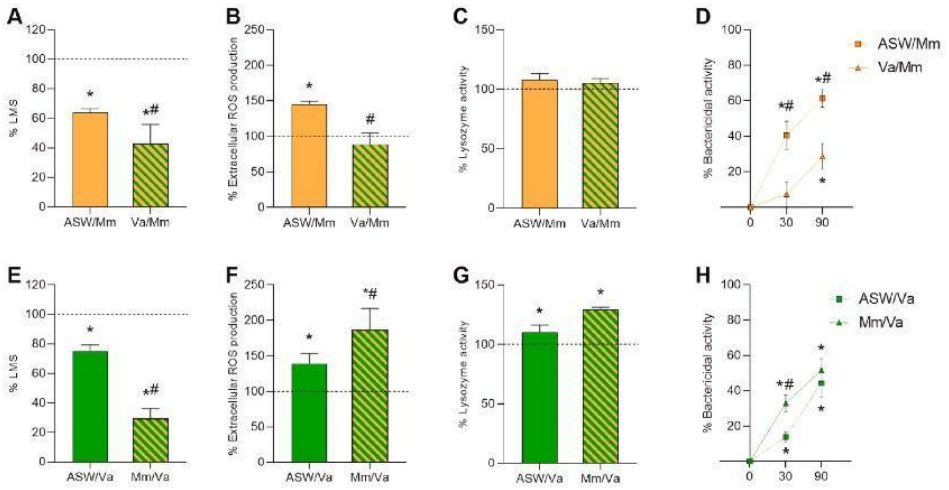

Fig. 4. Functional responses of hemolymph samples after in *vivo/in vitro* cross infection with Va and Mm. Mussels were injected with either Va or Mm (5×10^6 CFU/mL hemolymph) and then at 24 p.i. hemolymph samples were incubated *in vitro* with either Mm or Va.
A–D: hemolymph samples at 24 h p.i. with Va incubated *in vitro* with Mm (5×10^6 CFU/mL) for different times (see methods).
E–H: hemolymph samples at 24 h p.i. with Mm incubated *in vitro* with Va as described above.
A, E) lysosomal membrane stability (LMS); B, F) extracellular ROS production; C, G) lysozyme activity; D, H) bactericidal activity towards Va or Mm, respectively. In A-C and E-G data are reported as % values of negative controls (dotted lines), represented by samples at 24 p.i. with ASW and incubated *in vitro* with ASW only (ASW/ASW). In D-H data are reported at 30 and 90 min incubation with respect with time 0.
Data represent the mean ± SD of 3 experiments. Statistical analyses were performed by ANOVA followed by Tukey's multiple comparison test, $p < 0.05$. For bar charts * = all treatments vs control (ASW/ASW); # = between the 2 conditions. For bactericidal activity (D, H): * = all conditions vs time 0; # = differences between the 2 conditions for each time.

−18 %, $p < 0.05$). Pre-exposure to Va prevented the stimulation of extracellular ROS production by Mm (0 % vs +49 % in ASW/Mm samples, $p < 0.05$) (Fig. 6B), as well as the decrease in lysozyme activity induced by Mm (0 % vs −49 % in ASW/Mm samples, $p < 0.05$) (Fig. 6C). Accordingly, in Va/Mm samples, the bactericidal activity towards Mm was significantly lower with respect to the ASW/Mm group (54 % vs 83 %, $p < 0.05$) (Fig. 6D).

Effect of pre-challenge with Mm (E-H): in Mm-injected mussels, a large decrease in hemocyte LMS similar to that induced by Va alone was observed (−70 % and −60 %, respectively, $p < 0.05$). (Fig. 6E). However, pre-challenge with Mm prevented the inhibition of ROS production induced by Va alone (0 % vs −40 % in the ASW/Va group, $p < 0.05$) (Fig. 6F) and induced an increase in Lysozyme activity (+30 %, $p < 0.05$) that was not observed in the ASW/Va group (Fig. 6G). Accordingly, at 48 h p.s.i., the bactericidal activity towards Va was significantly higher in Mm/Va samples than in ASW/Va samples (38 % vs 22 %, respectively, $p < 0.05$) (Fig. 6H).

In Fig. S5 data obtained from *in vivo* experiments (24 h p.i. + 48 h p.s.i.) for all parameters in each respective control group are summarized, corresponding to 72 h after the first injection with either Va or Mm. In Va/ASW hemolymph samples, a large lysosomal destabilization still persisted over time (−48 %, $p < 0.05$) with respect to negative controls (ASW/ASW); that was much lower for Mm/ASW samples (−16 %, $p < 0.05$) (Fig. S5A). At 72 h, Va/ASW showed a small and late stimulation of ROS production (+29 %, $p < 0.05$) that was not observed in Mm/ASW samples (Fig. S5B). No changes in lysozyme activity were recorded (Fig. S5C). Interestingly, at 72 h Va/ASW samples also showed a substantial bactericidal activity towards Va, that at this time was negligible for Mm/ASW samples towards Mm (23 % and 5 % respectively) (Fig. S5D).

4. Discussion

Disease outbreaks and mass mortalities in bivalves are highly complex, often involving polymicrobial infections and/or abiotic factors [34,35]. Microbiome studies indicate that stressed or diseased animals frequently harbor pathogenic *Vibrio* and *Arcobacter*-like species [5,7,9]. However, while experimental infections with single bacterial strains are commonly used to assess pathogenicity, the roles of multiple pathogens remain unclear, and co-infection studies are needed to distinguish pathogenic from opportunistic isolates.

In the present work, responses of *M. galloprovincialis* to challenge with two bacterial strains, *V. aestuarianus* 106 and *M. marinus* R1, isolated from oyster mortality episodes in Spain [23,26] were investigated, both alone and in combination. Previous data showed that *M. marinus* is not pathogenic to adult mussels, where it can elicit efficient immune responses [26]. The effects of Va 106 on larval development in the 48 h embryotoxicity assay, as well as *in vitro* and *in vivo* immune responses of adult mussels infected with Va 106 were first evaluated, and the results were compared with those observed with Mm R1, in the same experimental conditions [26]. The results show that pathogenicity of Va towards early mussel larvae was low and comparable with that of Mm. It is generally accepted that mussel early developmental stages are likely to be more susceptible than adults to potential pathogens, not having fully developed the immune system [31]. In contrast, when tested in *in vitro* short term experiments on hemocytes from adult mussels, Va induced lysosomal stress, but no activation of extracellular immune defences (ROS production and lysozyme release). However, the *in vitro* bactericidal activity of hemolymph towards Va was comparable with that observed towards Mm, suggesting that the soluble serum fraction alone accounts for a major part of this activity.

The results obtained from *in vivo* challenge with Va at 24 h p.i. confirmed a distinct effect on immune responses of the host towards the two bacteria. With respect to Mm, Va induced smaller lysosomal stress

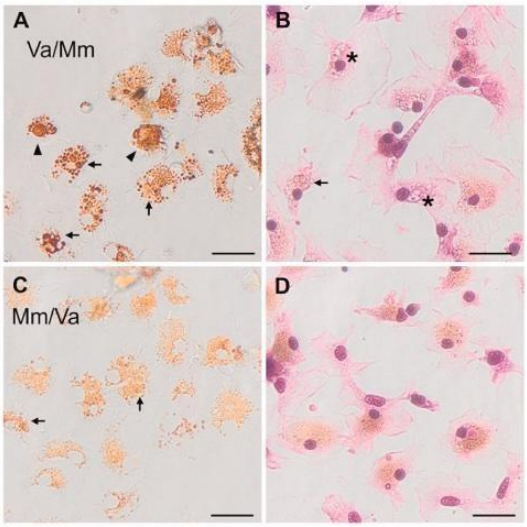

Fig. 5. Representative images of hemocytes of *M. galloprovincialis* from *vivo/in vitro* cross infection observed with different staining. Live hemocytes stained with Neutral Red (NR) for lysosomes (A, C) and fixed hemocytes stained with Giemsa (B, D).
A, B) hemolymph samples from mussels at 24 h p.i. with Va incubated *in vitro* with Mm for different times (30 min NR; 90 min Giemsa)
C, D: hemolymph samples from mussels at 24 h p.i. with Mm and incubated *in vitro* with Va as described above.
Arrow: lysosomal enlargement and fusion; arrowhead: rounded hemocyte, star: vacuolation.
Scale bars = 20 μm.

and lysozyme release in hemocytes, and inhibited, instead of stimulating, ROS production. This resulted in a much lower bactericidal activity of whole hemolymph samples towards Va than towards Mm (about 40 vs 80 %, respectively). Overall, both *in vitro* and *in vivo* data indicate that Va 106 could represent a potential pathogenic strain for adult mussels, in contrast with other *V. aestuarianus* strains. For example, the Va strain 01/032, originally isolated from an oyster mortality outbreak, also shown to be pathogenic to *C. gigas* [19], was shown to induce strong activation of both intracellular and extracellular immune defences in adult mussel hemocytes, leading to intra-lysosomal degradation and efficient bacterial clearance from the hemolymph [36]. These data, when compared with those of the present work, indicate that mussel immune defences are efficiently activated by Va strain 01/032, whereas, strain Va 106 may represent a potential pathogen not only for oysters but also for mussels.

As mentioned above, several reports on bivalve microbiome composition underline the increased *in vivo* abundance of members of the *Arcobacter-like* spp. in stressed or diseased bivalve species, suggesting that the interactions with the immune system of the host are extremely sensitive to infections with pathogens, resulting in a strongly opportunistic behavior of members of this group. In order to verify this hypothesis, sequential cross-infection experiments were subsequently performed in adult mussels, with the aim of understanding whether prior challenge with Va may affect subsequent immune responses to Mm or *vice versa*. *In vivo/in vitro* cross-exposure experiments were first performed, with the aim of evaluating possible differences in the immune responses at the cellular level in isolated hemocytes. The results showed that pre-challenge with Va reduced subsequent *in vitro* hemocyte responses to Mm, resulting in a lower bactericidal activity. This could be partly related to a cytotoxic effect, since in these conditions, hemocyte damage was also observed. In contrast, when hemocytes from Mm pre-injected mussels were incubated with Va, stimulation of extracellular defenses (ROS production and lysozyme release) prevailed, and the bactericidal activity towards Va was unaffected.

In order to verify these observations, *in vivo/in vivo* cross-exposure experiments were performed. Mussels were first challenged with Va and, at 24 p.i., they were subjected to a 2nd injection with Mm, and *vice versa*. At 48 h post 2nd challenge, hemolymph immune parameters were evaluated. The results show that pre-exposure to Va increased hemocyte stress and decreased ROS production, leading to a significant reduction in the bactericidal activity towards subsequent infection with Mm. In contrast, pre-exposure to Mm induced activation of extracellular immune responses (ROS production, lysozyme activity), thus contributing to increase the bactericidal activity towards subsequent challenge with Va.

Overall, both *in vitro* and *in vivo* data demonstrate that, in *M. galloprovincialis*, first infection with certain potential pathogens (i.e. Va 106) can weaken immune defences of the host, thus favoring the subsequent opportunistic behaviour of other non pathogenic bacteria (i.e. Mm R1). In this context, our data are consistent with findings from other polymicrobial infections in oysters, where OsHV-1 [9], or cytotoxic *Vibrio* species such as *V. harveyi* [8], by targeting host immunity and modifying the extracellular environment, facilitate the proliferation of co-infecting partners, including members of the genera *Vibrio* and *Arcobacter*. Conversely, prior infection with bacteria that elicit successful immune responses in the host (i.e. Mm), may even prevent subsequent establishment of other potential pathogens. The results indicate that the outcome of mussel responses (successful or susceptible to disease) depends on the timing of infection with different bacteria.

Overall, when considering all the *in vivo* data obtained from each 24 h injection with Va or Mm, along with the corresponding control values throughout the entire experiment (72 h) (see Figs. 3 and 6 and Fig. S5), a picture of the time course of cellular stress and immune defences in response to single and multiple challenge with Va and Mm can be drawn (Fig. 7). In single infection (Fig. 7, left panel) Mm rapidly induced cellular stress that was however accompanied by activation of immune defenses, leading to efficient bactericidal activity. By 72 h, lysosomal stress was largely reduced and immune responses returned to baseline levels, indicating that the infection has been successfully resolved. In contrast, Va-induced cellular stress in hemocytes was associated with reduction or no activation of immune responses, although some bactericidal activity could be observed, largely due to the activity of serum components (constitutive enzymes or antimicrobial peptides). However, lysosomal stress persisted with time, and it was accompanied by a late and modest activation of ROS production, resulting in a low bactericidal activity towards Va after 72 h from the first challenge. In multiple infections (Fig. 7, right panel) at least in the experimental setting used in the present work, the results indicate the existence of a potential window during which an opportunistic pathogen may exploit the mussel compromised condition characterized by high stress and lack of immune activation, to proliferate and invade the host, leading to potential risk of disease.

Further data are needed to understand the pathogenicity of different Va strains on bivalves, and the mechanisms involved (such as presence and expression of virulence genes). Mesnil et al. (2023) suggested that virulence factors, such as genes encoding copper resistance in *V. francensis* lineages, may enable these pathogens to adapt to oyster hosts [17]. The Ebro Delta is an important agricultural region where freshwater runs off from rice fields flows into the bays and copper-based compounds used in rice farming could select for copper-resistant strains. However, the role of this selection in facilitating multiple infections in mussels remains to be investigated.

Overall, the results suggest that the simple multiple-infection approach employed in this study used in *Mytilus*, a bivalve species generally considered resistant to bacterial infections, could be effectively applied to other, more susceptible bivalve species. These findings

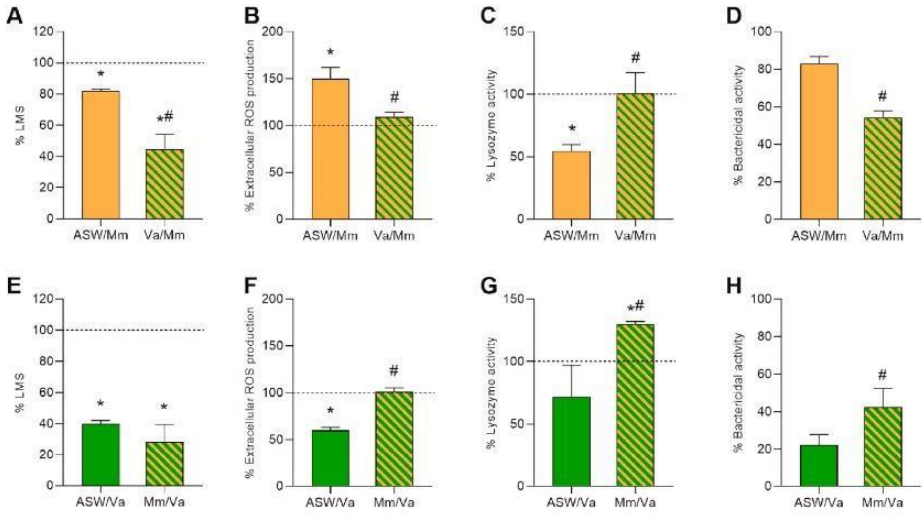

Fig. 6. Functional hemolymph parameters evaluated in mussels after in *vivo/in vivo* 48 h p.s.i cross infection with Va and Mm.
In all experimental conditions, a final nominal concentration of bacteria of 5x 10^6 CFU/mL hemolymph was used.
A–D: mussels first injected with Va and at 24 h p.i. re-injected with ASW or Mm.
E–F: mussels first injected with Mm and at 24 h p.i. re-injected with ASW or Va.
All parameters were evaluated at 48 after the 2nd injection (48 h p.s.i.).
A, E) lysosomal membrane stability (LMS); B, F) extracellular ROS production; C, G) lysozyme activity.
In A-G data are reported as % of negative controls (24 h p.i. ASW/48 h p.s.i ASW), represented by the dotted line. In D, H hemolymph bactericidal activity towards Mm or Va respectively, evaluated at 90 min with respect to time 0. Data represent the mean ± SD of 3 experiments. Statistical analyses were performed by ANOVA followed by Tukey's multiple comparison test, * = $p < 0.05$, all treatments vs control (ASW/ASW); # = $p < 0.05$ between the 2 conditions.

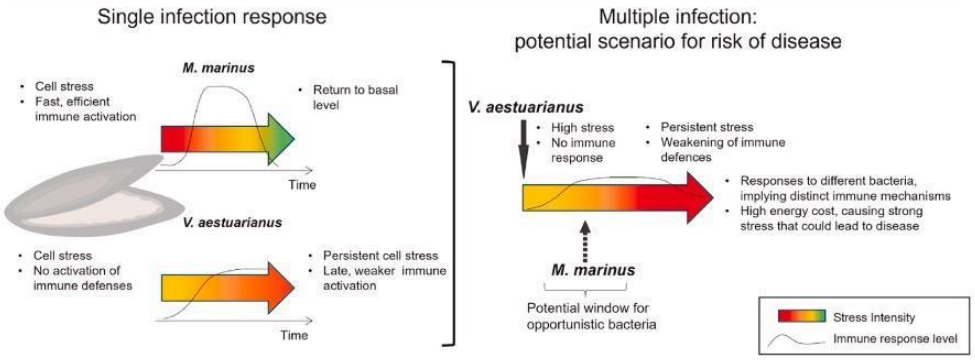

Fig. 7. Time course of stress conditions and immune activation in mussels after single (left) and multiple infection (right) with *M. marinus* R1 and *V. aestuarianus* 106.
Data are summarized from the different figures presented. Stress intensity was related to LMS data, the most sensitive parameter of stress in hemocytes and at whole organism level. The immune response level was generally summarized with data on the degree of extracellular defense produced by hemocytes (ROS and lysozyme) and bactericidal activity of hemolymph.

enhance our understanding of the potential dynamics of interactions between potential bacterial pathogens within bivalve hosts and help explaining the risk of disease outbreaks and mortality events in different bivalve species.

CRediT authorship contribution statement

Manon Auguste: Conceptualization, Data curation, Formal analysis, Investigation, Writing – original draft, Writing – review & editing. Martina Leonessi: Conceptualization, Data curation, Formal analysis, Investigation, Writing – original draft, Writing – review & editing. Caterina Oliveri: Formal analysis, Data curation. Teresa Balbi: Formal analysis, Data curation. Faiz Ur Rahman: Formal analysis. Luigi Vezzulli: Resources, Supervision, Writing – review & editing. Dolors Furones: Resources, Writing – review & editing. Laura Canesi: Resources, Supervision, Writing – original draft, Writing – review & editing.

Funding

Project funded under the National Recovery and Resilience Plan

(NRRP), Mission 4 Component 2 Investment 1.4 - Call for tender No. 3138 of December 16, 2021, rectified by Decree n.3175 of December 18, 2021 of Italian Ministry of University and Research funded by the European Union – NextGenerationEU; Award Number: Project code CN_00000033, Concession Decree No. 1034 of June 17, 2022 adopted by the Italian Ministry of University and Research, CUP D33C22000960007, Project title "National Biodiversity Future Center - NBFC". Faiz Ur Rahman fellowship funded by Marie Skł odowska-Curie Grant No. 713679.

Declaration of competing interest

None.

Appendix A. Supplementary data

Supplementary data to this article can be found online at https://doi.org/10.1016/j.fsi.2025.111064.

Data availability

Data will be made available on request.

References

[1] L. Avdelas, E. Avdic-Mravlje, A.C. Borges Marques, S. Cano, J.J. Capelle, N. Carvalho, M. Cozzolino, J. Dennis, T. Ellis, J.M. Fernández Polanco, J. Guillen, T. Lasner, V. Le Bihan, I. Llorente, A. Mol, S. Nicheva, R. Nielsen, H. Van Oostenbrugge, S. Villasante, S. Visnic, K. Zhelev, F. Asche, The decline of mussel aquaculture in the European Union: causes, economic impacts and opportunities, Rev. Aquacult. 13 (2021) 91–118, https://doi.org/10.1111/raq.12465.

[2] A.F. Rowley, C. Baker-Austin, A.S. Boerlage, C. Caillon, C.E. Davies, L. Duperret, S. A.M. Martin, G. Mitta, F. Pernet, J. Pratoomyot, J.D. Shields, A.P. Shinn, W. Songsungthong, G. Srijuntongsiri, K. Sritunyalucksana, J. Vidal-Dupiol, T. M. Uren Webster, S. Taengchaiyaphum, R. Wongwaradechkul, C.J. Coates, Diseases of marine fish and shellfish in an age of rapid climate change, iScience 27 (2024) 110838, https://doi.org/10.1016/j.isci.2024.110838.

[3] M.-A. Travers, K. Boettcher Miller, A. Roque, C.S. Friedman, Bacterial diseases in marine bivalves, J. Invertebr. Pathol. 131 (2015) 11–31, https://doi.org/10.1016/j.jip.2015.07.010.

[4] B. Petton, D. Destoumieux-Garzón, F. Pernet, E. Toulza, J. De Lorgeril, L. Degremont, G. Mitta, The Pacific oyster mortality syndrome, a polymicrobial and multifactorial disease: state of knowledge and future directions, Front. Immunol. 12 (2021) 630343, https://doi.org/10.3389/fimmu.2021.630343.

[5] A. Lasa, A. Di Cesare, G. Tassistro, A. Borello, S. Gualdi, D. Furones, N. Carrasco, D. Cheslett, A. Brechon, C. Paillard, A. Bidault, F. Pernet, L. Canesi, P. Edomi, A. Pallavicini, C. Pruzzo, L. Vezzulli, Dynamics of the Pacific oyster pathobiota during mortality episodes in Europe assessed by 16S rRNA gene profiling and a new target enrichment next-generation sequencing strategy, Environ. Microbiol. 21 (2019) 4548–4562, https://doi.org/10.1111/1462-2920.14750.

[6] L. Dantan, E. Toulza, B. Petton, C. Montagnani, L. Degremont, B. Morga, Y. Fleury, G. Mitta, Y. Gueguen, J. Vidal-Dupiol, C. Cosseau, Microbial education for marine invertebrate disease prevention in aquaculture, Rev. Aquacult. 16 (2024) 1229–1243, https://doi.org/10.1111/raq.12893.

[7] D. Destoumieux-Garzón, L. Canesi, D. Oyanedel, M. Travers, G.M. Charrière, C. Pruzzo, L. Vezzulli, *Vibrio* –bivalve interactions in health and disease, Environ. Microbiol. 22 (2020) 4323–4341, https://doi.org/10.1111/1462-2920.15055.

[8] D. Oyanedel, R. Rojas, K. Brokordt, P. Schmitt, Crassostrea gigas oysters from a non-intensive farming area naturally harbor potentially pathogenic vibrio strains, J. Invertebr. Pathol. 196 (2023) 107856, https://doi.org/10.1016/j.jip.2022.107856.

[9] J. De Lorgeril, A. Lucasson, B. Petton, E. Toulza, C. Montagnani, C. Clerissi, J. Vidal-Dupiol, C. Chaparro, R. Galinier, J.-M. Escoubas, P. Haffner, L. Dégremont, G.M. Charrière, M. Lafont, A. Delort, A. Vergnes, M. Chiarello, N. Faury, T. Rubio, M.A. Leroy, A. Pérignon, D. Régler, B. Morga, M. Alunno-Bruscia, P. Boudry, F. Le Roux, D. Destoumieux-Garzón, Y. Gueguen, G. Mitta, Immune-suppression by OsHV-1 viral infection causes fatal bacteraemia in Pacific oysters, Nat. Commun. 9 (2018) 4215, https://doi.org/10.1038/s41467-018-06659-3.

[10] M. Auguste, A. Lasa, T. Balbi, A. Pallavicini, L. Vezzulli, L. Canesi, Impact of nanoplastics on hemolymph immune parameters and microbiota composition in Mytilus galloprovincialis, Mar. Environ. Res. 159 (2020) 105017, https://doi.org/10.1016/j.marenvres.2020.105017.

[11] M. Richard, J.L. Rolland, Y. Gueguen, J. De Lorgeril, J. Pouzadoux, B. Mostajir, B. Bec, S. Mas, D. Parin, P. Le Gall, S. Mortreux, A. Fiandrino, F. Lagarde, G. Messiaen, M. Fortune, E. Roque d'Orbcastel, In situ characterisation of pathogen dynamics during a Pacific oyster mortality syndrome episode, Mar. Environ. Res. 165 (2021) 105251, https://doi.org/10.1016/j.marenvres.2020.105251.

[12] Y.-F. Li, N. Yang, X. Liang, A. Yoshida, K. Osatomi, D. Power, F.M. Batista, J.-L. Yang, Elevated seawater temperatures decrease microbial diversity in the gut of Mytilus coruscus, Front. Physiol. 9 (2018) 839, https://doi.org/10.3389/fphys.2018.00839.

[13] C. Paillard, F. Le Roux, J.J. Borrego, Bacterial disease in marine bivalves, a review of recent studies: trends and evolution, Aquat. Living Resour. 17 (2004) 477–498, https://doi.org/10.1051/alr:2004054.

[14] R. Beaz-Hidalgo, S. Balboa, J.L. Romalde, M.J. Figueras, Diversity and pathogenecity of *Vibrio* species in cultured bivalve molluscs, Environ Microbiol Rep 2 (2010) 34–43, https://doi.org/10.1111/j.1758-2229.2010.00135.x.

[15] J. Dubert, J.L. Barja, J.L. Romalde, New insights into pathogenic vibrios affecting bivalves in hatcheries: present and future prospects, Front. Microbiol. 8 (2017) 762, https://doi.org/10.3389/fmicb.2017.00762.

[16] D. Goudenège, M.A. Travers, A. Lemire, B. Petton, P. Haffner, Y. Labreuche, D. Tourbiez, S. Mangenot, A. Calteau, D. Mazel, J.L. Nicolas, A. Jacq, F. Le Roux, A single regulatory gene is sufficient to alter *V ibrio aestuarianus* pathogenicity in oysters, Environ. Microbiol. 17 (2015) 4189–4199, https://doi.org/10.1111/1462-2920.12699.

[17] A. Mesnil, M. Jacquot, C. Garcia, D. Tourbiez, L. Canier, A. Bidois, L. Dégremont, D. Cheslett, M. Geary, A. Vetri, A. Roque, D. Furones, A. Garden, P. Orozova, I. Arzul, M. Sicard, G.M. Charrière, D. Destoumieux-Garzón, M. Travers, Emergence and clonal expansion of *Vibrio aestuarianus* lineages pathogenic for oysters in Europe, Mol. Ecol. 32 (2023) 2869–2883, https://doi.org/10.1111/mec.16910.

[18] M.-A. Travers, D. Tourbiez, L. Parizadeh, P. Haffner, A. Kozic-Djellouli, M. Aboubaker, M. Koken, L. Dégremont, C. Lupo, Several strains, one disease: experimental investigation of Vibrio aestuarianus infection parameters in the Pacific oyster, Crassostrea gigas, Vet Res 48 (2017) 32, https://doi.org/10.1186/s13567-017-0438-1.

[19] M. Garnier, Y. Labreuche, J.-L. Nicolas, Molecular and phenotypic characterization of Vibrio aestuarianus subsp. francensis subsp. Nov., a pathogen of the oyster Crassostrea gigas, Syst. Appl. Microbiol. 31 (2008) 358–365, https://doi.org/10.1016/j.syapm.2008.06.003.

[20] D. Saulnier, S. De Decker, P. Haffner, Real-time PCR assay for rapid detection and quantification of Vibrio aestuarianus in oyster and seawater: a useful tool for epidemiologic studies, J. Microbiol. Methods 77 (2009) 191–197, https://doi.org/10.1016/j.mimet.2009.01.021.

[21] P. Azéma, J.-B. Lamy, P. Boudry, T. Renault, M.-A. Travers, L. Dégremont, Genetic parameters of resistance to Vibrio aestuarianus, and OsHV-1 infections in the Pacific oyster, Crassostrea gigas, at three different life stages, Genet. Sel. Evol. 49 (2017) 23, https://doi.org/10.1186/s12711-017-0297-2.

[22] N. Carrasco, I. Gairin, J. Pérez, K.B. Andree, A. Roque, M. Fernández-Tejedor, C. J. Rodgers, C. Aguilera, M.D. Furones, A Production Calendar Based on Water Temperature, Spat size, and husbandry practices reduce OsHV-1 µvar impact on cultured Pacific oyster Crassostrea gigas in the ebro Delta (Catalonia), Mediterranean Coast of Spain, Front. Physiol. 8 (2017), https://doi.org/10.3389/fphys.2017.00125.

[23] F. Ur Rahman, Potential Impact of Emerging Bacterial Pathogens on Shellfish Production, 2023.

[24] C. Zannella, F. Mosca, F. Mariani, G. Franci, V. Folliero, M. Galdiero, P.G. Tiscar, M. Galdiero, Microbial diseases of bivalve mollusks: infections, immunology and antimicrobial defense, Mar. Drugs 15 (2017) 182, https://doi.org/10.3390/md15060182.

[25] C. Lupo, S. Bougeard, V. Le Bihan, J.L. Blin, G. Allain, P. Azéma, F. Benoit, C. Béchemin, I. Bernard, P. Blachier, L. Brieau, M. Danion, A. Garcia, E. Gervasoni, P. Glize, A. Lainé, S. Lapègue, C. Mablouké, L. Poirier, J.C. Raymond, M. Treilles, C. Chauvin, S. Le Bouquin, Mortality of marine mussels *Mytilus edulis* and *M. galloprovincialis* : systematic literature review of risk factors and recommendations for future research, Rev. Aquacult. 13 (2021) 504–536, https://doi.org/10.1111/raq.12484.

[26] M. Auguste, F.U. Rahman, T. Balbi, M. Leonessi, C. Oliveri, G. Bellese, L. Vezzulli, D. Furones, L. Canesi, Responses of Mytilus galloprovincialis to challenge with environmental isolates of the potential emerging pathogen Malaciobacter marinus, Fish Shellfish Immunol. 131 (2022) 1–9, https://doi.org/10.1016/j.fsi.2022.09.048.

[27] F.U. Rahman, K.B. Andree, N. Salas-Massó, M. Fernandez-Tejedor, A. Sanjuan, M. J. Figueras, M.D. Furones, Improved culture enrichment broth for isolation of Arcobacter-like species from the marine environment, Sci. Rep. 10 (2020) 14547, https://doi.org/10.1038/s41598-020-71442-8.

[28] T. Balbi, M. Auguste, K. Cortese, M. Montagna, A. Borello, C. Pruzzo, L. Vezzulli, L. Canesi, Responses of Mytilus galloprovincialis to challenge with the emerging marine pathogen Vibrio coralliilyticus, Fish Shellfish Immunol. 84 (2019) 352–360, https://doi.org/10.1016/j.fsi.2018.10.011.

[29] ASTM AE724-21, Standard guide for conducting static short-term chronic toxicity tests starting with embryos of four species of saltwater bivalve molluscs. https://doi.org/10.1520/E0724-21, 2021.

[30] A. Lasa, M. Auguste, A. Lema, C. Oliveri, A. Borello, E. Taviani, G. Bonello, L. Doni, A.D. Millard, M. Bruto, J.L. Romalde, M. Yakimov, T. Balbi, C. Pruzzo, L. Canesi, L. Vezzulli, A deep-sea bacterium related to coastal marine pathogens, Environ. Microbiol. 23 (2021) 5349–5363, https://doi.org/10.1111/1462-2920.15629.

[31] P. Balseiro, R. Moreira, R. Chamorro, A. Figueras, B. Novoa, Immune responses during the larval stages of Mytilus galloprovincialis: metamorphosis alters immunocompetence, body shape and behavior, Fish Shellfish Immunol. 35 (2013) 438–447, https://doi.org/10.1016/j.fsi.2013.04.044.

[32] A. Romero, M. Costa, G. Forn-Cuní, P. Balseiro, R. Chamorro, S. Dios, A. Figueras, B. Novoa, Occurrence, seasonality and infectivity of Vibrio strains in natural

populations of mussels Mytilus galloprovincialis, Dis. Aquat. Org. 108 (2014) 149–163, https://doi.org/10.3354/dao02701.
[33] T. Balbi, M. Bozzo, M. Auguste, M. Montagna, A. Miglioli, K. Drouet, L. Vezzulli, L. Canesi, Impact of ocean warming on early development of the Mediterranean mussel Mytilus galloprovincialis: effects on larval susceptibility to potential vibrio pathogens, Fish Shellfish Immunol. 154 (2024) 109937, https://doi.org/10.1016/j.fsi.2024.109937.
[34] M. Charles, I. Bernard, A. Villalba, E. Oden, E.A.V. Burioli, G. Allain, S. Trancart, V. Bouchart, M. Houssin, High mortality of mussels in northern Brittany – evaluation of the involvement of pathogens, pathological conditions and pollutants, J. Invertebr. Pathol. 170 (2020) 107308, https://doi.org/10.1016/j.jip.2019.107308.
[35] L. Bracchetti, M. Capriotti, M. Fazzini, P. Cocci, F.A. Palermo, Mass mortality event of Mediterranean mussels (Mytilus galloprovincialis) in the middle adriatic: potential implications of the climate crisis for Marine ecosystems, Diversity 16 (2024) 130, https://doi.org/10.3390/d16030130.
[36] T. Balbi, R. Fabbri, K. Cortese, A. Smerilli, C. Ciacci, C. Grande, L. Vezzulli, C. Pruzzo, L. Canesi, Interactions between Mytilus galloprovincialis hemocytes and the bivalve pathogens Vibrio aestuarianus 01/032 and Vibrio splendidus LGP32, Fish Shellfish Immunol. 35 (2013) 1906–1915, https://doi.org/10.1016/j.fsi.2013.09.027.

Supplementary figures to: Deciphering Host–Pathogen Dynamics in *Mytilus galloprovincialis*: immune responses to multiple infections with bacterial isolates from bivalve mortality outbreaks

Manon Auguste[a,b,$*], Martina Leonessi[a,b,$], Caterina Oliveri[b], Teresa Balbi[a,b], Faiz Ur Rahman[c,d], Luigi Vezzulli[a,b], Dolors Furones[c], Laura Canesi[a,b]

[a]DISTAV, Dept. of Environmental, Earth and Life Sciences, University of Genoa, Italy
[b]National Biodiversity Future Center, Palermo, Italy
[c]IRTA La Ràpita Centre, Aquaculture Program, Spain
[d]Unit of Microbiology, Department of Basic Health Sciences, Faculty of Medicine and Health Sciences, IISPV, Universitat Rovira i Virgili, Reus, Spain
[$]Equally contributed to the work.

**Corresponding author*

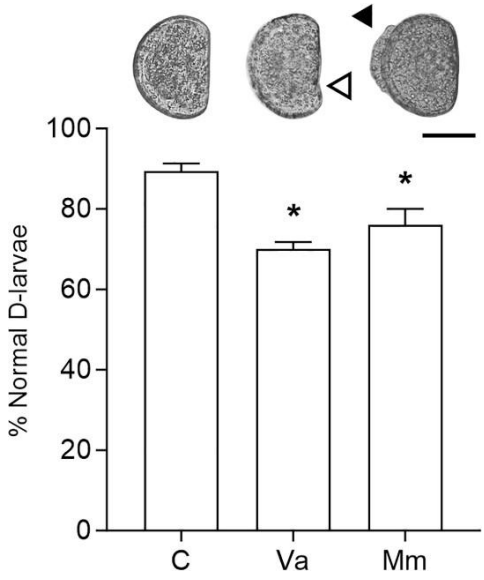

Fig. S1. Effect of *V. aestuarianus* 106 (Va, 10^6 CFU/mL) on *M. galloprovincialis* early larval development at 48 hpf. The results are compared with those previously obtained with the same concentration of *M. marinus* R1 (Mm) (Auguste et al., 2022). Representative images of control larvae and of the main larval phenotypes (lateral view) observed in different experimental conditions at 48 hpf. White arrow: convex hinge, black arrow: protruding mantle. Scale bar: 50 µm.
Data, representing the mean ± SD of 4 experiments carried out in 96-multiwell plates, were analyzed by Mann-Whitney U test, * = $p < 0.05$, bacteria-exposed *vs* controls.

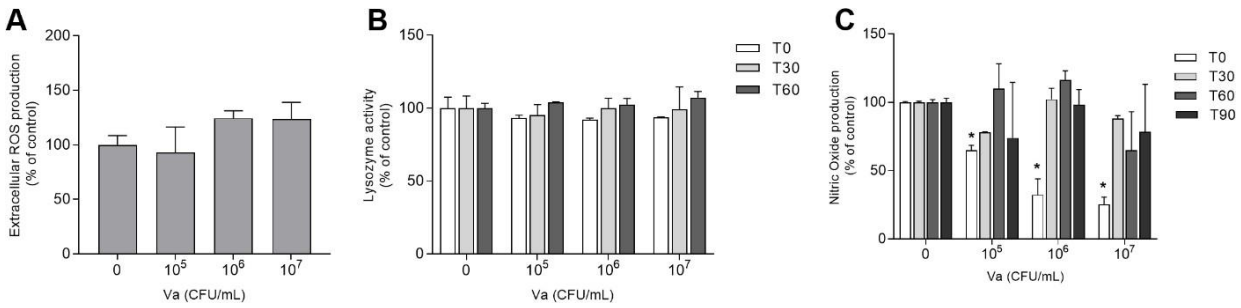

Fig. S2. *In vitro* effects of *V. aestuarianus* (Va) on immune response of *M. galloprovincialis* hemolymph.
A) Extracellular ROS production (after 30 min incubation). B) Lysosomal enzyme release; C) Nitric oxide-NO production, after incubation with Va at 10^5, 10^6, 10^7 CFU/mL from 30 min up to 90 min, according to the parameter measured. Data represent the mean ± SD of 3 experiments in triplicate. Statistical analyses were performed by ANOVA followed by Tukey's multiple comparison test, *=$p<0.05$.

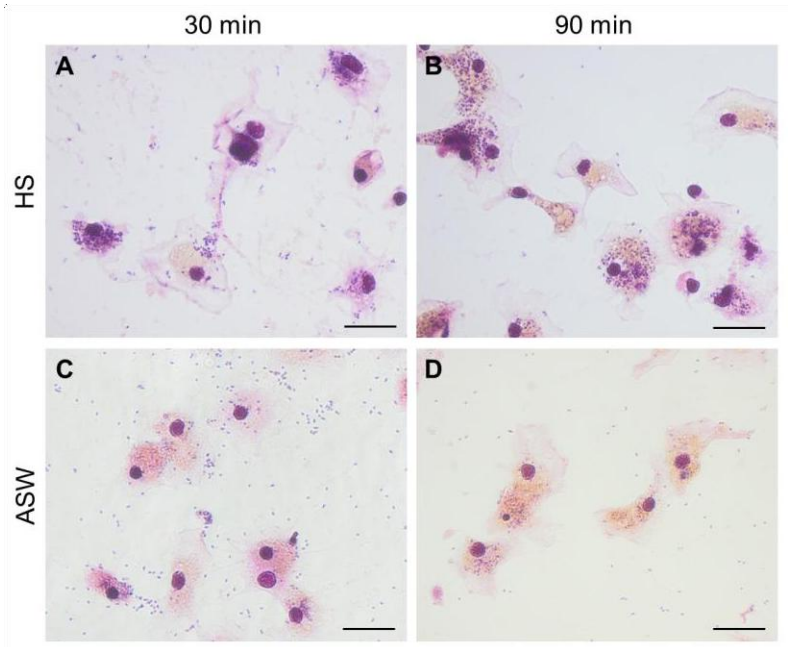

Fig. S3. Giemsa staining of *M. galloprovincialis* hemocytes incubated with *V. aestuarianus*.
Hemocytes were incubated for 30 and 90 min with bacteria (10^8 CFU/mL) resuspended in either hemolymph serum (HS) (A-B) or ASW (C-D) (for details see Auguste et al., 2022).
Progressive bacteria internalization by hemocytes was clearly more evident in HS (A, B), whereas in ASW most bacteria were in the extracellular medium. Scale bars: 20 µm.

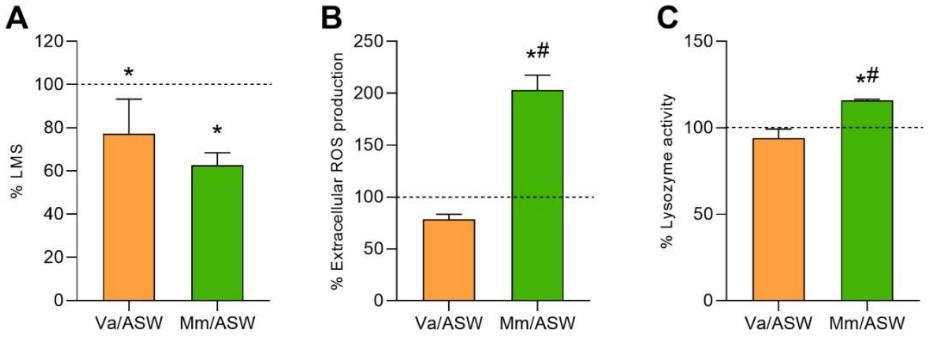

Fig. S4. ***In vivo/in vitro* cross experiments (*in vitro* controls).**
Functional parameters were evaluated in hemolymph samples at 24 p.i. with either Va or Mm (final concentration 5 × 10^6 CFU/mL hemolymph) incubated *in vitro* with ASW for 30 min.
A) lysosomal membrane stability; B) extracellular ROS production; C) lysozyme release. Data (mean ± SD of 3 experiments), are reported as % values of negative controls (dotted lines), represented by samples at 24 p.i. with ASW and incubated *in vitro* with ASW (ASW/ASW). Data represent the mean ± SD of 3 experiments. Statistical analyses were performed by ANOVA followed by Tukey's multiple comparison test, $p<0.05$. *= all treatments vs control (ASW/ASW); # = between the 2 conditions.

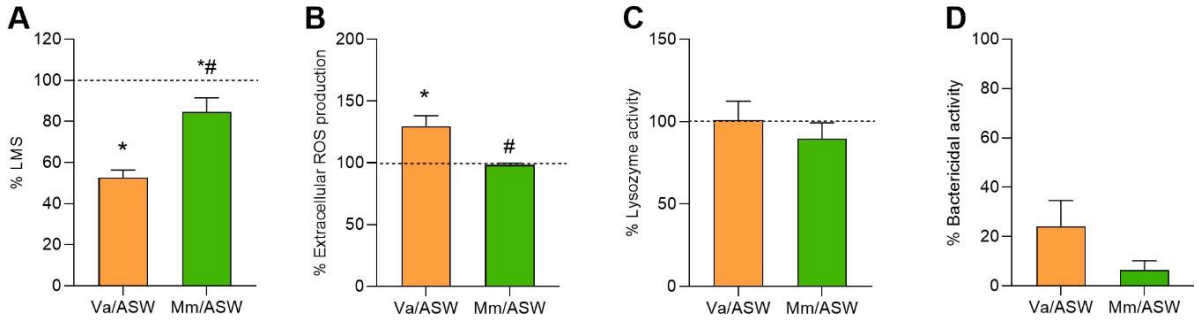

Fig. S5. *In vivo/in vivo* cross experiments (negative controls).
Functional parameters were evaluated in hemolymph samples from mussels pre-injected with either Va or Mm re-injected with ASW and at 24 h p.i., and data were collected at 48 h p.s.i. corresponding to an overall time of 72 h after the first injection.
A) lysosomal membrane stability; B) extracellular ROS production; C) lysozyme activity; D) bactericidal activity towards Va (Va/ASW) or Mm (Mm/ASW).
Data are reported as % of negative controls (24 h p.i. ASW/ 48 h p.s.i. ASW) (dotted line in A-C) or with respect to Time 0 (D). Data represent the mean ± SD of 3 experiments. Statistical analyses were performed by ANOVA followed by Tukey's multiple comparison test, $p<0.05$. *= all treatments vs control (ASW/ASW); # = between the 2 conditions.

Chapter 5:

Seasonal variations in immunocompetence of *Mytilus galloprovincialis* and its specificity towards different bacteria.

1. Introduction

Marine bivalves are key ecological components of coastal ecosystems and include several economically important aquaculture species, such as oysters, mussels, clams, and scallops, with a global production exceeding 15 million tonnes per year (FAO, 2018; Smaal et al., 2019). In a changing world, the climate crisis represents a major threat to species, biodiversity, and ecosystem functioning, affecting both individual organisms and their interactions (Bracchetti et al., 2024; Wernberg et al., 2024). In this context, mussel mortality events have become a growing concern, with an increasing number of reports documenting mass mortalities and disease outbreaks affecting both farmed and wild populations worldwide (Bracchetti et al., 2024; Charles et al., 2020a; Lattos et al., 2022; Lupo et al., 2021; Mandic et al., 2024).

Most studies report mussel mortality events occurring predominantly during the summer season. However, in a climate change scenario of ocean warming, the temporal window of mortality risk is likely to expand. Indeed, outbreaks are increasingly being reported earlier in the year, including during late winter and early spring. For example, in Brittany, (Charles et al., 2020a) documented significant mussel mortality events at the end of winter and in early spring 2017. Similarly, in the Netherlands, the first mass mortality event of mussel began in November 2015, with high mortality rates on culture plots persisting until autumn 2016. During this period, approximately 40–50% of mussels from all age classes were lost on culture plots, while 100% mortality was observed in wild seed beds. A second outbreak started in April–May 2019 and continued until the end of July, with mortality rates ranging from 20 to 100% across all age classes (Capelle et al., 2021).

However, the identification of the exact causes of these events is often challenging, as mortality outbreaks are generally considered to be both multifactorial and polymicrobial (Lupo et al., 2021). Indeed, seasonal fluctuations in biotic and abiotic factors can impose additional stress on mussel, affecting physiological homeostasis, including immunocompetence.

In the hemocytes of *M. galloprovincialis* farmed in the Ligurian sea (Italy) it has been demonstrated (Auguste et al., 2024; Balbi et al., 2017) that lysosomal membrane stability (LMS), a core biomarker of mussel health status directly correlated with physiological scope

for growth and protein turnover (Dagnino et al., 2007; Viarengo et al., 2007), is influenced by the natural stress associated with the final stages of gametogenesis and spawning. In mussels, gametogenesis is affected by various environmental factors and can vary from year to year, primarily depending on temperature and food availability. In particular, warmer temperatures have been shown to reduce the rate of gametogenesis in *M. galloprovincialis* (Fearman and Moltschaniwskyj, 2010).

A thorough knowledge on the natural variability of different immune biomarkers in farmed mussels is therefore needed for correctly interpreting mortality outbreak events. Moreover, monitoring immune responses towards different bacteria could provide insights into seasonal shift in immune defence strategies, and help understanding the contribution of specific mussel-bacteria interactions to these phenomena.

The present study was aimed at monitoring the natural seasonal dynamics of hemolymph immune biomarkers and at investigating the potential seasonal changes in specificity of hemolymph immune responses towards different bacteria. Specimens of *M. galloprovincialis* from the aquaculture plant of La Spezia (Italy), were analysed from January to December 2025. A set of hemolymph immune biomarkers (lysosomal membrane stability, serum lysozyme activity and bactericidal activity) were utilized to evaluate natural seasonal variability of immune defences. Moreover, the same parameters were evaluated in hemolymph samples challenged *in vitro* with different bacterial species and strains, in order to investigate the efficiency and specificity of hemolymph immune responses towards bacteria at different times of the year. To this aim, three model bacteria were selected: a non marine bacterium *E. coli* MG1655 (EC) (not pathogenic to bivalves, used as reference strain), and two vibrio isolates from bivalve mortality events *V. aestuarianus* 01/32 (VA) (pathogenic to oysters but not to mussels) and *V. tasmaniensis* LGP32 (VT) (pathogenic to both oysters and mussels) (see graphical abstract).

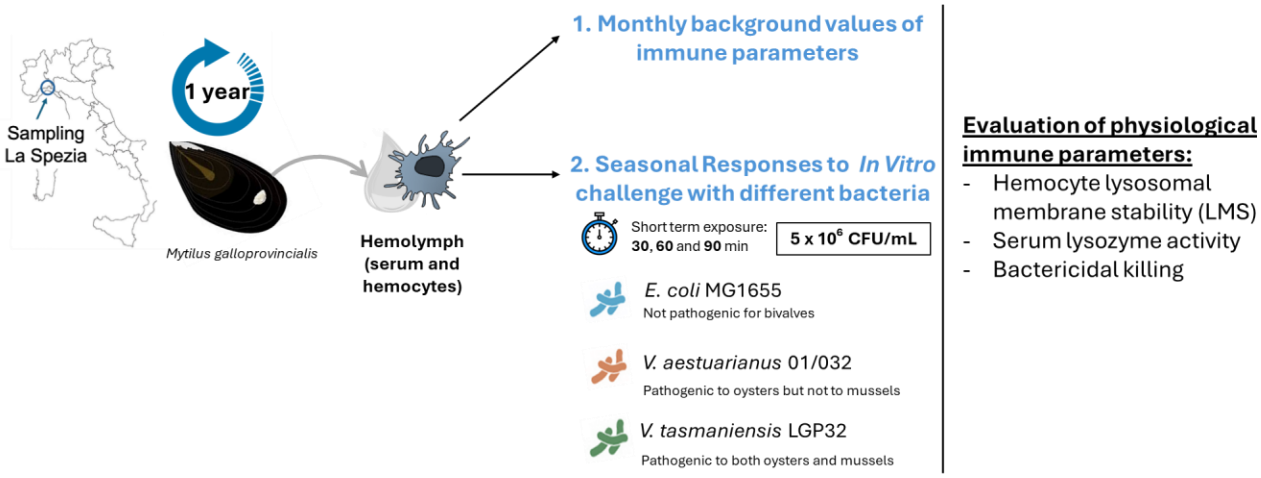

2. Methods

2.1. Mussel sampling

M. galloprovincialis were obtained from the aquaculture plant of La Spezia (Italy), approved for mussel commercialization after depuration (class B harvesting area, according to 91–492-EEC). The area is monitored for the marine ecosystem status and seawater quality by the Regional Agency for Environment Liguria (ARPAL), from which data on surface water temperature were obtained (https://www.arpal.liguria. it/). Monthly, mussels were freshly purchased from the local fish market all along 2025. Each month, at least 100 individuals of the same size (average length 4–5 cm) were utilized. The animals were acclimatized in static tanks in aerated artificial seawater (ASW) 1 L
/mussel, at 18 °C, 35 ppt salinity, for 24 h. The gonad reproductive stage was evaluated by microscopical observations of gonad smears as previously described (Balbi et al., 2017, p. 201).

2.2 Natural seasonal variability of immune parameters

Hemolymph was drawn from the posterior adductor muscle of 5 groups of 5 mussels each (n = 5) for the determination of basal immune parameters. For hemocyte monolayer preparation, 20 µL drops of the whole hemolymph were deposited on microscope slides and the cells were let to adhere for 20 min before removing the excess of hemolymph. Lysosomal membrane stability (LMS) of hemocyte monolayers was evaluated by the NRR (Neutral Red Retention time) assay (OSPAR Commission, 2013) as previously described (Auguste et al., 2020, 2019; Balbi et al., 2017). NRR time was evaluated by optical microscopy, and the endpoint of the assay was defined as the time at which 50% of the cells showed sign of lysosomal leaking (the cytosol becoming red and the cells rounded). Hemolymph lysozyme activity was determined at 450 nm using *Micrococcus lysodeikticus* (15 mg/100 mL in 66 mM phosphate buffer, pH 6.4) (Auguste et al., 2022) and expressed as Hen eggwhite (HEW) lysozyme equivalents (U/mg protein/mL). The hemolymph total protein content was determined by the Bradford method with bovine serum albumin (BSA) as a standard. All parameters were measured in triplicate.

2.3 *In vitro* challenge

At each month, hemolymph was sampled and pooled from 30 animals. The collected hemolymph was used to perform all *in vitro* challenges towards all three bacteria. Hemocyte monolayers or whole hemolymph samples (according to the endpoint, see the details in the next paragraph)

were incubated from 30 to 90 min, depending on the endpoint measured, with suspensions of *E. coli* MG1655 (EC),
V. aestuarianus 01/032 (VA) or *V. tasmaniensis* LGP032 (VT) suitably diluted in ASW to obtain a concentration of 10^6 CFU/mL. Untreated samples in ASW were run in parallel. Filter-sterilized ASW was utilized in all experiments. To obtain hemolymph serum-HS, the whole hemolymph was centrifuged at 100 × g for 10 min, and the supernatant was sterilized through a 0.22 µm-pore filter.

2.4 Bacterial cultures and inoculum preparations

E. coli MG1655 was cultured in LB Miller broth at 37 °C in static conditions overnight.
V. aestuarianus 01/032 and *V. tasmaniensis* LGP032 were cultured in Zobell medium at 23 °C in static conditions overnight. After overnight growth, the inocula were centrifuged (4500×g, 10 min) and washed once in ASW. The pellets were resuspended to obtain a concentration of about 5 x 10^8 colony forming units CFU/mL (determined spectrophotometrically as an Abs600 = 0.30 for EC, Abs600 = 0.80 for VA and Abs600 = 0.60). LB Miller plates for EC and LB 3% plates for VA and VT were used throughout the experiments.

2.5 Determination of functional parameters

All assays were carried out as previously described (Auguste et al., 2022; Balbi et al., 2017, 2013). Lysosomal membrane stability (LMS) was evaluated in hemocytes monolayers by the Neutral Red Retention Time (NRRT), as described above. Hemocyte monolayers were pre-incubated for 30 min with different bacteria suspensions of EC, VA or VT at 10^6 CFU/mL. All incubations were carried out at 18 °C. For the determination of Lysozyme release, aliquots of whole hemolymph were incubated with suspensions of EC, VA or VT (final concentrations 10^6) for 0, 30 and 60 min and the activity evaluated spectrophotometrically as described above. The hemolymph total protein content was determined by the Bradford method with bovine serum albumin (BSA) as a standard.

2.6 Bactericidal activity

For *in vitro* bactericidal activity, hemocyte monolayers were incubated with the bacterial suspensions (EC, VA or VT) in either ASW or HS (5 × 10^6 CFU/mL final concentration) as previously described (Auguste et al., 2022; Bosi et al., 2024). The bactericidal activity of HS alone was also evaluated. To check bacterial growth or death over experimental time, control samples of EC, VA or VT alone incubated in ASW were run in parallel. Immediately after the

addition of bacteria (T = 0) and after 30 and 90 min of incubation (at 18 °C), samples were collected and added with 0.05% Triton X-100 in ASW and vortexed for 10 s to lyse the hemocytes. The lysate was tenfold serially diluted in ASW and plated onto LB miller plates for EC samples and LB 3% for VA and VT samples. After incubation with different bacteria (24 h at 37 °C for EC and 48 h incubation at 23 °C for VA and VT, respectively, the number of CFU (colony forming units) for each condition (representing live, culturable bacteria) was determined. Percentages of killing were determined in comparison to values obtained at zero time. The number of CFU in control hemocytes never exceeded 0.1% of those enumerated in experimental samples.

3. Statistical analysis

Data on seasonal immune parameters represent the mean ± SD of at least 5 independent samples. Differences among individual months and mean value were analysed by the non-parametric Kruskal-Wallis test followed by Dunn's test ($p \leq 0.05$) using GraphPad Prism (version 7.03 for Windows). Data on *in vitro* challenges are expressed as mean ± SD of 3 technical replicates.

4. Results

4.1 Mussel gametogenic stage and seasonal changes in water temperature

In this work all animals were sampled from the Gulf of La Spezia (**Fig. 1A**). **Figure 1B** shows seasonal changes in surface seawater temperature at the site (left Y axis) and mussel gonad maturation stage (right Y axis). The average temperatures (mean values between 0.2 and 5 m depth) were lowest in January-March (12-13 °C) and highest in July-August (26 °C) (**Fig. 1B**), as previously observed in 2015/16 and 2020 (Balbi et al., 2017; Auguste et al., 2023) (See **Fig. S1**). The gametogenic stage was evaluated in mussels by microscopical observations of mantle tissue smears. Cumulative data are presented for both males and females. The maturation stage peaks in January (stage IV), when a strong spawning event was recorded in mussels during acclimation to laboratory conditions. From February to April and in December ripe gonads were observed with little spawning (stage III-IV). In the warmer months, T >18 °C (May-November), developing stages III-II were recorded. During the sampling period, no individuals with immature gonads (Stage 0-II) were observed.

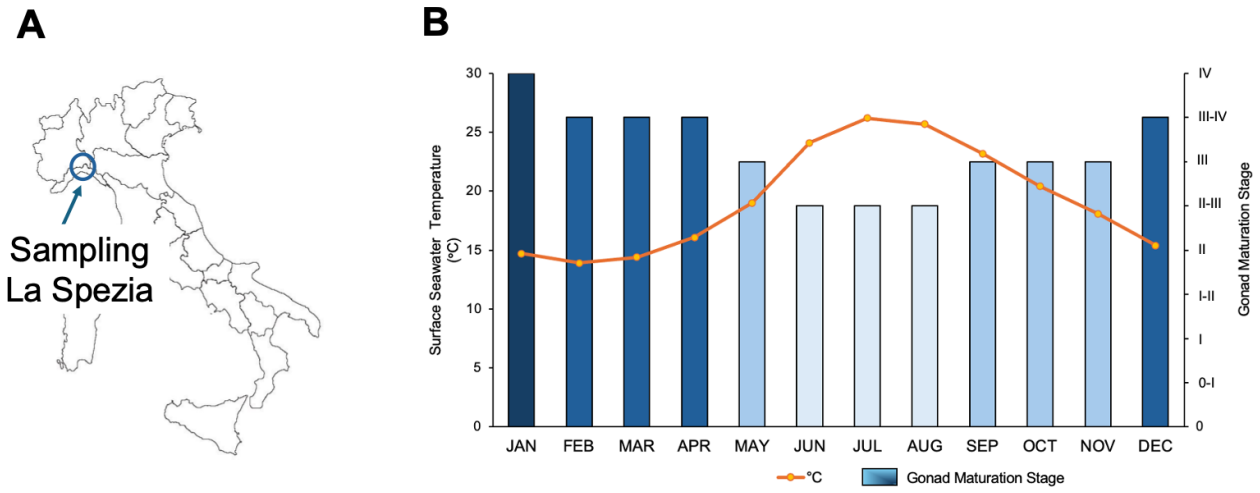

Figure 1: Study area, seasonal changes in surface seawater temperature and mussel gonad maturation stage. A) Location of the mussel farm in the Ligurian Sea, Italy; B) Average seawater temperature (°C) (https://www.arpal.liguria.it) in relation with gonad maturation stage: 0-II =early stage, III = developing/ripe, III-IV = ripe/spawning, IV = spawning.

4.2 Natural seasonal variability of immune parameters

LMS was first determined in hemocytes as a core stress biomarker at the cellular level (**Fig. 2A**). LMS showed average NRR times ≥ 100 min, indicating the absence of significant seasonal variations. However, data showed higher variability among pools in August and September, when some samples were rich in natural bacteria. In contrast, serum lysozyme activity showed highly fluctuating values (**Fig 2B**). Although a distinct seasonal trend was not observed (mean value 201.64 ± 80.00 U/mL/mg prot), highest values were observed again in August and September (300 U/mL/mg prot), this also reflecting responses to the presence of high amounts of natural bacteria.

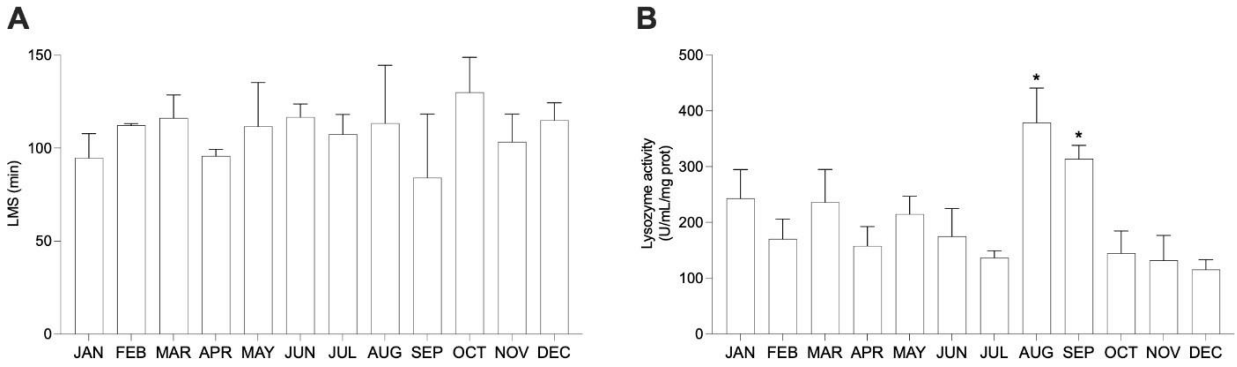

Figure 2: Seasonal changes in immune parameters in *M. galloprovincialis* hemolymph: A) hemocyte LMS expressed as NRRT (min), B) lysozyme activity in hemolymph serum (U/mL/mg prot). The

data are expressed as mean ± sd (N=5). Differences among individual months and mean value were analysed by the non-parametric Kruskal-Wallis test followed by Dunn's test, *p < 0.05.

4.3 *In vitro* challenge

The effects of 30 min *in vitro* incubation with different bacteria (EC, VA or VT respectively) at 5 x 10^6 CFU/mL on hemocyte LMS are reported in Fig 3.

All bacteria induced a general decrease in LMS with respect to controls. EC showed the mildest effects, inducing a marked decrease in LMS in winter (January-March, -40%), a small decrease in spring (April-June, -20%) and almost no effects in July-December (< -20%) (**Fig. 3A**). VA did not display a clear seasonal trend, with an average lysosomal destabilization of about - 40-50%, except for January, April and September, when VA exhibited the strongest effects (- 80%) (**Fig. 3B**). VT showed a progressive decrease in LMS over time, starting with approximately - 20% destabilization in January, and reaching almost complete destabilization (> -80%) in August. A partial recovery of LMS values was observed during the last months of the year (- 30-50 %) (**Fig. 3C**).

Lysozyme activity measured after 60 min of exposure did not show strong stimulation compared to the controls (**Fig. S1**). EC did not induce any increase in lysozyme activity. VA caused a slight increase (approximately +20%), but only during summer. In contrast, VT induced a modest increase in lysozyme activity (about +20%) throughout the entire sampling period (see **Fig. S2**).

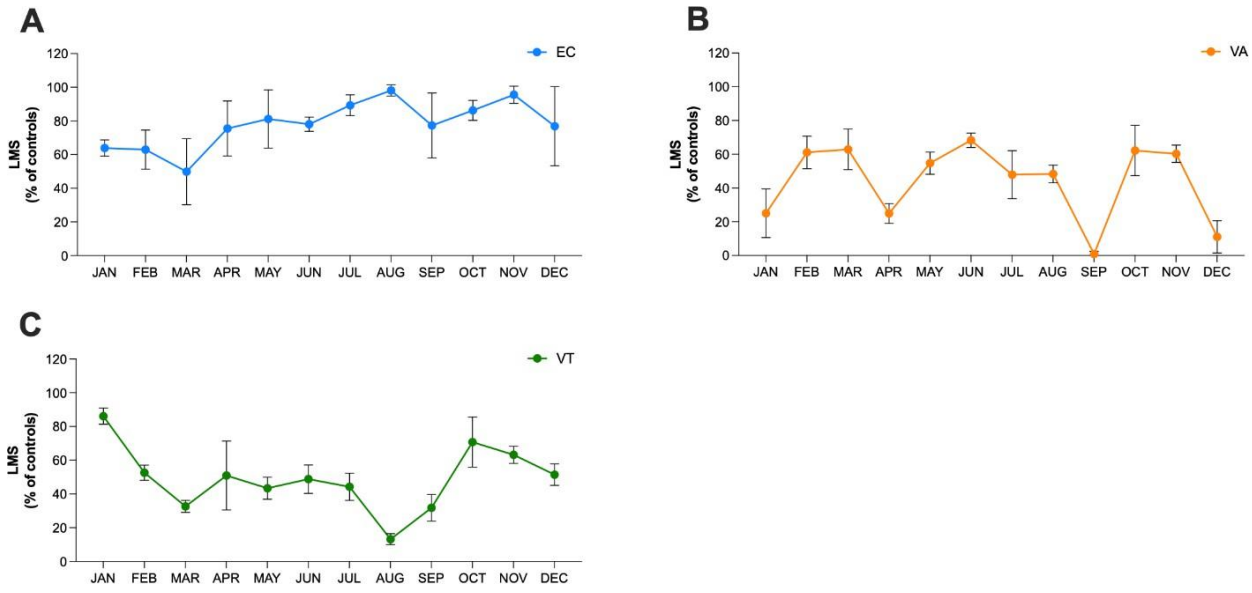

Figure 3: *In vitro* effects of EC (A), VA (B) and VT (C) strain on hemocyte lysosomal membrane stability-LMS throughout the year. EC: blue line; VA: orange line; VT: green

line. Data are expressed as mean ± sd of 3 technical replicates.

Finally, the bactericidal activity of mussel hemolymph components, hemocytes alone in ASW (HEM), hemolymph serum (HS), and whole hemolymph samples, towards EC, VA and VT (5 × 10^6 CFU/mL, 90 min) was evaluated (**Fig. 4A, B, C**). Data are expressed as the percentage of killed bacteria with respect to time zero.

HEM (**Fig. 4A**) exhibited constant bactericidal activity towards EC throughout the sampling period (about 50%). In contrast, killing of VA and VT showed clear seasonal fluctuations. The bactericidal activity of HEM alone towards VA was low from January to April (about 20- 30%) and progressively increased in spring-summer, with a maximum in July (up to 70%). After a large decrease observed in August and September (about 10%), a further rise was observed from October (almost 100 %). A similar, even more marked seasonal trend was observed with VT: bactericidal activity was low in January-April (about 10-20%), followed by increases in late spring (up to 90% in June). A subsequent drop was observed in summer (July-September). A second peak was observed in autumn (up to 99% in October),

HS alone showed generally higher bactericidal activities (**Fig 4B**), that for EC reached almost 100% from January to July, followed by a reduction from August to December (about 50–60%). In contrast, as for hemocytes, a clear seasonal pattern was observed with VA, with lower values in winter-early spring (January-April) (about 40%) followed by increases in warmer months (up to 60% in August). After a drop in September (17%), a large increase was observed in October (almost 100%), which persisted until the end of the year. HS showed high bactericidal activity against VT throughout most of the year (about 90%), except for January and February (<20%).

Finally, when HEM were combined with HS (**Fig. 4C**), the bactericidal activity for all bacteria followed trends similar to those observed with HS alone. Killing of EC was comparable to that observed with HS alone, while killing of VA followed the same seasonal pattern but with slightly higher magnitude. Killing of VT was also comparable with that of HS alone. No bacterial killing was observed in ASW alone (not shown).

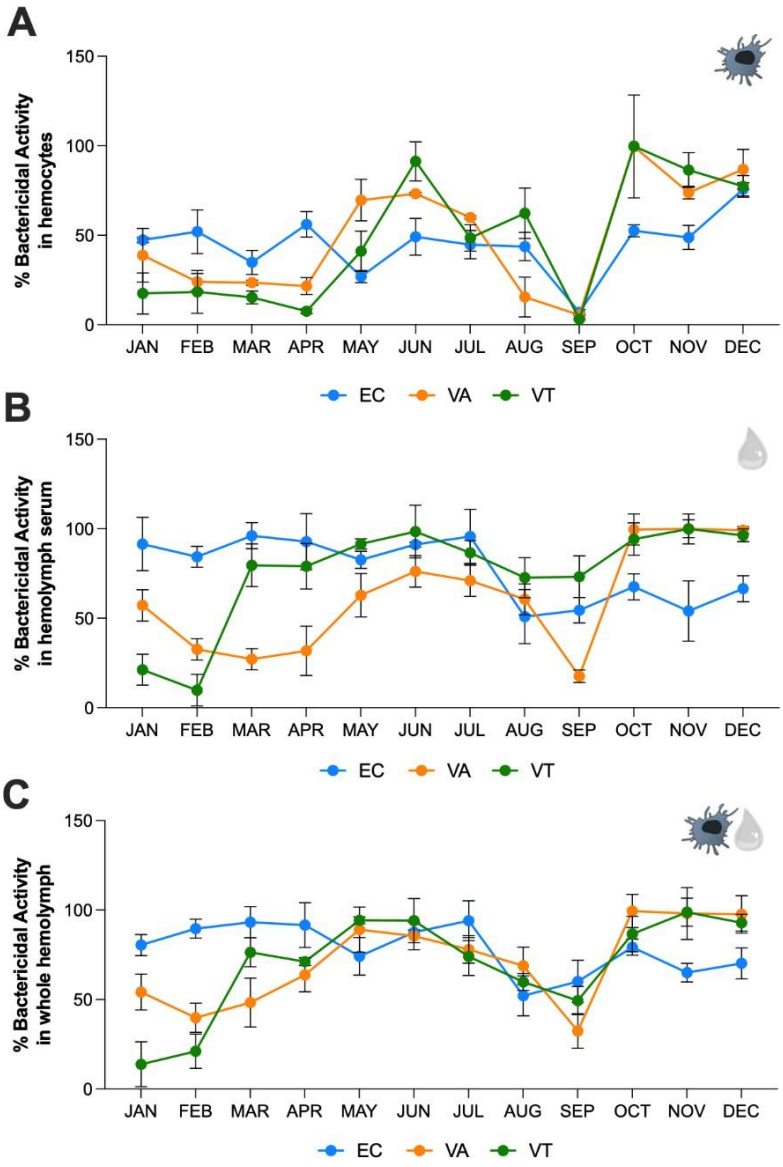

Figure 4: *In vitro* bactericidal activity of mussel hemocytes and serum towards EC, VA and VT after 90 min of exposure. A) bactericidal activity of hemocytes; B) bactericidal activity of hemolymph serum (HS); C) bactericidal activity of hemocytes resuspended in HS. Results are expressed as percentage values with respect to time zero. Data are expressed as mean ± sd of 3 technical replicates.

5. Discussion

5.1 Natural seasonal variability of immune parameters

The first part of this work focused on the evaluation of the natural seasonal immunocompetence of

M. galloprovincialis collected from an aquaculture farm in La Spezia (Italy). The study lasted one year, and samples were collected monthly from January to December 2025. In this period, water temperatures were always lower than 18 °C from January to May and in November-

December, allowing for almost continuous maturation of gametes, and thus confirming the relationship between water temperatures and gonadal maturation stages. However, it is worth noting that, in contrast to previous studies carried out on mussels from the same aquaculture site in 2015 and 2020 (Auguste et al., 2024; Balbi et al., 2017), mussels in early stages of gonad maturation (0-II) were never observed throughout the sampling period. Moreover, during mussel acclimatation in the laboratory prior to sampling, spawning episodes were recorded only in January. These findings suggest that, although mussels exhibited developing/mature gonads all over the year, the spawning window appears to be shorter in 2025 than those reported in previous studies (Auguste et al., 2024; Balbi et al., 2017). Actually, in 2025, slightly higher temperatures were observed from February to April (from 0.5 to 1 °C with respect to the previous years) (**Fig. S1**).

Lysosomal membrane stability (LMS) was determined in hemocytes as a core stress biomarker at the cellular level. In mussels, LMS is directly correlated with physiological scope for growth (SFG) and protein turnover. When LMS is evaluated by the NRR assay, animals are considered to be healthy if NRR is ≥120 min; stressed but compensating if < 120 min but ≥ 50 min, and severely stressed if < 50 min (Balbi et al., 2017; OSPAR Commission, 2013). In the present study LMS did not show a clear seasonal trend. Mean NRR values were generally ≥ 100 min, indicating a slightly stressed but compensating physiological status, with lower values observed in January, April, September, and November. In contrast, previous studies carried out at the same site reported highest LMS values (200 min) in summer (July – September) and lowest values (50%) in winter (January-April) during the spawning season (Balbi et al., 2017; Auguste et al., 2023). Summer is generally considered the season associated with the highest LMS in mussel hemocytes, as favorable environmental conditions, increased food availability, and the absence of energetically demanding reproductive processes collectively support cellular homeostasis and immune competence (OSPAR Commission, 2013). In contrast, one of the main confounding factor is the adverse effect of the final stage of gametogenesis and spawning occurring in winter, which is a naturally stressful process (Balbi et al., 2017).
In the present study, average LMS values were generally lower (about 100 min) across the whole year, with no seasonal variations. The results suggest a potential change in the seasonal pattern of hemocyte LMS that may be caused by both endogenous and environmental factors. With regards to the influence of the gametogenic cycle, despite the persistent presence of ripening gonads, a shorter spawning window was observed in the present study with respect to previous years. Moreover, the presence of a high bacterial background in hemolymph observed

in August and September, as observed by optical microscopy (not shown), could have slightly affected hemocyte LMS. In the context of ocean warming, increasing temperatures may have impacts not only on physiological homeostasis and health status of the host, but also on increased virulence and range expansion of potentially pathogenic bacteria (Cohen et al., 2018), this potentially affecting host-bacteria interactions. Similarly to LMS, lysozyme activity, which represents one the most important functional extracellular defences in mussel hemolymph, did not show a clear seasonal trend, as previously reported. However, peaks in August and September were observed, probably due to the response to the presence of natural bacteria.

5.2 *In vitro* challenge

The same parameters described above were evaluated to determine the ability and specificity of mussel immune system to respond to *in vitro* challenge with different bacterial species and strains (5 x 10^6 CFU/mL): a non marine bacterium *E. coli* MG1655 (EC), and two vibrio isolates from bivalve mortality events *V. aestuarianus* 01/32 (VA) and *V. tasmaniensis* LGP32 (VT). These bacteria were selected based on their different characteristics.

E. coli is a very common gram-negative bacterium, representing a major foodborne pathogen in humans; most strains colonize the gastrointestinal tract of humans without consequences; however, there are pathogenic *E. coli* strains that causes infections (Li et al., 2010). For this reason, *E. coli* is usually used as a model for enteric bacteria released in the marine environment (Canesi et al., 2016). Our results indicate evident, but moderate responses of mussel hemolymph components (both in terms of LMS and bactericidal activity) to this model exogenous bacterium. In particular, in the present work, the strain *E. coli* MG1655 was utilized, expressing D-mannose-sensitive adhesins (MSHA), called type 1 fimbriae on the bacterial surface. Previous *in vitro* studies demonstrated that MSHA are easily recognized by the extrapallial protein precursor (MgEP) present in the hemolymph serum of *M. galloprovincialis* (Canesi et al., 2016, 2002). The presence of MgEP increased the bactericidal killing towards *E. coli* MG1655 by promoting bacterial opsonization and its adhesion to hemocytes (Canesi et al., 2016, 2002). Consistent with the literature, our results demonstrated that hemocytes efficiently killed EC (≥50%) throughout the year, and that the bactericidal activity was increased by the presence of HS, indicating a synergistic effect between cellular and humoral immune components. Interestingly, the killing efficiency of HS alone towards EC showed seasonal variations, with highest values (almost 100%) in the first part of the year and 50-60% after the summer. These observations suggest seasonal variations in the levels of

MgEP serum protein, or other components with similar function, in mussel hemolymph.

The second bacterium tested was *V. aestuarianus* 01/032. *V. aestuarianus* is a gram-negative marine bacterium originally isolated from adult moribund oysters during a French disease outbreak in 2001 (Garnier et al., 2008, 2007). The 01/032 strain produces extracellular products (ECPs) containing the main virulence factor of *V. aestuarianus*: the metalloprotease Vam (Labreuche et al., 2010).

In vitro and *in vivo* data on interactions of *V. aestuarianus* 01/032 with bivalve hemocytes revealed an opposite outcome in oysters and mussels. In *M. gigas*, where *V. aestuarianus* 01/032 expresses its pathogenic potential, it is able to avoid phagocytosis (Labreuche et al., 2006), whereas in mussels, where it does not cause disease, 01/032 is opsonized by the MgEP serum protein and efficiently killed by the hemocytes (Balbi et al., 2013; Pezzati et al., 2015). This is in line with the presence, also in this strain, of the MSHA adhesin (Pezzati et al., 2015). Our results indicate that VA significantly affected hemocyte LMS and slightly stimulated extracellular lysozyme release, to a different extent at different times of the year. Moreover, bactericidal assays demonstrated the capacity of mussel hemolymph to cope with VA challenge, confirming previous data (Balbi et al., 2013), with hemocytes and HS acting in synergy as also reported by (Pezzati et al., 2015). A clear seasonality in bactericidal activity was observed under all three experimental conditions, starting from lowest values in the first three months of the year and progressively increasing to reach a maximum in October. However, such a trend was distinct from that observed with EC, suggesting a role not only for MgEP, but also other HS soluble factors (AMPs, hydrolytic enzymes) in the bactericidal activity towards VA.

Finally, the third bacterium tested was a *V. tasmaniensis* strain. *V. tasmaniens* belongs to *Splendidus* clade, which is commonly reported in association with hatchery or field bivalve mortality events (Travers et al., 2015). The strain utilised, *V. tasmaniensis* LGP32, was originally isolated from moribund *M. gigas* oysters (Gay et al., 2004). LGP32 has been described as a facultative intracellular pathogen of oyster immune cells: although the bacterium is recognized by oyster immune system, inducing antimicrobial defences based on AMPs, ROS and heavy metals (Rubio et al., 2019), inside the phagosome it is able to avoid acidic vacuole formation. In mussels, LGP32 shows a lower pathogenic potential and induces smaller hemocyte damage than in oysters (Balbi et al., 2013). Our results showed a seasonal variation

in the effects of VT on hemocyte LMS, with stronger effects from January to August followed by smaller lysosomal destabilization thereafter. LGP32 also stimulated lysozyme release. What is more, the bactericidal activity of hemocytes alone showed dramatic seasonal variations, from negligible values observed at the beginning of the year and in September, confirming previous data (Balbi et al., 2013), to peaks of about 100% killing in summer and autumn. In addition, the highest killing was recorded in HS, indicating the presence of specific soluble factors directed against VA. However, the bactericidal activity of HS was extremely low in January, February, at the peak of the gametogenic cycle, indicating strong seasonal variations.

Finally, it is worth to noting that hemocytes alone showed lowest bactericidal activities towards all bacteria in September. This reduction, not in line with the trends, may be partly ascribed to the high abundance of natural bacteria in hemolymph during this period, as described in the analysis of seasonal baseline immune parameters. Under these conditions, hemocytes could be unable to mount an efficient immune response to the additional *in vitro* challenge.

6. Conclusions and perspectives

- The results obtained on **natural fluctuations of functional immune parameters** further support the hypothesis that biotic factors (gametogenic stage) and related abiotic factors (i.e. temperature) can influence immune capacity of *M. galloprovincialis* of mussel hemolymph. In this light, increasing background knowledge on possible seasonal changes in immune defences of mussel populations (natural or farmed) utilized in laboratory trials can contribute to a better understanding of immune responses to different potential pathogens.

- Data from ***in vitro*** **short-term experiments with different bacteria** highlight clear species-specific differences in immune responses of *M. galloprovincialis* hemolymph towards different bacterial species and strains, confirming and extending previous data (Balbi et al., 2013; Canesi and Pruzzo, 2016, p. 201; Ciacci et al., 2017, 2010). Immune responses obtained in *in vitro* experiments can help understanding the interactions between each bacterium and hemolymph components; however, further *in vivo* studies carried out using mussels sampled at different times of the year are needed to evaluate the full immune responses to different bacteria.

- The results underline the **key role of mussel hemolymph serum** in bactericidal activity. These data indicate the presence, in the hemolymph of unstimulated mussels, the presence of soluble factors able to recognize and kill bacteria, with some degree of specificity, as evidenced by distinct seasonal killing patterns observed for each bacteria. These may include a number of different antibacterial peptides (AMPs), and hydrolytic enzymes other than lysozyme. Seasonal and year to year variations in expression of mussel AMP have been observed in *Mytilus* spp. (Li et al., 2010; Yang et al., 2022). However, knowledge on possible seasonal variations of hemolymph soluble components is still limited and deserves further investigation. Hemocyte samples have been collected in order to evaluate possible seasonal changes in immune gene expression.

The physiological health status of the animals, that can be influenced by biotic and environmental factors, appears to be fundamental for effective immune activation (Balbi et al., 2017; Hemraj and Russell, 2025; Sokolova, 2021). Given the specificity of mussel immune system towards different bacteria, and the seasonal variations in efficiency of the immune response, our data underline how studies on challenge with individual pathogenic or opportunistic bacteria should take into account the seasonal variations in immunocompetence for each mussel population (farmed or natural). This is the case for example of data obtained on VT LPG32: previous data showed that mussel hemocytes were unable to mount an efficient immune response against this strain (Balbi et al., 2013); however, the present results underline large seasonal variation in hemolymph bactericidal activity, from negligible values to almost 100% killing activity. In contrast, the results confirm the capacity of mussel hemolymph to cope with both EC and VA 01/032, although variable along the year.

The ability to cope with infection should be considered a multifactorial process (Bracchetti et al., 2024; Charles et al., 2020b), requiring the integration of multiple physiological and environmental aspects. For instance, the increased presence of natural bacteria in the hemolymph may be associated with site contamination linked to elevated water temperatures, which are known to favour bacteria proliferation (Baker-Austin et al., 2024). Moreover, our data point at a time window (Jan-Feb) of higher susceptibility of mussel hemolymph to bacterial challenge, independent of the type of bacteria, corresponding, in the mussel population studied, to the peak of the gametogenic cycle. This information has some relevance also in the light of the polymicrobial infections that occur in the natural environment.

Taken together, the results highlight how the immune function of mussel hemolymph can be influenced by multiple factors. The results further underline the complexity of host-pathogen

interactions and emphasize the need for further investigations into immune mechanisms towards different bacteria that can represent potential pathogenic or opportunistic species affecting mussel populations.

7. References

Auguste, M., Lasa, A., Balbi, T., Pallavicini, A., Vezzulli, L., Canesi, L., 2020. Impact of nanoplastics on hemolymph immune parameters and microbiota composition in Mytilus galloprovincialis. Mar. Environ. Res. 159, 105017. https://doi.org/10.1016/j.marenvres.2020.105017

Auguste, M., Lasa, A., Pallavicini, A., Gualdi, S., Vezzulli, L., Canesi, L., 2019. Exposure to TiO2 nanoparticles induces shifts in the microbiota composition of Mytilus galloprovincialis hemolymph. Sci. Total Environ. 670, 129–137. https://doi.org/10.1016/j.scitotenv.2019.03.133

Auguste, M., Leonessi, M., Balbi, T., Doni, L., Oliveri, C., Vezzulli, L., Canesi, L., 2024. Seasonal fluctuations of hemolymph microbiota and immune parameters in Mytilus galloprovincialis farmed at La Spezia, Italy. Aquaculture 578, 740028. https://doi.org/10.1016/j.aquaculture.2023.740028

Auguste, M., Rahman, F.U., Balbi, T., Leonessi, M., Oliveri, C., Bellese, G., Vezzulli, L., Furones, D., Canesi, L., 2022. Responses of Mytilus galloprovincialis to challenge with environmental isolates of the potential emerging pathogen Malaciobacter marinus. Fish Shellfish Immunol. 131, 1–9. https://doi.org/10.1016/j.fsi.2022.09.048

Baker-Austin, C., Lake, I., Archer, E., Hartnell, R., Trinanes, J., Martinez-Urtaza, J., 2024. Stemming the rising tide of Vibrio disease. Lancet Planet. Health 8, e515–e520. https://doi.org/10.1016/S2542-5196(24)00124-4

Balbi, T., Fabbri, R., Cortese, K., Smerilli, A., Ciacci, C., Grande, C., Vezzulli, L., Pruzzo, C., Canesi, L., 2013. Interactions between Mytilus galloprovincialis hemocytes and the bivalve pathogens Vibrio aestuarianus 01/032 and Vibrio splendidus LGP32. Fish Shellfish Immunol. 35, 1906–1915. https://doi.org/10.1016/j.fsi.2013.09.027

Balbi, T., Fabbri, R., Montagna, M., Camisassi, G., Canesi, L., 2017. Seasonal variability of different biomarkers in mussels (Mytilus galloprovincialis) farmed at different sites of the Gulf of La Spezia, Ligurian sea, Italy. Mar. Pollut. Bull. 116, 348–356. https://doi.org/10.1016/j.marpolbul.2017.01.035

Bosi, E., Taviani, E., Avesani, A., Doni, L., Auguste, M., Oliveri, C., Leonessi, M., Martinez-Urtaza, J., Vetriani, C., Vezzulli, L., 2024. Pan-Genome Provides Insights into *Vibrio* Evolution and Adaptation to Deep-Sea Hydrothermal Vents. Genome Biol. Evol. 16, evae131. https://doi.org/10.1093/gbe/evae131

Bracchetti, L., Capriotti, M., Fazzini, M., Cocci, P., Palermo, F.A., 2024. Mass Mortality Event of Mediterranean Mussels (Mytilus galloprovincialis) in the Middle Adriatic: Potential Implications of the Climate Crisis for Marine Ecosystems. Diversity 16, 130. https://doi.org/10.3390/d16030130

Canesi, L., Gallo, G., Gavioli, M., Pruzzo, C., 2002. Bacteria–hemocyte interactions and phagocytosis in marine bivalves. Microsc. Res. Tech. 57, 469–476. https://doi.org/10.1002/jemt.10100

Canesi, L., Grande, C., Pezzati, E., Balbi, T., Vezzulli, L., Pruzzo, C., 2016. Killing of Vibrio cholerae and Escherichia coli Strains Carrying D-mannose-sensitive Ligands by Mytilus Hemocytes is Promoted by a Multifunctional Hemolymph Serum Protein. Microb. Ecol. 72, 759–762. https://doi.org/10.1007/s00248-016-0757-1

Canesi, L., Pruzzo, C., 2016. Chapter 6 - Specificity of Innate Immunity in Bivalves: A Lesson From Bacteria, in: Ballarin, L., Cammarata, M. (Eds.), Lessons in Immunity. Academic Press, pp. 79–91. https://doi.org/10.1016/B978-0-12-803252-7.00006-0

Capelle, J.J., Garcia, A.B., Kamermans, P., Engelsma, M.Y., Jansen, H.M., 2021. Observations on recent mass mortality events of marine mussels in the Oosterschelde, the Netherlands.
Aquac. Int. 29, 1737–1751. https://doi.org/10.1007/s10499-021-00713-6

Charles, M., Bernard, I., Villalba, A., Oden, E., Burioli, E.A.V., Allain, G., Trancart, S., Bouchart, V., Houssin, M., 2020a. High mortality of mussels in northern Brittany – Evaluation of the involvement of pathogens, pathological conditions and pollutants. J. Invertebr. Pathol. 170, 107308. https://doi.org/10.1016/j.jip.2019.107308

Charles, M., Trancart, S., Oden, E., Houssin, M., 2020b. Experimental infection of *Mytilus edulis* by two *Vibrio splendidus* -related strains: Determination of pathogenicity level of strains and influence of the origin and annual cycle of mussels on their sensitivity. J. Fish Dis. 43, 9–21. https://doi.org/10.1111/jfd.13094

Ciacci, C., Betti, M., Canonico, B., Citterio, B., Roch, P., Canesi, L., 2010. Specificity of anti-Vibrio immune response through p38 MAPK and PKC activation in the hemocytes of the mussel Mytilus galloprovincialis. J. Invertebr. Pathol. 105, 49–55. https://doi.org/10.1016/j.jip.2010.05.010

Ciacci, C., Manti, A., Canonico, B., Campana, R., Camisassi, G., Baffone, W., Canesi, L., 2017. Responses of Mytilus galloprovincialis hemocytes to environmental strains of Vibrio parahaemolyticus, Vibrio alginolyticus, Vibrio vulnificus. Fish Shellfish Immunol. 65, 80–87. https://doi.org/10.1016/j.fsi.2017.04.002

Cohen, R., James, C., Lee, A., Martinelli, M., Muraoka, W., Ortega, M., Sadowski, R., Starkey, L., Szesciorka, A., Timko, S., Weiss, E., Franks, P., 2018. Marine Host-Pathogen Dynamics: Influences of Global Climate Change. Oceanography 31. https://doi.org/10.5670/oceanog.2018.201

Dagnino, A., Allen, J.I., Moore, M.N., Broeg, K., Canesi, L., Viarengo, A., 2007. Development of an expert system for the integration of biomarker responses in mussels into an animal health index. Biomarkers 12, 155–172. https://doi.org/10.1080/13547500601037171

FAO (Ed.), 2018. Meeting the sustainable development goals, The state of world fisheries and aquaculture. Rome.

Fearman, J., Moltschaniwskyj, N.A., 2010. Warmer temperatures reduce rates of gametogenesis in temperate mussels, Mytilus galloprovincialis. Aquaculture 305, 20–25. https://doi.org/10.1016/j.aquaculture.2010.04.003

Garnier, M., Labreuche, Y., Garcia, C., Robert, M., Nicolas, J.-L., 2007. Evidence for the Involvement of Pathogenic Bacteria in Summer Mortalities of the Pacific Oyster Crassostrea gigas. Microb. Ecol. 53, 187–196. https://doi.org/10.1007/s00248-006-9061-9

Garnier, M., Labreuche, Y., Nicolas, J.-L., 2008. Molecular and phenotypic characterization of Vibrio aestuarianus subsp. francensis subsp. nov., a pathogen of the oyster Crassostrea gigas. Syst. Appl. Microbiol. 31, 358–365. https://doi.org/10.1016/j.syapm.2008.06.003

Gay, M., Berthe, F., Le Roux, F., 2004. Screening of Vibrio isolates to develop an experimental infection model in the Pacific oyster Crassostrea gigas. Dis. Aquat. Organ. 59, 49–56. https://doi.org/10.3354/dao059049

Hemraj, D.A., Russell, B.D., 2025. Consistency in marine heatwave experiments for ecological relevance and application: Key problems and solutions. Limnol. Oceanogr. Lett. 10, 1–4. https://doi.org/10.1002/lol2.10418

Labreuche, Y., Le Roux, F., Henry, J., Zatylny, C., Huvet, A., Lambert, C., Soudant, P., Mazel, D., Nicolas, J.-L., 2010. Vibrio aestuarianus zinc metalloprotease causes lethality in the Pacific oyster Crassostrea gigas and impairs the host cellular immune defenses. Fish Shellfish Immunol. 29, 753–758. https://doi.org/10.1016/j.fsi.2010.07.007

Labreuche, Y., Soudant, P., Goncalves, M., Lambert, C., Nicolas, J., 2006. Effects of extracellular products from the pathogenic Vibrio aestuarianus strain 01/32 on lethality and cellular immune responses of the oyster Crassostrea gigas. Dev. Comp. Immunol. 30, 367–379. https://doi.org/10.1016/j.dci.2005.05.003

Lattos, A., Papadopoulos, D.K., Feidantsis, K., Karagiannis, D., Giantsis, I.A., Michaelidis, B., 2022. Are Marine Heatwaves Responsible for Mortalities of Farmed Mytilus galloprovincialis? A Pathophysiological Analysis of Marteilia Infected Mussels from Thermaikos Gulf, Greece. Animals 12, 2805. https://doi.org/10.3390/ani12202805

Li, H., Venier, P., Prado-Alvárez, M., Gestal, C., Toubiana, M., Quartesan, R., Borghesan, F., Novoa, B., Figueras, A., Roch, P., 2010. Expression of Mytilus immune genes in response to experimental challenges varied according to the site of collection. Fish Shellfish Immunol. 28, 640–648. https://doi.org/10.1016/j.fsi.2009.12.022

Lupo, C., Bougeard, S., Le Bihan, V., Blin, J.L., Allain, G., Azéma, P., Benoit, F., Béchemin, C., Bernard, I., Blachier, P., Brieau, L., Danion, M., Garcia, A., Gervasoni, E., Glize, P., Lainé, A., Lapègue, S., Mablouké, C., Poirier, L., Raymond, J.C., Treilles, M., Chauvin, C., Le Bouquin, S., 2021. Mortality of marine mussels *Mytilus edulis* and *M. galloprovincialis* : systematic literature review of risk factors and recommendations for future research. Rev. Aquac. 13, 504–536. https://doi.org/10.1111/raq.12484

Mandic, M., Gvozdenović Nikolić, S., Kokić, I., Jokanović, S., 2024. Mass mortality of farmed mussels – a phenomenon without explanation? https://doi.org/10.5281/ZENODO.12749090

OSPAR Commission, 2013. Background documents and technical annexes for biological effects monitoring. p. 239.

Pezzati, E., Canesi, L., Damonte, G., Salis, A., Marsano, F., Grande, C., Vezzulli, L., Pruzzo, C., 2015. Susceptibility of *V ibrio aestuarianu* s 01/032 to the antibacterial activity of *M ytilus* haemolymph: identification of a serum opsonin involved in mannose-sensitive
interactions. Environ. Microbiol. 17, 4271–4279. https://doi.org/10.1111/1462-2920.12750

Rubio, T., Oyanedel, D., Labreuche, Y., Toulza, E., Luo, X., Bruto, M., Chaparro, C., Torres, M., De Lorgeril, J., Haffner, P., Vidal-Dupiol, J., Lagorce, A., Petton, B., Mitta, G., Jacq, A., Le Roux, F., Charrière, G.M., Destoumieux-Garzón, D., 2019. Species-specific mechanisms of cytotoxicity toward immune cells determine the successful outcome of *Vibrio* infections.
Proc. Natl. Acad. Sci. 116, 14238–14247. https://doi.org/10.1073/pnas.1905747116

Smaal, A.C., Ferreira, J.G., Grant, J., Petersen, J.K., Strand, Ø. (Eds.), 2019. Goods and Services of Marine Bivalves. Springer International Publishing, Cham. https://doi.org/10.1007/978-3- 319-96776-9

Sokolova, I., 2021. Bioenergetics in environmental adaptation and stress tolerance of aquatic ectotherms: linking physiology and ecology in a multi-stressor landscape. J. Exp. Biol. 224, jeb236802. https://doi.org/10.1242/jeb.236802

Travers, M.-A., Boettcher Miller, K., Roque, A., Friedman, C.S., 2015. Bacterial diseases in marine bivalves. J. Invertebr. Pathol. 131, 11–31. https://doi.org/10.1016/j.jip.2015.07.010

Viarengo, A., Lowe, D., Bolognesi, C., Fabbri, E., Koehler, A., 2007. The use of biomarkers in biomonitoring: A 2-tier approach assessing the level of pollutant-induced stress syndrome in sentinel organisms. Comp. Biochem. Physiol. Part C Toxicol. Pharmacol. 146, 281–300. https://doi.org/10.1016/j.cbpc.2007.04.011

Wernberg, T., Thomsen, M.S., Baum, J.K., Bishop, M.J., Bruno, J.F., Coleman, M.A., Filbee-Dexter, K., Gagnon, K., He, Q., Murdiyarso, D., Rogers, K., Silliman, B.R., Smale, D.A., Starko, S., Vanderklift, M.A., 2024. Impacts of Climate Change on Marine Foundation Species. Annu. Rev. Mar. Sci. 16, 247–282. https://doi.org/10.1146/annurev-marine-042023- 093037

Yang, J., He, J., Liu, L., He, M., Zhang, X., Buttino, I., Guo, B., Yan, X., Liao, Z., 2022. Expression profiles of antimicrobial peptides in Mytilus coruscus. Aquaculture 548, 737709. https://doi.org/10.1016/j.aquaculture.2021.737709

Supplementary

Material Results

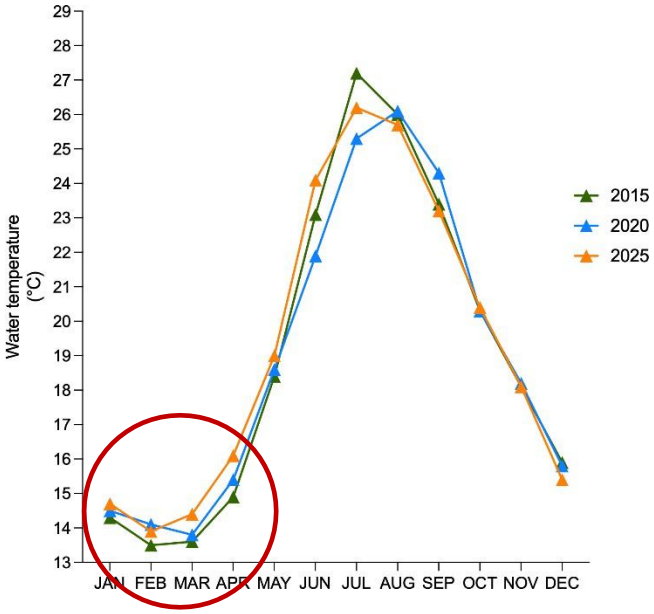

Figure S1: Seasonal trends in surface seawater temperatures at the Gulf of La Spezia, Italy from 2015 to 2025 (https://www.arpal.liguria.it/). Note the slight increases observed in 2025 with respect to the previous years in Feb-April (red circle).

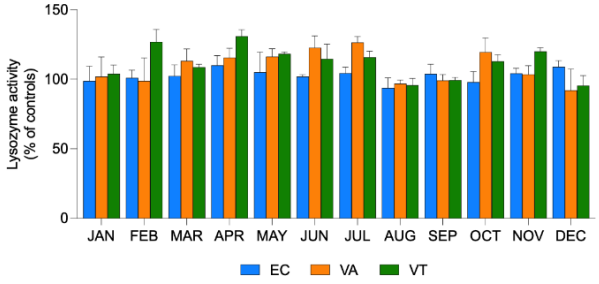

Figure S2: *in vitro* effects of EC, VA and VT on extracellular lysozyme release. Lysozyme activity was evaluated after incubation with EC, VA or VT at 5 x 10^6 CFU/mL in ASW. Data are expressed as mean ± sd of 3 technical replicates.

Conclusions and Perspectives

The main outcomes of the present thesis and conclusive points could be summarized as follows. **Health of farmed bivalves in a global change scenario: immune responses of *Mytilus galloprovincialis* to potential bacterial pathogens.**

The results reported in **Chapters 1- 3** are focused on the oyster larval pathogen *V. ostreicida*. From the first isolation and characterization of *V. ostreicida* strains from samples of cultivated *M. galloprovincialis* during a mortality event, the interactions between *V. ostreicida* and mussel and oyster (*Magallana gigas*) hemolymph were first investigated in *in vitro* studies. The results underlined differences in immune responses towards *V. ostreicida* between mussels and oysters, with the hemolymph serum of mussels playing a key role in immune defences and bactericidal activity, indicating species-specific interactions. Subsequent *in vivo* studies of mussel infection indicated partial horizontal transfer of *V. ostreicida* from infected to un-infects individuals, as well as bacterial uptake from the water. However, *V. ostreicida* induced transient stressful conditions and hemolymph responses in mussels. Overall, the results represent the first data on interactions between *V. ostreicida* isolates and *M. galloprovincialis*, indicating that mussels are able to cope with challenge with this Vibrio species, that appears to be moderately pathogenic to adult mussels under the established experimental conditions.

In **Chapter 4** data are reported on immune responses of mussels to polymicrobial infections, using two bacterial strains isolated from an oyster mortality event: *Vibrio aestuarianus* 106 (Va) and *Malaciobacter marinus* R1 (Mm). The results of single infection with either bacterium show species- specific interactions manner with the mussel immune system. Both in vivo/in vitro and in vivo/in vivo cross-infections were then performed to determine whether prior exposure to either isolate could influence immune responses to subsequent challenge with the other. The results demonstrate that first infection with Va weakened mussel immune defences, thus favoring the subsequent opportunistic behaviour of Mm and not vice versa. Moreover*, in vivo/in vivo* cross-infections indicate the existence of a potential temporal window during which an opportunistic pathogen may exploit the mussel compromised condition characterized by high stress and lack of immune activation, to proliferate and invade the host, leading to potential risk of disease. The results underline the specificity of mussel immune responses to different potentially pathogenic or opportunistic bacteria, and the need of further studies on polymicrobial infections.

In **Chapter 5** data are reported on seasonal variations of functional immune parameters in mussel hemolymph during a 12 months period, and their responses to *in vitro* challenge with different bacteria. The results show specific and season-related trends in immune responses

towards different bacterial species, and underline the key role of soluble hemolymph components in bactericidal activity. Moreover, the results support the hypothesis that the physiological health status of the animals, that can be influenced by multiple biotic and abiotic factors, is fundamental for effective immune activation. In order to better identify potential time windows of higher susceptibility to bacterial infection, *in vivo* studies are in progress to evaluate seasonal changes in immunocompetence to different potential pathogens.

Overall, these data highlight the complexity of interactions between the mussel immune system and bacteria and the numerous variables that can influence their outcome. The results point at the need for further studies on polymicrobial infections and on identification of periods of higher susceptibility of the mussel host, potentially leading to disease. Moreover, due to the close relationship between immune effectors and the microbiome, further studies are needed on possible changes in composition and dynamics of the hemolymph microbiota after infection with different environmental isolates from bivalve mortality episodes. This information would help understanding, and eventually predicting the occurrence and development of diseases.
This is of particular importance in the light of ongoing global changes in the oceans, where environmental variables may strongly affect mussel health status and consequent immune responses.

SECTION II

Monitoring growth and physiological conditions of fish from an offshore farm in the Ligurian Sea using a multibiomarker approach

Introduction

1. Marine fish aquaculture

In 2022, global production of marine and coastal aquaculture reached 35.3 million tonnes. Consumer demand is expected to double by 2030, representing a major challenge to the aquaculture industry (FAO, 2024). In Europe, marine finfish represent 21% of the total volume (267.000 tonnes) and the 41% of the production value (€ 1.76 billion) (European Commission. Joint Research Centre. and Scientific, Technical and Economic Committee for Fisheries., 2025a).

Inevitably, concerns about environmental sustainability and animal welfare in fish aquaculture, raised 20 years ago, are increasing nowadays (Alfonso et al., 2023). Offshore mariculture is emerging as a promising solution to reconcile high production demands with sustainability goals (Brian Austin et al., 2022). In offshore facilities, cages are located in deep and open waters, in less sheltered sites with stronger sea currents. These conditions, designed to produce large volumes of fish, allow better water quality and oxygen supply, and at the same time, help reducing the environmental impacts (Buck et al., 2018; Giangrande et al., 2021; Naylor et al., 2021). In this context, it is fundamental to assess strategies that could combine environmental sustainability in offshore aquaculture with the welfare of farmed fish (Alfonso et al., 2023; Gentry et al., 2017).

The gilthead seabream *Sparus aurata* (L. 1758), is one of the most intensively cultured species in the Mediterranean Sea and the most important in terms of production volume (Llorente et al., 2020) reaching a total of 103,130 metric tons (about 286 million) and a value of € 537 million (data related to EU27 in APROMAR - the Spanish Aquaculture Business Association, 2023) in 2022. These figures remained stable in 2023 and 2024 (European Commission. Joint Research Centre. and Scientific, Technical and Economic Committee for Fisheries., 2025b). The seabream sector has achieved stability in terms of annual production volumes over the past five years: Italy is the fourth and third EU producer of adult and juvenile seabream, respectively (FEAM report 2025), with the offshore cages segment showing resilience in profitability, driven by significant cost reductions and investments in productivity, compared to the tanks and race-ways segment. In the Italian marine aquaculture sector, seabream is generally farmed together with the European seabass *Dicentrarchus labrax*, with different production volumes, depending on the specific farm. Seabass EU catches have experienced a strong downward trend (- 42%) over the past decade (2013-2022). The main reason for this strong drop is the decline of seabass natural resource, especially in the northern Atlantic, due to an increase in fishing pressure, this trend favoring aquaculture production (EUMOFA. and

European Commission. Directorate General for Maritime Affairs and Fisheries., 2024). Indeed, the total aquaculture production of seabass *D. labrax* in Europe in 2021 was 97,137 tonnes, the highest ever recorded (+ 54% compared to 2012)(EUMOFA. and European Commission. Directorate General for Maritime Affairs and Fisheries., 2024).

The high demand and profitability of *S. aurata* and *D. labrax* underline the importance of early monitoring of their health status, for ensuring high productivity, minimizing disease outbreaks, and maintaining environmental sustainability. However, evaluating the welfare of commercially-reared fish remains challenging due to the influence of farming conditions (Bordignon et al., 2025). Roque et al., 2020 identified 4 key categories of welfare indicators: good feeding, good housing, good health and appropriate indicators. Within each category, different welfare measures are identified and classified based on their scope as: animal-based, management-based and environment-based. The animal-based indicators specifically assess the health status and growth of farmed fish. However, their use remains limited: in this light, EFSA's vision is to develop new methodologies (quantitative and qualitative) for assessing animal welfare of food-producing animals across EU by 2027 and to start collecting standardized and good quality data to assess animal welfare by 2030 (Paulović et al., 2024). A list of the main indicators of fish health is provided in Tab. 1.

Table 1 – Overview of the grouped indicators for evaluating farmed fish health (adapted from (Paulović et al., 2024).

Domain	Grouped indicator	Description	Link to welfare consequences
Environment	*Physical water quality*	All indicators of physical quality, measured on the water itself (e.g. ammonia, oxygen, nitrate	Sensory under and/or over stimulation
	Water quality, animal-based	Animal-based indicators of water quality such as gulping, surface behaviour, standingat inlet	Sensory under and/or over stimulation
	Restriction of movement	Number of fish per tank, etc.	Restriction of movement
Health	*Soft tissue and integument damage*	Discoloration, haemorrhages, lesions, wounds	Soft tissue and integument damage
	Fin condition	Damaged or injured fins (all fins)	Soft tissue and integument damage
	Gill condition	Damaged or injured gills, pathogens, lamellae	Soft tissue and integument damage
	Deformities	Spina, jaw, gill cover deformation	
	Mortality	Mortality documentation, dead fish	
Mental state	*Cortisol*	Measured in blood, scales, etc.	
Nutrition	*Body condition*	Emaciation, length, weight, growth	Prolonged hunger
	Feed intake/appetite	Feed intake and appetite	Prolonged hunger

However, their use remains limited: in this light, EFSA's vision is to develop new methodologies (quantitative and qualitative) for assessing animal welfare of food-producing animals across EU by 2027 and to start collecting standardized and good quality data to assess animal welfare by 2030 (Paulović et al., 2024). Thus, in 2022, EFSA identified the need to develop an action Roadmap for the *More Welfare project: towards new risk assessment methodologies and harmonized animal welfare data in the EU* (Paulović et al., 2024). The general objective is to map existing animal welfare assessment methods, tools, and data collection activities for different species of food-producing animals. The roadmap aims to identify data and knowledge gaps as well as challenges towards research areas that require further development (i.e., working areas), but also highlights collaboration opportunities and priority strategies (actions and project proposals) necessary for achieving EFSA's vision. In this broader context, the focus of the roadmap is given to on-farm welfare assessment of selected animal species: among finfish, salmon, trout, carp, seabream, tuna.

In this light, the application of other, more sensitive indicators represents a step forward in monitoring health and welfare of most common farmed fish. This is of particular importance for marine species, that represent a large sector in European aquaculture.

Biomarkers are biological parameters measured from molecular to organism level utilized in marine biomonitoring programs (OSPAR) that, by providing sensitive, quantitative, early-warning indicators of physiological stress and environmental impacts, can reveal the health status of individuals before visible symptoms appear. Biomarkers can be classified as general and specific: general biomarkers (stress biomarkers) are all those responses of an organism to different types of environmental stress; specific biomarkers (biomarkers of exposure) are the molecular and biochemical responses detectable in organisms as a consequence of exposure to a particular agent or class of contaminants. Biomarkers are essential tools in monitoring and protecting marine ecosystems (OSPAR), whose application practices are being extended to the Mediterranean region, thus enhancing the ability to assess and manage the health of Mediterranean species, including fish and invertebrates (unep). Despite the biomarker approach has long been utilized worldwide in biomonitoring the health status of fish in different environmental conditions, it has been less frequently applied to the aquaculture sector (Oliveira et al., 2024).

Composition of the gut microbiome is another parameter closely related to fish health (Hoseinifar et al., 2018; Oliveira et al., 2024; Perry et al., 2020; Quero et al., 2023). The gut

commensal microbiota, in addition to protect the host against pathogenic bacteria invasion, are able to modulate many processes involved in health status, such as the stimulation of epithelial proliferation, nutrient metabolism, and innate immune responses, promoting intestinal homeostasis. Then, any interference on the microbiota composition may impair gut condition and health, leading to disease-related dysbiosis (Firmino et al., 2019). At present, most of available data on the health status of aquacultured fish, including seabream and seabass, come from feeding trials and are generally related to growth, immune response, and resistance to disease (Alfonso et al., 2023; Fontinha et al., 2021; Hoseinifar et al., 2018; Naya-Català et al., 2021; Orduna et al., 2023; Parma et al., 2016; Tarricone et al., 2024). While a large amount of knowledge is available on growth performance and physiological indicators in adult gilthead seabream and European seabass reared in different experimental conditions (different diets, temperature, salinity) (Kousoulaki et al., 2015; Mhalhel et al., 2023), no data are available on the application of monitoring programs of fish throughout the production cycle in offshore farms.

2. The models:

2.1 *Sparus aurata*

Sparus aurata (Linnaeus, 1758) is a teleost fish belonging to the family Sparidae, order Perciformes, class Actinopterygii (Moretti et al., 1999).

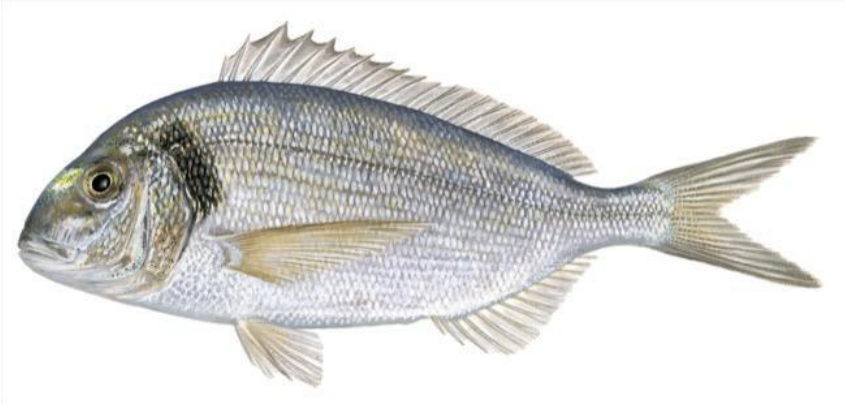

Figure 1: *Sparus aurata* (Linneaeus, 1758)

The species name refers to the silver-gray coloration of the body, characterized by a distinctive black spot that covers the upper part of the opercular bone, and by a golden band between the eyes. The dorsal fin is gray-blue and comprises 11 rigid rays and 13 soft rays. The pectoral fins are long and pointed, whereas the pelvic fins are shorter. The grey-greenish caudal fin has

pointed and lobed extremities bordered in black (Moretti et al., 1999). The body has an oval shape, very high and laterally compressed. The eyes are relatively small, and the mouth is positioned low and slightly oblique, with thick lips. The cheeks are covered with scales, whereas the preopercular bone lacks squamation. The lower jaw is shorter than the upper jaw; both jaws have anterior caniniform teeth (4–6), followed posteriorly by 3–5 rows of blunt molariform teeth. The teeth of the outer rows are particularly robust and are adapted for destroying shells and crustacean carapaces. Indeed, *S. aurata* is predominantly carnivorous, although occasional herbivore behaviors have been reported; its diet consists mainly of mollusks, crustaceans, worms, and holothurians. The morphology of the buccal apparatus therefore closely reflects its feeding ecology (Bertolino and Ferranti, 2018; Sola, 2007). The buccal cavity is followed by the esophagus, which exhibits a stratified mucosa composed of epithelial and mucous cells in the proximal portion, and regions of single epithelium in the distal portion. The esophagus enters the Y-shaped stomach. The beginning of the intestine is marked by four short pyloric caeca, at the base of which the ductus hepaticus and the ductus pancreaticus discharge. The stomach is composed by a single columnar epithelium underlain by gastric glands. The intestine is relatively short and simple, a typical feature of carnivorous species (in contrast to the longer and more convoluted intestine of herbivorous fishes adapted for the digestion of starch and cellulose); the intestinal epithelium consists of columnar cells and mucous cells (Cataldi et al., 1987). The digestive enzymes of *S. aurata* include trypsin, chymotrypsin, amylase, carboxypeptidase and pepsin. Except for pepsin, which is localized in the stomach, these enzymes do not show a strict regional localization. This suggests that digestive processes are not restricted to a single region of the gastrointestinal tract but are spatially distributed, with pancreatic secretions supplying enzymes to multiple intestinal sections (Deguara et al., 2003). Enzymatic activity is strongly influenced by pH, as each enzyme exhibits a specific optimal pH range; deviations from these values can markedly reduce enzymatic efficiency (Deguara et al., 2003). Several authors have proposed that this diffuse enzymatic distribution represents an adaptive response to the variable diet encountered in natural environments, allowing for a flexible digestive strategy in which different nutrients are progressively digested as they transit through the intestine (Deguara et al., 2003).

Sparus aurata is widely distributed throughout the Mediterranean Sea, the northeastern Atlantic Ocean, and the Black Sea. As an euryhaline species, it performs seasonal migrations to and from coastal brackish lagoons and estuarine environments for feeding and reproduction (Franchini et al., 2012). Additional migratory movements have been documented along the eastern Atlantic coastline, from the Iberian Peninsula to the British Isles (Sola, 2007). *S. aurata*

is a benthopelagic species and is usually found on rocky and seaweed bottoms, although it is also frequently caught on sandy grounds. It is most abundant in coastal areas and exhibits sedentary and demersal behavior. Individuals are generally solitary but may form small aggregations. Juveniles typically occur at shallow depths (approximately 30–40 m), whereas adults may reach depths of up to 150 m (Sola, 2007).

Gilthead seabream is a protandrous hermaphrodite. Individuals initially develop as functional males during the first two years of life and subsequently undergo sex reversal to females when reaching body lengths of about 30 cm (Moretti et al., 1999). Males reach sexual maturity at approximately 1– 2 years old (20–30 cm total length), whereas females mature at 2–3 years (33–40 cm). During the spawning season, which extends from October to December, females release between 20,000 and 80,000 eggs per day (Sola, 2007). The eggs are spherical and transparent, with a diameter slightly less than 1 mm (Moretti et al., 1999). The planktonic larval stage occurs in waters with temperatures ranging from 17 to 18 °C and may last approximately 50 days (Sola, 2007). Fry live in offshore waters during winter and migrate to shallower, warmer coastal habitats in early spring, where food availability is higher. Juveniles are highly sensitive to low temperatures and therefore return to offshore waters in late autumn, coinciding with the reproductive period of adults (Moretti et al., 1999).

2.3 *Dicentrarchus labrax*

Dicentrarchus labrax (Linnaeus, 1758) is the European seabass belonging to the family Moronidae, order Perciformes, class Actinopterygii (Moretti et al., 1999).

Figure 2: *Dicentrarchus labrax* (Linnaeus, 1758)

The species has an elongated body, dark grey on the dorsal part, gradually fading to a silver colour in the ventral region. Marine specimens display a much paler coloration compared to

individuals inhabiting estuarine environments. Juveniles exhibit a livery characterized by small dark spots on the anterior part of the body or on the head, which disappear with age. A characteristic dark spot remains on the operculum, which also bears two robust spines directed posteriorly. The lateral line is clearly visible but does not extend onto the caudal fin (Bertolino and Ferranti, 2018). The two dorsal fins are separated: the first has 8–10 spiny rays, while the second has 12–13 rays, of which only the first is spiny. The anal fin has 3 spiny rays and 10–12 soft rays, and the caudal fin is bilobed with a broad caudal peduncle (Bertolino and Ferranti, 2018; Moretti et al., 1999). Overall, *D. labrax* is a medium- sized fish, reaching commonly about 50 cm in length, although it can grow up to 1 m and attain a maximum weight of approximately 12 kg.

The snout is pointed, with a large, slightly protrusible mouth and numerous teeth on the jaws and vomer, but lacking caniniform teeth. Like the gilthead seabream, the European seabass is a carnivorous species, and its buccal apparatus and digestive system reflect its diet. It feeds on small fish and a wide variety of invertebrates. Feeding behavior is size-dependent: juveniles eat mainly crustaceans and small fish (approximately one quarter of the diet), whereas adults larger than 20 cm also include shrimps and crabs in their diet (IUCN, 2008; Moretti et al., 1999). The digestive system has the same general structure described for *S. aurata*, and the liver and gills remain the most sensitive tissues to external environmental variations. Intestinal pH depends on dietary composition and consequently influences enzymatic activities, which vary according to the type of food ingested.

The European seabass is distributed in the eastern Atlantic Ocean (from Norway to Morocco, including the Canary Islands and Senegal), as well as in the Mediterranean Sea and the Black Sea, but is absent from the Barents, Baltic, and Caspian seas (IUCN, 2008). *D. labrax* is a gregarious, eurythermal, and euryhaline species, with limited territoriality associated with feeding and reproduction. It is more tolerant to salinity fluctuations and less sensitive to low temperatures than gilthead seabream. Consequently, it inhabits both marine and brackish environments, such as coastal lagoons and sandy estuarine areas (usually during winter), and occasionally ascend river courses. During the early stages of its life cycle, it exhibits behavior similar to *S. aurata* (Frimodt, 1995 in Kousoulaki et al., 2015).

The European seabass is a gonochoric species with separate sexes. Females exhibit a deeper body and a longer, more pointed head. Gonadal maturation and reproduction require specific environmental conditions (temperature, photoperiod, and salinity), which determine variations in the spawning period. The eggs are pelagic, float due to the presence of an oil droplet, hatch

after approximately three days, and are followed by a larval development lasting about 40 days (Moretti et al., 1999). After spawning, the eggs develop their characteristic spherical shape, with size varying according to latitude (Moretti et al., 1999). Eggs and larvae show a high dispersal capacity during the first three months of life, and adults are capable of migrating over several hundred kilometres (Froese, 2006). Sexual maturity in males is reached at approximately 1–2 years, whereas females mature later, at around 3–5 years old. Females spawn once per year, during winter in the Mediterranean Sea (from December to March), and up to June in Atlantic populations. Fecundity is high, and reproduction generally begins when individuals exceed a body weight of 2 kg (Froese, 2006).

References

Alfonso, S., Mente, E., Fiocchi, E., Manfrin, A., Dimitroglou, A., Papaharisis, L., Barkas, D., Toomey, L., Boscarato, M., Losasso, C., Peruzzo, A., Stefani, A., Zupa, W., Spedicato, M.T., Nengas, I., Lembo, G., Carbonara, P., 2023. Growth performance, gut microbiota composition, health and welfare of European sea bass (Dicentrarchus labrax) fed an environmentally and economically sustainable low marine protein diet in sea cages. Sci. Rep. 13, 21269. https://doi.org/10.1038/s41598-023-48533-3

APROMAR - the Spanish Aquaculture Business Association, 2023. Aquaculture in Spain.

Bertolino, M., Ferranti, M.P., 2018. PINNEGGIANDO NEI MARI ITALIANI – Atlante della flora e della fauna. HOEPLI.

Bordignon, F., Ferrarese, L., Solimeo, A., Di Leva, V., Trocino, A., 2025. Animal-based measures for operational welfare indicators at wholesale level in gilthead seabream (Sparus aurata) reared in the Mediterranean Sea. Aquaculture 603, 742417. https://doi.org/10.1016/j.aquaculture.2025.742417

Brian Austin, Addison Lee Lawrence, Erkan Can, Cristian Carboni, Jack Crockett, Nida Demirtaş Erol, Delano Dias Schleder, Jatobá, A., Sevki Kayis, Ulviye Karacalar, Volkan Kizak, Aysun Kop, Kim Thompson, Carlos Andres Mendez Ruiz, Osman Serdar, Şafak Seyhaneyildiz Can, Steve Watts, Güzel Yücel Gier, 2022. Selected topics in sustainable aquaculture research: Current and future focus. https://doi.org/10.5281/ZENODO.7032804

Buck, B.H., Troell, M.F., Krause, G., Angel, D.L., Grote, B., Chopin, T., 2018. State of the Art and Challenges for Offshore Integrated Multi-Trophic Aquaculture (IMTA). Front. Mar. Sci. 5,165. https://doi.org/10.3389/fmars.2018.00165

Cataldi, E., Cataudella, S., Monaco, G., Rossi, A., Tancioni, L., 1987. A study of the histology and morphology of the digestive tract of the sea-bream, *Sparus aurata*. J. Fish Biol. 30, 135–145. https://doi.org/10.1111/j.1095-8649.1987.tb05740.x

Deguara, S., Jauncey, K., Agius, C., 2003. Enzyme activities and pH variations in the digestive tract of gilthead sea bream. J. Fish Biol. 62, 1033–1043. https://doi.org/10.1046/j.1095-8649.2003.00094.x

EUMOFA., European Commission. Directorate General for Maritime Affairs and Fisheries., 2024. Study on the challenges of aquaculture products in food outlets. Publications Office, LU.

European Commission. Joint Research Centre., Scientific, Technical and Economic Committee for Fisheries., 2025a. The 2024 aquaculture economic report (STECF 24-14). Publications Office, LU.

European Commission. Joint Research Centre., Scientific, Technical and Economic Committee for Fisheries., 2025b. The 2024 aquaculture economic report (STECF 24-14). Publications Office, LU.

FAO, 2024. The State of World Fisheries and Aquaculture 2024. FAO. https://doi.org/10.4060/cd0683en

Firmino, J., Furones, M.D., Andree, K.B., Sarasquete, C., Ortiz-Delgado, J.B., Asencio-Alcudia, G., Gisbert, E., 2019. Contrasting outcomes of Vibrio harveyi pathogenicity in gilthead seabream, Sparus aurata and European seabass, Dicentrachus labrax. Aquaculture 511, 734210. https://doi.org/10.1016/j.aquaculture.2019.734210

Fontinha, F., Magalhães, R., Moutinho, S., Santos, R., Campos, P., Serra, C.R., Aires, T., Oliva- Teles, A., Peres, H., 2021. Effect of dietary poultry meal and oil on growth, digestive capacity, and gut microbiota of gilthead seabream (Sparus aurata) juveniles. Aquaculture 530, 735879. https://doi.org/10.1016/j.aquaculture.2020.735879

Franchini, P., Sola, L., Crosetti, D., Milana, V., Rossi, A.R., 2012. Low levels of population genetic structure in the gilthead sea bream, Sparus aurata, along the coast of Italy. ICES J. Mar. Sci. 69, 41–50. https://doi.org/10.1093/icesjms/fsr175

Froese, R., 2006. Cube law, condition factor and weight-length relationships: history, meta-analysis and recommendations. J. Appl. Ichthyol. 22, 241–253. https://doi.org/10.1111/j.1439- 0426.2006.00805.x

Gentry, R.R., Lester, S.E., Kappel, C.V., White, C., Bell, T.W., Stevens, J., Gaines, S.D., 2017. Offshore aquaculture: Spatial planning principles for sustainable development. Ecol. Evol. 7, 733–743. https://doi.org/10.1002/ece3.2637

Giangrande, A., Gravina, M.F., Rossi, S., Longo, C., Pierri, C., 2021. Aquaculture and Restoration: Perspectives from Mediterranean Sea Experiences. Water 13, 991. https://doi.org/10.3390/w13070991

Hoseinifar, S.H., Sun, Y.-Z., Wang, A., Zhou, Z., 2018. Probiotics as Means of Diseases Control in Aquaculture, a Review of Current Knowledge and Future Perspectives. Front. Microbiol. 9, 2429. https://doi.org/10.3389/fmicb.2018.02429

IUCN, 2008. Abramis brama: Freyhof, J. & Kottelat, M.: The IUCN Red List of Threatened Species 2008: e.T135696A4184980. https://doi.org/10.2305/IUCN.UK.2008.RLTS.T135696A4184980.en

Kousoulaki, K., Saether, B.-S., Albrektsen, S., Noble, C., 2015. Review on European sea bass (*Dicentrarchus labrax,* Linnaeus, 1758) nutrition and feed management: a practical guide for optimizing feed formulation and farming protocols. Aquac. Nutr. 21, 129–151. https://doi.org/10.1111/anu.12233

Mhalhel, K., Levanti, M., Abbate, F., Laurà, R., Guerrera, M.C., Aragona, M., Porcino, C., Briglia, M., Germanà, A., Montalbano, G., 2023. Review on Gilthead Seabream (Sparus aurata) Aquaculture: Life Cycle, Growth, Aquaculture Practices and Challenges. J. Mar. Sci. Eng. 11, 2008. https://doi.org/10.3390/jmse11102008

Moretti, A., Fernandez-Criado, M.P., Cittolin, G., Guidastri, R., 1999. Manual on hatchery production of seabass and gilthead seabream- Volume 1.

Naya-Català, F., Wiggers, G.A., Piazzon, M.C., López-Martínez, M.I., Estensoro, I., Calduch-Giner, J.A., Martínez-Cuesta, M.C., Requena, T., Sitjà-Bobadilla, A., Miguel, M., Pérez-Sánchez, J., 2021. Modulation of Gilthead Sea Bream Gut Microbiota by a Bioactive Egg White Hydrolysate: Interactions Between Bacteria and Host Lipid Metabolism. Front. Mar. Sci. 8, 698484. https://doi.org/10.3389/fmars.2021.698484

Naylor, R.L., Hardy, R.W., Buschmann, A.H., Bush, S.R., Cao, L., Klinger, D.H., Little, D.C., Lubchenco, J., Shumway, S.E., Troell, M., 2021. A 20-year retrospective review of global aquaculture. Nature 591, 551–563. https://doi.org/10.1038/s41586-021-03308-6

Oliveira, J., Oliva-Teles, A., Couto, A., 2024. Tracking Biomarkers for the Health and Welfare of

Aquaculture Fish. Fishes 9, 289. https://doi.org/10.3390/fishes9070289
Orduna, C., De Meo, I., Rodríguez-Ruiz, A., Cid-Quintero, J.R., Encina, L., 2023. Seasonal Length–Weight Relationships of European Sea Bass (Dicentrarchus labrax) in Two Aquaculture Production Systems. Fishes 8, 227. https://doi.org/10.3390/fishes8050227
OSPAR, n.d. https://www.ospar.org.
Parma, L., Candela, M., Soverini, M., Turroni, S., Consolandi, C., Brigidi, P., Mandrioli, L., Sirri, R., Fontanillas, R., Gatta, P.P., Bonaldo, A., 2016. Next-generation sequencing characterization of the gut bacterial community of gilthead sea bream (Sparus aurata, L.) fed low fishmeal based diets with increasing soybean meal levels. Anim. Feed Sci. Technol.
222, 204–216. https://doi.org/10.1016/j.anifeedsci.2016.10.022
Paulović, T., Jong, I. de, Ouweltjes, W., Martin Valls, G.E., Llonch Obiols, P., Ko, H., Kieffer, V., Lapeyre, C., Campana, C., Wille, H., Jasinska, A., Spoolder, H., 2024. Development of a roadmap for action for the project More Welfare: towards new risk assessment methodologies and harmonised animal welfare data in the EU. EFSA Support. Publ. 21. https://doi.org/10.2903/sp.efsa.2024.EN-8566
Perry, W.B., Lindsay, E., Payne, C.J., Brodie, C., Kazlauskaite, R., 2020. The role of the gut microbiome in sustainable teleost aquaculture. Proc. R. Soc. B Biol. Sci. 287, 20200184. https://doi.org/10.1098/rspb.2020.0184
Quero, G.M., Piredda, R., Basili, M., Maricchiolo, G., Mirto, S., Manini, E., Seyfarth, A.M., Candela, M., Luna, G.M., 2023. Host-associated and Environmental Microbiomes in an Open-Sea Mediterranean Gilthead Sea Bream Fish Farm. Microb. Ecol. 86, 1319–1330. https://doi.org/10.1007/s00248-022-02120-7
Roque, A., Castanheira, M.F., Toffan, A, Arechavala-Lopez, P., Brun, E., Vilarroel, M, Gisbert, E, Mylonas, Muniesa, A, Estevez, A., Dalmau, A, Basurco, B, 2020. Report on fish welfare and list of operational welfare indicators in sea bream. Deliverable 4.5 of the Horizon 2020 project MedAID (GA number 727315), published in the project web site on 17.02.2020: http://www.medaid-h2020.eu/index.php/deliverables/.
Sola, 2007. Gilthead Sea Bream - aquatrace.
Tarricone, S., Ragni, M., Carbonara, C., Giannico, F., Bozzo, F., Petrontino, A., Caputi Jambrenghi, A., Colonna, M.A., 2024. Growth Performance and Flesh Quality of Sea Bass (Dicentrarchus labrax) Fed with Diets Containing Olive Oil in Partial Replacement of Fish Oil—With or Without Supplementation with Rosmarinus officinalis L. Essential Oil.
Animals 14, 3237.
https://doi.org/10.3390/ani14223237 unep, n.d.
https://www.unep.org.

Aim and objectives

The research activity carried out in the second section of this thesis was developed within the framework of the Italian National Recovery and Resilience Plan (PNRR), Activity 3, Task 3.3, focusing on Improvement of health and welfare of farmed fish.
In the present work, a multibiomarker approach was applied to monitor the health status of 2 fish species reared in an offshore farm:

1. *S. aurata*: sampled along two years, from fry to marketable size.
2. *D. labrax*: sampled along 9 months, from juvenile to marketable size.

Morphometric and physiological parameters related to growth were measured at the organism level. At the tissue level, enzymatic biomarkers of oxidative stress and biotransformation were evaluated in both gills and liver. The microbiota composition of anterior intestine samples from both species was also analysed by 16S rRNA gene amplification and sequencing. In *S. aurata*, histopathology in gills, liver, and anterior intestine were also evaluated.

This activity was carried out in collaboration with the aquaculture offshore farm Aqua de Ma (Lavagna, Italy), who provided the animals all over the sampling periods.

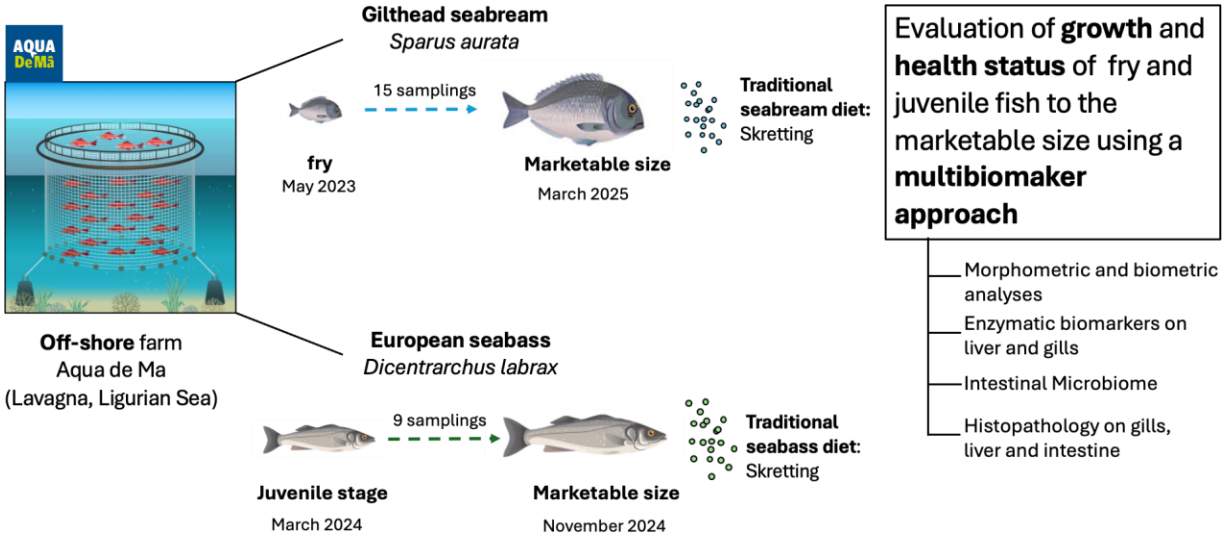

Materials and Methods

1. Sampling site

The offshore Aqua de Ma farm (AQUADEMA) is situated in the Golfo del Tigullio (Liguria, Italy), at 1 mile from the coast (latitude: 44° 17' 22''; longitude: 9° 20' 49''). It represents the only fish aquaculture site in the Ligurian Sea. The location is characterized by a strong hydro dynamism, including currents that maintain the sea floor and the nearest areas clean from waste products. Fish are grown in 16 rounded floating, submersible cages, with a diameter of 19 m and a depth of 12 m (3,800 m^3), suspended at 30 m over the sea bottom. The cages are made of high density polyethylene (HPDE) tube rings, and closed in the upper part by a net to prevent predation from marine birds and evasion of the fish when the cages are submerged. The cage was designed with three main flotation pipes with inner-fillings of Styrofoam cylinders. The main upper pipes at surface are connected to each other by brackets and a hand-rim 1 m above the water surface all around the bracket lines.

2. Fish rearing conditions and feeding regimen

2.1 Gilthead seabream

Gilthead seabream *S. aurata* fry (with an initial mean body weight of 2.44 ± 0.03 g and mean length of 5.90 ± 0.02 cm) were obtained from a seabream hatchery located in Torre Canne (Brindisi, Italy), and transferred to the cage-farm site. The cage contained a fish population of about 140,000 individuals, with a maximal stocking density from 8 to 10 kg/m^3 at 350 g fish body weight. Water temperature was measured daily, and oxygen, salinity and pH were measured 3 times a month by using the YSI multi-parameter device (Polaris C, OxyGuard, Denmark).

Fish were fed commercial sea bream diets (Skretting Italia S.p.A, Italy), supplied on a dry matter basis according to fish body weight (%/BW), that was periodically measured. Both standard and variant feeds were utilized in 4 different pellet diameters (Perla MPL, Perla MPT, 1P and 2P, corresponding to 1.5 mm, 1.9 mm, 3.0 mm and 4.0 mm, respectively), selected on the basis of the fish weight as indicated by the manufacturers. Perla MPL and Perla MPT feeds were utilized for fish up to about 10 g weight, and from 10 to 20 g weight, respectively. Fish from 20 to 100 g weight were fed Shield Bream 1P. This feed, containing essential oils such as garlic, is formulated to prevent blood-feeding parasites, particularly *Sparicotyle chrysophrii* (a gill parasite of gilthead seabream) which can cause high mortality in fish smaller than 100 g and decrease the growth rate of bigger individuals.

For fish > 100 g weight, different types of 2P feeds were utilized. 'Protec', for acclimatation to

low temperatures (from 18-16 °C) during the winter period, until return to T of 18 °C, fish were fed 'Protec Bream', a feed variant containing natural ingredients (mix of functional oils such as cinnamon) with anti-inflammatory properties that prevent intestinal inflammation. At higher temperatures, 'Alterna Bream' was utilized. The feeding regimen (feeding days/month) was chosen according to the season, with a higher frequency in warmer months (max 30 feeding days/month). The feeding regimen and the type of feed administered along the whole period, from May 2023 to Mar 2025, as well as sea water temperatures, are shown in **Fig. 1A**. The total amount of fats in different feeds did not exceed 16%, except for 'Protec' (18% total fat) that was administered only in two months (Nov-Dec 2024). The gross composition of different feeds, as declared by the manufacturers, is reported in **Tab. S1**.

2.2 European seabass

D. labrax was grown in the same conditions and feeding regimen utilized for *S. aurata* until February 2024. From March 2024, they were fed a standard commercial sea bass diet (Alterna bass 2P, Skretting Italia S.p.A., Italy), containing 20% total fat, throughout the monitoring period. The feeding regimen is reported in **Fig. 1B**.

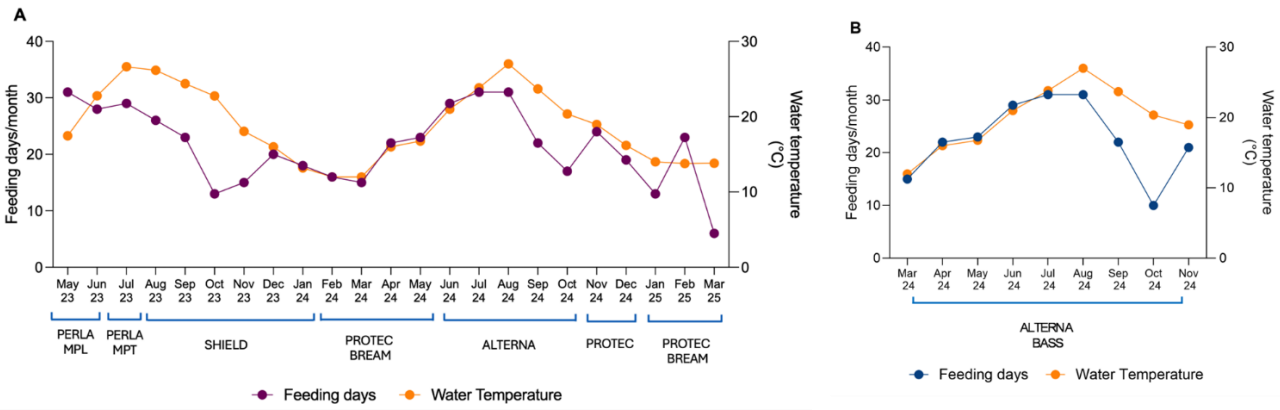

Figure 1 – Feeding regimen (feeding days/month) (left Y axis) and water temperature (right Y axis) during *S. aurata* (A) and *D. labrax* (B) growth in an off-shore cage at the Aqua farm (Lavagna, Genoa, Italy). *S. aurata*: the monitoring period was from May 2023 (1-2 months old fry, about 2.4 g BW) to March 2025, when fish reached the marketable size (about 400 g BW). *D. labrax*: the monitoring period was from March 2024 (about 150 g BW) to November 2024, when fish reached the marketable size (about 400 g BW). On the X axis, the type of feed administered at different periods of growth and times of the year, depending on fish weight and water temperature, is also indicated.

3. Sample collection

3.1 Gilthead seabream

The monitoring program of *S. aurata* was carried out from May 2023 (1-2 months old fry) to March 2025 (marketable size animals). A total of 150 fish were examined. At each sampling month, fish were randomly collected from the same cage by net and by using attractiveness of feed, immediately put in sea water/ice aboard a boat, and transported to the onshore facility for commercial distribution. Here, a set of specimens (from 15 to 6 gilthead seabream depending on the fish size) were randomly collected and transported in ice to the laboratory. Only dead fish were collected from the harvests. All fish were examined for gross alterations, presence of parasites or lesions by a stereo microscope, and morphometric parameters (length, width and total body weight) were recorded. Subsequently, tissues (liver, gills and intestine) were quickly dissected and weighted. Aliquots of gills and livers (about 0.5 g) were frozen for subsequent determination of enzymatic biomarkers. Portions (approximately 1 cm) of the anterior intestine were stored at -80 °C for microbiota analyses. The remaining tissues were collected for histopathological analyses.

3.2 European seabass

D. labrax sampling was carried out from March 2024 (juvenile stage; ~160 g) to November 2024 (marketable size; ~ 400 g), for a total of 9 months, with 6 fish examined at each sampling time (N = 6). The same type of samples of *S. aurata* were collected, except for those for histological analyses.

4. Morphometric and physiological parameters

Fish condition was evaluated by calculating Fulton's condition factor (K) (Omnes et al., 2015):

$$\text{K factor (\%)} = \frac{\text{total body weight (g)}}{\text{length}^3} \times 100$$

The specific growth rate (SGR %) was calculated according to the following equation (Ducros et al., 2023):

$$\text{SGR in weight (\%.day}^{-1}\text{)} = \frac{\ln(\text{weight}_{t2}) - \ln(\text{weight}_{t1})}{\Delta \text{ days}} \times 100$$

The length-weight relationship, used to determine allometric growth in fish, was calculated according to (Yýldýrým Korkut and Gurkan, 2018):

$$W = aL^b$$

W = mean weight (g)
L = mean length (cm)
a = rate of change of weight with length (intercept)
b = weight at unit length (slope)

The Hepatosomatic index (HSI) was calculated as percent ratio of liver to the total body weight (OSPAR Commission, 2013):

$$HSI\ (\%) = \frac{\text{weight of liver (g)}}{\text{Total body weight (g)}} \times 100$$

The gonadosomatic index (GSI) was calculated as percent ratio of gonad weight to the total body weight (OSPAR Commission, 2013):

$$GSI\ (\%) = \frac{\text{gonad weight (g)}}{\text{total body weight (g)}} \times 100$$

5. Enzymatic biomarkers

For *S. aurata* fish up to 5 g body weight (from May to June 2023), due to the small size of the animals, 5 pools of tissues were made from 3 individuals (N = 5 for each month). From July 2023, enzyme activities were evaluated in individual tissue samples (N = 6). All *D. labrax* enzyme activities were evaluated in individual tissue samples (N=6).

Catalase (CAT), Glutathione-S-Transferase (GST) and 7-ethoxyresorufin O-deethylase (EROD) activities were evaluated in gills and liver as described in Maradonna et al., 2014, with slight modifications. Briefly, for CAT and GST tissues were homogenized in Tris buffer (0.15 M, EDTA 1 mM, pH 7.5) at 1:4 (gills) and 1:6 (liver) w/v ratio, centrifuged at 500 × g for 15 min at 4 °C. The supernatants were then centrifuged at 14,000 × g for 40 min. The resulting supernatants were utilized for spectrophotometric determination of CAT (decomposition of H_2O_2 at 240 nm) and GST (conjugation with CDNB at 340 nm) activities.

For EROD activity, livers were homogenized at 1:4 w/v ratio in phosphate buffer (K_2HPO_4/KH_2PO_4 100 mM, KCl 150 mM, EDTA 1mM, DTT 1 mM, pH 7.4), centrifuged at 10,000 x g for 20 min at 4°C. EROD was measured fluorometrically in the resulting supernatants (λex 535 nm, λem 585 nm for 10 min) as the amount of resorufin (pmol) generated per minute.

Protein content was determined using the Bradford method with bovine serum albumin (BSA) as a standard. Data are expressed as μmol/mg prot/min, nmol/mg prot/min and pmol/mg prot/min respectively for CAT, GST and EROD activities.

6. Histology

Gilthead seabream tissues dissected from 4 fish from each sampling time (gills, liver, and intestine) were preserved in 10 % buffered formalin (Sigma-Aldrich, Germany) and maintained at 4 °C for 24 h, washed in phosphate buffer saline 0.1M pH 7.4 (PBS) dehydrated in ethanol, cleared in BioClear (Bio-Optica, Italy) and paraffin-embedded (Noga, 2010). Tissue sections (5 μm thick) were obtained by using a rotary microtome (Microtome Reichert-Jung 2065 Supercut, Leica, Germany) and subsequently stained with Mayer's haematoxylin and eosin. Histological slides were observed using a light microscope Leica DMRB (Leica Microsystems, Wetzlar, Germany) equipped with a Moticam 3+ (Motic Europe, Spain).

Images were analysed using the software ImageJ. For each tissue, three optical field were analysed from three photographs taken from three different sections, yielding a total of nine replicates per individual. In the liver, lipid content (expressed as relative surface over the considered area) were estimated.

7. Microbiome analysis

7.1 DNA extraction

For each sampling, 2 pools of tissue from 3 animals (200 mg for each fish) were utilised. Nucleic acids were extracted from frozen intestine samples using the QIAamp PowerFecal Pro DNA Kit (Qiagen, Germany) according to the manufacturer's instructions. The amount of DNA extracted was determined by a QuantiFluorTM dsDNA System using a QuantiFluorTM fluorometer (Promega Italia srl, Milano, Italy).

7.2 16S rRNA gene amplification and sequencing

16S rRNA PCR amplicon libraries were generated from genomic DNA extracted from fish intestine samples using primers amplifying the V3 – V4 variable regions of bacterial 16S rRNA gene. Libraries were generated using the Illumina 16S Metagenomic Sequencing Library preparation protocol. The primers used are listed in **Table S2**. Libraries were sequenced by the Illumina MiSeq platform, using MiSeq Reagent Kit v3 and 300 bp paired-end.

7.2.1 Bioinformatic analyses

Raw amplicons were denoised with AmpWrap (Doni et al., 2025). Briefly, after the denoising step including primer removal, quality filtering, and chimera removal amplicon sequence variants (ASVs) were inferred. A total of 2801368 reads from the 25 sequenced samples, ranging from 92400 to 249188 reads per sample (on average 112055 per sample), were assigned to 4711 ASVs. Non- bacterial, mitochondrial and chloroplast sequences were removed and samples were normalized by total sum scaling (TSS). Microbial community composition and diversity analyses were performed using the phyloseq R package (McMurdie and Holmes, 2013) and visualizations were generated with ggplot2 (Wickham, 2016). Alpha diversity was assessed using observed richness and the Chao1 estimator on raw count data, while Shannon and Simpson diversity indices were computed on TSS- normalized data. A bubble plot was used to visualize taxonomic composition, displaying the relative abundance of the top 15 most abundant phyla and the top 20 most abundant families across samples.

8. Statistical analysis

Growth, physiological and enzymatic data were first analysed for normal distribution using the Shapiro-Wilk's test ($P > 0.05$) followed by one way ANOVA (p value < 0.05). Differences among individual months and mean values along the whole growth period were analyzed by Tukey's or Dunnet's multiple comparison tests, respectively.

Data correlation was calculated using the non parametric Spearman rank correlation test ($p < 0.05$).

Statistical analyses were performed using GraphPad Prism version 7.03 for Windows, GraphPad Software, San Diego, CA, USA.

References

AQUADEMA, n.d. https://www.aquadema.it/.

Ducros, L., Touaibia, M., Pichaud, N., Lamarre, S.G., 2023. Resilience and phenotypic plasticity of Arctic char (*Salvelinus alpinus*) facing cyclic hypoxia: insights into growth, energy stores and hepatic metabolism. Conserv. Physiol. 11, coad099. https://doi.org/10.1093/conphys/coad099

Maradonna, F., Nozzi, V., Dalla Valle, L., Traversi, I., Gioacchini, G., Benato, F., Colletti, E., Gallo, P., Di Marco Pisciottano, I., Mita, D.G., Hardiman, G., Mandich, A., Carnevali, O., 2014. A developmental hepatotoxicity study of dietary bisphenol A in Sparus aurata juveniles. Comp. Biochem. Physiol. Part C Toxicol. Pharmacol. 166, 1–13. https://doi.org/10.1016/j.cbpc.2014.06.004

McMurdie, P.J., Holmes, S., 2013. phyloseq: An R Package for Reproducible Interactive Analysis and Graphics of Microbiome Census Data. PLoS ONE 8, e61217. https://doi.org/10.1371/journal.pone.0061217

Noga, M.S., 2010. Fish Disease: Diagnosis and Treatment.

Omnes, M.H., Silva, F.C.P., Moriceau, J., Aguirre, P., Kaushik, S., Gatesoupe, F.J., 2015. Influence of lupin and rapeseed meals on the integrity of digestive tract and organs in gilthead seabream (*Sparus aurata* L.) and goldfish (*Carassius auratus* L.) juveniles. Aquac. Nutr.
21, 223–233. https://doi.org/10.1111/anu.12162

OSPAR Commission, 2013. Background documents and technical annexes for biological effects monitoring. p. 239.

Wickham, H., 2016. ggplot2: Elegant Graphics for Data Analysis. Wickham, H., 2016. ggplot2: Elegant Graphics fSpringer-Verlag, New York.

Yýldýrým Korkut, Y.K.A., Gurkan, S., 2018. Length-weight relationship and condition factor as an indicator of growth and feeding intensity of Sea bream (Sparus aurata L, 1758) given feed with different protein contents. Indian J. Anim. Res. https://doi.org/10.18805/ijar.B-998

Results

Chapter 6:

Sparus aurata

All analyses were carried out in all seabream samples, for a total of 15 sampling times.

Growth and physiological parameters

At the onset of monitoring in May 2023, seabream mean length, width and body weight were 6.42 ±

0.44 cm, 2.37 ± 0.30 cm and 3.8 ± 0.58 g, respectively **(Fig. S1A,B,C**). By March 2025, fish reached the commercial size, with a mean body weight of 388.54 ± 38.27 g and mean length and width of

28.93 ± 0.85 cm and 9.73 ± 0.15 cm, respectively (**Fig. S1A,B,C**).

Data on physiological parameters are reported in **Fig. 2**. Condition factor (K), a parameter for assessing fish health and robustness, showed fairly constant values throughout the sampling period and growth, irrespectively of changes in temperature (mean = 1.45 ± 0.20) (**Fig. 2A**).

In contrast, Specific Growth Rate (SGR), an indicator of fish growth performance over time, showed large seasonal variations (**Fig. 2B**). The highest SGR value was recorded in June 2023 (3.21), corresponding to the first period of growth and to the beginning of the warmer season, while the lowest value was observed during the coldest months, with a minimum in February 2024 (0.01). SGR data were positively correlated with seawater temperature ($r = 0.73^*$, p value < 0.01, Spearman correlation test).

The length-weight relationship was described by the equation $W = 0.0074L^{3.2491}$ with a scaling exponent $b = 3.2491 > 3$, indicating positive allometric growth all over the sampling period (Yýldýrým Korkut and Gurkan, 2018) (**Fig. 2C**).

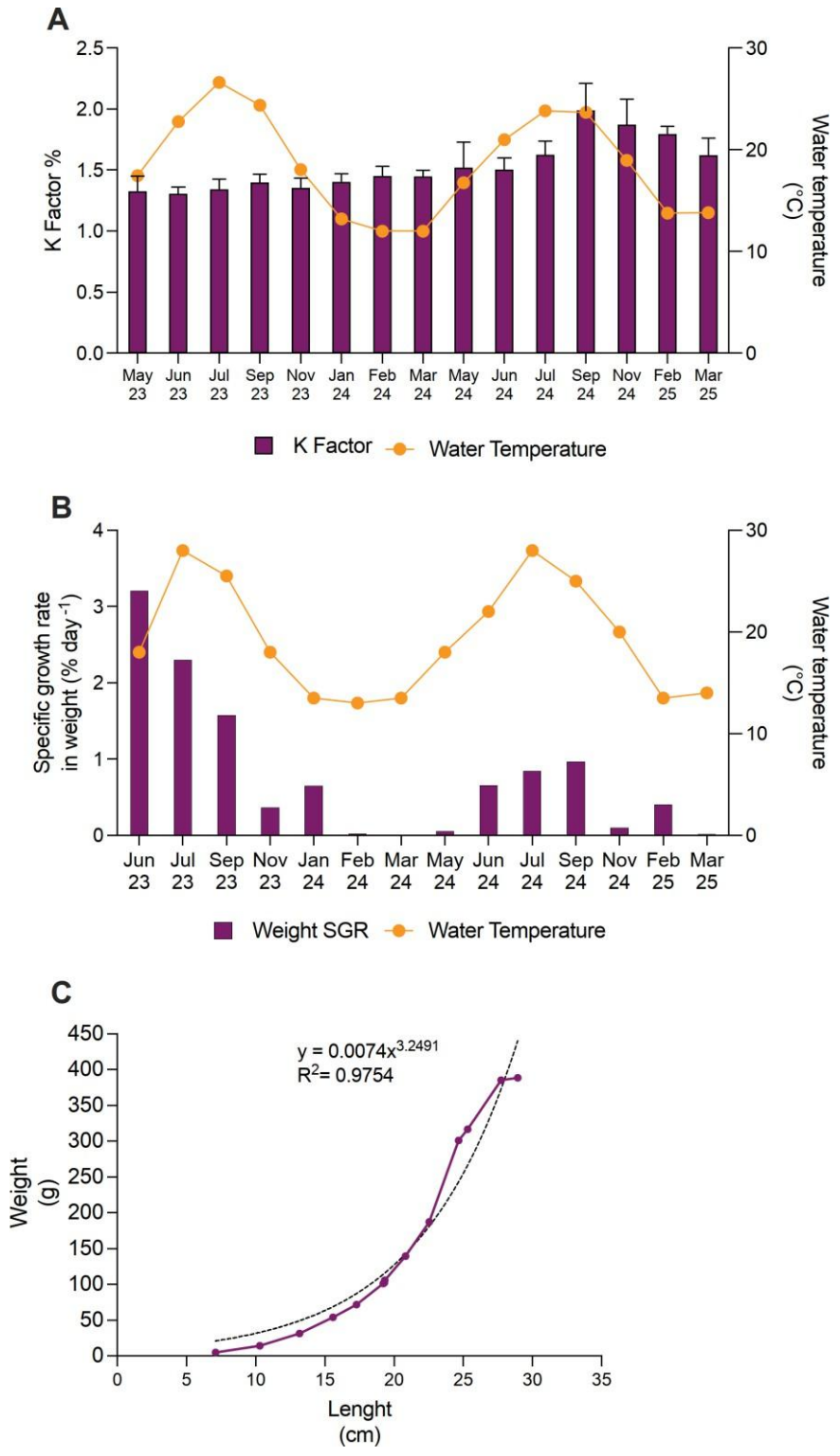

Figure 2 - Indicators of physiological growth performance in *S. aurata*: A) Condition factor (K); B) Specific Growth Rate (SGR), C) Length-Weight relationship. In A and B, changes in water temperature values are indicated by the orange lines. Data are expressed as means ± sd (N= 15 for May to June 2023 and N= 6 for the following months).

The hepatosomatic index (HSI) showed a mean value of 1.78 ± 0.55 along the whole period (**Fig. 3A**). The highest HSI was recorded in May 2023, at the beginning of the growth process (2.69 ± 0.46 in May 2023). Seasonal fluctuations were subsequently observed along growth, that were inversely correlated with changes in seawater temperature ($r = -0.65$, $p < 0.01$, Spearman correlation test).

The Gonado Somatic Index (GSI) was also calculated. Developing male gonads could be observed only in individuals sampled from July 2024, when body weight and length reached values > 200 g and > 20 cm, respectively, in about 80% of individuals. However, low GSI values were observed (< 0.4%), indicating first stages of gonad development (**Fig. 3B**).

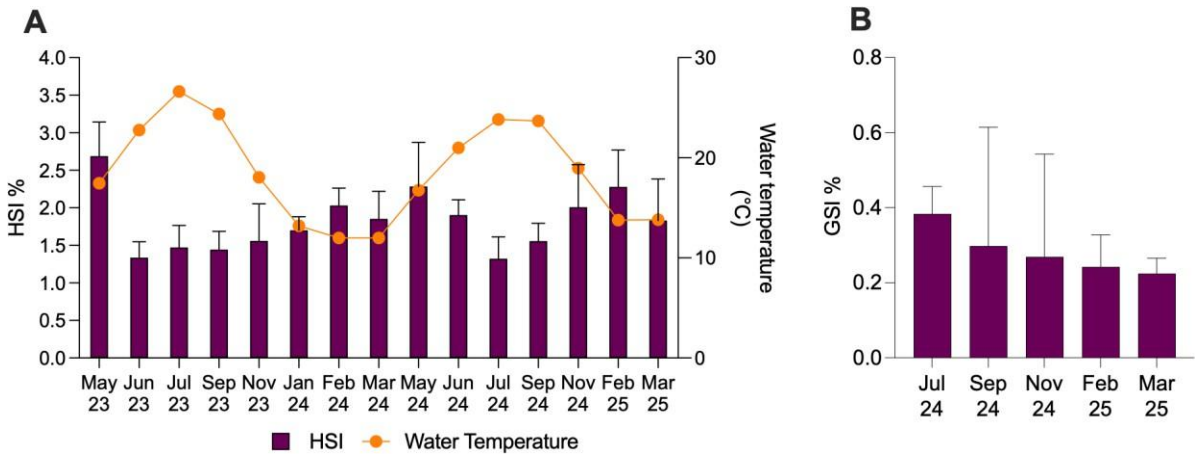

Figure 3 - Seasonal variations of HSI (A) and GSI (B) in *S. aurata* along growth. Data are expressed as means ± sd. (N= 15 for May to June 2023 and N= 6 for the following months).

Histological analyses

Histological observations were carried out on liver, gills and intestine. All tissues showed a generally normal appearance throughout the sampling period (representative images are reported **Fig. S2 A, B, C** for each tissue, respectively). Although some histopathological alterations were occasionally observed, these occurred randomly in a small proportion of samples (<5%) and were not associated with growth stage or environmental temperature.

Since HSI is often correlated to liver lipid accumulation (Ibarz et al., 2007; Yıldız et al., 2006), the lipid content was compared in liver tissue sections of the same samples. Data, expressed as percent lipid surface over the whole tissue areas analysed, are reported in **Fig. 4.** The results (**Fig. 4A**) indicate a distinct trend in liver lipid content along the two years of growth. Lowest values were observed in summer 2023 (June-September 2023) (**Fig. 4B**), corresponding to the first period of weight gain (See **Fig S1C**)**,** followed by an increase in winter, reaching average values

of about 10% liver lipid content between November 2023 and February 2024, followed by a peak in March (18%) (**Fig. 4C**) and a minimum in July 2024 (about 5%). In the whole period, liver lipid content showed a negative correlation with temperature (-0.51 $p = 0.05$) and a positive correlation with HIS (0.62, $p < 0.02$).

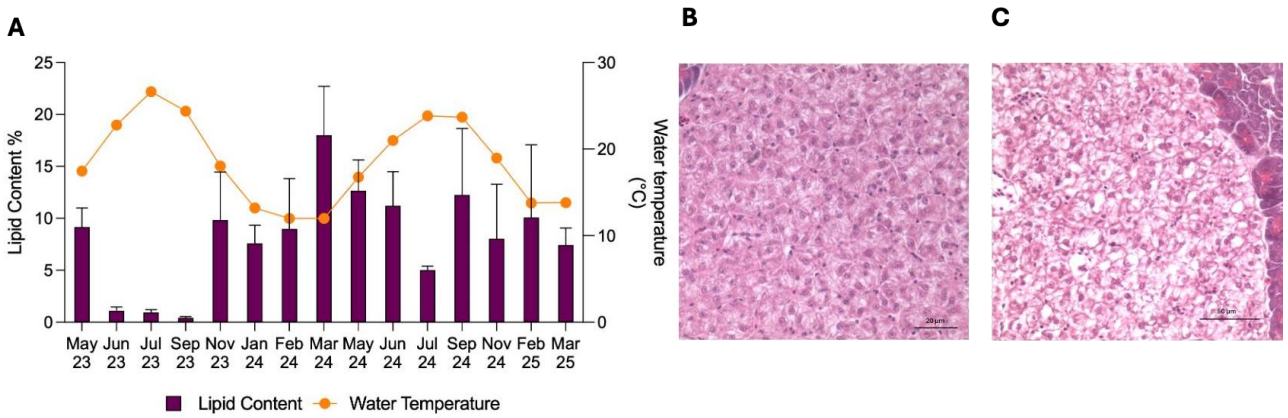

Figure 4 - Seasonal variations of liver lipid content in *S. aurata* along growth. Data were evaluated on histological tissue sections (9 sections per individual, 4 individuals, N = 4 for each sampling time) and are reported as % lipid surface over the considered area. Seasonal changes in water temperature are indicated by the red lines (A). In B and C, representative images of liver tissue sections of samples with low (June 2023) and high (June 2024) lipid content, respectively, are reported.

Enzymatic biomarkers

Data on enzymatic biomarkers of oxidative stress and biotransformation measured in liver and gills of *S. aurata* are presented in **Fig. 4**. CAT activity was higher in liver than in gills, with mean values of 139.5 ± 29.4 µmol/min/mg prot and 24.6 ± 14.1 µmol/min/mg prot, respectively, over the whole sampling period **(Fig. 4A**). Similarly, higher GST activities were detected in liver (434.9 ± 152.9 nmol/min/mg prot) with respect to gills (213.5 ± 87.1 nmol/min/mg prot) (**Fig. 4B**). Although fluctuations in activities of both enzymes were recorded over the sampling period, with significant differences between some months and mean values (**Fig. 4A** and **4B**), no clear trends could be observed with growth and season for either enzyme and tissue. The same applies to hepatic EROD activity, that showed a mean value of 3.6 ± 2.8 pmol/min/mg prot, with a maximum observed in January 2024 (5.6 ± 1.3) (**Fig. 3C**). Accordingly, no correlation was found between antioxidant and biotransformation enzyme activities in either tissue and water temperature, fish growth or age, not between liver biotransformation activities and lipid content.

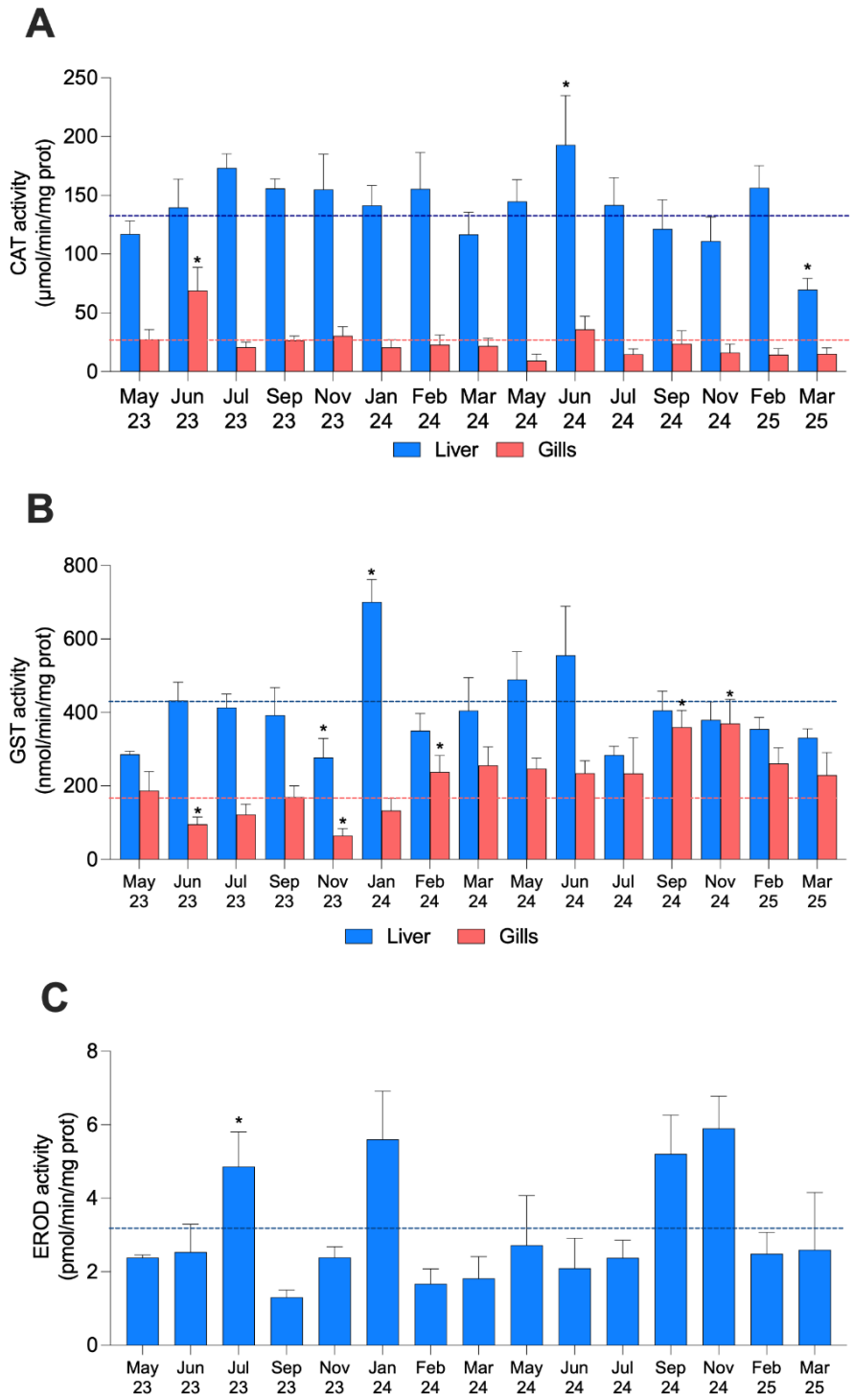

Figure 5 - Evaluation of enzymatic biomarkers of oxidative stress (in liver and gills) and biotransformation (in liver) of *S. aurata* along growth. A) Catalase (CAT) activity, B) Glutathione-S- Transferase (GST) activity and C) EROD activity. Values are expressed as mean ± sd (N= 5 for May to June 2023 and N= 6 for the following months). Statistical analyses were performed by one way ANOVA followed by Dunnett's multiple comparisons test, * = $p < 0.05$; monthly data *vs* mean data recorded across the whole sampling period (indicated by the dotted line). May and June 2023 were evaluated in 5 pools of 3 animals each, for the following months enzyme activities were evaluated in individual tissue samples.

Gut microbiome

A first analysis of the anterior intestine microbiome was carried out in 5 selected seabream samples, from T0, corresponding to fry at the beginning of the monitoring period (May2023), to different growth stages and season, T1 (Jul 2023), T2 (Feb2024), T3 (Jul 2024) and T4, at the end of the growth cycle (Mar2025). Fish body weight, feeding days and seawater temperature at these time points are summarized in **Table S3**. 16S rRNA PCR amplicon libraries were generated from genomic DNA extracted from fish intestine samples using primers amplifying the V3 – V4 variable regions of bacterial 16S rRNA gene. Libraries were generated using the Illumina 16S Metagenomic Sequencing Library preparation protocol.

Raw amplicons were denoised with AmpWrap (Doni et al., 2025). Rarefaction curves calculated for total ASVs abundance reached the plateau, indicating that a good sequencing depth to capture most of the total bacterial diversity (**Fig. S3).**

Taxonomic composition at the phylum level (**Fig. 6A**) highlighted the dominance in all samples of Pseudomonadota (aka Proteobacteria) (mean 46.86 ± 32.52%) and Bacillota (aka Firmicutes) (19.94 ± 20.27 %) followed by Bacterioidota (16.04 ± 11.32 %), Spirochaetota (10.24 ± 6.88%) and Patescibacteria (2.12±1.47%). All other families showed abundances < 1%. For more details see **Tab. S4A**.

Among these, T0 samples showed highest abundance of Pseudomonadota (62%), followed by Bacteroidota (13.5%), Bacillota (10.2%) and Spirochaetota (3.5%). A dramatic decrease in Pseudomonadota was observed in T1 samples (8.1%), that were dominated by Bacillota and Spirochaetota (>70%). At T2, the initial relative composition was partially re-established (Pseudomonadota 53.6%); however, abundance of Spirochaetota was still higher (12.9%) with respect to T0. Another major shift was observed in T3 samples, that were totally dominated by Pseudomonadota (88.9%) and Spirochaetota (10.2%). Finally, T4 showed a heterogenenous composition, more resembling that of T0, with Bacterioidota, Bacillota and Pseudomonadota representing over 80% of total abundance, and a return to lower abundance of Spirochaetota (4.1%).

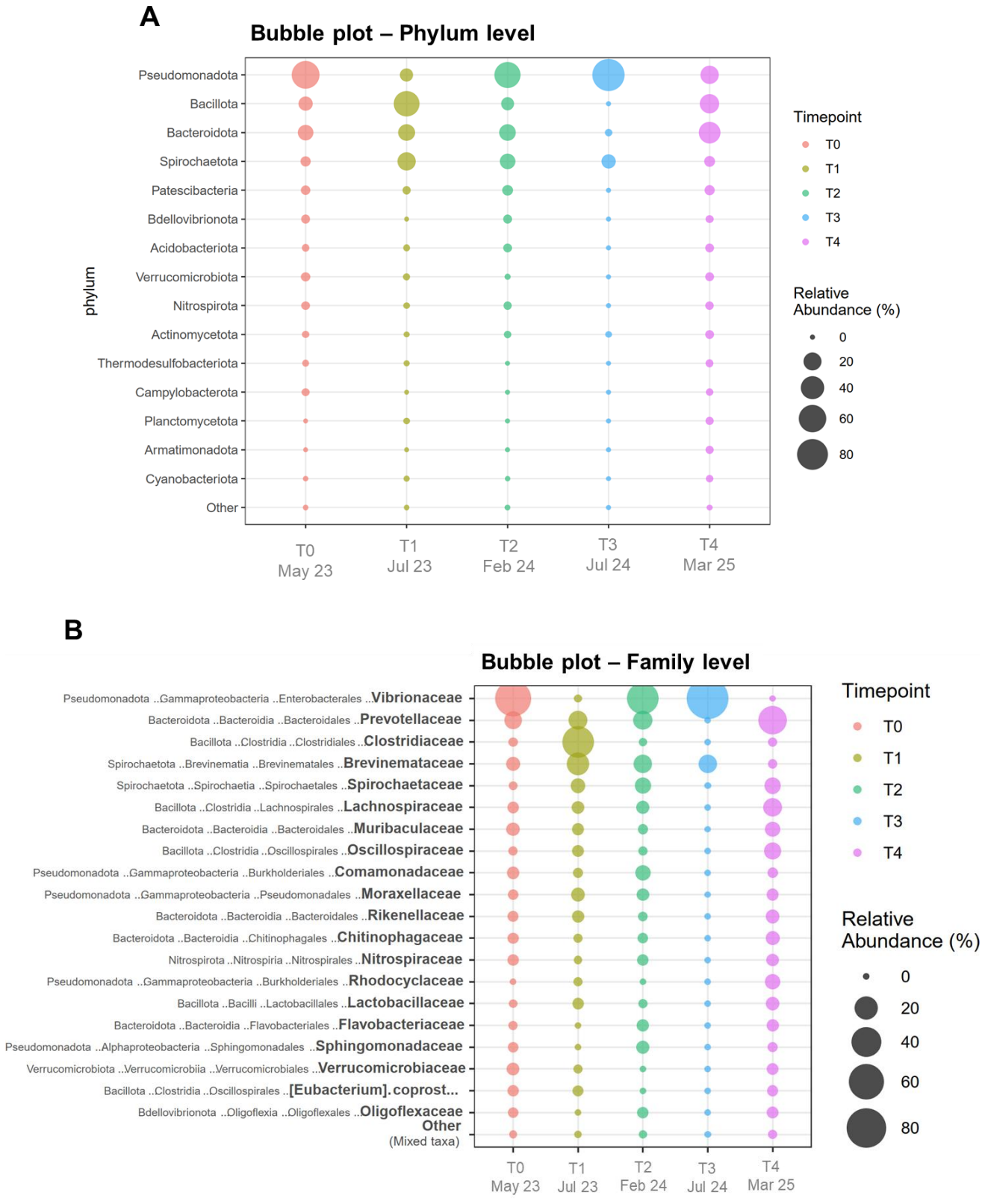

Figure 6 - Bubble plots representing the seabream gut bacterial community at two phylogenetic levels: A) Top 15 Phyla; B) Top 20 Families. Mean data from 2 pools for each sampling time.

At the family level (**Fig. 6B**) the most represented group was that of Vibrionaceae (40%) followed by Prevotellaceae (13%), Clostridiaceae (9%) and Brevinemataceae (9%). Other less represented families were Spirochetaceae, Lachnospiraceae, Muribaculaceae, Comamonadaceae, Oscillospiraceae and Rikenellaceae (about 1-4%). For more details see **Tab. S4B**.

At T0, samples were characterized by dominance of Vibrionaceae (62.8%), followed by Prevotellaceae (9.3%), Brevinemataceae (4.2%), Muribaculaceae (3.6%), Verrucomicrobiaceae (2.8%) and Comamonadaceae (2.7%) and many other families with abundances from 2 to 1%. A dramatic shift was observed in T1, showing the almost complete disappearance of Vibrionaceae (0.2%), that were substituted by Clostridiaceae (45.8%) and Brevinemataceae 18.80%). Changes in several less represented families were also observed.

At T2, samples showed a relative composition resembling that of T0: the abundance of Vibrionaceae was restored, and those of Clostridiaceae and Brevinemataceae fell to 0.3 % and 10.4% respectively. In July 2024 (T3), the bacterial composition was totally represented by Vibrionaceae and Brevinemataceae, these two families accounting for almost 100% total abundance. As observed at the phylum level, T4 samples were characterized by a more heterogeneous composition, with high abundance of Prevotellaceae (34.5%), followed by Lachnospiraceae (10.4%), Oscillospiraceae and Spirochaetaceae (8.1 and 7.4%, respectively), Muribaculaceae (5.6%), Rikenellaceae and Chitinophagaceae (4.1%) and many other families with abundance of about 1%. A dramatic fall in Brevinemataceae was also observed (0.6%).

Alpha-diversity analysis using the Chao1 index showed that bacterial diversity increased over time in parallel with fish growth, with the highest values observed at T4, when animals reached marketable size (**Fig. 7**). Similarly, the Shannon index, which reflects both richness and evenness of bacterial communities, increased over time, again showing the highest diversity at T4 (**Fig. 7**). In contrast, the lowest alpha-diversity and richness values were recorded at T3. This result is in line with microbiota composition data, as the T3 community was almost entirely represented by Pseudomonadota (90%), mainly represented by the family Vibrionaceae (90%).

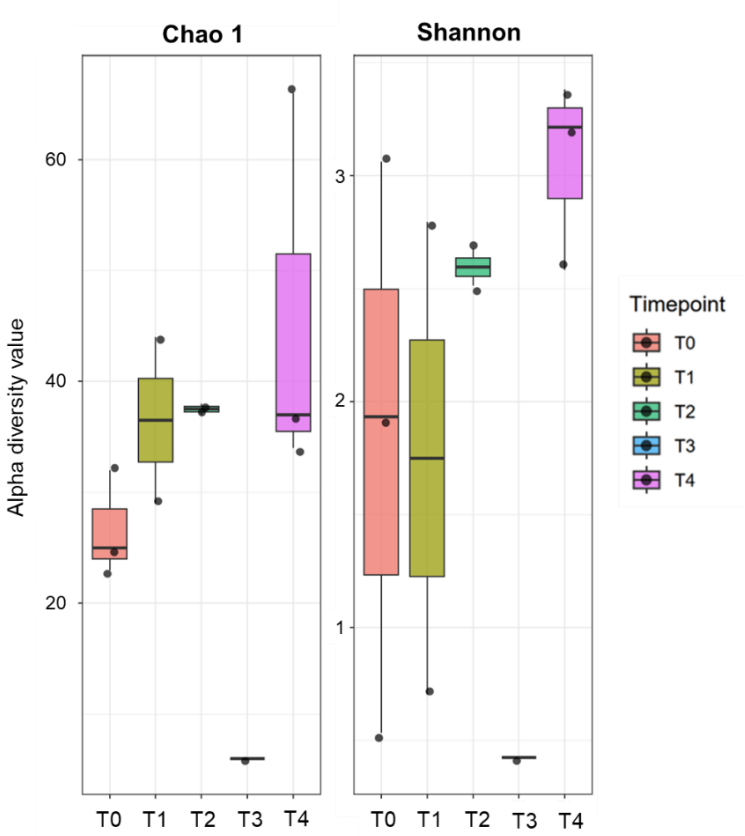

Figure 7 - Box plots representing the median, minimum and maximum of richness estimates of the Alfa-diversity estimator Chao1 and Shannon diversity index of anterior intestine microbial populations of gilthead seabream at each sampling time T0, T1, T2, T3, T4 at family level.

Supplementary material

Materials and methods

Table S1: Proximate % composition of Skretting feed variants, as provided by the manufacturers: Protec, Protec Bream and Alterna Bream.
MPL, MPT, 1P and 2P: pellet diameters, corresponding to 1.5 mm, 1.9 mm, 3.0 mm and 4.0 mm, respectively.

PERLA		
Composition %	**MPL**	**MPT**
Moisture	20.5	24.1
Crude protein	54.0	51.0
Crude fat	15.0	15.0
Crude fibers	1.0	1.5
Ash	8.0	7.0
Phosphorus	1.5	1.4
DE (MJ/kg)	17.0	17.0

SHIELD BREAM	
Composition %	**1P**
Moisture	19.7
Crude protein	51.0
Crude fat	16.0
Crude fibers	3.5
Ash	8.5
Phosphorus	1.3
DE (MJ/kg)	17.0

PROTEC	
Composition %	**2P**
Moisture	24.4
Crude protein	46.0
Crude fat	18.0
Crude fibers	3.0
Ash	7.5
Phosphorus	1.1
DE (MJ/kg)	17.0

PROTEC BREAM	
Composition %	**2P**
Moisture	26.0
Crude protein	47.0
Crude fat	16.0
Crude fibers	3.5
Ash	6.5
Phosphorus	1.0
DE (MJ/kg)	17.0

ALTERNA BREAM	
Composition %	**2P**
Moisture	24.3
Crude protein	48.0
Crude fat	16.0
Crude fibers	4.0
Ash	6.7
Phosphorus	1.0
DE (MJ/kg)	17.0

DE: digestible energy

Table S2: List of primers used for the amplification of the V3-V4 hypervariable region of the 16S rRNA gene.

Primer	**Primer sequence**
Forwards	CCTACGGGNGGCWGCAG
Reverse	GACTACHVGGGTATCTAATCC

Results

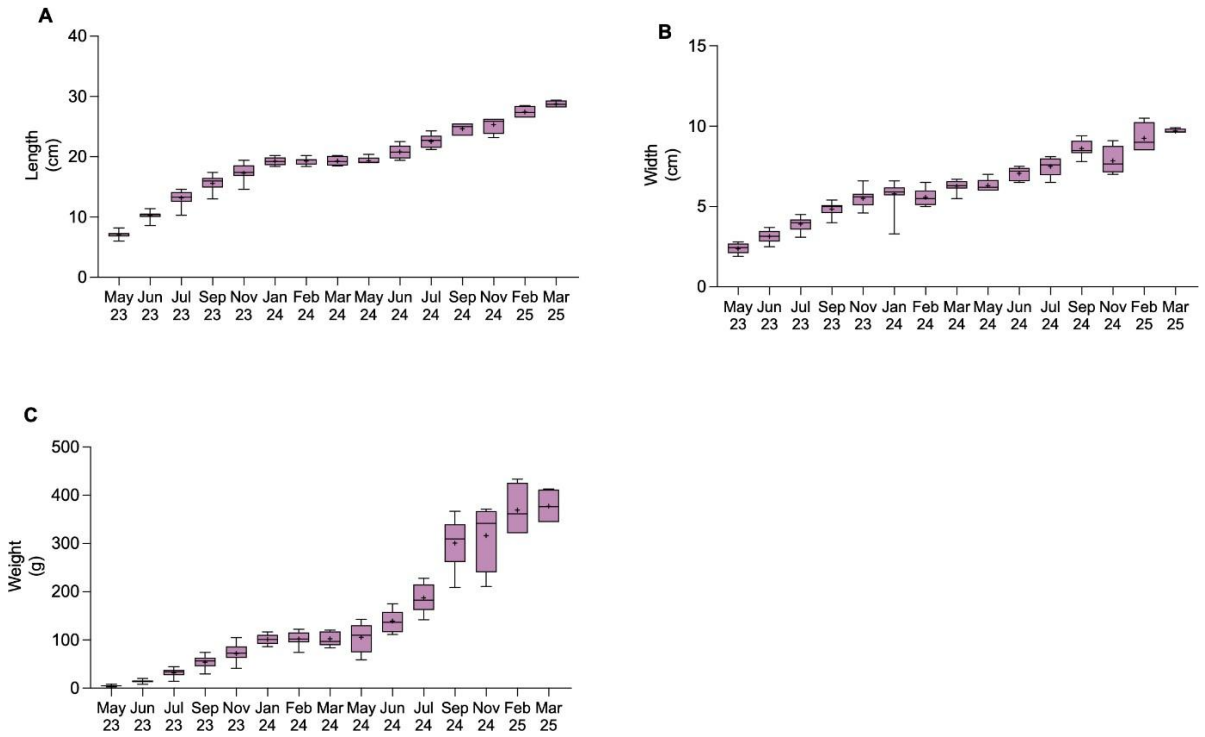

Figure S1 - Morphometric parameters of *S. aurata* overtime: A) Length; B) width and C) weight. Boxplots indicate the median (—), the mean (+), 5th and 75th percentiles (box), min and max range (whiskers).

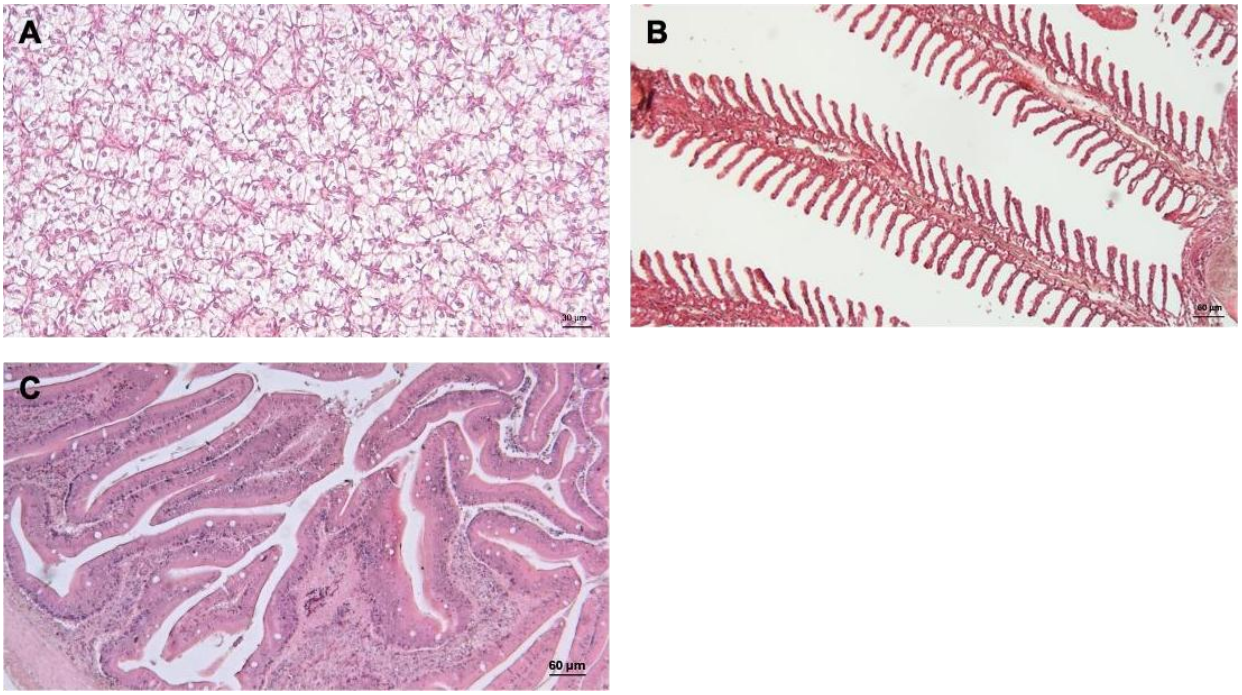

Figure S2 – Representative images of microscopical images of *S. aurata* liver (A), gills (B) and intestine (C)

In gills, mean length of filaments, frequency of lamellae, mean height of lamellae and hyperplasia of filaments were evaluated (Hughes, 1984). In the intestine, the parameters considered were: number of goblet cells, fusion of villi (absent / basal fusion/ few fused/ many fused), presence of granulocytes (absent/ in the submucosa/in the villi), villi wall condition (good/ partially damaged/ destroyed), and presence of parasites (no/ yes) (Pacorig et al., 2022). Although some histopathological alterations were occasionally observed, these occurred randomly in a small proportion of samples (<5%) and were not associated with growth stage or environmental temperature (not shown).

Table S3: Sampling times for microbiome analysis of anterior intestine samples of *S. aurata*

	T0 MAY 23	T1 JUL 23	T2 FEB 24	T3 JUL 24	T4 MAR 25
Body weight (mean ± SD)	4.8 ± 1.3	31.5 ± 8.4	102.1 ± 15.1	187.4 ± 31.5	388.5 ± 38.3
Water Temperature (°C)	17.5	26.6	12	23.8	13.8
Feeding (days/month)	31	29	16	31	6

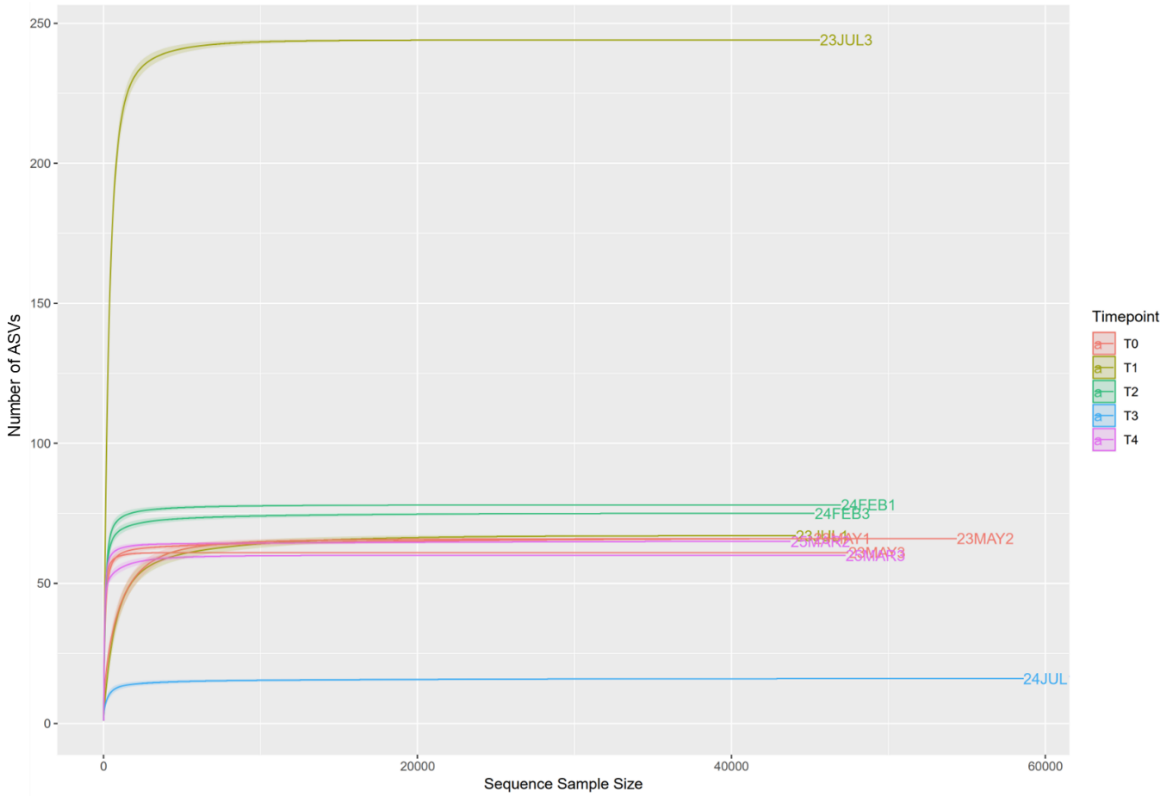

Figure S3: Alpha-diversity metrics rarefaction curves (number of total ASVs calculated from 16rDNA gene-based profiling analysis) in *S. aurata* anterior intestine for each pool (n=2) of each timepoint

Tab S4: Seabream gut bacterial community abundance in % of the 15 most present phyla (A) and of the 20 most present families (B). Data are expressed as a mean of 2 pools.

	T0 May 23	T1 Jul 23	T2 Feb 24	T3 Jul 24	T4 Mar 25
Pseudomonadota	62	8.1	53.6	88.9	21.7
Bacillota	10.2	51.6	7.7	0	25.2
Bacteroidota	13.5	16.3	16.4	0.6	33.4
Spirochaetota	3.5	20.5	12.9	10.2	4.1
Patescibacteria	2.3	1.3	3.8	0	3.2
Bdellovibrionota	2	0	1.8	0	1
Acidobacteriota	0.9	0.5	1.7	0	1.8
Verrucomicrobiota	2.1	0.5	0.2	0	1.9
Nitrospirota	1.5	0.3	1.4	0	1.3
Actinomycetota	0.6	0.1	0.7	0.3	1.7
Thermodesulfobacteriota	0.5	0.2	0	0	1
Campylobacterota	1	0	0	0	0.6
Planctomycetota	0	0.3	0	0	1.2
Armatimonadota	0	0	0	0	1.1
Cyanobacteriota	0.1	0.2	0	0	0.8
Other	0.1	0	0.1	0	0.1

B	T0 May 23	T1 Jul 23	T2 Feb 24	T3 Jul 24	T4 Mar 25
Vibrionaceae	62.8	0.2	46	89.7	0
Prevotellaceae	9.3	10.8	11.5	0	34.5
Clostridiaceae	0.6	45.8	0.3	0	0.6
Brevinemataceae	4.2	18.8	10.4	10.3	0.6
Spirochaetaceae	0.4	5	6.8	0	7.4
Lachnospiraceae	1.9	2.6	3.2	0	10.4
Muribaculaceae	3.6	2.3	1	0	5.6
Oscillospiraceae	0.6	2	0.6	0	8.1
Comamonadaceae	2.7	0.9	5.9	0	1.2
Moraxellaceae	1	4	2.6	0	2.3
Rikenellaceae	1.5	2.5	0.6	0	3.9
Chitinophagaceae	1.7	0.5	1.2	0	4.1
Nitrospiraceae	2	0.3	1.9	0	2.6
Rhodocyclaceae	0	0.6	0	0	5.8
Lactobacillaceae	0.3	1.8	0.5	0	3.3
Flavobacteriaceae	0.5	0	2.6	0	2.5
Sphingomonadaceae	1.2	0	3	0	1
Verrucomicrobiaceae	2.8	0.5	0	0	1.8
[Eubacterium].coprost	1.7	1.4	0	0	1.6
Oligoflexaceae	1	0	1.8	0	2
Other	0.2	0.1	0.3	0	0.6

References

Hughes, G.M., 1984. Measurement of gill area in fishes: practices and problems. J. Mar. Biol. Assoc. U. K. 64, 637–655. https://doi.org/10.1017/S0025315400030319

Ibarz, A., Beltrán, M., Fernández-Borràs, J., Gallardo, M.A., Sánchez, J., Blasco, J., 2007. Alterations in lipid metabolism and use of energy depots of gilthead sea bream (Sparus aurata) at low temperatures. Aquaculture 262, 470–480. https://doi.org/10.1016/j.aquaculture.2006.11.008

Pacorig, V., Galeotti, M., Beraldo, P., 2022. Multiparametric Semi-quantitative Scoring System for the histological evaluation of marine fish larval and juvenile quality. Aquac. Rep. 26, 101285. https://doi.org/10.1016/j.aqrep.2022.101285

Yıldız, M., Sener, E., Timur, M., 2006. Effect of Seasonal Change and Different Commercial Feeds on Proximate Composition of Sea Bream (Sparus aurata) Turkish Journal of Fisheries and Aquatic Sciences 6: 99-104 (2006).

Yýldýrým Korkut, Y.K.A., Gurkan, S., 2018. Length-weight relationship and condition factor as an indicator of growth and feeding intensity of Sea bream (Sparus aurata L, 1758) given feed with different protein contents. Indian J. Anim. Res. https://doi.org/10.18805/ijar.B-998

Chapter 7:

Dicentrarchus labrax

All analyses were carried out in selected samples, for a total of 6 sampling times.

Growth and physiological parameters

At the onset of monitoring in March 2024, seabass mean length, width and body weight were 24.59 ± 1.18 cm, 3.98 ± 0.37 cm, and 158.55 ± 20.77 g, respectively (**Fig. S1A,B,C**). By November 2024, fish reached the commercial size, with a mean body weight of 400.45 ± 58.90 g and mean length and width of 30.88 ± 2.45 cm and 7.21 ± 0.65 cm, respectively (**Fig. S1A,B,C**).

Data on physiological parameters are reported in **Fig. 2**. Condition factor (K) showed fairly constant values throughout the sampling period and growth, irrespectively of changes in temperature, showing generally lower values that those observed for seabream in the same period (mean = 1.11 ± 0.03) (**Fig. 2A**).

Specific Growth Rate (SGR) showed large fluctuations (**Fig. 2B**), with values comparable with those observed for seabream in the same period and highest in July; however, SGR data were not correlated with seawater temperature ($r = 0.60$, p value < 0.5, Spearman correlation test).

The length-weight relationship was $W = 0.0061L^{3.1847}$ with a scaling exponent $b = 3.1847 > 3$, indicating positive allometric growth also for seabass all over the sampling period (Kop et al., 2019) (**Fig. 2C**).

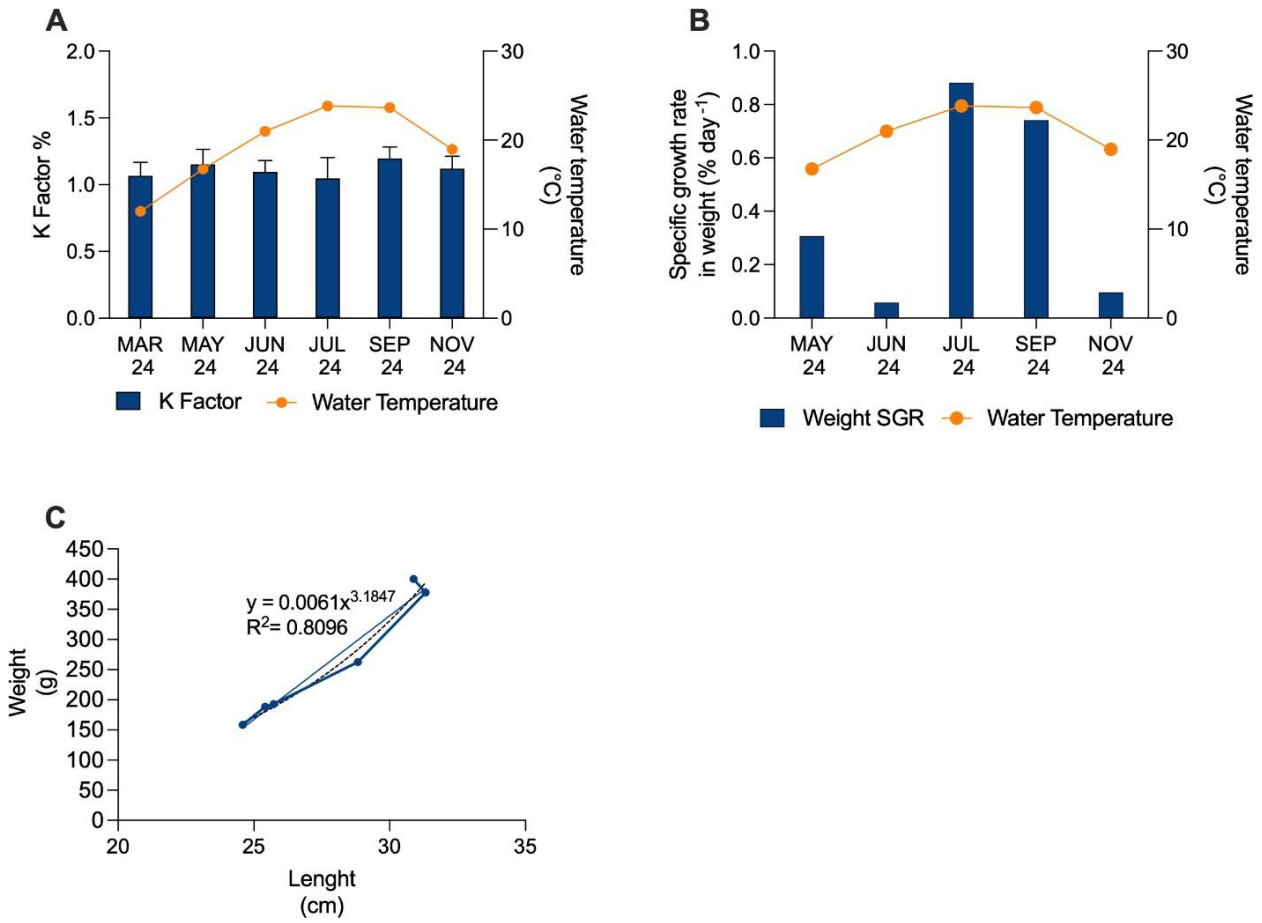

Figure 2 - Indicators of physiological growth performance in *D. labrax*: A) Condition factor (K); B) Specific Growth Rate (SGR), C) Length-Weight relationship. In A and B, changes in water temperature values are indicated by the orange lines. Data are expressed as means ± sd (N= 6).

The hepatosomatic index (HSI) showed a mean value of 1.73 ± 0.12 along the whole period (**Fig. 3A**) and fairly constant values throughout the sampling period and growth, irrespectively of changes in temperature.

The Gonado Somatic Index (GSI) was also calculated. As for seabream, only developing male gonads were observed. Highly fluctuating values were registered (**Fig. 3B**). Gonads were observed in 95% of the individuals.

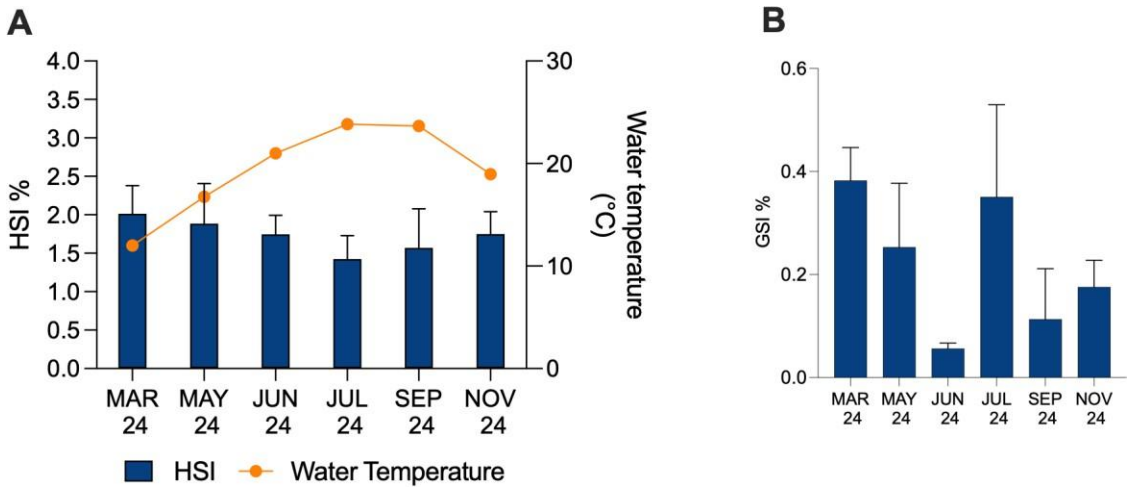

Figure 3 - Seasonal variations of HSI (A) and GSI (B) in *D. labrax* along growth. Data are expressed as means ± sd. (N= 6).

Enzymatic biomarkers

Data on enzymatic biomarkers of oxidative stress and biotransformation measured in liver and gills of *D. labrax* are presented in **Fig. 4**. CAT activity was higher in liver than in gills, with mean values of 176.70 ± 81.55 µmol/min/mg prot and 78.56 ± 39.24 µmol/min/mg prot, respectively, over the whole sampling period (**Fig. 4A**). Similarly, higher GST activities were detected in liver (120.67 ± 12.89 nmol/min/mg prot) with respect to gills (37.88 ± 7.47 nmol/min/mg prot) (**Fig. 4B**). Although fluctuations in activities of both enzymes were recorded over the sampling period, with significant differences between some months and mean values (**Fig. 4A** and **4B**), no clear trends could be observed with growth and season for either enzyme and tissue. The same applies to hepatic EROD activity, that showed a mean value of 3.04 ± 0.51 pmol/min/mg prot from March to September. A maximum activity was observed in November (16.69 ± 0.89) (**Fig. 3C**). Accordingly, no correlation was found between antioxidant and biotransformation enzyme activities in either tissue and water temperature, fish growth or age.

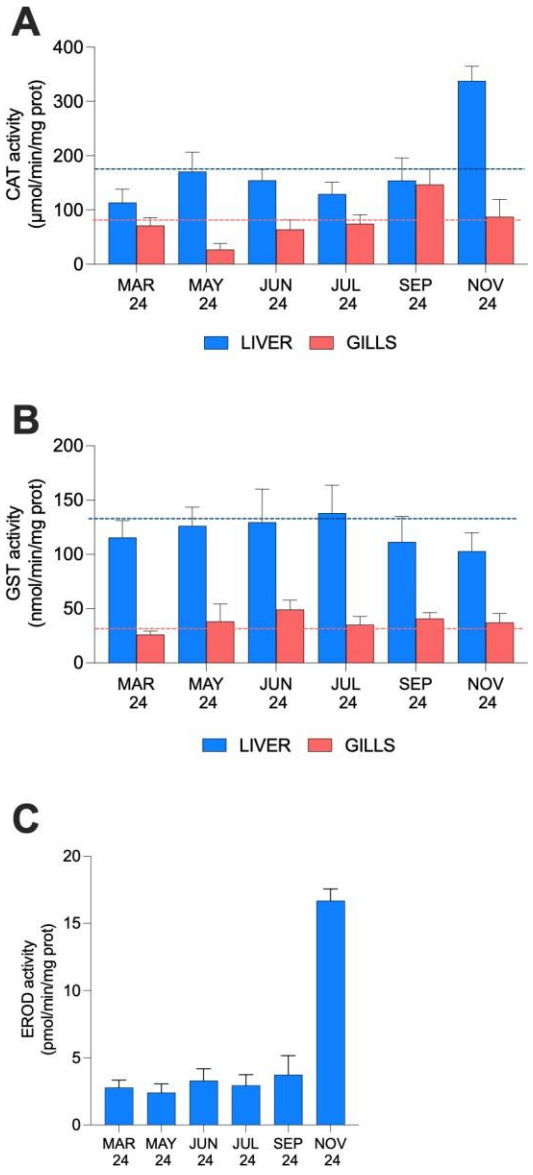

Figure 4 - Evaluation of enzymatic biomarkers of oxidative stress (in liver and gills) and biotransformation (in liver) of *D. labrax* along the sampling period. A) Catalase (CAT) activity, B) Glutathione-S-Transferase (GST) activity and C) EROD activity. Values are expressed as mean ± sd (N= 6). Statistical analyses were performed by one way ANOVA followed by Dunnett's multiple comparisons test, * = $p < 0.05$; monthly data *vs* mean data recorded across the whole sampling period (indicated by the dotted line).

Gut microbiome

Microbiome analysis was carried out on six selected samples from March 2024, corresponding to juvenile stage, to November 2024, at the end of the growth cycle. Fish body weight, feeding days and seawater temperature at these time points are summarized in **Tab. S2**.

16S rRNA PCR amplicon libraries were generated from genomic DNA extracted from fish intestine samples using primers amplifying the V3 – V4 variable regions of bacterial 16S rRNA gene. Libraries were generated using the Illumina 16S Metagenomic Sequencing Library preparation protocol.
Raw amplicons were denoised with AmpWrap (Doni et al., 2024).
Rarefaction curves calculated for total ASVs abundance reached the plateau, indicating a good sequencing depth to capture most of the total bacterial diversity (**Fig. S2**).

Taxonomic composition at the phylum level (**Fig. 5A**) highlighted the dominance in all samples of Bacterioidota (aka Firmicutes) (30.51 ± 8.91 %), Pseudomonadota (aka Proteobacteria) (mean 25.37 ± 6.62%) and Bacillota (22.87 ± 9.11 %), followed by smaller abundances of Patescibacteria (3.45 ± 1.89 %), Verrucomicrobiota (3.2 ± 1.58 %), Acidobacteriota (2.32 ± 3.19 %) and Spirochaetota (2.08 ± 2.36 %). All other families showed abundances < 2%. For more details see **Tab. S4**.

In March 2024, samples showed high abundance of Bacteroidota (30.1%), followed by Pseudomonadota (15.2%), Bacillota (14.2%) and Acidobacteriota (8.7%), and lower amounts of Patescibacteria (6.9%), Campylobacteriota (5.3%), Bdellovibrionota (4.5%). May was totally dominated by Bacteroidota (35.5%), Pseudomonadota (30.2%) and Bacillota (20.3%), together representing the 85% of all phyla, whereas abundance of other less represented groups was largely decreased; for example, Acidobacteriota fell to abundance < 1%. A similar composition was observed in June for the three most represented phyla: Bacteroidota (39%), Bacillota (24.6%), and Pseudomonadota (21.5 %). However, a large increase of Thermodesulfobacteriota (9.6%) was observed with respect to the previous months (< 0.5).
A dramatic decrease in Bacteroidota was observed in July samples (13%), that were dominated by Bacillota and Pseudomonadota (about 70%). Patescibacteria and Verrucomicrobiota were present at
3.7 and 3.4% respectively, whereas abundances of other groups were <2%. In September, Bacteroidota returned to values similar to those of the previous months (32.4 %), followed by Pseudomonadota (30.6%), Bacillota (14.2%) and Verrucomicrobiota (5%). In September, an increase of Spirochaetota (5.3%) was observed with respect to the previous months (always < 2%). Such a composition remained quite stable in November: Bacteroidota (33.3%), Bacillota (24.7%), Pseudomonadota (21.6%) and Spirochaetota (5.8%).

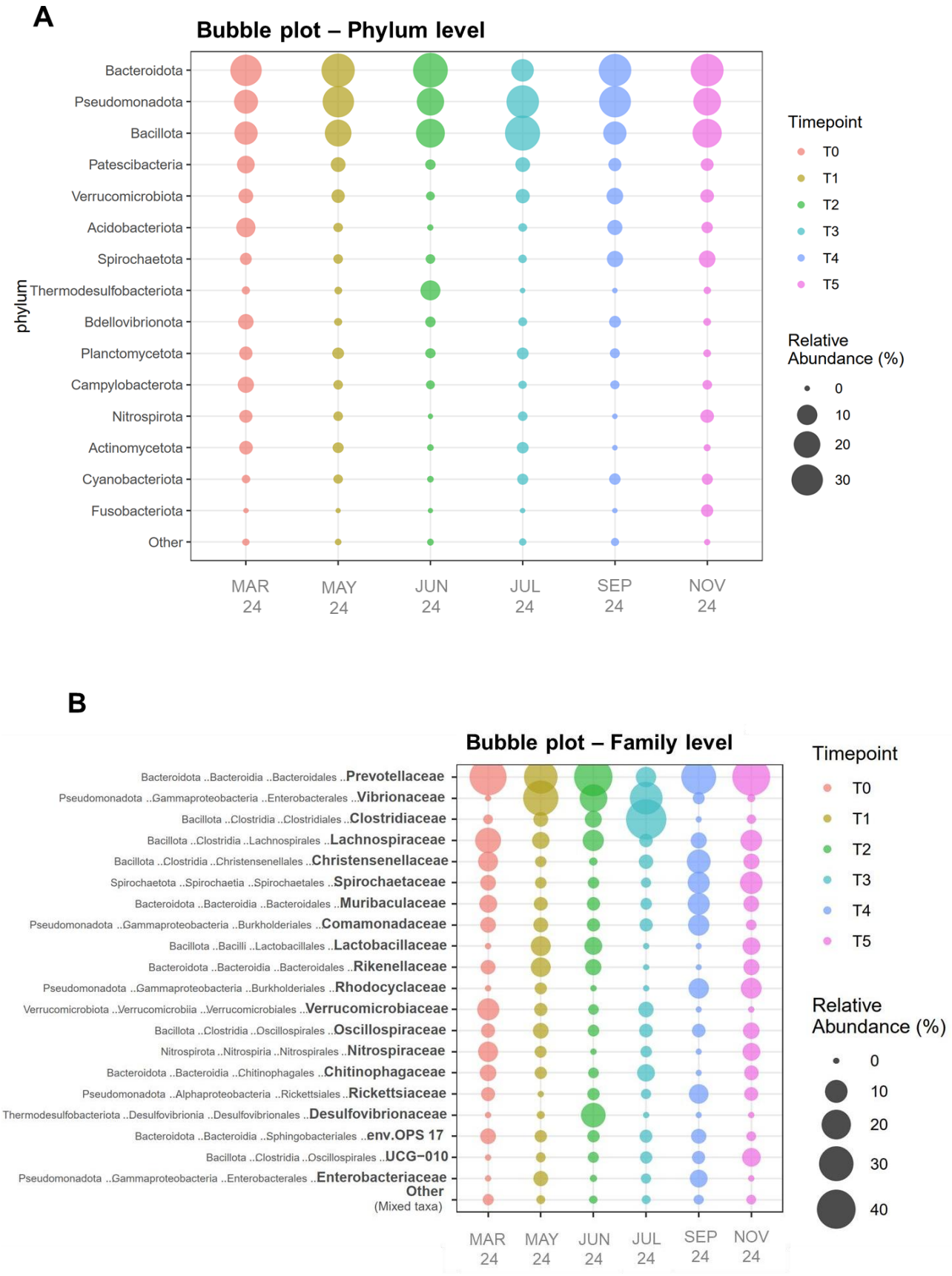

Figure 5 - Bubble plots representing the seabass gut bacterial community at two phylogenetic levels: A) Top 15 Phyla; B) Top 20 Families. Mean data from 2 pools for each sampling time.

At the family level (Fig. 5B), the most represented group was Prevotellaceae (29%) followed by Vibrionaceae (12.5%), Clostridiaceae (8.5%), Lachnospiraceae (7%), Christensenellaceae (4.3%) and Spirochetaceae (4.1%). Other less represented families were Muribaculaceae, Lactobacillaceae, Rikenellaceae and Comamonadaceae (<4%). For more details see **Tab. S4**.
In March, samples were characterized by Prevotellaceae (34.6%), followed by Lachnospiraceae (14.3%), Verrucomicrobiaceae (9.4%), Nitrospiraceae (7.3%) and Muribaculaceae (5%), and many other families with abundances between 3 and 1%. A dramatic shift was observed in May, showing the dominance of Vibrionaceae (30.8%), not detected in the previous sampling, followed by Prevotellaceae (27.5%) and the increase in Lactobacillaceae (from 0% to 7.2%) and Rikenellaceae (from 2.6% to 6.7%). Changes in several less represented families were also observed. In June, the abundance of Prevotellaceae was restored to 38.5% and a decrease of Vibrionaceae (16.9%) was observed. An increase of Desulfovibrionaceae was observed (12.5%), which in previous months was always <0.1. In July 2024, a dramatic decrease of Prevotellaceae (7.3%) and increase of Clostridiaceae (43.3%) were observed. Vibrionaceae slightly increased (26.1%). In September, Clostridiaceae and Vibrionaceae fell to 0% and 1.3% respectively. September was characterized by a more heterogeneous composition: Prevotellaceae (29.9%), Christensenellaceae (11.8%) and Spirochaetaceae and Muribaculaceae, both at 9.3%, and more families with abundances between 8% and 3% of abundance. November sample composition was dominated by Prevotellaceae (37.1%), followed by Spirochaetaceae (9.7%) and Lachnospiraceae (8.8%). Decrease in Christensenellaceae (3.5%) and Muribaculaceae (3.4%) were observed. Clostridiaceae and Vibrionaceae were at 0.4% and 0.1% respectively. The remaining composition was characterized by a heterogeneous abundance of less present families (between 8% and 2%).

Alpha-diversity analysis using the Chao1 index showed that bacterial diversity was similar among all samples, with slightly lower values in June and July (**Fig. 6**). The Shannon index, which reflects both richness and evenness of bacterial communities, showed a decrease from May to July. These results are in line with microbiota composition data, showing that bacterial communities were almost entirely represented by Prevotellaceae and Desulfovibrionaceae in June and Clostridiaceae in July.

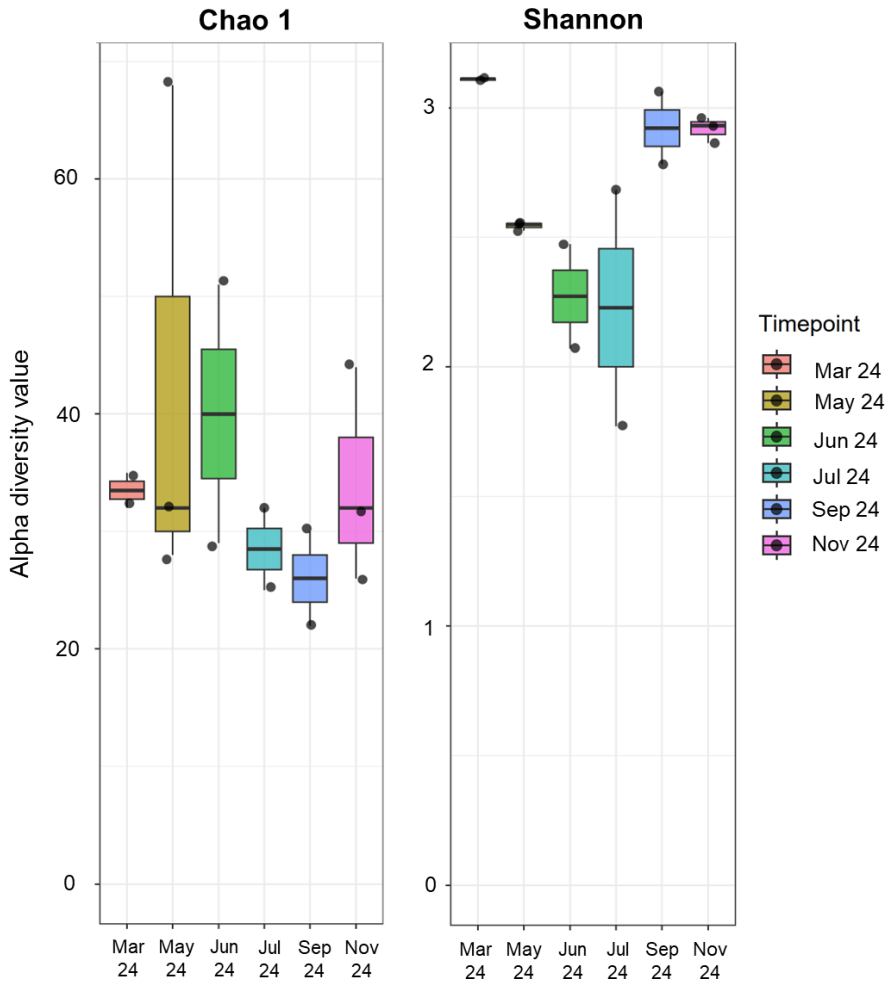

Figure 6 - Box plots representing the median, minimum and maximum of richness estimates of the Alfa-diversity estimator Chao1 and Shannon diversity index of anterior intestine microbial populations of seabass at each sampling time Mar24, May24, Jun24, Jul24, Sep24 and Nov24 at family level.

Supplementary material

Materials and methods

Table S1: Proximate % composition of Alterna Bass Skretting as provided by the manufacturers 2P: pellet diameter corresponding 4.0 mm.

ALTERNA BASS	
Composition %	**2P**
Moisture	22.2
Crude protein	45.0
Crude fat	20.0
Crude fibers	4.0
Ash	7.7
Phosphorus	1.1
DE (MJ/kg)	17.5

Results

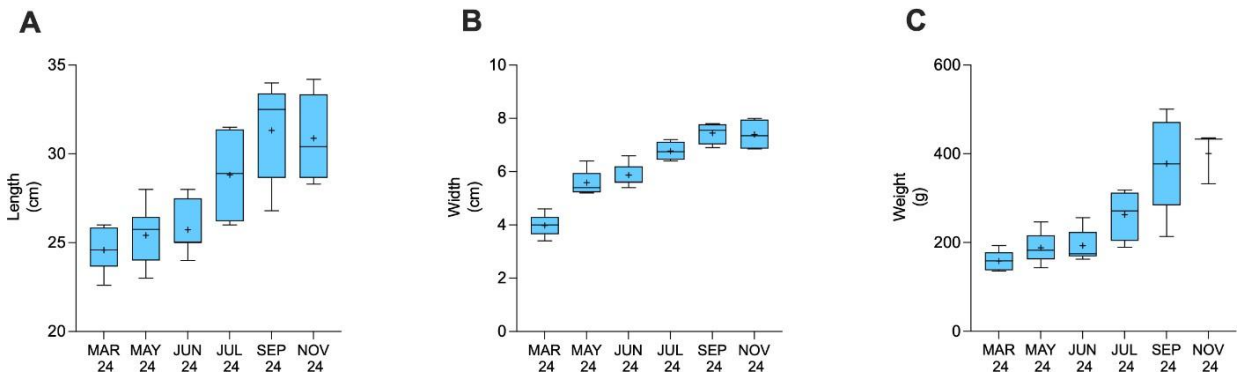

Figure S1 - Morphometric parameters of *D. labrax* overtime: A) Length; B) width and C) weight. Boxplots indicate the median (—), the mean (+), 5th and 75th percentiles (box), min and max range (whiskers).

Table S2 – Sampling times for microbiome analysis of anterior intestine samples of *D. labrax*

	MAR	MAY	JUN	JUL	SEP	NOV
Body weight (mean ± SD)	158.5 ± 20.8	188.3 ± 33.7	192.9 ± 34.7	262.6 ± 57.9	377.7 ± 108.1	400.5 ± 58.9
Water Temperature (°C)	12.0	16.8	21	23.8	23.7	19.0
Feeding (days/month)	15	23	29	31	22	21

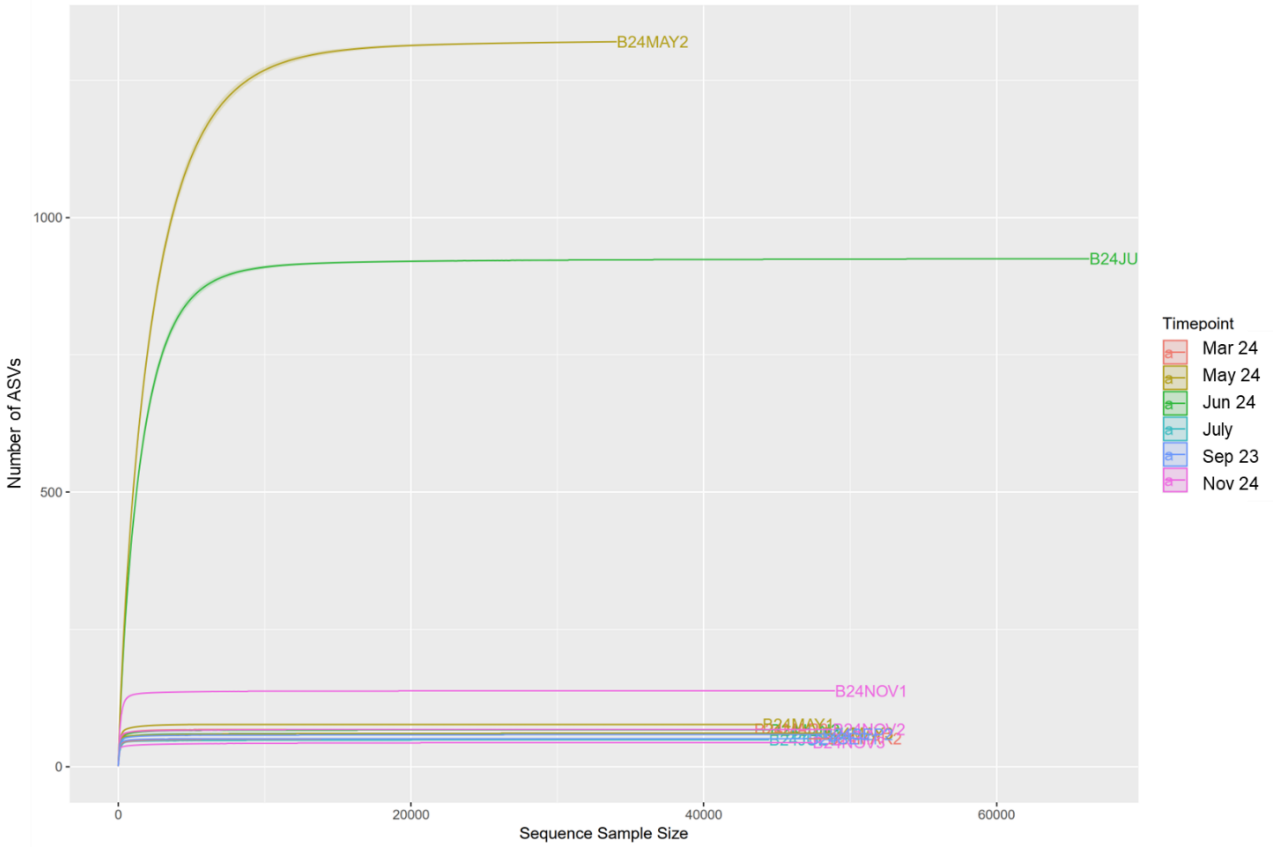

Figure S2 - Alpha-diversity metrics rarefaction curves (number of total ASVs calculated from 16rDNA gene-based profiling analysis) in *D. labrax* anterior intestine for each pool (n=2) of each timepoint.

Tab S3: Seabass gut bacterial community abundance in % of the 15 most present phyla (A) and of the 20 most present families. Data are expressed as a mean of 2 pools.

A	Mar 24	May 24	Jun 24	Jul 24	Sep 24	Nov 24
Bacteroidota	30.1	35.3	39	13	32.4	33.3
Pseudomonadota	15.2	30.2	21.5	33.1	30.6	21.6
Bacillota	14.2	20.3	24.6	39.2	14.2	24.7
Patescibacteria	6.9	4	1.2	3.7	2.6	2.3
Verrucomicrobiota	3.8	3	0.5	3.4	5.6	2.9
Acidobacteriota	8.7	0.8	0	0.5	4.1	1.6
Spirochaetota	1.9	0.8	0.7	0.4	5.3	5.8
Thermodesulfobacteriota	0.3	0.2	9.6	0	0	0.2
Bdellovibrionota	4.5	0.3	1.2	0.5	1.8	0.2
Planctomycetota	2.9	1.6	1	1.8	0.9	0.2
Campylobacterota	5.3	0.7	0.6	0.4	0.6	0.8
Nitrospirota	2.6	0.8	0	0.7	0	2.8
Actinomycetota	2.9	1.3	0.1	1.7	0	0.1
Cyanobacteriota	0.4	0.6	0.1	1.5	1.5	1.4
Fusobacteriota	0	0	0	0	0	2.1
Other	0.1	0.1	0.1	0.1	0.3	0

B	Mar 24	May 24	Jun 24	Jul 24	Sep 24	Nov 24
Prevotellaceae	34.6	27.5	38.5	7.3	29.9	37.1
Vibrionaceae	0	30.8	16.9	26.1	1.3	0.1
Clostridiaceae	0.5	2.7	4.2	43.3	0	0.4
Lachnospiraceae	14.3	4.6	8.5	1.9	3.8	8.8
Christensenellaceae	7.1	0.9	0.2	2.5	11.8	3.5
Spirochaetaceae	3.3	1.1	0.9	0.6	9.3	9.7
Muribaculaceae	5	2.1	1.8	1	9.3	3.4
Comamonadaceae	3.2	2.6	1.8	1	9.3	3.4
Lactobacillaceae	0	7.2	4.9	0	0	4.8
Rikenellaceae	2.6	6.7	3.6	0	0	3.7
Rhodocyclaceae	0	1.2	0	0	7.4	7.9
Verrucomicrobiaceae	9.4	1.8	0.6	3.2	0	0
Oscillospiraceae	2.3	3.4	1.1	2.1	1.8	3.9
Nitrospiraceae	7.3	1.2	0	0	7.4	7.9
Chitinophagaceae	3.9	1.2	0.8	4.8	0	4.8
Rickettsiaceae	2.2	0	1.3	0.6	6.8	2.2
Desulfovibrionaceae	0	0.1	12.5	0	0	0
env.OPS 17	3.4	1.4	1.3	1.6	2.9	0.4
UCG−010	0	0.5	0.8	1.3	1.8	5.6
Enterobacteriaceae	0	2.9	0	0.6	5	0
Other	0.9	0.2	0.2	0.3	0.6	0.5

References

Doni, L., Marotta, A., Vezzulli, L., Bosi, E., 2024. AmpWrap: a one-line fully automated amplicon metabarcoding 16S and 18S rRNA gene analysis. Bioinforma. Adv. 5, vbaf312. https://doi.org/10.1093/bioadv/vbaf312

Discussion

In order to get a general overview of the health status of fish from the same aquaculture farm, the results presented in Chapter 6 and 7 for *S. aurata* e *D. labrax*, respectively, are discussed together.

Background

Seabream and seabass farming requires between a year and a half and two years to produce commercial-size fish of 300 - 500 g, depending on rearing conditions, and seasonal variations in water temperature and photoperiod (FAO, 2024).

With regards to temperature, most of the studies on *S. aurata* and *D. labrax* cultured in the Mediterranean indicate optimal growth conditions between 20 and 25 °C (Mhalhel et al., 2023; Pelusio et al., 2021). In contrast, both species are highly sensitive to low temperatures, *S. aurata* in particular. In farming conditions, the decrease in temperature becomes critical for gilthead seabream, and below 13 °C fish lowers its metabolic activity, with significant decrease in feed consumption and growth performance (Ibarz et al., 2007; Kousoulaki et al., 2015; Sánchez-Nuño et al., 2018; Silva et al., 2014). Several studies have been focused on the effects of winter feeds *in S. aurata* to overcome metabolic alterations, nutritional disorders, immune suppression that can occur in colder months, often resulting in the 'winter syndrome', a multifactorial pathology affecting cultured gilthead seabream in cold water, characterized by chronic mortality in winter and acute episodes when temperatures rise (Cascarano et al., 2021 and refs therein). Rising water temperatures also represent a major challenge, especially for gilthead seabream, which exhibits lower thermal tolerance compared with European seabass (Cascarano et al., 2021).

Therefore, environmental temperature and feeding regimen are considered the main factors affecting growth and health performance of aquacultured seabream and seabass.

In both *S. aurata* and *D. labrax* aquaculture, about 45% of the production cost is attributed to the diet (FEAP, 2025; García García et al., 2019). This gave rise to a large number of experimental trials with different diets (containing different lipid and protein contents and sources, addition of functional ingredients, etc.) to optimize growth and health conditions, in seabream in particular. In general, the total lipid content varies between 15 and 21% on a dry weight basis; however, especially at temperatures below 13° C, excess in dietary lipids can be accumulated as a fat depot in perivisceral tissue due to low metabolic activity (Ibarz et al., 2007). Overall, a large number of studies report data on growth and physiological status of farmed seabream in different controlled experimental conditions (diet composition, environmental parameters)(reviewed in Mhalhel et al., 2023). Actually, a PubMed search for 'seabream, diet, growth' gave 214 hits in the last 10 years (January 2026). Less information is available on seabass: indeed, the same PubMed

search for “seabass, diet, growth” gave only 39 results.

In contrast to the amount of studies carried out in experimental trials, much less studies are focused on seabream and seabass along the growth cycle in offshore farming (Fazio et al., 2013; Kaya Öztürk et al., 2020; Klinger et al., 2017). Due to the relatively strict environmental requirements of early life stages of fish, this production is maintained on land, in controlled temperature conditions to maximize health and production per unit of feed. The juvenile stages (e.g. 5–100 g), are then transferred to open ocean cages, where the major constraint to growth and production is represented by water temperatures (García García et al., 2019; Klinger et al., 2017).

Actually, monitoring fish growth performance and health parameters in the actual offshore farming conditions can represent a significant help for producers, suggesting adaptation measures, such as the use of different feeds, to overcome the negative effects of environmental temperature, and provide information to consumers and regulatory authorities on welfare of farmed fish, at the same time contributing to environmental sustainability. These topics have become of great concern in the last decade, being widely accepted that fish in good health and welfare state will grow better (Ashley et al., 2007).

Results

The results obtained in this work (Chapter 6 and 7) represent the first data on monitoring growth and health status of seabream and seabass reared in an offshore farm in Italy, from fry and juvenile stage to marketable size, respectively. Both fish species were fed commercial diets applying a feeding regimen established by the farmers, based on individual growth and water temperature, including the utilization of feed variants with natural additives to protect animals from the decrease in temperatures, inflammation and common parasites.

A limitation of the present study, with respect to experimental feeding trials, is the lack of information on the exact composition of different commercial feeds and feed variants utilized by the farmers, that are not at present provided by the manufacturers. All feeds were specifically developed for either seabream or seabass, and declared the presence of both fish meal and plant meal, but the proportion of different sources was not provided. In this light, first analyses on detailed chemical composition of each feed have been commissioned by the Aqua company.

The only quantitative information available was that on proximate % composition of main dietary components (See SI). For seabream feeds, average fat content was always 16% along the whole growth cycle; the protein content in different feed variants was higher in the first year of

growth (54- 51%) and lower in the second (47-48%). Only for a two months period (Nov-Dec 2024) the feed had higher lipid content (18%) and lower proteins (46%) (see Methods and Table S1). For seabass, the same seabream feeding regimen was utilized until a body weight of about 150 g. Afterwards, from the beginning to the end of the monitoring period, fish were fed a specific seabass diet, containing a higher proportion of fat (20%) and lower protein content (46%).

Common indicators of fish growth and health include biometry, condition indexes, morphological and skeletal anomalies and caudal fin erosion (Bordignon et al., 2025; Noble et al., 2026). In the present work, macroscopical observation did not reveal any sign of disease, presence of parasites, or altered morphology at individual and tissue level. Morphometric and physiological parameters related to growth were first evaluated. The results indicate, for both species, high values of the condition factor K (>1) across the whole period, indicating good/ excellent conditions (Faggio et al., 2014; Yýldýrým Korkut and Gurkan, 2018).

In *S. aurata,* periods of weight gain were identified between May and November in both 2023 and 2024, corresponding to warmer months (T > 22 °C), followed by stable body weights in winter (from January to March), corresponding to lower water temperatures (about 14 °C). Specific Growth Rate (SGR), showed large seasonal variations; obtained values showed a significant positive correlation with temperature along the whole monitoring period. Lowest SGR values observed in winter are in line with previous literature data describing a 'winter growth arrest' in experimental conditions where seabream were brought from 22 to 14 °C (Pelusio et al., 2021; Sánchez-Nuño et al., 2018). This is due to the decrease in the fish metabolic rates and in the amount of feed consumed at lowering water temperatures.

D. labrax was monitored across a much shorter period. Fish growth is typically faster during the first year of life (Menna O et al., 2021), whereas the European seabass in the present study were already one year old and exhibited SGR values not exceeding 0.8, in line with studies on fish juveniles (Alfonso et al., 2023). Although a clear seasonal growth trend was not identified, higher SGR values were recorded in July and September, corresponding to the warmest months. Moreover, SGR values were generally comparable with those observed in *S. aurata* from June 2024, when the individuals were also approximately one year old.

Fish may show isometric growth, negative allometric growth or positive allometric growth. According to the formula $W = aL^b$, isometric growth (b=3) means that the body shape does not change as an organism grows. Negative allometric growth (b<3) means that a fish becomes thinner as its weight increases; positive allometric growth (b>3) means that its body becomes

relatively broader as the length increases (Riedel et al., 2007). Our data show a positive allometric growth along the whole monitoring period for both species (b = 3.2491 and b = 3.1847 for seabream and seabass respectively). In contrast, literature data reported slightly negative allometric growth for seabream reared in the Mediterranean Sea (Yýldýrým Korkut and Gurkan, 2018, and refs. therein). However, this was ascribed to gonadal development during the period of study. In *S. aurata*, sexual maturity first develops in males at 2 years of age (20-30 cm) and in females at 2-3 years (33-40 cm). Accordingly, in the present work, development of male gonads was observed only from July 2024, when fish reached a body length > 20 cm and weight > 200 g, as indicated by GSI data. Overall, standard morphometric and physiological measurements at the whole organism level indicate good growth performance and health conditions.

Less information is available on seabass. A study conducted on European seabass farmed in off-shore cages situated along Portuguese Atlantic coast reported negative allometric growth during summer and positive allometric growth in spring and autumn (Orduna et al., 2023). As the specimens examined in the present study were already older than 1 year, all individuals have reached the size for developing gonads. Accordingly, development of male gonads was observed in 95% of samples throughout the monitoring period.

HSI represents a key indicator of a fish energy reserves, liver health, and overall body condition; this parameter is generally used to assess environmental stress, pollution, diet, and reproductive status, often changing with season, temperature, and migration (Schilling et al., 2025). Our data on *S. aurata* show seasonal changes in HIS that were inversely correlated with temperature. Higher HSI values recorded at lower temperatures in winter are in line with other literature data, indicating that such a physiological response to decreasing T is ascribed to hepatic deposition of lipids due to their higher mobilization from other tissues (Ibarz et al., 2007; Mininni et al., 2014). Accordingly, liver lipid content was higher at lower temperatures, and positively correlated with HSI values. Other histological observations of liver, gills and intestine, showed a generally normal appearance and absence of significant present of parasites across the whole sampling period.

In seabass, HSI did not display a seasonal trend; these results in line literature and with seabass being more tolerant towards temperature fluctuations (Arafat et al., 2025). No histopathological analyses were conducted in seabass tissues.

At the tissue level, enzymatic biomarkers related to oxidative stress and biotransformation activities, CAT, GST and EROD, were evaluated. CAT is directly involved in degradation of hydrogen peroxide, thus representing a primary antioxidant defense against production of oxygen

reactive species (ROS) and their derivatives; GST is major second-phase detoxification enzyme, playing a role in preventing oxidative damage by generating less toxic/more hydrophilic compounds through the conjugation of breakdown products of lipid peroxidase to glutathione (Martınez-Alvarez et al., 2005). EROD activity represents a specific biomarker of Phase I biotransformation of lipophilic compounds (OSPAR, 2013). Mean values of each enzymatic biomarkers are in line with those recorded in healthy specimens of *S. aurata* (Capó et al., 2021; Maradonna et al., 2014; Telli-Karakoç and Barlas, 2019) and *D. labrax* (Amaral et al., 2023; Guerreiro et al., 2015; Sinha et al., 2015). For both species the results indicate the absence of a significant trend in activity of each enzyme in both gills and liver along growth at different temperatures. The peak in seabass liver EROD activity observed in November 2024 was not apparently related to steroid metabolism during gonad maturation, as GSI values were not increased with respect to the previous months; however, it could be partly ascribed to the large increase in the amount of feed with respect previous month.
Overall, these data indicate the absence of oxidative stress conditions or induction of biotransformation processes of lipophilic compounds and confirm the absence of stressful conditions at the tissue level throughout the monitoring study in both species.

The characterization and monitoring of the intestinal microbiota represent essential components of health assessment in aquaculture. Gut microbiota studies are emerging as effective approaches for promoting farmed fish health, contributing to improve the productivity of the aquaculture sector (Brugman et al., 2018; Egan et al., 2020; Egerton et al., 2018). In this regard, it is noteworthy that measurements of gut microbiota diversity are considered a good indicator of animal health, with dietary factors representing one of the main regulators of intestinal microbial diversity (Moschen et al., 2012). Moreover, the fish gut microbiome is heavily influenced by factors such as water temperature, salinity, oxygen concentration, diet, feeding habits, habitat community, and intrinsic factors such as genetics and developmental stages (Feijão et al., 2025). The vast available literature describing the intestinal microbiota of gilthead sea bream agrees on a general pattern with a dominance of the phylum Proteobacteria, followed by Bacillota (aka Firmicutes), Actinobacteriota and Bacteroidota (Naya-Català et al., 2022; Pelusio et al., 2021; Quero et al., 2023; Ruiz et al., 2023; Solé-Jiménez et al., 2021; Tapia-Paniagua et al., 2019). Most of these studies report data on gut microbiota composition of farmed seabream in different controlled experimental conditions (diet composition, supplement feeds, environmental parameters), but little information is available on seabream microbiota variations along the growth cycle in offshore farming (Piazzon et al., 2019).

The results of the present work represent the first data on microbiota composition of anterior intestine of *S. aurata* grown in an open sea farm, from fry to marketable size. All samples were dominated by Pseudomonadota (aka Proteobacteria), followed by Bacillota (aka Firmicutes) and Bacterioidota. Proteobacteria (facultative anaerobic organisms) are one of the most abundant symbionts in marine fish, because of their highly flexible metabolic properties (Ikeda-Ohtsubo et al., 2018; Tarnecki et al., 2017). However, large shifts in abundance of this phylum were recorded along growth: a drop was observed at T1 (July 2023), followed by a subsequent increase in the following summer (with a maximum at T3, July 2024). Within Proteobacteria, high abundances were found for the Vibrionaceae family in all samples, reaching up to 90% at T3. Members of this family help to digest organic substances due to the production of lipases, amylases and proteases; however, some species can also produce harmful enzymes like neuraminidases and act as causative agents of fish pathologies (Egerton et al., 2018). Interestingly, in samples where Pseudomonadota showed lower abundance, they were represented by various families other than Vibrionaceae (Moraxellaceae, Rhodocyclaceae, and Comamonadaceae).

The second and third most abundant phyla in all groups were Bacillota and Bacteroidota. Bacteroidota, represented by different families, were rather stable along growth, except for T3 samples. Bacillota showed an opposite trend with respect to Proteobacteria, with highest and lowest abundance at T1 and T3, respectively. These fluctuations were reflected at the family level. At T1, Bacillota were mainly represented by Clostridiaceae, normally present in the intestinal microbiota of fish, where they are crucial for the degradation of complex carbohydrates—especially in herbivorous species—and they produce butyrate, a short-chain fatty acid that is essential for intestinal health and nutrient absorption (Li et al., 2024).

However, our data show some differences with respect to those of literature data on seabream gut microbiome; in all samples, Actinomycetota were present with low abundance at the phylum level, and absent from the top 20 most represented taxa at the family level. A decreased abundance of Actinobacteria (which are often associated with healthy, diverse gut flora) can alter the fish ability to cope with potential stress-induced changes in the intestinal mucosa. Emerging contaminants and pollutants often lead to imbalances in the gut microbiota, particularly reducing beneficial bacteria like Actinobacteria (Song et al., 2025 and refs therein). Moreover, in T1-T3 samples, Spirochaetota were generally detected at higher abundance, mainly represented by Brevinemataceae and Spirochaetaceae. In a recent study, increases in members of Spirochaetota have been observed in seabream gut microbiome following high temperature stress, that were almost completely reversed by the use of dietary emulsifiers in combination with low energized

diets (Domingo-Bretón et al., 2025). However, high abundance of this taxon were recorded also in T2 samples, collected at low temperatures in February. The abundance of this taxonomic group has been found in fish fed a low marine protein diet and can be due to some of the feed ingredients such as yeast protein, fermented soya and sunflower meal, and to the increased supply of complex/non-digestible carbohydrates in carnivorous fish (Alfonso et al., 2023, and refs. therein),

Overall, the results show a progressive increase in bacterial diversity along seabream growth, from fry to marketable size. These changes are in line with the results obtained by morphological, physiological, and biomarker data, indicating good health and growth conditions. Therefore, shifts in microbiota composition observed among samples may be mainly related to the type/amount of feed utilized along the production cycle. However, at present, the exact composition of each feed variant is not provided by the manufacturers. Moreover, the possible role of environmental factors, including the presence of emerging contaminants, cannot be ruled out.

Similarly, the microbiome composition of European seabass anterior intestine was evaluated from juvenile stage (March 2024) to marketable size (November 2024). It is worth noting, as already previously mentioned, that much less information is available on microbiome composition of *D. labrax*, essentially from feeding trials.

The intestinal microbiota in this study was dominated by Bacteroidota, Pseudomonadota (aka Proteobacteria), and Bacillota (aka Firmicutes) throughout most sampling periods, with lower contributions from Patescibacteria, Verrucomicrobiota, Acidobacteriota, and Spirochaetota. This phylum-level structure aligns with previous work on the gut microbiota of *D. labrax*, which consistently reports Proteobacteria and Bacillota as major components, often accompanied by Bacteroidota and Actinobacteria, regardless of diet in both experimental and aquaculture settings (Alfonso et al., 2023; Serra et al., 2021). Among Bacteroidota, the most abundant family was represented by Prevotellaceae, whose members are important primary fermenters in fish intestine, through which complex carbohydrates enter the microbial metabolic network and provide soluble sugars and amino acids available for all type of cells (Ikeda-Ohtsubo et al., 2018).

Among Pseudomonadota, a transient bloom of Vibrionaceae was recorded in July, associated with reduced diversity indexes. Clostridiaceae, belonging to the third most represented phylum, Bacillota, were highly present in July, where, together with Vibrionaceae, represented almost the 70% of the family abundance. Members of the Clostridiaceae family are anaerobic fermentative

bacteria with carbohydrolytic potential, not only associated with pathogenic strains; indeed, many positive effects on animal health, including anti-inflammatory properties, epithelial barrier strengthening, and disease resistance have been reported (Piazzon et al., 2020, 2019).

The restoration of a richer bacterial community at family level was observed in September and November, that dominated by Prevotellaceae, followed by an heterogeneous abundance of less present families, indicating a return toward a balanced microbiota after seasonal perturbations (Egerton et al., 2018; Pérez-Pascual et al., 2021).

Overall, these data seem to support the high variability and sensitivity of seabass microbiome to different type of factors; however, seabream gut microbiota is apparently more sensitive and plastic— it shifts quickly in response to both internal (diet, age) and external (environment, farming practices) factors with respect to that of seabream.

For seabream microbiome, the high sensitivity is a double-edged sword: it enables adaptation, but also makes the system fragile, in particular in aquaculture systems, influencing feed efficiency, resistance to disease, welfare and survival. Key sensitivity drivers are the diet (strongest factor), with plant-based diets causing major microbial shifts, anti-nutritional factors (soy saponins, fibers) that can destabilize microbiota and promote dysbiosis, environmental conditions, developmental stage (early-life microbiota is especially sensitive and critical for immune development). Other factors are represented by administration of antibiotics and chemotherapeutics or stress conditions (handling, stocking density), that do not apply to the farming practises utilized in the present study. These changes can in turn affect production of short-chain fatty acids, induce shifts in immune modulation, impact on nutrient absorption and growth performance.

Therefore, the results presented, although preliminary since obtained at selected time points, underline how the evaluation of gut microbiota can highlight possible changes occurring in seabream gut metabolism and function during its growth cycle, thus representing a useful tool to provide additional information for farmers to optimize the rearing conditions. Ongoing analysis of gut microbiota along the whole growth cycle may also help understanding its relationship with growth stage, temperature, and amount/type of feed.

Conclusions and Perspectives

European Union seabream and seabass sales are projected to grow from 2025 to 2035 (about 156.5% total growth), with demand forecast to expand at a compound annual growth rate (CAGR) in the next decade. According to the globally cited FMI Food Intelligence Database, the overall industry size is expected to grow by nearly 2.6X during the same period, supported by the increasing consumer preference for premium white fish species, growing awareness of Mediterranean diet health benefits, expanding aquaculture production capabilities across Mediterranean regions, and rising demand for sustainable seafood throughout European foodservice and retail channels (future Market Insights, n.d.).

Over the past twenty years, the gilthead seabream and European seabass aquaculture industry has undergone a rapid development, with impressive advancements in knowledge on rearing methods, disease management, nutrition. The quality of fish, as perceived by consumers, depends on morphological and organoleptic features that should closely resemble those of wild fish. However, with increasing knowledge on fish physiology and changes in their health status in response to different stressors, evaluation of their health status and welfare during growth under different farming conditions is becoming a key issue in fish aquaculture, and an important tool for early monitoring the quality of production across the whole growth cycle. In a global change scenario, this is particularly relevant in open-ocean aquaculture, where the heterogeneous effects of climate changes at a regional scale may result in changes in growth rates and production (Klinger et al., 2017). Such an approach is also in line with the One Health perspective, developed for managing aquatic animal health and successful industry outcomes, particularly in respect to aquaculture (Stentiford et al., 2020).

Overall, the results of the present work, that combine standard morphometric and physiological parameters with tissue biomarkers and microbiome analyses in a multi- parameter approach, represent a first step forward in knowledge on monitoring growth and health status of *S. aurata* and *D. labrax* from an offshore farm in Italy. This kind of data can be utilized as a feedback loop that will help understanding the conditions for maintenance and improvement of health and welfare of farmed seabream and seabass for a sustainable aquaculture. This would greatly help the implementation of health management approaches: as suggested by the Standing Committee on Agricultural Research (SCAR) reports on welfare priorities and fish diseases, fish health and welfare is an issue of high research priority for European fish farming, as it affects not only the productivity and profitability of the sector but also the public perception and acceptance of aquaculture products (FAO, 2024, p. 202).

References

Alfonso, S., Mente, E., Fiocchi, E., Manfrin, A., Dimitroglou, A., Papaharisis, L., Barkas, D., Toomey, L., Boscarato, M., Losasso, C., Peruzzo, A., Stefani, A., Zupa, W., Spedicato, M.T., Nengas, I., Lembo, G., Carbonara, P., 2023. Growth performance, gut microbiota composition, health and welfare of European sea bass (Dicentrarchus labrax) fed an environmentally and economically sustainable low marine protein diet in sea cages. Sci. Rep. 13, 21269. https://doi.org/10.1038/s41598-023-48533-3

Amaral, D., Filipe, D.M., Cavalheri, T.F., Vieira, L., Magalhães, R.P., Belo, I., Peres, H., Ozório, R.O.D.A., 2023. Solid-State Fermentation of Plant Feedstuff Mixture Affected the Physiological Responses of European Seabass (Dicentrarchus labrax) Reared at Different Temperatures and Subjected to Salinity Oscillation. Animals 13, 393. https://doi.org/10.3390/ani13030393

Arafat, M., Hassan, Z., Farid, O.A.-H.A., Zaki, V.H., Zahran, E., 2025. Comparative analysis of biomarkers and energy metabolism in parasitized and non-parasitized European seabass (Dicentrarchus labrax). Aquac. Int. 33, 717. https://doi.org/10.1007/s10499-025-02371-4

Ashley, P.J., Sneddon, L.U., McCrohan, C.R., 2007. Nociception in fish: stimulus–response properties of receptors on the head of trout Oncorhynchus mykiss. Brain Res. 1166, 47–54. https://doi.org/10.1016/j.brainres.2007.07.011

Bordignon, F., Ferrarese, L., Solimeo, A., Di Leva, V., Trocino, A., 2025. Animal-based measures for operational welfare indicators at wholesale level in gilthead seabream (Sparus aurata) reared in the Mediterranean Sea. Aquaculture 603, 742417. https://doi.org/10.1016/j.aquaculture.2025.742417

Brugman, S., Ikeda-Ohtsubo, W., Braber, S., Folkerts, G., Pieterse, C.M.J., Bakker, P.A.H.M., 2018. A Comparative Review on Microbiota Manipulation: Lessons From Fish, Plants, Livestock, and Human Research. Front. Nutr. 5, 80. https://doi.org/10.3389/fnut.2018.00080

Capó, X., Company, J.J., Alomar, C., Compa, M., Sureda, A., Grau, A., Hansjosten, B., López-Vázquez, J., Quintana, J.B., Rodil, R., Deudero, S., 2021. Long-term exposure to virgin and seawater exposed microplastic enriched-diet causes liver oxidative stress and inflammation in gilthead seabream Sparus aurata, Linnaeus 1758. Sci. Total Environ. 767, 144976. https://doi.org/10.1016/j.scitotenv.2021.144976

Cascarano, M.C., Stavrakidis-Zachou, O., Mladineo, I., Thompson, K.D., Papandroulakis, N., Katharios, P., 2021. Mediterranean Aquaculture in a Changing Climate: Temperature Effects on Pathogens and Diseases of Three Farmed Fish Species. Pathogens 10, 1205. https://doi.org/10.3390/pathogens10091205

Domingo-Bretón, R., Cools, S., Moroni, F., Belenguer, A., Calduch-Giner, J.A., Croes, E., Holhorea, P.G., Naya-Català, F., Boon, H., Pérez-Sánchez, J., 2025. Intestinal microbiota shifts by dietary intervention during extreme heat summer episodes in farmed gilthead sea bream (Sparus aurata). Aquac. Rep. 40, 102566. https://doi.org/10.1016/j.aqrep.2024.102566

Egan, S., Fukatsu, T., Francino, M.P., 2020. Opportunities and Challenges to Microbial Symbiosis Research in the Microbiome Era. Front. Microbiol. 11, 1150. https://doi.org/10.3389/fmicb.2020.01150

Egerton, S., Culloty, S., Whooley, J., Stanton, C., Ross, R.P., 2018. The Gut Microbiota of Marine Fish. Front. Microbiol. 9, 873. https://doi.org/10.3389/fmicb.2018.00873

Faggio, C., Piccione, G., Marafioti, S., Arfuso, F., Fortino, G., Fazio, F., 2014. [No title found]. Turk. J. Fish. Aquat. Sci. 14. https://doi.org/10.4194/1303-2712-v14_2_28

FAO, 2024. The State of World Fisheries and Aquaculture 2024. FAO.

https://doi.org/10.4060/cd0683en

Fazio, F., Marafioti, S., Arfuso, F., Piccione, G., Faggio, C., 2013. Comparative study of the biochemical and haematological parameters of four wild Tyrrhenian fish species. Veterinární Medicína 58, 576–581. https://doi.org/10.17221/7139-VETMED

FEAP, 2025. European Aquaculture Production Report 2017-2023.

Feijão, E., Duarte, I.A., Pereira, M., Pascoal, P., Nunes, M., Tanner, S.E., Dias, R., Duarte, B., Matos, A.R., Figueiredo, A., Fonseca, V.F., 2025. Gilthead sea bream gut bacteriome as a valuable tool for seafood provenance analysis. Appl. Environ. Microbiol. 91, e01508-25. https://doi.org/10.1128/aem.01508-25

future Market Insights, n.d. Demand for Sea Bream in EU.

García García, B., Rosique Jiménez, C., Aguado-Giménez, F., García García, J., 2019. Life Cycle Assessment of Seabass (Dicentrarchus labrax) Produced in Offshore Fish Farms: Variability and Multiple Regression Analysis. Sustainability 11, 3523. https://doi.org/10.3390/su11133523

Guerreiro, I., Couto, A., Pérez-Jiménez, A., Oliva-Teles, A., Enes, P., 2015. Gut morphology and hepatic oxidative status of European sea bass (*Dicentrarchus labrax*) juveniles fed plant feedstuffs or fishmeal-based diets supplemented with short-chain fructo-oligosaccharides and xylo-oligosaccharides. Br. J. Nutr. 114, 1975–1984. https://doi.org/10.1017/S0007114515003773

Ibarz, A., Beltrán, M., Fernández-Borràs, J., Gallardo, M.A., Sánchez, J., Blasco, J., 2007. Alterations in lipid metabolism and use of energy depots of gilthead sea bream (Sparus aurata) at low temperatures. Aquaculture 262, 470–480. https://doi.org/10.1016/j.aquaculture.2006.11.008

Ikeda-Ohtsubo, W., Brugman, S., Warden, C.H., Rebel, J.M.J., Folkerts, G., Pieterse, C.M.J., 2018. How Can We Define "Optimal Microbiota?": A Comparative Review of Structure and Functions of Microbiota of Animals, Fish, and Plants in Agriculture. Front. Nutr. 5, 90. https://doi.org/10.3389/fnut.2018.00090

Kaya Öztürk, D., Öztürk, R., Baki, B., Karayücel, İ., Karayücel, S., 2020. Monthly variation of growth, biochemical composition, fatty and amino acids patterns of gilthead sea bream (*Sparus aurata*) in offshore cage systems under brackish water conditions in the Black Sea. Aquac. Res. 51, 4961–4983. https://doi.org/10.1111/are.14833

Klinger, D.H., Levin, S.A., Watson, J.R., 2017. The growth of finfish in global open-ocean aquaculture under climate change. Proc. R. Soc. B Biol. Sci. 284, 20170834. https://doi.org/10.1098/rspb.2017.0834

Kousoulaki, K., Saether, B.-S., Albrektsen, S., Noble, C., 2015. Review on European sea bass (*Dicentrarchus labrax,* Linnaeus, 1758) nutrition and feed management: a practical guide for optimizing feed formulation and farming protocols. Aquac. Nutr. 21, 129–151. https://doi.org/10.1111/anu.12233

Li, M., Liang, H., Yang, H., Ding, Q., Xia, R., Chen, J., Zhou, W., Yang, Y., Zhang, Z., Yao, Y., Ran, C., Zhou, Z., 2024. Deciphering the gut microbiome of grass carp through multi-omics approach. Microbiome 12, 2. https://doi.org/10.1186/s40168-023-01715-7

Maradonna, F., Nozzi, V., Dalla Valle, L., Traversi, I., Gioacchini, G., Benato, F., Colletti, E., Gallo, P., Di Marco Pisciottano, I., Mita, D.G., Hardiman, G., Mandich, A., Carnevali, O., 2014. A developmental hepatotoxicity study of dietary bisphenol A in Sparus aurata juveniles. Comp. Biochem. Physiol. Part C Toxicol. Pharmacol. 166, 1–13. https://doi.org/10.1016/j.cbpc.2014.06.004

Menna O, E.-D., Younis M, Y., El-Dakar, A.Y., Salem M, A., Kassem S, A., Ahmed M, A.-B., 2021. Age, growth and mortality of the European Seabass, (Dicentrarchus Labrax) in Bardawil lagoon, North Sinai, Egypt. Int. J. Aquac. Fish. Sci. 042–046. https://doi.org/10.17352/2455- 8400.000072

Mhalhel, K., Levanti, M., Abbate, F., Laurà, R., Guerrera, M.C., Aragona, M., Porcino, C., Briglia, M., Germanà, A., Montalbano, G., 2023. Review on Gilthead Seabream (Sparus aurata) Aquaculture: Life Cycle, Growth, Aquaculture Practices and Challenges. J. Mar. Sci. Eng. 11, 2008. https://doi.org/10.3390/jmse11102008

Mininni, A.N., Milan, M., Ferraresso, S., Petochi, T., Di Marco, P., Marino, G., Livi, S., Romualdi, C., Bargelloni, L., Patarnello, T., 2014. Liver transcriptome analysis in gilthead sea bream upon exposure to low temperature. BMC Genomics 15, 765. https://doi.org/10.1186/1471- 2164-15-765

Moschen, A.R., Wieser, V., Tilg, H., 2012. Dietary Factors: Major Regulators of the Gut's Microbiota. Gut Liver 6, 411–416. https://doi.org/10.5009/gnl.2012.6.4.411

Naya-Català, F., Piazzon, M.C., Torrecillas, S., Toxqui-Rodríguez, S., Calduch-Giner, J.À., Fontanillas, R., Sitjà-Bobadilla, A., Montero, D., Pérez-Sánchez, J., 2022. Genetics and Nutrition Drive the Gut Microbiota Succession and Host-Transcriptome Interactions through the Gilthead Sea Bream (Sparus aurata) Production Cycle. Biology 11, 1744. https://doi.org/10.3390/biology11121744

Noble, C., Abbink, W., Alvestad, R., Ardó, L., Bégout, M., Bloecher, N., Burgerhout, E., Calduch-Giner, J., Chivite-Alcalde, M., Císař, P., Durland, E., Espmark, Å.M., Falconer, L., Føre, M., Georgopoulou, D.G., Heia, K., Helberg, G.A.N., Izquierdo Gomez, D., Johansen, L., Johansson, G.S., Jónsdóttir, K.E., Kolarevic, J., Krasnov, A., Kumaran, S.K., Kvæstad, B., Larsson, T., Lazado, C.C., Madaro, A., Moroni, F., Måge, I., Nilsson, J., Ortega, S., Papandroulakis, N., Pérez-Sánchez, J., Prentice, P.M., Rey Planellas, S., Roth, B., Smith, A., Solberg, L.E., Stavrakidis-Zachou, O., Stien, L.H., Striberny, A., Svalheim, R.A., Sæther, B., Timmerhaus, G., Toften, H., Tschirren, L., Van De Vis, H., Ytteborg, E., Zena, L.A., Østbye, T.K., 2026. Welfare Indicators for Aquaculture Research: Toolboxes for Five Farmed European Fish Species. Rev. Aquac. 18, e70109. https://doi.org/10.1111/raq.70109

Orduna, C., De Meo, I., Rodríguez-Ruiz, A., Cid-Quintero, J.R., Encina, L., 2023. Seasonal Length–Weight Relationships of European Sea Bass (Dicentrarchus labrax) in Two Aquaculture Production Systems. Fishes 8, 227. https://doi.org/10.3390/fishes8050227

Pelusio, N.F., Scicchitano, D., Parma, L., Dondi, F., Brini, E., D'Amico, F., Candela, M., Yúfera, M., Gilannejad, N., Moyano, F.J., Gatta, P.P., Bonaldo, A., 2021. Interaction Between Dietary Lipid Level and Seasonal Temperature Changes in Gilthead Sea Bream Sparus aurata: Effects on Growth, Fat Deposition, Plasma Biochemistry, Digestive Enzyme Activity, and Gut Bacterial Community. Front. Mar. Sci. 8, 664701. https://doi.org/10.3389/fmars.2021.664701

Pérez-Pascual, D., Vendrell-Fernández, S., Audrain, B., Bernal-Bayard, J., Patiño-Navarrete, R., Petit, V., Rigaudeau, D., Ghigo, J.-M., 2021. Gnotobiotic rainbow trout (Oncorhynchus mykiss) model reveals endogenous bacteria that protect against Flavobacterium columnare infection. PLOS Pathog. 17, e1009302. https://doi.org/10.1371/journal.ppat.1009302

Piazzon, M.C., Naya-Català, F., Perera, E., Palenzuela, O., Sitjà-Bobadilla, A., Pérez-Sánchez, J., 2020. Genetic selection for growth drives differences in intestinal microbiota composition and parasite disease resistance in gilthead sea bream. Microbiome 8, 168. https://doi.org/10.1186/s40168-020-00922-w

Piazzon, M.C., Naya-Català, F., Simó-Mirabet, P., Picard-Sánchez, A., Roig, F.J., Calduch-Giner, J.A., Sitjà-Bobadilla, A., Pérez-Sánchez, J., 2019. Sex, Age, and Bacteria: How the Intestinal Microbiota Is Modulated in a Protandrous Hermaphrodite Fish. Front. Microbiol. 10, 2512. https://doi.org/10.3389/fmicb.2019.02512

Quero, G.M., Piredda, R., Basili, M., Maricchiolo, G., Mirto, S., Manini, E., Seyfarth, A.M., Candela, M., Luna, G.M., 2023. Host-associated and Environmental Microbiomes in an Open-Sea Mediterranean Gilthead Sea Bream Fish Farm.

Microb. Ecol. 86, 1319–1330. https://doi.org/10.1007/s00248-022-02120-7
Riedel, R., Caskey, L.M., Hurlbert, S.H., 2007. Length-weight relations and growth rates of dominant fishes of the Salton Sea: implications for predation by fish-eating birds. Lake Reserv. Manag. 23, 528–535. https://doi.org/10.1080/07438140709354036
Ruiz, A., Andree, K.B., Furones, D., Holhorea, P.G., Calduch-Giner, J.À., Viñas, M., Pérez-Sánchez, J., Gisbert, E., 2023. Modulation of gut microbiota and intestinal immune response in gilthead seabream (Sparus aurata) by dietary bile salt supplementation. Front. Microbiol. 14, 1123716. https://doi.org/10.3389/fmicb.2023.1123716
Sánchez-Nuño, S., Eroldogan, O., Sanahuja, I., Özşahniğlu, I., Blasco, J., Fernández-Borràs, J., Fontanillas, R., Guerreiro, P., Ibarz, A., 2018. Cold-induced growth arrest in gilthead sea bream Sparus aurata: metabolic reorganisation and recovery. Aquac. Environ. Interact. 10, 511–528. https://doi.org/10.3354/aei00286
Schilling, J.W., Hussey, N.E., Hedges, K.J., Barkley, A.N., 2025. Non-invasive ultrasound measurements for determination of hepato-somatic index in GREENLAND halibut (*Reinhardtius hippoglossoides*). J. Fish Biol. 107, 1313–1322. https://doi.org/10.1111/jfb.70089
Serra, C.R., Oliva-Teles, A., Enes, P., Tavares, F., 2021. Gut microbiota dynamics in carnivorous European seabass (Dicentrarchus labrax) fed plant-based diets. Sci. Rep. 11, 447. https://doi.org/10.1038/s41598-020-80138-y
Silva, T.S., Da Costa, A.M.R., Conceição, L.E.C., Dias, J.P., Rodrigues, P.M.L., Richard, N., 2014. Metabolic fingerprinting of gilthead seabream (*Sparus aurata*) liver to track interactions between dietary factors and seasonal temperature variations. PeerJ 2, e527. https://doi.org/10.7717/peerj.527
Sinha, A.K., Zinta, G., AbdElgawad, H., Asard, H., Blust, R., De Boeck, G., 2015. High environmental ammonia elicits differential oxidative stress and antioxidant responses in five different organs of a model estuarine teleost (Dicentrarchus labrax). Comp. Biochem. Physiol. Part C Toxicol. Pharmacol. 174–175, 21–31. https://doi.org/10.1016/j.cbpc.2015.06.002
Solé-Jiménez, P., Naya-Català, F., Piazzon, M.C., Estensoro, I., Calduch-Giner, J.À., Sitjà-Bobadilla, A., Van Mullem, D., Pérez-Sánchez, J., 2021. Reshaping of Gut Microbiota in Gilthead Sea Bream Fed Microbial and Processed Animal Proteins as the Main Dietary Protein Source. Front. Mar. Sci. 8, 705041. https://doi.org/10.3389/fmars.2021.705041
Song, W., Chen, C., Du, X., Zhang, R., Zhao, J., 2025. Patterns and influencing factors of intestinal microbiota from different groupers. Anim. Microbiome 7, 96. https://doi.org/10.1186/s42523-025-00461-5
Stentiford, G.D., Bateman, I.J., Hinchliffe, S.J., Bass, D., Hartnell, R., Santos, E.M., Devlin, M.J., Feist, S.W., Taylor, N.G.H., Verner-Jeffreys, D.W., Van Aerle, R., Peeler, E.J., Higman, W.A., Smith, L., Baines, R., Behringer, D.C., Katsiadaki, I., Froehlich, H.E., Tyler, C.R., 2020. Sustainable aquaculture through the One Health lens. Nat. Food 1, 468–474. https://doi.org/10.1038/s43016-020-0127-5
Tapia-Paniagua, S.T., Fumanal, M., Anguís, V., Fernández-Díaz, C., Alarcón, F.J., Moriñigo, M.A., Balebona, M.C., 2019. Modulation of Intestinal Microbiota in Solea senegalensis Fed Low Dietary Level of Ulva ohnoi. Front. Microbiol. 10, 171. https://doi.org/10.3389/fmicb.2019.00171
Tarnecki, A.M., Burgos, F.A., Ray, C.L., Arias, C.R., 2017. Fish intestinal microbiome: diversity and symbiosis unravelled by metagenomics. J. Appl. Microbiol. 123, 2–17. https://doi.org/10.1111/jam.13415
Telli-Karakoç, F., Barlas, N., 2019. Determination of the healthiness of aquaculture fish by enzymes and histopathological methods. Mar. Pollut. Bull. 149, 110535.

https://doi.org/10.1016/j.marpolbul.2019.110535
Yýldýrým Korkut, Y.K.A., Gurkan, S., 2018. Length-weight relationship and condition factor as an indicator of growth and feeding intensity of Sea bream (Sparus aurata L, 1758) given feed with different protein contents. Indian J. Anim. Res. https://doi.org/10.18805/ijar.B-998

Acknowledgement

Financial support was received for the research and/or publication of this article. Project funded under the National Recovery and Resilience Plan (NRRP), Mission 4 Component 2 Investment 1.4 - Call for tender No. 3138 of 16 December 2021, rectified by Decree n.3175 of 18 December 2021 of Italian Ministry of University and Research funded by the European Union – NextGenerationEU; Award Number: Project code CN_00000033, Concession Decree No. 1034 of 17 June 2022 adopted by the Italian Ministry of University and Research, CUP D33C22000960007, Project title “National Biodiversity Future Center - NBFC”.